Development of Virtual Patients for use in Mechanical Ventilation

Sophie Elizabeth Morton

A thesis presented for partial fulfilment of the

requirements for the degree of Doctor of Philosophy

in

Mechanical Engineering

at the

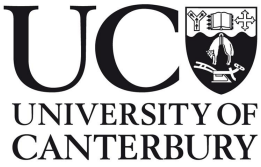

University of Canterbury

Christchurch, New Zealand

August 2019

For my mother, Diana Clair Morton, whose laugh I miss more than anything.

In between many other things, she taught me that few challenges in life seem as insurmountable when approached with a sense of humour, grittiness, and a soundtrack of upbeat 70s music.

Acknowledgements

There are several people I would like to thank for helping me along the path to completing this thesis.

My primary supervisor, Geoff Chase. Thank you for giving me the opportunity to pursue this PhD, and for allowing me to work through it at my own pace. Your technical knowledge and seemingly endless supply of analogies to explain every part of biomedical research have been invaluable. Thank you for encouraging me to both publish my results and present them at conferences, and for your tireless removal of unnecessary qualifiers in my abstracts and conclusions.

To both of my co-supervisors, Jennifer Knopp and Paul Docherty. Thank you for always being so approachable, sharing your expertise with me, and your willingness to guide me in translating ideas into models. Jennifer, thank you for the proof-reading, including your exceptional ability to find the kind of minor errors in my algebra proofs and/or 700 lines of code that cause things like the modelled pressure to exceed the number of atoms in the known universe. Paul, thank you for answering my system identification questions, and your constant vigilance in removing all traces of hospital blue from my presentations.

My associate supervisors Merryn Tawhai, Geoff Shaw, Yeong Shiong Chiew, Thomas Desaive and Knut Möller. Thank you for your brilliant technical insight, for being so forthcoming with clinical data, and for proofreading papers, occasionally at very short notice. My thanks also go to Chris Pretty for frequently checking up on me and always

being prepared with excellent explanations of how to approach the issues I faced during this process.

The residents of the UC Bioengineering Centre for the support, the discussions, the comedy, and for helping me to hone my paper plane skills.

Thank you to all my friends and flatmates who have provided me with many welcome distractions from my PhD over the years (Webb, 2016). Gemma and Mary, thank you both for your unwavering support through the more challenging times.

Alex, for your love, your understanding and your patience, and for your almost guaranteed presence in the office last year providing me with extra motivation to do work on Saturday afternoons.

To my family, thank you for everything you do for me. Dad, for always encouraging and supporting my scientific curiosity, even when you discovered I was intentionally cultivating penicillin in the kitchen. To my sisters, Amanda and Katie, thank you for always being there for me, and for the often well timed dog and wombat photos that appear in my Facebook inbox after I've had a long day. I would also like to thank André and Will for their continued commitment to beating me at card games. Victoria, for all the joy you bring into my life, and Arthur, for providing motivation to finish this thesis on time. Rosie, thank you for often acting as an alarm clock when you felt it was an appropriate time for your morning walk. To my grandparents: Kathy, John, and Daphne, thank you for all the support and love you have each given me over the years.

Finally, I would like to thank Prince Rogers Nelson and Tupac Shakur. Without their musical genius, the late nights working on my thesis would have felt much longer.

Abstract

Mechanical ventilation (MV) is a core life-support therapy for patients suffering respiratory failure or acute respiratory distress syndrome (ARDS). Respiratory failure is a secondary outcome of a range of injuries and diseases, and results in almost half of all intensive care unit (ICU) patients receiving some form of MV. Funding the increasing demand for ICU is a major issue and MV, in particular, can double the cost per day due to significant patient variability, over-sedation, and the large amount of clinician time required for patient management. Reducing the cost in this area requires both a decrease in the average duration of MV by improving care, and a reduction in clinical workload.

Model-based methods offer a way of using individual patient physiology and response to MV to suggest optimal ventilator settings. In particular, models and data can be used to gain insight into specific lung mechanics, such as pulmonary elastance and resistance. Importantly, these models can be used to quantify aspects of patient lung physiology over time, capturing a patient's time-dependent disease state as patient condition evolves. These models have the potential to enable predictive, personalised, and potentially automated, approaches to MV.

The research in this thesis explores creating a more effective method of clinical trial

design for mechanical ventilation trials. The high level of patient variability and the non-normal distribution of the key clinical outcome, length of mechanical ventilation, means many MV clinical trials struggle to achieve statistical significance. As a result, very large sample sizes are required to achieve statistical power to prevent inconclusive findings that cannot be extrapolated to other care units. Equally, non-significant findings do not inform the field or allow it to improve. A Monte-Carlo simulation method was developed and used to investigate several outcome metrics of ventilation treatment. As these metrics have highly skewed distributions, it also included the impact of imposing objective clinically relevant exclusion criteria on study power to enable better design for significance. This method combined with the use of composite outcome metrics, such as ventilator free days, enables high powered studies to be developed with substantially lower sample size requirements, enabling better study design and outcomes.

This thesis primarily focusses on the development of virtual patients. Virtual patients are used to personalise and optimise care for each individual patient by predicting response to a change in treatment prior to implementing the change. This personalisation is especially critical for ICU patients, who exhibit a great deal of variation in condition, and response to treatment. In particular, these virtual patient models predict the effects of a recruitment manoeuvre (RM) on lung elastance to minimise the risk of ventilator induced lung injury (VILI) while also maximising lung recruitment, and thus oxygenation.

The model was developed using physiologically relevant basis function models describing the effects of alveolar recruitment, lung distension, and airway resistance on overall lung elastance and resistance over pressure, volume and flow. The goal was to ensure the virtual patients model predictions and information provided was clinically relevant. It was validated using clinical data from two diverse sets of data from trials in

New Zealand (the CURE trial) and Germany (McREM trial). A high level of fitting accuracy (RMS error) was seen for predictions of PEEP changes of up to 10 cmH_2O, indicating the selected basis functions accurately describe the behaviour of the dominant lung mechanics in an RM and could have potential as a diagnostic tool.

The model showed a high level of accuracy with predicted peak inspiratory pressure error (median [IQR]) of 6.3 [4.5 - 8.3]% in the CURE cohort and 6.2 [5.0 - 9.1] % in the McREM cohort, even for PEEP changes up to 10 cmH_2O. This capability to accurately predict pressure so far ahead in an RM provides important clinical insight, as it can enable the clinician to assess early in a RM when increases should either be stopped, or when much smaller incremental changes should be made. This knowledge could significantly aid in the efficiency of RMs, reducing clinical workload and improving patient care and outcomes.

A less studied impact of increasing PEEP is the added pressure results in an increased end-expiratory (recruited) lung volume, or dynamic function residual capacity. It is essentially the residual additional lung volume additional lung volume (V_{frc}), due to alveolar recruitment at this higher pressure. Determining V_{frc} is invasive, typically requiring imaging that either cannot be carried out at the bedside or is not available in every care unit. A model-based method to predict additional recruited lung volume (V_{frc}) gained throughout a recruitment manoeuvre was developed and validated against clinical data. Results were promising with high accuracy shown in both approximating V_{frc} and using this information to predict lung behaviour at higher PEEP levels. The results offer a clinical opportunity to titrate PEEP based on the estimated lung volume recruited, a direct indication of the success of an RM. Combined with prediction of the point of minimum elastance and prediction of peak inspiratory pressure this information would allow clinicians to optimise the trade-off between the risk of VILI and lung recruitment, in real-time as patient condition evolves, improving patient care and out-

comes.

The incorporation of virtual patient methods into mechanical ventilation will aid the healthcare sector in meeting increasing demand in intensive care units. In particular, a change from more generic protocols to the use of predictive, patient-specific models will improve individual patient outcomes while also reducing clinical workload. The efficacy of the physiologically relevant model in determining lung behaviour throughout an entire RM in ventilation indicates it could be used as a diagnostic clinical tool. The future use of virtual patients and cohorts will also allow new treatments and therapies to be safely and more efficiently tested, allowing for faster advancements in the field.

Publications

Over the course of this research, a number of papers have been published. The research demonstrated in these papers is based on the work presented in this thesis.

Journal Papers

- **Morton, SE**, Knopp, JL, Chase, JG, Möller, K, Docherty, P, Shaw, GM, Tawhai, M, (2019). ”Authors’ Response to Drs. Ece Salihoglu and Ziya Salihoglu’s Letter to the Editor”. *Annals of Biomedical Engineering*, https://doi.org/10.1007/s10439-019-02339-5
- **Morton, SE**, Knopp, JL, Chase, JG, Docherty, P, Howe, SL, Möller, K, Tawhai, M, (2019). ”Optimising mechanical ventilation through model-based methods and automation”. *Annual Reviews in Controls*. http://dx.doi.org/10.1016
- **Morton, SE**, Knopp, JL, Chase, JG, Möller, K, Docherty, P, Shaw, GM, Tawhai, M, (2019), “Predictive Virtual Patient Modelling of Mechanical Ventilation: Impact of Recruitment Function”. *Annals of Biomedical Engineering*, DOI :10.1007/s10439-019-02253-w.
- **Morton, S.E.**, Docherty, P. D., Dickson, J. L., Chase, J. G. (2018). ”An analysis of the impact of the inclusion of expiration data on the fitting of a predictive pulmonary

elastance model". *Current Directions in Biomedical Engineering*, 4(1), 255–258.

- **Morton, SE**, Dickson, JL, Chase, JG, Docherty, PD, Desaive, T, Howe, SL, Shaw, GM and Tawhai, M,(2018),"A virtual patient model for mechanical ventilation". *Computer Methods and Programs in Biomedicine*,vol. 165, pp. 77–87.

- **Morton, SE**, Chiew, YS, Pretty, CG, Moltchanova, E, Scarrot, C, Redmond, D, Shaw, GM and Chase, JG, (2017) "Effective sample size estimation for a mechanical ventilation trial through Monte-Carlo simulation: Length of mechanical ventilation and Ventilator Free Days". *Mathematical Biosciences*, vol. 284, pp. 21–31, **(invited)**

Conference Papers

- **Morton, SE**, Dickson, JL, Chase, JG, Docherty, PD, Howe, SL, Shaw, GM and Tawhai, M (2018). "Development of a Predictive Pulmonary Elastance Model to Describe Lung Mechanics throughout Recruitment Manoeuvres," *10th IFAC Symposium on Biological and Medical Systems (BMS 2018)*, September 3-5, Sao Paulo, Brazil, 6-pages, (invited).

- **Morton, SE**, Knopp, JL, Docherty, PD, Shaw, GM and Chase, JG (2018). "Validation of a Model-based Method for Estimating Functional Volume Gains during Recruitment Manoeuvres in Mechanical Ventilation," *10th IFAC Symposium on Biological and Medical Systems (BMS 2018)*, September 3-5, Sao Paulo, Brazil, 6-pages, (invited).

- **Morton, SE**, Dickson, JL, Chase, JG, Docherty, PD, Howe, S, Shaw, GM and Tawhai, M (2018). "Basis function identification of lung mechanics in mechanical ventilation for predicting outcomes of therapy changes: A first virtual patient," *18th IFAC Symposium on System Identification (IFAC SYSID)*, Stockholm, Sweden, July 9-11, 6-pages, (invited).

- **Morton, S**, Dickson, JL, Docherty, PD, Shaw, GM and Chase, JG (2017). "Develop-

ment of a Predictive Model for Pulmonary Elastance," Medtech CoRE Conference, Auckland, NZ, June 20, 2-pages.

- **Morton, S,** Dickson, JL, Docherty, PD, Chiew, YS, Shaw, GM, Desaive, T and Chase, JG (2017). "Development of Virtual Patients for use in Mechanical Ventilation," HRSC Grand Rounds, Christchurch, NZ, May 26, 1-pages; In: *NZ Medical Journal*, July 2017, Vol 130(1459), pp. 80.

- **Morton, S**, Chiew, YS, Pretty, CG, Shaw, GM and Chase, JG (2016). "Impact of Sedative Drug Use on Length of Mechanical Ventilation," Medtech CoRE Conference, Auckland, NZ, June 20, 2-pages.

- **Morton, S**, Chiew, YS, Pretty, CG, Chase, JG and Shaw, GM (2016). "Impact of sedative drug use on the length of mechanical ventilation," *36th International Symposium on Intensive Care and Emergency Medicine (ISICEM)*, Brussels, Belgium, March 15-18, 1-page.

- Chase, JG, **Morton, SE**, Knopp, JL, (2019) "Virtual Patients for Managing Mechanical Ventilation in the ICU", *41st Annual International Conference of the IEEE Engineering in Medicine and Biology Society (EMBC)*, Berlin, Germany (invited)

- Howe, S. L., Chase, J. G., Redmond, D. P., **Morton, S. E.**, Kim, K. T., Pretty, C. G.,Shaw, G.M, Tawhai, M.,Desaive, T. (2018). Estimation of Inspiratory Respiratory Elastance Using Expiratory Data. *IFAC-PapersOnLine*, 51(27), 204–208.

- Uyttendaele, V., Dickson, J. L., **Morton, S. E.,** Shaw, G. M., Desaive, T., Chase, J. G. (2018). Changes in Identified , Model-based Insulin Sensitivity can be used to Improve Risk and Variability Forecasting in Glycaemic Control. *IFAC-PapersOnLine*, 51(15), 311–316.

- Redmond, D. P., Kim, K. T., **Morton, S. E.**, Howe, S. L., Chiew, Y.-S., Chase, J. G. (2017). A Variable Resistance Respiratory Mechanics Model. *IFAC-PapersOnLine*, 50(1), 6660–6665. http://doi.org/10.1016/j.ifacol.2017.08.1533

- Kim, K. T., Redmond, D. P., **Morton, S. E.,** Howe, S. L., Chiew, Y.-S., Chase, J. G. (2017). Quantifying patient effort in spontaneously breathing patient using negative component of dynamic Elastance. *IFAC-PapersOnLine*, 50(1), 5486–5491.

Contents

List of Figures

List of Tables

List of Abbreviations

ALI Acute Lung Injury

ARDS acute respiratory distress syndrome

BIPAP bi-level positive airway pressure

COPD Chronic Obstructive Pulmonary Disease

CPAP continuous positive airway pressure

$\triangle$ **Effect** change in treatment effect

$\triangle$ **LoMV** change in length of mechanical ventilation

E_{drs} Dynamic lung elastance

ETT Endotracheal Tube

FEA Finite Element Analysis

FRC functional residual capacity

ICU Intensive Care Unit

I/E ratio inspiration:expiration ratio

KS-Test Kolmogorov-Smirnov Test

LoMV length of mechanical ventilation

LoMV$_{28}$ length of mechanical ventilation within 28 days

MV Mechanical Ventilation

PCV Pressure Controlled Ventilation

PEEP positive end-expiratory pressure

PaO_2/FiO_2 ratio PaO_2/FiO_2 ratio

PIP peak inspiratory pressure

PUMP PEEP adjustment and Monitoring Procedure

PV curve pressure-volume curves

RCT randomised control trial

R_{rs} lung resistance

RM recruitment manoeuvre

RMS Root Mean Square

TCP threshold closing pressure

TOP threshold opening pressure

(lognormal) T-Test (lognormal)Student T-Test

VCV Volume Controlled Ventilation

VFD Ventilator Free Days

V_{frc} additional lung volume

VILI ventilator-induced lung injury

WR-Test Wilcoxon-Ranksum Test

ZEEP zero end-expiratory pressure

CHAPTER 1

Introduction

1.1 Introduction

Mechanical Ventilation (MV) is a core life-support therapy for patients suffering from respiratory failure or acute respiratory distress syndrome (ARDS) (de Matos et al., 2012; Girard & Bernard, 2007; Herridge et al., 2003; Lorx et al., 2010; Petrucci & De Feo, 2013; Slutsky, 1993; Slutsky & Tremblay, 1998; Sundaresan et al., 2009). Respiratory failure is a secondary outcome of a range of injuries and diseases, resulting in 30%-50% of Intensive Care Unit (ICU) patients receiving some form of MV (Dasta, McLaughlin, Mody, & Piech, 2005; Metnitz et al., 2009). While improvements in therapy have reduced mortality rates in ventilated patients since 1995 (Maca et al., 2017), the variability and severity of patient-specific condition makes care difficult to optimise. Thus, MV still has an overall mortality rate of 30.5% (Wunsch et al., 2010), where the sub-group diagnosed with ARDS have a mortality rate of 45% (Maca et al., 2017). Overall, MV is a common therapy operating at the forefront of life support and preservation in the ICU.

A primary, if not singular, issue facing healthcare sectors is funding for increasing demand. Intensive care is one of the most expensive hospital departments and MV, in

particular, is an expensive treatment due to patient variability and the resulting over-sedation, and the large amount of clinician time required (Cohen & Booth, 1994; Dasta et al., 2005). In fact, MV doubles the cost of an ICU stay (Dasta et al., 2005). Reducing the cost of this expensive therapy requires both a decrease in the average duration of MV by improving and personalising care, and a reduction in clinical workload. Both might be safely achieved by automating some or all aspects of clinical MV care.

Incorporating model-based methods into MV care could allow clinicians to gain insight into patient condition and improve safety on a patient level through the forward prediction of outcomes, such as peak inspiratory pressure (PIP) and volume gain with changes in treatment. On a cohort level, development of virtual patient models and methods would be essential for design and efficient testing of clinical protocols with a lower patient burden (Chase, Desaive, & Preiser, 2016; Chase et al., 2018).

1.2 Mechanical Ventilation

The ultimate aim of MV is to maintain adequate gas exchange in the alveoli. Alveolar collapse is common in ARDS, leading to seriously inhibited gas exchange and hypoxaemia (Ashbaugh, Bigelow, Petty, & Levine, 1967). To induce alveolar opening, a pressure differential must be applied physically across the lungs (Corrado & Gorini, 2002). This can be achieved with either negative or positive pressure ventilation.

Historically, this differential was achieved through devices such as the iron lung that exposed the patient's torso to negative pressure to facilitate lung expansion and thus inspiration (Corrado & Gorini, 2002; Maxwell, 1986; Thomson, 1997). This approach was useful for patients who were presenting with a condition, such as polio, where paralysis of the chest muscles and diaphragm meant that they could not carry out the muscle contractions required for inspiration. It allows for some patient-controlled breathing, as it is primarily designed to provide extra breathing support. The development of a polio vaccination along with the development of more efficient methods of positive-

pressure ventilation meant that iron lungs are no longer commonly used.

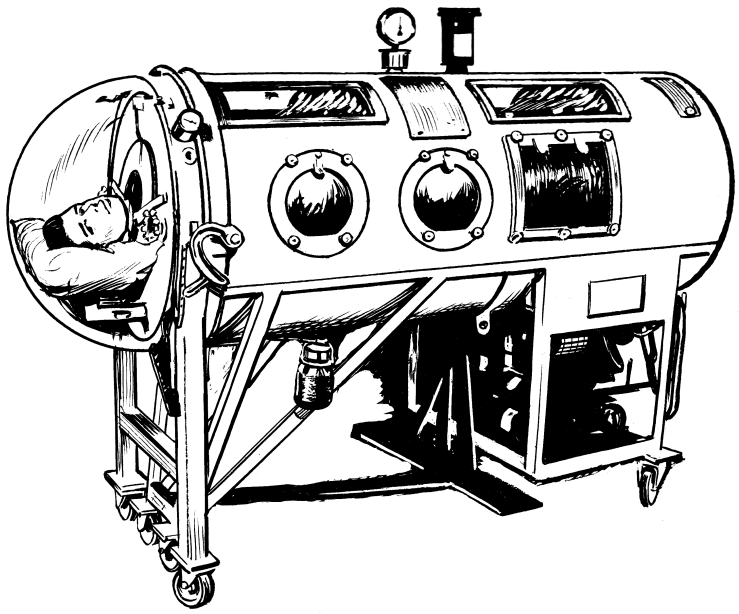

Figure 1.1: A diagram of a typical iron lung used throughout the polio epidemic of the 20th century.

Today, positive pressure ventilators are used to treat most patients suffering from acute respiratory failure. A clinician-set inspiratory pressure is applied directly to the airways of the lungs. This positive pressure ventilation is achieved either invasively via an Endotracheal Tube (ETT) or tracheotomy, or non-invasively using a continuous positive airway pressure (CPAP) or bi-level positive airway pressure (BIPAP) mask (Brochard et al., 1994; Kárason, Antonsen, & Aneman, 2002). This thesis will focus on invasive ventilation delivered through an ETT.

Both positive and negative pressure ventilators can cause mechanical lung damage, known as ventilator-induced lung injury (VILI), if incorrect ventilator settings are used (Albaiceta & Blanch, 2011; Alviar et al., 2018; M. Amato, Barbas, Medeiros, Magaldi, & Schettino, 1998; de Matos et al., 2012; DiRocco, Carney, & Nieman, 2007; Herridge et al., 2011; Jandre, Modesto, Carvalho, & Giannella-Neto, 2008; Major, Shaw, & Chase, 2018; Marini, 1994; Pinhu, Whitehead, Evans, & Griffiths, 2003; Ranieri et al., 2011; Simonis et al., 2015; Slutsky & Ranieri, 2014; Slutsky & Tremblay, 1998; Terragni, Rosboch, Lisi,

Viale, & Ranieri, 2003). This lung damage can result in additional lung injuries, such as alveolar-capillary lesions, alterations in permeability and oedema (M. Amato et al., 1998). In particular, VILI occurs as a result of the ventilator applying excessive pressure or tidal volume (Chiumello et al., 2008; Lipes, Bojmehrani, & Lellouche, 2012; Zick et al., 2013). This exacerbates the existing condition and extends the patient's stay in the ICU. This is a particularly significant problem for patients presenting with ARDS or Acute Lung Injury (ALI), heterogeneous lung diseases causing regional lung collapse (Carvalho et al., 2007; Chiew, Pretty, Moltchanova, et al., 2015; S. Grasso et al., 2009; Kheir et al., 2013), with a mortality rate of approximately 40-50% (Brower et al., 2000). However, equally, not enough pressure can result in lung units not opening enough, potentially causing hypoxaemia and atelectotrauma due to repeated opening and closing (Blanch & Villagrá, 2004; Crotti et al., 2001; Halter et al., 2003; Jobe, 2009; Pelosi et al., 2001; Slutsky, 1999; Suarez-Sipmann, 2014). Hence, optimising ventilator settings is a careful balance between two forms of risk, where too little or too much is problematic (Major et al., 2018).

The current standard of MV therapy in the ICU relies heavily on either clinician intuition, or on a generalised and protocolised approach (Briel et al., 2010; Brower et al., 2004; Meade, Cook, Griffith, et al., 2008; Slutsky & Ranieri, 2000). These generalised approaches target improved outcomes for the cohort. However, they disregard the heterogeneity of many lung diseases and patient variability, lacking patient-specificity. In addition, a generalised approach ignores the wide range of breathing data available for each individual patient. Thus, a method to guide patient-specific MV therapy is needed to improve individual patient outcomes beyond care using generalised protocols.

To achieve this goal, a combination of numerical methods along with an understanding of the physiological processes carried out in breathing enables the development of models to guide clinical decisions.

1.3 Physiology

While the warm blooded nature of mammals means they can respond to stimuli immediately, this requires a steady supply of energy. The great bulk of this energy is generated in the mitochondria using an oxygen requiring process of oxidative phosphorylation where the body effectively burns reduced fuels such as carbohydrates and lipids to carbon dioxide and water. Hence, oxygen induced energy generation, and thus oxygen, are critical to physiological function.

1.3.1 Structure of the Lungs

The airways of the lungs are a series of branching tubes; starting with the trachea, bifurcating into the left and right bronchi, and continuing to divide until they reach the terminal bronchioles (West, 2012). These branches are the extent of the conducting part of the airways which transport oxygen from the outside to the gas exchanging regions of the lungs. As the conducting airways do not carry out gas exchange, they are described as the anatomic dead space (West, 2012).

Past this point, the terminal bronchioles continue to split into respiratory bronchioles, which contain some alveoli and can carry out gas exchange. The process of bifurcation continues until the airways reach the estimated 480 million alveolar sacs where gas exchange occurs (Ochs et al., 2004). The thin walls of the alveoli combined with a total surface area of over 100m^2 allows for sufficient diffusion of oxygen from the alveoli to the capillaries wrapped around them (West, 2012). The process works in reverse for carbon dioxide. The rate of this diffusion is dependent on the partial pressure difference between the alveoli and the capillaries.

1.3.2 Ventilation

The lung does not participate in the actual muscular movement required for inflation. This action is carried out by the diaphragm and intercostal muscles. There is no me-

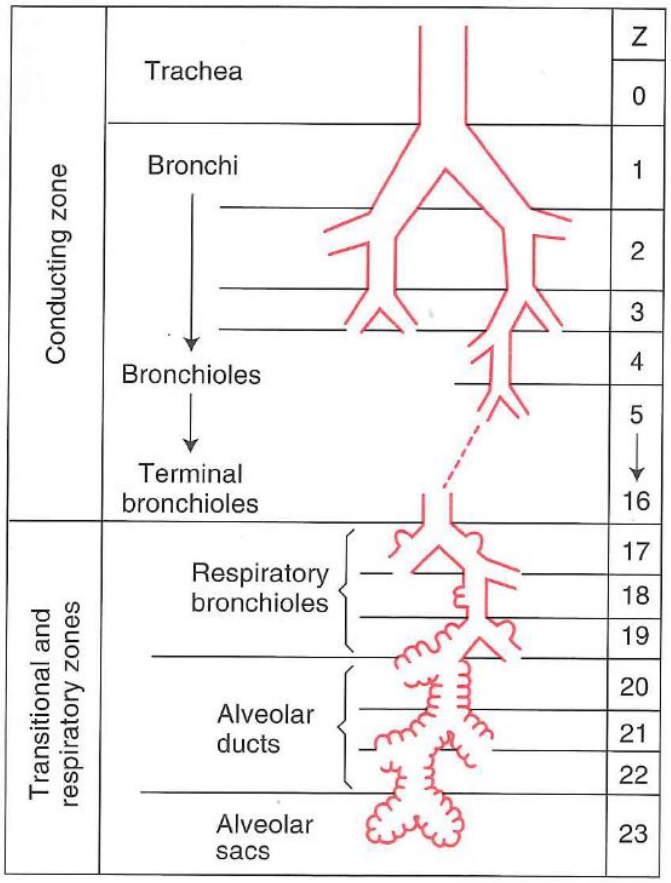

Figure 1.2: Structure of the lung airways (West, 2012)

chanical connection between the lungs and surrounding tissues. Instead, inflation is based on a transmural pressure gradient between the thoracic cavity and the lung.

This motion is created by the contraction of the respiratory muscles, causing a negative pressure gradient between the thoracic cavity and the lung. In turn, this gradient creates a negative pressure between the lung and the environment. Air is drawn into this lung to equate the pressure gradient, creating the inspiratory pattern of normal breathing. Negative pressure ventilators, such as the iron lung shown in Figure 1.1, seek to replicate this behaviour by periodically altering intrathoracic pressure. Positive pressure ventilation is more commonly used in care units, and involves the ventilator providing pressure to the airways to open the alveoli for gas exchange (F. Grasso et al., 2008).

Gravity also impacts the level of ventilation throughout the lungs (Surrowes, 2005; Swan, Clark, & Tawhai, 2012). The amount of inhaled air follows a topographic distribution caused by posture, airway tree shape and tissue deformation (Swan et al., 2012). Understanding the influence of these factors on respiration is significant because, while the human lung often operates in the upright position, mechanical ventilation is administered while the patient is either in the supine or prone position. A large scale effect of the effect of gravity is preferential ventilation in parts of the lung (Kim et al., 2002; Swan et al., 2012).

1.3.3 Perfusion

The lungs deliver oxygen to the bloodstream to deliver to the tissues. Thus, one of the primary functions of the lungs is perfusion, extracting oxygen from the air we breathe and releasing this oxygen into the bloodstream. The second is its exchange with CO_2.

In mechanical ventilation, oxygen levels need to be carefully monitored to prevent low blood oxygen, or hypoxaemia (Tehrani, 2012). In addition, excessive levels of oxygen can cause lung collapse, oxygen toxicity, or blindness in infants (Luecke & Pelosi, 2005; Wheatley, Dickinson, Mackey, Craig, & Sale, 2002). The saturation of oxygen in the bloodstream, typically measured as arterial SaO_2 or pulse oximetry, is an indication of how much of the haemoglobin present is oxygenated (Trundle & Rawat, 2011) . It is most typically monitored using a pulse oximeter (Jubran, 2015).

Alveoli are thin-walled air sacs located on the terminal branches of the bronchial tree. They are surrounded by pulmonary capillaries, and carry out gas exchange of oxygen and carbon dioxide to and from the bloodstream. The large number of alveoli combined with their small diameter and thin walls allows for sufficient surface diffusion across from the alveoli to the capillaries.

An alveolus has two states, open and closed. Gas exchange is only possible when an alveolus is open. Alveoli have a pressure at which they will open or ‘recruit’ during

inspiration, threshold opening pressure (TOP) and one at which they will close again during expiration threshold closing pressure (TCP) (Crotti et al., 2001). Working out the threshold pressures for the population of alveoli is generally done with using pressure-volume curves (PV curve). These PV curve and other data are often presented in real time on the ventilator (Lucangelo, Bernabè, & Blanch, 2007). The curve changes dramatically at the TCP and TOP as larger numbers of alveoli close or recruit (Hickling, 1998).

1.4 Lung Pathologies

Mechanical ventilation is used as a therapy for patients who are suffering from some form of respiratory failure (Slutsky, 1993). Respiratory failure is often a secondary symptom from a range of diseases, many causing lung damage that is mixed in effect and severity (Breen, Churches, Hawker, & Torzillo, 2002). This heterogeneity has made it difficult for the field to standardise care to optimise outcomes for all patients (Stenqvist, 2003).

Respiratory failure is caused by inadequate gas exchange in the lungs. This inadequacy is defined as it failing at one or both of insufficient oxygenation (hypoxaemia), or carbon dioxide elimination (hypercapnia). There are subsequently two types of respiratory failure defined, Type 1 and Type 2.

Type 1 is a low level of oxygen in the blood, without an increased level of carbon dioxide. It is often caused by the volume of air entering and exiting the lungs not being matched by the flow of blood to the lungs. This is defined as a ventilation-perfusion (V/Q) mismatch, where ventilation is the air that reaches the alveoli and perfusion is blood reaching the alveoli from the capillaries. Common conditions causing Type 1 respiratory failure in an ICU are:

- **Ventilation–perfusion mismatch** which can be caused by pulmonary embolisms
- **Problems with diffusion** which can be caused by pneumonia or ARDS (The ARDS

Definition Task Force, 2012)

- **Shunt** where oxygenated blood has mixed with non-oxygenated blood from the venous system (Fletcher & Barber, 1966).

Type 2 respiratory failure is caused by inadequate alveolar ventilation, where the exchange of both oxygen and carbon dioxide is affected. It often results in a build-up of carbon dioxide in the lungs (Ahrens, 2004). Common causes of this failure are:

- Increased airway resistance caused by Chronic Obstructive Pulmonary Disease (COPD) or asthma.
- A decrease in the working parts of the lungs, caused by diseases such as bronchitis.

In addition to these classifications, respiratory failure may also be defined as acute or chronic. Acute conditions develop suddenly and are often treated as an emergency. Meanwhile, chronic conditions develop over a longer period of time and require long term treatment, and monitoring.

1.4.1 ARDS

ARDS (Ashbaugh et al., 1967) is an extreme form of acute respiratory failure, caused by either direct or indirect lung injury (Petty & Ashbaugh, 1971). It is a severe inflammatory response inside the lung, resulting in mass alveoli collapse and characterised by oedema and severe hypoxaemia (Donahoe, 2011; Laufer et al., 2017). Common causes include pneumonia, sepsis, trauma, asthma, COPD, pancreatitis, burns, and near drowning (Chiew, 2013; Laufer et al., 2017).

ARDS encompasses a wide range of pulmonary dysfunctions, making it both complex and highly heterogeneous (Laufer et al., 2017). The hallmark of the disease is hypoxaemia and carbon dioxide retention caused by extensive alveolar collapse. The disease can develop over a timeframe ranging from hours to a few days (Bastarache & Blackwell, 2009). It is clinically defined by an PaO_2/FiO_2 ratio (PaO_2/FiO_2 ratio) less than 300 mmHg (Aboab, Louis, Jonson, & Brochard, 2006; The ARDS Definition Task Force, 2012).

Other indicators include poor intrapulmonary shunt fraction, oxygen index or arterial to alveolar O_2 difference (Aboab et al., 2006). The culmination of the various aspects of ARDS causes reduced O_2 supply and CO_2 removal, impacting upon other organs and tissues, causing significant physiological stress. ARDS is created by a reduction in the alveolar-capillary barrier, along with a flooding of the airspaces (Bastarache & Blackwell, 2009).

ARDS has been defined multiple times over the years with the most recent consensus definition by the Acute Respiratory Distress Network in 2012. This definition has simplified it to being solely classified by a PaO_2/FiO_2 ratio (The ARDS Definition Task Force, 2012):

- Mild ARDS ($200 < PaO_2/FiO_2$ ratio ≤ 300 mmHg)
- Moderate ARDS ($100 < PaO_2/FiO_2$ ratio ≤ 200 mmHg)
- Severe ARDS (PaO_2/FiO_2 ratio ≤ 100 mmHg)

The acute time frame is defined to be within one week. Overall, it is clear ARDS defines respiratory failure. In particular, it is defined by the failure to achieve adequate gas exchange (Chiew, 2013).

Due to respiratory failure being a secondary outcome and the heterogeneous nature of the ARDS lung, developing a standard care protocol to treat these patients is challenging. A range of randomised control trials (RCTs) have studied different treatment strategies to optimise care (Breen et al., 2002; Brower et al., 2004, 2000; Meade, Cook, Griffith, et al., 2008; Mercat et al., 2008). To date, none have provided an effective or generalisable solution (Major et al., 2018).

In addition to hypoxemia, ARDS lungs are more prone to VILI. This increased incidence of VILI is due to a combination of the heterogeneous nature of the lung, and because there is a much higher proportion of collapsed alveoli (Ashbaugh et al., 1967; Gattinoni & Pesenti, 2005; Petty & Ashbaugh, 1971). As the alveoli in ARDS lungs struggle

to open with each breathing cycle, it is critical to ensure as many of them stay open as possible. Increasing the number of open alveoli during mechanical ventilation is a process known as recruitment (Bates & Irvin, 2002; Blanch & Villagrá, 2004; Das et al., 2015; Dellamonica et al., 2011; Jobe, 2009; Kheir et al., 2013; Meade, Cook, Griffith, et al., 2008; Rocco, Pelosi, & de Abreu, 2010; Tusman et al., 2014). However, lungs can be damaged by repeated recruitment and decruitment over time (Blanch & Villagrá, 2004; Jobe, 2009; Slutsky, 1999; Suarez-Sipmann, 2014). Consequently, reducing the amount of times a diseased alveolus must recruit or open and close is advisable for ARDS patients (Blanch & Villagrá, 2004). This outcome is typically achieved by applying positive end-expiratory pressure (PEEP), a non-zero pressure at the end of each breath to maintain recruited alveoli in an open state (Das et al., 2015; Dellamonica et al., 2011; Jobe, 2009).

Improved outcomes in ARDS patients have been connected to the use of lower tidal volumes, higher PEEP settings, and ventilation in the prone position (M. Amato et al., 1998; Malhotra, 2008; Sundaresan & Chase, 2012; Terragni et al., 2007; Villar, Kacmarek, Perez-Mendez, & Aguirre-Jaime, 2006; Villar & Slutsky, 1996). Lower tidal volumes avoid over distension (Brower et al., 2000). PEEP ensures damaged lung units remain recruited, minimising damage. They are two of the most contentiously debated MV settings (Major et al., 2018).

1.5 Ventilator Induced Lung Injury

Ventilation strategies such as ARDSnet among others (Briel et al., 2010; Brower et al., 2004, 2000; Deans et al., 2005; Major et al., 2018; Meade, Cook, Griffith, et al., 2008; Mercat et al., 2008; Nieman et al., 2017; Slutsky & Ranieri, 2000) tend to follow a set generalised protocol and are not patient-specific. However, as acute respiratory failure is a secondary outcome of a range of diseases, applied MV will have very different pressure-flow outcomes in different patients for the same ventilator settings. Sub-optimal settings can lead to several types of VILI (M. Amato et al., 1998; Brower et al.,

2000; Hodgson et al., 2011; Meade, Cook, Griffith, et al., 2008; Slutsky & Tremblay, 1998; Valentini, Aquino-Esperanza, Bonelli, & Maskin, 2014), including alveolar-capillary lesions, alterations in permeability, oedema, and others, all of which hinder recovery and thus increase the length and cost of MV (M. Amato et al., 1998). Hence, intra- and inter-patient heterogeneity and variability over time makes it difficult to select ventilator settings to optimise oxygenation and gas exchange, while minimising VILI (Garcia et al., 2006).

The mechanics of, and strategies for, preventing VILI are contentious (Major et al., 2018). Historically, it has been assumed VILI is caused by either excessive global pressure (barotrauma) or excessive volume (volutrauma) in a ventilation mode dependent manner. For example, in Pressure Controlled Ventilation (PCV), pressure is the controlled variable and volume delivered is dependent on lung elastance, thus volutrauma is the risk. The converse is true for Volume Controlled Ventilation (VCV), where volume delivery is the controlled variable, and dependent pressure makes barotrauma a possible outcome. However, such an approach is potentially over-simplified, and the mechanics of VILI are likely much more complex and patient- and/or breath-specific. Studies have recommended both inspiratory plateau pressure and tidal volume should be limited as both barotrauma and volutrauma can occur within a given ventilation mode (Hager, Krishnan, Hayden, & Brower, 2005).

More recent research has cast light on mechanisms of injury and strategies for mitigation of VILI. Dreyfuss and Saumon (Dreyfuss & Saumon, 1998) postulated alveolar strain due to the transpulmonary pressure gradient could cause injury (Nieman et al., 2018), which was later confirmed (Mols, Priebe, & Guttmann, 2006). In addition, closed alveoli can be subjected to very high levels of shear stress when exposed to the same pressures as adjacent open healthy alveoli (Mols et al., 2006). Excessive shear stress can be mitigated using lung protective strategies (M. Amato et al., 1998; Brower et al., 2000; Donahoe, 2011; Laufer et al., 2017; Meade, Cook, Griffith, et al., 2008; Petrucci &

De Feo, 2013; Pintado et al., 2013; Sundaresan & Chase, 2012), such as the use of lower tidal volumes, personalised PEEP, and moderating driving pressure (M. B. Amato et al., 2015; Brower et al., 2004, 2000; Futier et al., 2013; Girard & Bernard, 2007; Iglesias et al., 2008; Jobe, 2009; Meade, Cook, Griffith, et al., 2008; Mercat et al., 2008; Nieman et al., 2018; Petrucci & De Feo, 2013; Zick et al., 2013).

1.6 Lung protective strategies and recruitment manoeuvres

Lung protective strategies have improved patient outcomes by reducing VILI and improving oxygenation (M. Amato et al., 1998). This improvement has, in turn, resulted in reduced time on MV and thus a reduced ICU cost (Dasta et al., 2005). Recruitment manoeuvres (RM) when performed safely can also be an effective way of increasing and maintaining alveolar recruitment (Bates & Irvin, 2002; Dyhr, Laursen, & Larsson, 2002; Gattinoni, Carlesso, Brazzi, & Caironi, 2010; Hess, 2015; Spieth & Gama de Abreu, 2012). However, if performed poorly, RMs can expose patients to an increased risk of lung injury due to heterogeneity in lung and patient condition, and their response to care.

To avoid injury and enhance recovery, recruitment of closed lung alveoli is desirable. Alveoli may collapse due to disease or injury (Mols et al., 2006), and recruitment is often achieved by applying tidal volume (Crotti et al., 2001) and PEEP to prevent derecruitment during expiration (Kacmarek et al., 2016). Alveoli have threshold opening pressures, which are typically higher than their threshold closing pressures (Sundaresan et al., 2009; Yuta, 2007). Titration of PEEP through a staircase RMs can open closed alveoli, improving arterial oxygenation (Brower et al., 2004) and help clinicians determine the lowest PEEP needed to ensure sustained ventilation of recruited lung (Kacmarek et al., 2016).

Optimal PEEP is used to prevent the repetitive opening and closing of injured alveoli, which causes atelectrauma (M. Amato et al., 1998; Briel et al., 2010; Cavalcanti et al., 2017; Crotti et al., 2001; Gong, Krueger-Ziolek, Moeller, Schullcke, & Zhao, 2015; Jandre et al., 2008; Jobe, 2009; Kacmarek et al., 2016; Meade, Cook, Griffith, et al., 2008; Mercat et al., 2008; Mols et al., 2006; Nieman et al., 2017; Pintado et al., 2013). Evidence suggests titrating PEEP to the point of minimum elastance (maximum compliance), which is found using a staircase recruitment manoeuvre (RM), could improve patient outcomes (M. B. Amato et al., 2015; Carvalho et al., 2007; Chiew, Pretty, Shaw, et al., 2015; Lambermont et al., 2008; Pintado et al., 2013). In this manner, the minimum elastance strategy maximises recruitment, while minimising the risk of volutrauma or barotrauma.

In a staircase RM carried out at the beginning of ventilation, PEEP is typically increased in steps of 2 cmH_2O or 4 cmH_2O until a set limit of plateau pressure (pressure controlled ventilation) or tidal volume (volume controlled ventilation) is reached. It is then stepped down to the initial PEEP level. A first RM can be used to recruit collapsed alveoli, while maintaining recruitment of those already open. The process can be immediately repeated to titrate PEEP and determine the PEEP level where minimum elastance is achieved (Pintado et al., 2013). After this second RM is completed, a new PEEP setting can be selected (Chiew, Pretty, Shaw, et al., 2015).

The optimal RM pressure range is contentious (Cavalcanti et al., 2017; Hodgson et al., 2011; Mercat et al., 2008), as the higher pressures in a RM carry risk of barotrauma or volutrauma, where short exposures to damaging MV may reverse any improvements in patient state (Carvalho et al., 2007; Cavalcanti et al., 2017; Hodgson et al., 2011; Suarez-Sipmann et al., 2007). Thus, forward prediction of lung mechanics throughout a staircase RM would allow clinicians to manage the trade-off between the risk of barotrauma and volutrauma caused by the increased pressures and/or volumes in the RM, while maximising the benefit of additional lung volume being recruited. Such an approach would enable safer RM application with greater insight into desired outcomes and po-

tential risks.

Increases in PEEP throughout an RM also results in additional lung volume (V_{frc}) due to alveolar recruitment (Dellamonica et al., 2011; Morton, Knopp, Docherty, Shaw, & Chase, 2018; van Drunen, Chase, Chiew, Shaw, & Desaive, 2013; Wallet et al., 2013). Determining V_{frc}, is often invasive, or requires imaging (Computed Tomography (CT) or Electrical Impedance Tomography (EIT)) that either cannot be carried out at the bedside (Chase et al., 2014; van Drunen, Chase, et al., 2013) or is not available in every care unit. Model-based predictions of V_{frc} across each RM step could aid PEEP optimisation, and minimise the risk of unintended volutrauma. Potentially, PEEP could even be titrated based on V_{frc}, as this recruited additional lung volume is the direct goal of applying PEEP.

Due to the nature of respiratory disease (Albert et al., 2009; Bates & Irvin, 2002; Ma & Bates, 2010; Marini, 1994), alveoli opened by an RM can collapse despite optimal PEEP settings. Therefore, multiple RMs can be required during a full course of MV (Morton, Dickson, Chase, Docherty, Howe, et al., 2018b; Stahl et al., 2006) to re-open collapsed alveoli and sustain oxygenation, along with providing a means of monitoring V_{frc} (Chiew, Pretty, Shaw, et al., 2015; van Drunen, Chase, et al., 2013). These RMs can often involve a clinician carrying out single or a few steps up and down in PEEP. Development of a predictive model of lung mechanics would allow this process to be optimised and automated, including monitoring of patient-specific condition and regularly optimising PEEP as patient condition evolves, which would in turn reduce clinical load and potentially improve outcomes via personalised care (Morton, Dickson, Chase, Docherty, Howe, et al., 2018b).

Overall, MV is an important and widely used ICU therapy. Currently, most MV protocols are generalised and fail to address the heterogeneity of MV patients. Tailoring MV to patient condition is thus currently reactive, ad hoc, and variable in application. To avoid VILI, ventilator settings need to be optimised to individual patient-specific lung

mechanics, and the evolving condition. Thus, there is a need for greater personalisation of MV. Model-based methods are ideally suited to meet these needs. Current model based methods are covered in Chapter 3.

1.7 Necessity of virtual patients

Virtual patients can be developed to model the responses one may expect from an individual, or a cohort-wide scale (Chase et al., 2016, 2018). Virtual patients are used to personalise and optimise care for an individual patient by predicting response to a change in treatment prior to implementing the change. This personalisation is especially critical for ICU patients, who exhibit a great deal of variation in condition, and response to treatment (J. L. Dickson, Gunn, & Chase, 2014). As noted, for intubated patients, personalisation would be used to predict the effects of an RM on lung elastance to minimise the risk of VILI while also maximising lung recruitment, and thus, oxygenation.

Virtual cohorts offer a method of safely and efficiently validating the effect that testing new treatments can have on a population of patients (Chase et al., 2016). A validated in-silico virtual trial platform could reduce the number of Phase II and III human trials (Chase et al., 2018). It would thus be a substantial development in mechanical ventilation, as two of the main metrics for judging an improvement in treatment across a cohort (length of mechanical ventilation (LoMV) and Ventilator Free Days (VFD) Schoenfeld and Bernard (2002)) are both highly skewed (Morton, Chiew, et al., 2017). This skew requires a large number of patients in a given clinical trial to reach statistical power ((Morton, Chiew, et al., 2017). Capitalising on the recent FDA change to recognising virtual trials (Smalley, 2018) as a method of testing medical treatments, having virtual cohorts to test new mechanical ventilation protocols would allow the field to move forward much faster.

CHAPTER 2

Non-Parametric Sample Size Estimation for Mechanical Ventilation Trials

2.1 Introduction

While it is a relatively straightforward treatment, optimising mechanical ventilation without causing damage to the lung is complex in practice (Major et al., 2018; Sundaresan & Chase, 2012). A range of randomised control trials (RCT) have been carried out to assess methods of improving MV care (Major et al., 2018). However, many have had non-significant findings, and the field remains uninformed about consistent action that might improve outcomes (Brower et al., 2004, 2000; Meade, Cook, Griffith, et al., 2008; Mercat et al., 2008). Aside from the efficacy of the proposed treatment intervention, the outcome metrics and sample sizes of the trial can significantly affect the resulting outcome statistical significance. All these factors thus impact trial design (Bhardwaj, Camacho, Derrow, Fleischer, & Feldman, 2004; Schoenfeld & Bernard, 2002).

Because respiratory failure is often a secondary symptom from a range of diseases, many causing lung damage that is mixed in effect and severity (Breen et al., 2002), the generalised *"one size fits all"* treatment proposed in some RCTs may not provide the best possible treatment for all patient types (Chase et al., 2018). In addition, non-significant RCT results may also be partly due to difficulty in determining the efficacy of mechanical ventilation therapy. Aside from patient mortality, other metrics used to assess the quality of mechanical ventilation treatment include cardiopulmonary and haemodynamic responses, patient physiological or acuity scores, and patient ventilator dependency, such as length of mechanical ventilation (LoMV) and Ventilator Free Days (VFD) (Schoenfeld & Bernard, 2002). However, all these metrics have limitations.

To ensure a study has a sufficiently high sample size for statistically significant results, it must have enough power, along with a significance greater than a pre-determined threshold (Motulsky, 1995). Statistical significance is a measure of the chance that the observed results could be caused by random chance. However, the power of a study is the probability that a test of significance will pick up on an effect that is present. Alternatively, this is defined as the probability of avoiding a Type II statistical error: when the null hypothesis is false, but erroneously fails to be rejected. Low power is often caused by a sample size that is too small to accurately detect a difference in outcomes between two groups. A study carried out by Moher et al (Moher, Dulberg, & Wells, 1994) reviewed 383 RCTs. They found that of 102 null trials in this study, only 36% had 80% power to detect a difference of 50% in outcome between each group. Only 16% had 80% power to detect a more probable difference of 25% Moher et al (Moher et al., 1994; Whitley & Ball, 2002). Only 32% of the null trials investigated stated the sample size of the study in the results (Whitley & Ball, 2002).

However, having a study with a sample size that is too large can not only require an excessive amount of resources, but may also be unethical due to requiring a larger than necessary number of participants to receive placebo, control, or otherwise inferior

treatment (Whitley & Ball, 2002). Determining the optimal sample size heavily depends on the estimation of the difference in treatment outcome between each group, often dependent on clinical judgment. Hence, the sample sizes determined from statistical methods are intended as approximate guides as opposed to exact numbers (Whitley & Ball, 2002).

LoMV or VFD are the two most common metrics used to assess MV efficacy in many trials, describing patient ventilator dependency and weaning, along with the mortality rate for the cohort (Schoenfeld & Bernard, 2002). They also assess the economic impact, as ventilator dependency is associated with a higher cost (Dasta et al., 2005). For a clinical trial to be successful, it must have both useful results and statistical significance (Bhardwaj et al., 2004). Table 2.1 shows a range of mechanical ventilation RCTs that use LoMV or VFD as one of their outcome metrics (M. B. Amato et al., 2015; Brower et al., 2004, 2000; Hodgson et al., 2011; Meade, Cook, Griffith, et al., 2008; Mercat et al., 2008; Pintado et al., 2013). These studies ranged in size from 70–2300 patients, with only 3 able to reach statistical significance of $p < 0.05$. When clinical significance was not found, it was often due to ineffective treatment or inability to effectively treat all patients. However, high levels of patient variability, as well as insufficient sample sizes, can significantly impact the ability of a clinical study to achieve significance (Altman & Bland, 1995; Van Der Lee, Tanck, Wesseling, & Offringa, 2009).

In an earlier study by Chiew et al. (Chiew, Pretty, Moltchanova, et al., 2015), it was noted the commonly used sample size estimation methods for a powered study (Petrie, Bulman, & Osborn, 2002), such as the Altman Nomogram, were not feasible for LoMV clinical data that were heavily skewed with a very long upper tail (Bland & Altman, 1986). Thus, it is not possible to truly assess whether trial design or sample size, or trial inefficacy are the cause of failure to achieve statistical significance. Hence, a simulation-based method using retrospective clinical cohort data may provide a better, much more precise, estimation of a well-powered sample size for a desired outcome metric and pa-

tient cohort (Richardson, 2003).

Table 2.1: Summary of several randomised control trials assessing LoMV and VFD. Where **[1]:** (Brower et al., 2000), **[2]:** (Brower et al., 2004), **[3]:** (Mercat et al., 2008), **[4]:** (Meade, Cook, Arabi, et al., 2008), **[5]:** (Blum et al., 2015), **[6]:** (Pintado et al., 2013)

Study Name	**Metric Used**	**Total Number of Patients in Study**	**Groups LoMV or VFD (mean ± SD or median [IQR])**		**p-value achieved**
ARDSNet [1]	VFD	861	Low Tidal Volume 12±11	High Tidal Volume 10±11	0.0070
ALVEOLI [2]	VFD	549	Lower PEEP 14.5±10.4	Higher PEEP 13.8±10.6	0.5000
EXPRESS [3]	VFD	767	Minimal distension 3 [0-17]	Increased recruitment 7 [0-19]	0.0400
LOVS [4]	LoMV	982	Control 10 [6-16]	Lung open 10 [6-17]	0.9200
Meta-Analysis [5]	VFD	2299	Lower PEEP 11 [0-21]	Higher PEEP 13 [0-22]	0.1000
Individualised PEEP [6]	VFD	70	Control 0 [0-15.75]	Intervention 1 [0-18]	0.1600

This chapter presents a Monte-Carlo simulation-based method to estimate sample sizes for a powered and significant RCT for a range of outcome metrics relating to ventilator dependency. The outcome metrics investigated in this study were LoMV, VFD, and a modified LoMV. A case study for determining the sample sizes of a planned RCT is also presented, where patient selection criteria are simulated to replicate the planned RCT as closely as possible (Gastañaga, McLaren, & Delfino, 2006). Overall, this non-parametric simulation based method is readily generalisable for trial design.

2.2 Methods

Monte-Carlo simulations are used to assess the sample size required for 80% power and a p-value less than a specified significance value in the case of interventions causing specified outcome differences in the underlying population. Two populations from which trial participants may be drawn are examined:

- Cohort A is all MV patients and covers the case where no additional exclusion criteria are applied.

- Cohort B is drawn from Cohort A with exclusion criteria applied.

This analysis thus examines the effect of inclusion criteria , statistical test, and sample size on statistical power for an interventional trial, while directly using the true underlying distribution of patient clinical data.

2.2.1 Sample size analysis metric

Three outcome metrics for sample size estimation were investigated:

- Length of mechanical ventilation (LoMV)
- Ventilator Free Days (VFD) (Schoenfeld & Bernard, 2002)
- Length of mechanical ventilation within 28 days (length of mechanical ventilation within 28 days (LoMV_{28})).

VFD and LoMV_{28} are modified LoMV distributions that also include mortality information where deceased patients have 0 VFD or 28 days of LoMV. Table 2.2 shows a more detailed description of each outcome metric used in this study.

Table 2.2: Outcomes metrics used in analysis

Outcome Metric	Description
LoMV	The total duration of mechanical ventilation.
LoMV_{28}	Length of MV within 28 days, where: • LoMV_{28} = 28: if the patient dies before 28 days • LoMV_{28} = LoMV: if the patient is successfully weaned from MV within 28 days • LoMV_{28} = 28: if the patients required MV for 28 days or more.
VFD	The number of days free of MV within a 28 day period. VFD is defined by Schoenfeld and Bernard (2002) as • VFD = 0 if the patient dies before 28 days • VFD = (28 – LoMV) if the patient is successfully weaned from MV within 28 days. • VFD = 0 if the patients requires MV for 28 days or more

2.2.2 Retrospective patient cohort data (Cohort A)

Retrospective data from 5176 patients admitted to the Christchurch Hospital Intensive Care Unit (ICU) from 2011 to 2014 was considered in this study. All APACHE III diagnostic codes, ICU mortality and length of mechanical ventilation (LoMV) were recorded. Of this number, 3896 (75%) patients required MV therapy and 3383 (63%) received invasive ventilation either through tracheotomy or intubation. The breakdown of the LoMV of these patients is shown in Figure 2.1. A breakdown of patient numbers for each year studied is shown in Table 2.3.

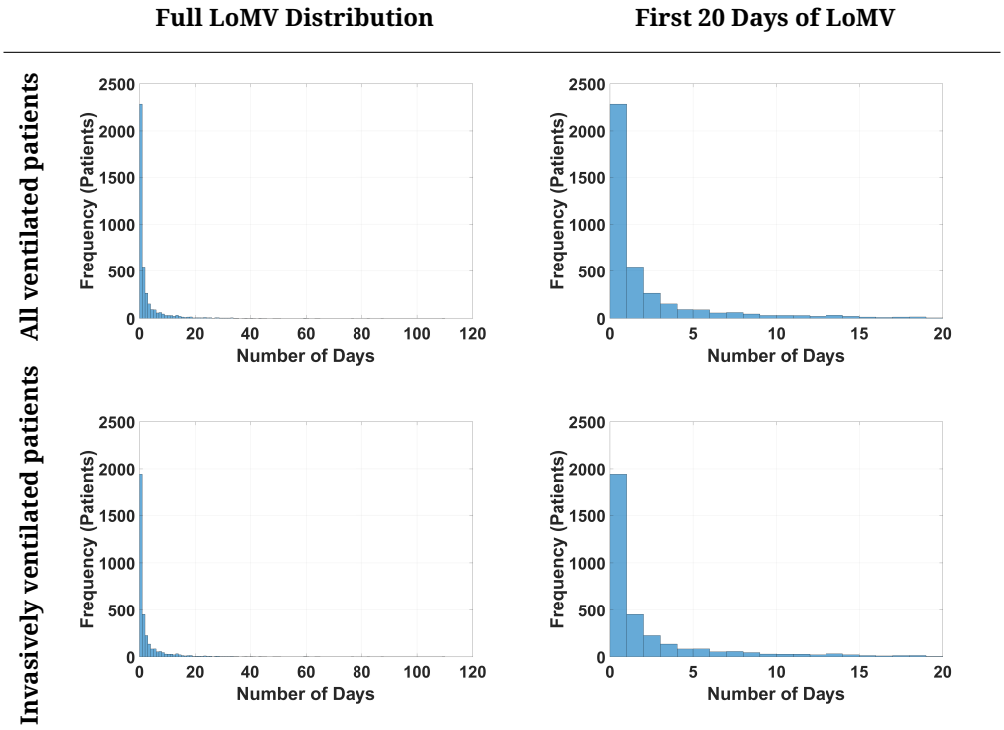

Figure 2.1: LoMV distribution of cohorts studied. The histograms on the left show the entirety of the distribution including outliers of 110 days LoMV, while those on the right truncate the data at a maximum LoMV of 20 days for clarity.

Table 2.3: Patient number and distribution

Cohort	**Number of Patients**				
	2011	**2012**	**2013**	**2014**	**Total**
All ICU Patients	1279	1284	1344	1269	5176
All Ventilated Patients	1004	953	963	977	3897
Invasively Ventilated Patients	878	825	830	850	3383

In this study, only patients who were invasively ventilated are considered, which thus comprises the largest possible cohort for an MV trial focussing on ETT ventilation, and is delineated Cohort A in this study. The median[IQR] LoMV was 0.73 [0.24 - 2.48] (mean = 2.95 ± 6.50 days) . The detailed patient distribution for this cohort and their corresponding LoMV and mortality distribution can be found in Tables 2.4, 2.5 and 2.6.

Table 2.4: Patient LoMV Distribution (Mean ± SD)

Cohort	**LoMV (Days) (Mean ± SD)**				
	2011	**2012**	**2013**	**2014**	**Total**
All Ventilated Patients	2.54±6.12	2.90±6.61	2.98±6.49	2.88±6.16	2.82±6.34
Invasively Ventilated Patients	2.66±6.38	3.06±6.92	3.24±6.86	2.88±5.79	2.95±6.50

Table 2.5: Patient LoMV Distribution (Median [IQR])

Cohort	**LoMV (Days) (Median [IQR])**				
	2011	**2012**	**2013**	**2014**	**Total**
All Ventilated Patients	0.62 [0.24-1.91]	0.73 [0.25-2.20]	0.79 [0.24-2.48]	0.83 [0.31-2.76]	0.74 [0.25-2.29]
Invasively Ventilated Patients	0.62 [0.24-1.94]	0.72 [0.24-2.32	0.81 [0.24-2.75]	0.80 [0.26-2.70]	0.73 [0.24-2.48]

Table 2.6: ICU Mortality Distribution

Cohort	**ICU Mortality Rate (%)**				
	2011	**2012**	**2013**	**2014**	**Total**
All ICU Patients	8.68%	11.99%	8.93%	10.48%	10.01%
All Ventilated Patients	10.66%	15.22%	11.84%	12.59%	12.55%
Invasively Ventilated Patients	11.85%	16.12%	12.65%	13.53%	13.51%

2.2.3 Simulating realistic clinical trial cohorts (Cohort B)

Not all invasively ventilated patients may benefit from optimised MV. For example, some patient groups receive MV only for brief post-surgical periods, and thus usually would not be part of such a trial. One major difficulty is exclusion criteria in many trials are subjective and thus can add unintended variability, bias and/or dimensionality to the study, affecting the potential outcome in ways not included in the study design.

Using Monte-Carlo simulation, an objective patient cohort can be created and simulated from Cohort A. This objective cohort (Cohort B) aims to capture the realistic character-

istics of a patient cohort expected to be used in a planned clinical trial. In particular, using quantifiable exclusion criteria.

Objective patient selection is enabled using the APACHE III diagnostic code to simulate the actual clinical trial inclusion and exclusion criteria. Many of these criteria have been used in prior studies (Brower et al., 2004, 2000; Hodgson et al., 2011; Meade, Cook, Arabi, et al., 2008; Mercat et al., 2008; Pintado et al., 2013). Objective, explicit criteria for all exclusions would ensure a more robust design and implementation.

The exclusion criteria typically used are listed below and the studies they are used in are referenced. These criteria include:

1. Patients who are likely to be discontinued from MV within 24 hours (Pintado et al., 2013; Strøm, Martinussen, & Toft, 2010)
2. Patients with raised intracranial pressure (Brower et al., 2004, 2000; Hodgson et al., 2011; Meade, Cook, Arabi, et al., 2008; Mercat et al., 2008; Pintado et al., 2013; Strøm et al., 2010)
3. Patients who have significant weakness from any neurological disease (Brower et al., 2004, 2000; Meade, Cook, Arabi, et al., 2008; Mercat et al., 2008; Pintado et al., 2013)
4. Patients who have asthma as the primary presenting condition, or a history of significant chronic obstructive pulmonary disease (Brower et al., 2004, 2000; Meade, Cook, Arabi, et al., 2008; Mercat et al., 2008)

In this study, a sample of clinical inclusion and exclusion criteria for a randomised controlled trial is used (ANZCTR number: ACTRN12614001069640). Inclusion criteria are set to target every patient that is eligible for the study (Cohort A). The exclusion criteria are chosen based on the clinical implication these patients may not benefit from a MV intervention, or could be harmed in some cases – as listed above.

In this study, the objective cohort (Cohort B) was established by excluding all patients under APACHE III diagnostic codes as shown in Appendix Table A.12, which are rele-

vant to the 4 main criteria typically used and listed above. The use of diagnostic codes also avoids subjective choices in both simulation and implementation, where such subjectivity is difficult to model and induces unintended variability from what might actually occur. It could also be easily and objectively implemented in a real trial, which would better ensure that the trial design and the actual study matched. Thus, the following specific APACHE III diagnostic codes were also excluded in implementing the typical exclusion criteria listed previously:

- 206 – Chronic obstructive pulmonary disease
- 209 –Asthma
- 400 – Neurological non-operative
- 601 –Head trauma with or without multi trauma
- 604 –Multi trauma with spinal injury
- 605 – Isolated cervical spine injury
- 1500 – Neurological post-operative
- 1601 –Post operation patients: head trauma with or without multi-trauma.
- 1604 –Post operation patients: Multi trauma with spinal injury.
- 1605 –Post operation patients: isolated cervical spine injury.

This approach makes the criteria objective and easy to implement both in simulation and in a clinical trial. After imposing the exclusion criteria, the number of patients eligible for the study is reduced from 5176 to 974 (18.8% of total patients admitted to ICU or 28.8% of patients requiring invasive MV), and is denoted as Cohort B. A more detailed comparison of the actual trial exclusion criteria and simulation method is shown in Table 2.7.

2.2.4 Sample size determination using Monte-Carlo simulation

A Monte-Carlo simulation was performed to determine the power of the study at a range of sample sizes. This simulation allows a range of intervention effect sizes to be simulated, and the corresponding sample sizes required to detect the significance at a power, to be calculated. The patients were separated into two cohorts of increasing sample

Table 2.7: Exclusion criteria used in clinical trial, and in simulation

Inclusion Criteria	
Actual clinical protocol	**Simulation method**
Patients requiring invasive MV Patients with PaO_2/FiO_2 ratio $<$300 mmHg Arterial line in situ.	Patients requiring invasive MV
Exclusion Criteria	
Patients who are likely to be discontinued from MV within 24 hours.	Exclude patient with LoMV $<$1 days.
Patients with age $<$16 years.	Exclude patient with age $<$16 years.
Any medical condition associated with a clinical suspicion of raised intracranial pressure and/or a measured intracranial pressure $<$20 cmH2O.	Exclude patient with head trauma using APACHE III diagnostic Code: • 601 - Head trauma with or without multi-trauma • 1601 - Post operation patients: head trauma with or without multi-trauma
Patients who have a high spinal cord injury with loss of motor function and/or have significant weakness from any neurological disease.	Exclude patient using APACHE III diagnostic Code: • 400 - Neurological non-operative • 604 - Multi trauma with spinal injury • 605 - Isolated cervical spine injury • 1500 - Post-operative: Neurological patients • 1604 - Post-operation patients: Multi-trauma with spinal injury • 1605 - Post operation patients: isolated cervical spine injury
Patients who have a barotrauma (pneumothorax, pneumomediastinum, subcutaneous emphysema or any intercostal catheter for the treatment of air leak).	No action performed
Patients who have asthma as the primary presenting condition or a history of significant COPD disease.	Exclude APACHE III diagnostic code: • 206 - COPD • 209 - Asthma
Patients who are moribund and/or not expected to survive for $>$72 hours.	No action performed
Patients who have already received MV for $>$48 hours (including time spent ventilated in a referring unit).	No action performed
Lack of clinical equipoise by intensive care unit (ICU) medical staff managing the patient.	No action performed

sizes from 100:10:2000. This was done using the datasample function in MATLAB. Randomly selected patients were selected (from a uniform distribution), with replacement

from the dataset. Replacement was used to allow the 2000/arm sample sizes to be analysed.

The intervention effects of a 10%, 15%, 20%, and 25% reduction in LoMV were implemented in the randomly selected intervention arm. The LoMV of the entire group was reduced by the specified percentage reduction. A 10,000 iteration Monte-Carlo simulation was run over the data to determine the required sample size for each trial arm to achieve 80% power. In this study, the sample sizes for Cohort A and Cohort B were examined. All simulations were performed using MATLAB.

The hierarchical steps followed to carry out the Monte-Carlo design analysis are outlined in Table 2.8. Both double-sided and single-sided (lognormal) T-Test, Wilcoxon-Ranksum Test (WR-Test) and a Kolmogorov-Smirnov Test (KS-Test) were used for significance testing of the difference in mean and other distribution characteristics (median and variability). The change into VFD and $LoMV_{28}$ metrics is carried out after the LoMV difference has been imposed on the intervention group (Step 3) and before the statistical testing (Step 4).

Table 2.8: Steps followed in Monte Carlo Simulation

	Step	Description	Tested Group
1.	**Patient Cohorts**	Select a patient cohort 1. Cohort A includes all invasively ventilated patients 2. Cohort B is created from Cohort A by imposing exclusion criteria	• Cohort A • Cohort B
2.	**Sample Size Estimation**	1. Randomly select patients from the patient cohort and assign each patients to a treatment group. 1) Control group or 2) Intervention group. 2. Patient is selected with replacement. 3. Various sample size of each treatment group is tested.	Total sample size N= 100, 110, 120… 2000 patients
3.	**Difference in LoMV**	1. Impose an intervention effect to simulate differences in LoMV between the two groups. 2. The LoMV in Intervention group is reduced by the chosen percentage. 3. LoMV intervention = LoMV patient × (100% -Percentage reduction) 4. The difference in LoMV ranges from 10 to 25% of total LoMV.	Difference of LoMV = 10%, 15%, 20%, 25%
4.	**Metric Conversion**	Calculation of VFD and LoMV-28 using given LoMV.	• Cohort A
5.	**Statistical Test**	1. Perform statistical test comparing the metrics (LoMV, VFD or LoMV-28) between two groups. 2. Using parametric and non-parametric tests. 3. A p-value < 0.05 indicates that LoMV for the intervention group is significantly different from control group	1. (lognormal) T-Test 2. WR-Test 3. KS-Test
6.	**Power Analysis**	1. Each Monte-Carlo simulation iteration will generate a p-value for each statistical test. 2. For a given sample size and significance level α, statistical power is evaluated as the proportion of iterations for which p $< \alpha$.	E.g. for 10000 Monte-Carlo iterations, if p $< \alpha$ for 84% (8400 iterations), Power = 0.84.

2.2.5 Baseline characteristics of each outcome metric

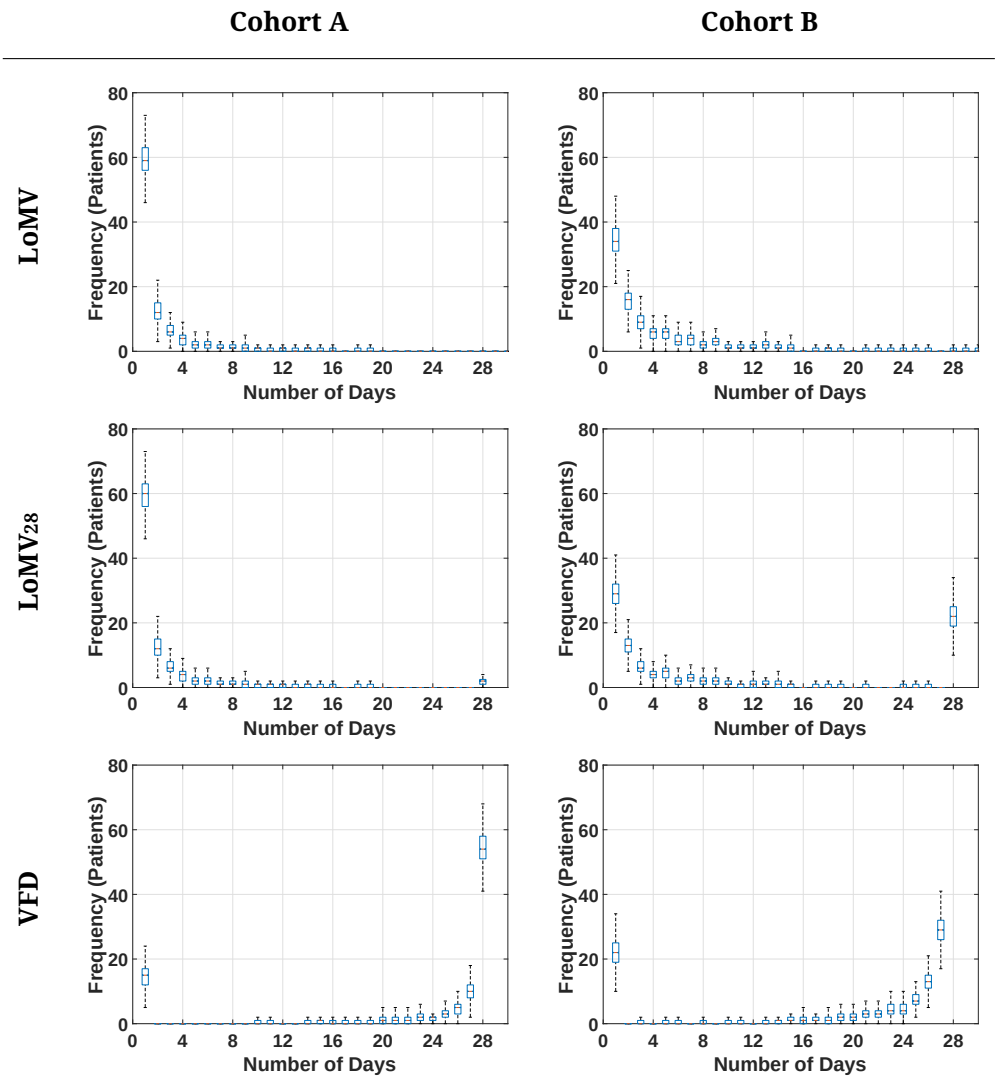

Figure 2.2: Outcome metric distributions for sample size of 100 patients.

Figure 2.2 shows a distribution of the LOMV, VFD and LoMV$_{28}$ distribution for 10,000 cohorts of 100 patients selected from Cohort A and Cohort B prior to implementing an intervention effect. Patient selection was iterated 10,000 times using random selection with replacement (Table 2.8, Step 2) to create the boxplots. As can be seen, both the LoMV and LoMV$_{28}$ cohorts have significantly skewed log-normal distributions, whereas VFD shows a reverse log-normal distribution that is highly skewed towards 28 days.

The distribution spikes at the start of the VFD, and end of the LoMV$_{28}$ plots are due

to the impact of mortality data on these metrics. This feature clearly shows how any change in mortality due to an intervention can have a further significant effect on the distribution shape. Finally, the LoMV$_{28}$ and VFD metrics are also not lognormal given these spikes, which could cause further issues when using a trial design method based on a normal distribution assumption, even if the data was logged first (Bland & Altman, 1986). Consequently, use of sample size estimation methods that require a Gaussian distribution, which is the common approach, would not have been appropriate for these outcome metrics (Chiew, Pretty, Moltchanova, et al., 2015; Petrie et al., 2002). Consequently, non-parametric statistics and Monte-Carlo analysis, as proposed, should provide a more accurate solution. These analyses will thus also show the impact of these choices.

2.2.6 Statistical Comparisons

The (lognormal) T-Test, KS-Test and WR-Test are common test for establishing differences between populations. The (lognormal) T-Test is gaussian, but is often used with logged data to establish greater normality. The KS-Test and WR-Test are both non-parametric. Each cohort size for N = 100-2000 with a 10 patient step size is analysed as follows:

Analysis 1. Sample size estimation for each cohort.

- **Cohorts Studied:** Cohort A, Cohort B
- **Outcome Metrics:** LoMV, VFD, LoMV$_{28}$.

Intervention arms for a defined outcome difference (10-25% difference in LoMV in steps of 5%). Analysis 1 uses a two-tailed test to assess what impact the trial exclusion criteria has on the sample size required to reach 80% power.

Analysis 2. Single vs double-tailed tests

- **Cohorts Studied:** Cohort B
- **Outcome Metrics:** LoMV, VFD, LoMV_{28}.

Two-tailed tests can separate whether the intervention yields a better or worse outcome. A one-tailed test assumes the intervention is better or not better, but cannot show it is worse. A one-tailed test at $p < 0.025$ is considered equivalent to a two-tailed test at $p < 0.05$ (Motulsky, 1995). However, clinically, an intervention that is not better is potentially enough of an answer, as clinicians seek better treatment. Therefore, Analysis 2 also considers the impact of single-tail testing in this approach for Cohort B.

Analysis 3. Impact of mortality differential between control and intervention groups.

- **Cohorts Studied:** Cohort B
- **Outcome Metrics:** VFD, LoMV_{28} metrics.

Finally, both **Analysis 1** and **Analysis 2** assume equivalent mortality as simulated. However, a good intervention might be expected to reduce mortality, which in turn affects VFD and LoMV_{28}. This aspect was also simulated, by randomly selecting patients to have their mortality changed in the intervention cohort, and repeating Analysis #1:

The three fundamental analyses clearly delineate the impact on trial design and trial size, using such nonlinear distributions and metrics, for explicit exclusion criteria in cohort selection **(Analysis #1)**, statistical test used **(Analysis #2)**, and the impact of mortality when using mortality affected metrics **(Analysis #3)**.

2.3 Results

2.3.1 Impact of exclusion criteria on sample size estimation (Analysis #1)

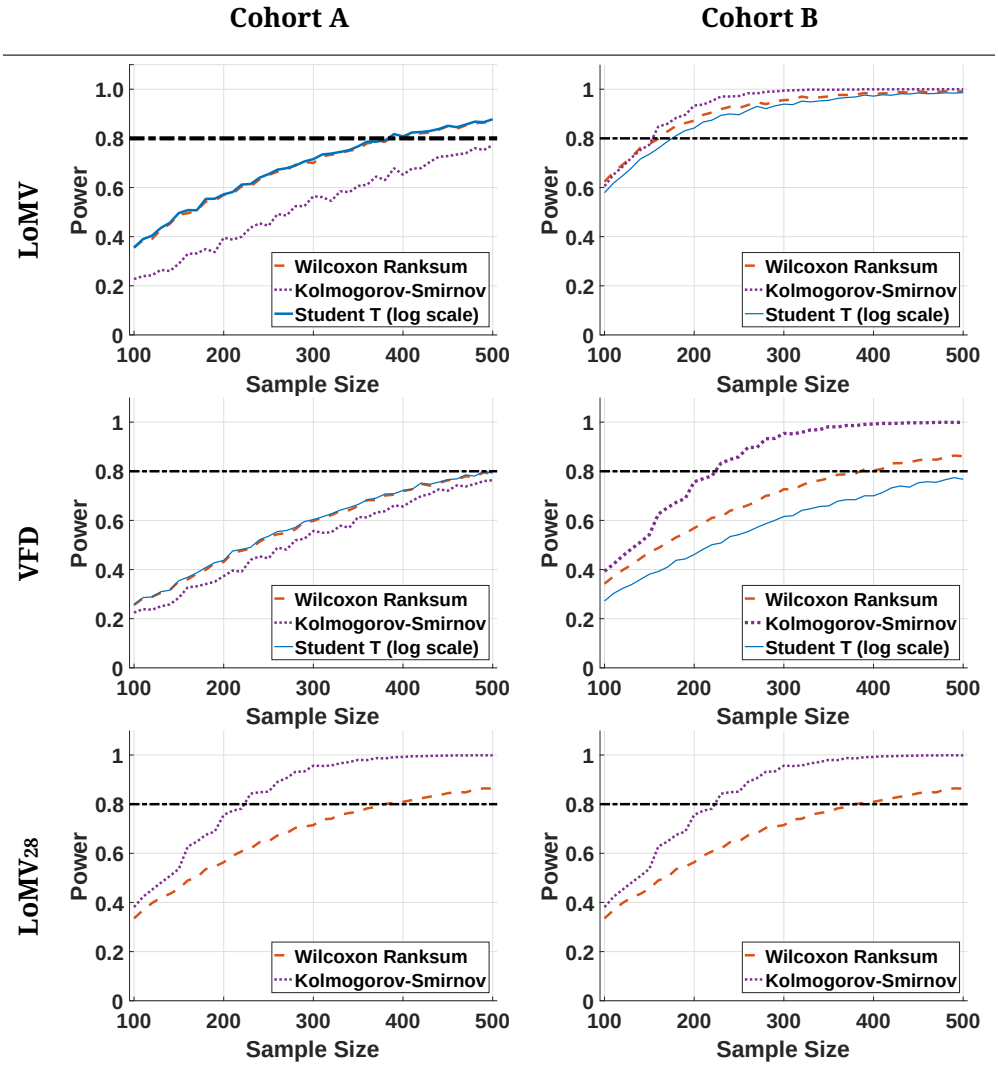

Figure 2.3: Results of Monte Carlo simulation for 25% LoMV difference.

Graphical results for sample size estimation with a 25% difference in LoMV between control and intervention groups are shown in Figure 2.3. The X-axis shows the samples size and the Y-axis shows the corresponding power obtained through the 10,000 iteration Monte-Carlo simulation at each sample size. Cohort A, which included all in-

vasively ventilated patients, had a much lower power compared to Cohort B. Due to the negatively skewed distribution of the VFD metric, as shown in Figure 2.2, a log-transformed student t-test was not suitable for the significance testing. This issue is often not noted in the many trial designs that use VFD, yet it clearly can have a major effect.

The power analysis was carried out for each metric at change in length of mechanical ventilation (△ LoMV) of 10%, 15%, 20% and 25% and the estimated sample sizes per trial arm are shown in Table 2.9. These effect sizes are realistic based on the trials summarised in Table 2.1.

Table 2.9: Estimated sample sizes per trial arm for LoMV outcome metric sizes of 10-25% in 5% increments, for both Cohorts A and B, using all 3 statistical tests.

△LoMV						
	Wilcoxon-Ranksum		**Kolmogorov-Smirnov**		**Student T-Test (log scale)**	
Cohort	**A**	**B**	**A**	**B**	**A**	**B**
10%	2000+	1350	2000+	750	2000+	2000+
15%	1340	530	1530	370	1330	670
20%	670	270	850	240	670	310
25%	400	160	530	160	390	180
△VFD						
	Wilcoxon-Ranksum		**Kolmogorov-Smirnov**		**Student T-Test (log scale)**	
Cohort	**A**	**B**	**A**	**B**	**A**	**B**
10%	2000+	2000+	2000+	850	T-Tests were not able to be used for the VFD metric	
15%	2000+	2000+	1800	500		
20%	1460	700	1030	330		
25%	790	390	650	220		
△LoMV-28						
	Wilcoxon-Ranksum		**Kolmogorov-Smirnov**		**Student T-Test (log scale)**	
Cohort	**A**	**B**	**A**	**B**	**A**	**B**
10%	2000+	2000+	2000+	860	2000+	2000+
15%	2000+	2000+	860	480+	2000+	2000+
20%	700	700	330	330	1160	1160
25%	490	380	510	230	490	540

Transferring the input parameter uncertainties to ranges is achievable. The uncertainty in patient types and which patients might arrive at a given trial period was covered

parametrically by the dimensions N_{cohort}, change in treatment effect (Δ Effect) and a reduced mortality on the VFD and $LoMV_{28}$ metrics, as well as by using 4-years of patient data from the trial centre. Thus, the resulting, Monte-Carlo range of p-values from each Monte-Carlo run yields the power at a significance level of 0.05, as seen in Figure 2.4 and Table 2.9.

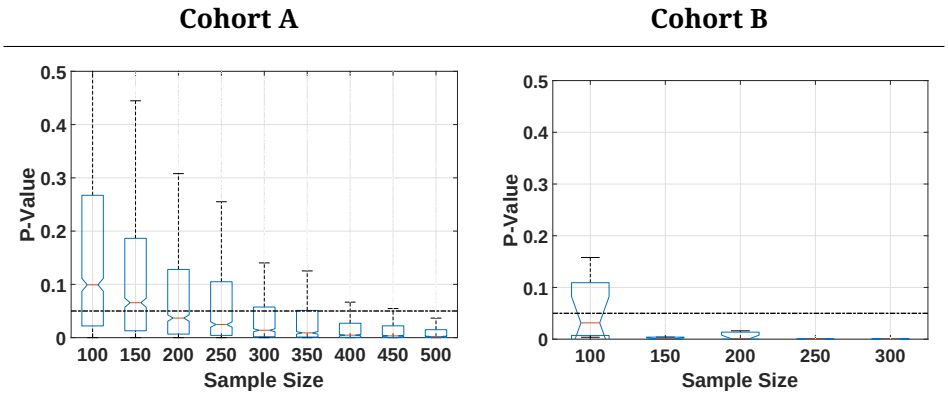

Figure 2.4: Results of each Monte-Carlo simulation for 25% LoMV difference in box and whiskers format for both Cohorts A and B, with p <0.05 shown. The percentage of results below p = 0.05 indicates the power at that sample size.

For clarity, Figure 2.3 demonstrates the ability of this method to also show the range of p-values that dictate whether or not the sample size can achieve a power of 80%. The box and whisker plots show the results from a 25% LoMV difference, as in Figure 2.2, but with the full range of Monte-Carlo run results, where Cohort B has the objective trial exclusion criteria applied.

2.3.2 Single vs double-tailed tests (Analysis #2)

Single (upper) tailed WR-Test and (lognormal) T-Tests were carried out on each metric with a set significant level of α = 0.05 to assess whether this had an impact on the results. At a Δ LoMV of 25%, there is no difference in the required sample size in LoMV and $LoMV_{28}$, as shown in Table 2.10. However, for the VFD metric, a significant reduction of required sample size to achieve 80% power was found.

Table 2.10: Sample size comparison between single-tailed and double-tailed statistical tests for LoMV, LoMV-28 and VFD when the intervention effect is 25% reduction in LoMV

	△ LoMV		△ VFD		△ LoMV-28	
	Single Tailed	**Double Tailed**	**Single Tailed**	**Double Tailed**	**Single Tailed**	**Double Tailed**
WR-Test	160	160	290	390	380	380
KS-Test	160	160	170	230	230	230
(lognormal) T-Test	180	180	N/A	N/A	550	540

2.3.3 Impact of mortality difference (Analysis #3)

Schoenfeld et al. (Schoenfeld & Bernard, 2002) hypothesised using VFD to determine intervention differences would require a much higher sample size than LoMV if there was not a significant difference in mortality rates. To this end, concomitant mortality rate reductions of 5% and 10% were simulated in the intervention cohort for the $LoMV_{28}$ and VFD metrics (Brower et al., 2004). The sample sizes for a 25% LoMV difference and 5 to 10% of mortality rate difference for the WR-Test and KS-Test analyses are shown in Table 2.11, and in Figures 2.5 and 2.6.

Table 2.11: Impact of simulating a mortality differential between control and intervention cohorts for VFD and LoMV-28 outcome metrics.

	No Mortality Difference		**5% Mortality Difference**		**10% Mortality Difference**	
	WR-Test	**KS-Test**	**WR-Test**	**KS-Test**	**WR-Test**	**KS-Test**
$LoMV_{28}$	380	230	190	190	110	140
VFD	280	220	130	130	90	100

As can be seen, the sample size required to reach 80% power is significantly reduced if a mortality differential of 5% occurs between each cohort. Such an improvement is reasonably possible for a targeted cohort receiving better care. To capitalise on these findings, it is recommended that the mortality rate is accounted for at the end of the trial to assess the efficacy of the intervention treatment.

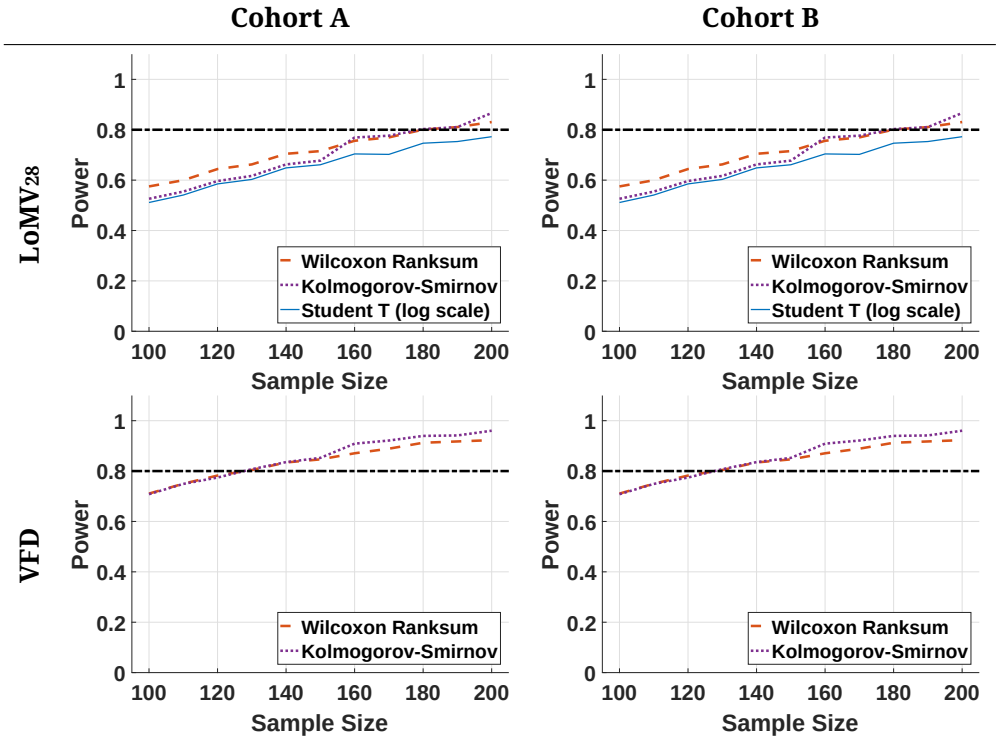

Figure 2.5: Results of Monte Carlo simulation for 25% LoMV difference and a 5% mortality differential.

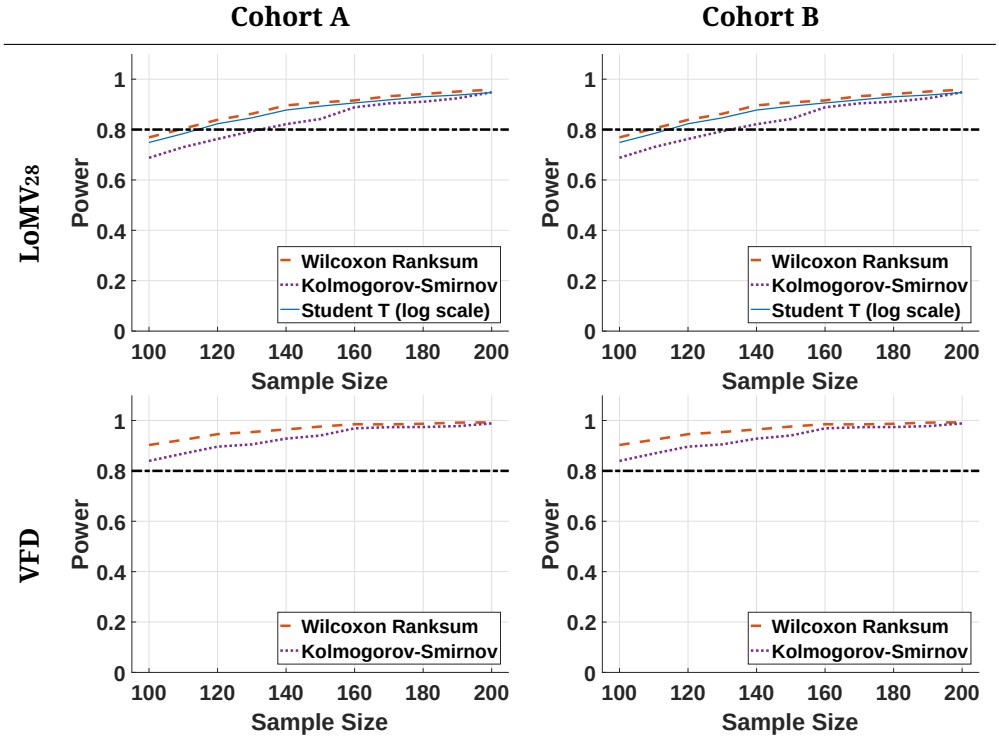

Figure 2.6: Results of Monte Carlo simulation for 25% LoMV difference and a 10% mortality differential.

2.4 Discussion

The Monte-Carlo simulation based design method was able to estimate the sample size required for a clinical trial to detect a significant difference with set power. When the intervention effect is 10%, large sample sizes of more than 2,000 patients per trial arm are required as compared to larger intervention effects, as expected. This larger sample size from the typical design method is due to the skewed and highly variable distribution of ventilation duration of the cohort, and is indicative of the range of patients underlying conditions that require mechanical ventilation. Importantly, these distributions in Figure 2.2 are typical and, more critically, do not match the assumptions made by typical design tools.

When exclusion criteria are implemented in the simulation, the required sample sizes per arm at the same intervention effect, is further reduced. From Figure 2.2, it is clear if Cohort A was considered as the trial cohort, the sample size required for clinical significance and a well-powered study is much higher compared to targeting a specific patient cohort (Cohort B). This result shows targeting a specific cohort through implementing objective and easily defined inclusion and exclusion criteria available at patient admission can result in a narrower metric distribution, which is important. Thus, a clinical trial that aimed to reduce LoMV, or increase VFD, should be designed to target specific patient groups by diagnostic codes who are likely to benefit from the treatment and whose distribution of patient-specific LoMV is amended to seeing a change for reasonable sample size (Chiew, Pretty, Moltchanova, et al., 2015) .

Finally, and importantly, trial sizes also impact patient risk. A trial with equipoise in its hypothesis includes the risk of the intervention possibly having a negative effect on patient outcome. Thus, the fewer the number of patients in the trial design that are needed to achieve significance and power, achieved here with a non-parametric Monte-Carlo simulation design approach, the lesser the risk to patients in determining

the impact and safety of the intervention.

2.4.1 Impact of different outcome metrics and intervention effect

Sample sizes for different outcome metrics were examined in this study. The LoMV metric was found to have the smallest sample size required to achieve significance with 80% power compared to the other 2 metrics. This result was attained with 160 patients required per trial arm for a 25% LoMV reduction difference in Cohort B. However, at a difference of 20% this value increases to 270 patients per arm. Choosing 15% and 10% differences sees a rise to 1,000 patients per arm for an 80% powered study. This finding also shows the perils of these outcome metrics and one possible reason behind non-significant RCTs aside from non-effective clinical interventions. If sample sizes are too small, the probability of not observing a true underlying difference increases. If a large intervention effect, which is difficult to achieve, cannot be obtained trial sizes grow rapidly along with the likelihood of other risks to the trial.

Both the VFD and LoMV_{28} outcome metrics were studied with the hypothesis that the inclusion of mortality would affect the power of the study. The VFD metric was specifically designed with the intention that a new treatment that either reduced the length of ventilation, or mortality, would be more likely to show a significant difference in a trial (Schoenfeld & Bernard, 2002). However, this simulation does not include any changes in mortality and thus the effect is minimal and both metrics have led to a lower powered study than the standard LoMV outcome. It is expected the discrepancy in the t-test results for the LoMV_{28} metric is due to the change in distribution shape due to the peak at 28 days. This issue obstructs the ability of the typically used statistical testing method to detect a significant difference.

2.4.2 Impact of different statistical tests

Incorrect assumptions about the distribution of data can result in an inconclusive and under-powered study (Van Der Lee et al., 2009). A two sample unpaired t-test requires

data with a Gaussian distribution. The log-normal distribution of the LoMV and $LoMV_{28}$ allowed a (lognormal) T-Test to be carried out on the data. This distribution shape was verified by the similar results from the WR-Test analysis. The negatively skewed VFD metric did not meet the Gaussian distribution assumption for a t-test, even when log-transformed, showing its significant limitations when used in typical trial design.

The impact of using a single-tailed test with a significance level of 0.025 was assessed for the LoMV and $LoMV_{28}$ outcome metrics and found to be minimal. However, it showed a significant improvement in the study power for the VFD metric in Table 2.10. While it is possible to use a single-tailed test to determine optimal sample size for a trial, the risk of the intervention group having worse clinical outcomes than the control arm can increase risk. The criteria for choosing one statistical method over another has often been due to statistical correctness, a limitation of resources for the trial favouring lower numbers, or due to ethics committee or independent statistician requirements. If it is known that a treatment is not improving prognoses, it is not ethical to continue with it.

Thus, with skewed data sets, such as LoMV, it is often preferable to use a non-parametric statistical test. Hence, of the three tests used in this study (KS-Test, WR-Test and (lognormal) T-Test), only the t-test assumes a distribution, which is then log corrected. Ideally, either of the two non-parametric tests would be used, where the KS-Test is more sensitive to differences in distribution spread, while WR-Test is more sensitive to differences in the data set median. Which test should be used would depend on what a given trial is aiming to achieve.

2.4.3 Absolute vs percentage decrease in intervention effects for VFD outcome metric

As shown in Tables 2.10 and 2.11, the VFD outcome metric displayed a considerably lower power than $LoMV_{28}$. This result was unexpected, as the distributions of each metric are mirrored, and non- parametric tests were used. The inconsistency is due

to the use of percentage LoMV reductions. Percentage reductions imply less change for shorter stay patients, which is clinically reasonable versus an absolute change that has lesser impact for longer stay patients. Table 2.12 demonstrates the discrepancy in percentage changes for an initial LoMV of 5 days, with intervention of 20% LoMV.

Table 2.12: Differences between absolute and percentage reductions, for initial median LoMV of 5 days

	Pre-Intervention Value	**Post-Intervention Value**	**% Change**
LoMV	5	4	20%
LoMV-28	5	4	20%
VFD	28-5 = 23	28-4 = 24	4%

In this case, the VFD metric with a typically seen median LoMV of 5 days means a large change in LoMV and thus LoMV_{28} as a percentage is a relatively small change in VFD. At LoMV = 14 days the effect would be equal, and over 14 days the situation would reverse with greater effect for VFD and an easier ability to detect change in this metric. This latter case is shown in Table 2.13 with an initial LoMV of 20 days, and a percentage reduction of 20%.

Table 2.13: Differences between absolute and percentage reductions, for an initial LoMV of 20 days

	Pre-Intervention Value	**Post-Intervention Value**	**% Change**
LoMV	20	16	20%
LoMV-28	20	16	20%
VFD	28-20 = 8	28-16 = 12	33%

Hence, the choice of LoMV_{28} or VFD should depend primarily on the given initial distribution, of retrospective data informing the trial design, and this outcome would apply more generally to other trial design approaches with similar metrics. In addition, Using LoMV as the root outcome to test in simulation is important, as well as knowing the exact distribution. This Monte-Carlo approach can do this simulation, unlike other commonly used statistical assumption based design methods.

2.4.4 Statistical significance and power

A significant problem in many trials is concentrating on the clinical results, while neglecting the statistical significance (Bhardwaj et al., 2004). Conducting a power analysis allows the probability of correctly detecting a difference between the control and intervention groups to be determined (Bhardwaj et al., 2004). This process is complicated when analysing highly variable data that is not normally distributed. This analysis used Monte-Carlo simulation, combined with clinically relevant exclusion criteria as a viable method of determining the power of a study that uses a primary outcome metric of LoMV.

If the specific RCT assessed in this paper solely analysed LoMV, 160 patients in each arm would be sufficient to achieve a statistically significant result with 80% power and an intervention difference of 25%. However, using an outcome metric that also considers mortality data, such as VFD or LoMV_{28}, could be beneficial if there is a mortality difference between each cohort. Using the VFD metric with the same intervention effect can reduce the number of patients required to 130/arm with a mortality differential of 5%. Due to the high variability and skewed distribution of LoMV data, it is a difficult metric to use to assess the power of a clinical trial (Chiew, Pretty, Moltchanova, et al., 2015). However, it remains one of the most effective methods of determining the efficacy of MV treatment. In addition due to the high cost of ventilator therapy, reductions in ventilator duration have significant economic impacts for care units and hospitals (Dasta et al., 2005).

2.4.5 Limitations

Use of data from a specific ICU

The study was undertaken with the assumption the data used in the simulation was indicative of that which would be used in the RCT. However, use of LoMV distribution data from a single, specific Intensive Care Unit (ICU) may mean the results are not

universally applicable, and only able to be used in those with similar characteristics (Van Der Lee et al., 2009). Nevertheless, the approach followed in this study is general enough to be able to be repeated and utilised for most centres or across multiple centres in either randomised or centre randomised trials. If information on LoMV distribution is required, then a small and centre-specific pilot study could be carried out. In the case of a multi-centre study, information from multiple centres should be used.

2.4.6 Overall impact of Monte Carlo simulation method, cohorts and analyses

The struggle the design of many mechanical ventilation trials face is the excessive dimensionality of patient factors (diagnosis, age, sex) and MV care factors (how they are treated, and thus the size of the intervention effect). The key to this method and trial design approach is it collapses that dimensionality in two ways. First, the objective exclusion criteria, eliminate unintended subjectivity and patient dimensions, where subjectively patients may be either included or excluded, creating variability between the trial cohort and the intended target cohort who might benefit. Second, it does so through the use of repeated simulation, thus covering all possible or likely cohort outcomes, where the use of 4-years of data from the trial unit provides a final means of reducing potential un- intended variability in this model-based approach. Thus, the use of objective inclusion and exclusion in-silico criteria reduces a lot of dimensionality and uncertainty that would otherwise occur.

The overall non-parametric simulation methods and design approach was selected as it would be feasible in a clinical trial. The objectivity implemented in a manner where it can be used in the actual trial ensures the desired lower dimensionality is preserved. In turn, this outcome provides an increased chance of reaching significance through better control of the trial design and the actual trial so that the trial design is a far better match for what occurs in implementation, increasing the likelihood that if the assumed intervention benefit is observed the trial will be significant.

2.5 Summary

This chapter presented a generalisable Monte-Carlo simulation approach to determine required sample sizes for RCTs with highly skewed outcome metrics. In addition, the use of relevant exclusion criteria was found to reduce the required number of patients in each arm to reach statistical power, as well as inintended added dimensionality. Use of LoMV as an outcome metric required 160 patients/arm to reach 80% power with a clinically expected intervention difference of 25% LoMV if clinically relevant exclusion criteria were applied to the cohort, but 400 patients/arm if they were not. However, only 130 patients/arm would be required for the same statistical significance at the same intervention difference if VFD was used. Assessment of Δ LoMV in response to treatment should be considered to avoid an under-powered study. Monte-Carlo simulation, combined with objective patient selection criteria provides better design of ventilation studies. Finally, the overall approach used here is readily generalisable to most trials where the outcome measures are based on a log-normal or otherwise skewed data set, such as most length of care outcomes commonly used in medical research trials.

CHAPTER 3

Overview of Current Pulmonary Mechanics Models

3.1 Introduction

A range of models have been developed to describe lung mechanics from simple compartments models to complex finite element analyses. There is a limited amount of information and computational power available at the bedside. As a result of this, bedside models need to be able to convey critical information about patient condition with limited input data. The benefit of identifying aspects of the complexity and variability of lung physiology and lung injury or disease is currently ambiguous and thus, to date, has not justified the high costs of high fidelity data collection. In short, for a model to have clinical relevance and widespread use it needs to be structured simply enough to ensure clinical relevance and be mathematically identifiable using information readily available at the bedside (Chase et al., 2018; Chiew, Chase, Shaw, Sundare-

san, & Desaive, 2011; Cobelli & DiStefano, 1980; Docherty, Chase, Lotz, & Desaive, 2011; Ljung, 1999; Riedlinger, Kretschmer, & Möller, 2015; Schranz, Docherty, Chiew, Chase, & Möller, 2012).

Currently, only airway pressure and flow are measured during standard practice mechanical ventilation in most Intensive Care Unit (ICU) settings. The data is thus limited compared to pulmonary model complexity in the literature. In addition, respiratory failure is a secondary outcome to many disease or injury states, complicating the application of Mechanical Ventilation (MV) in a broad clinical cohort.

Thus, an evaluation of a range of pulmonary models is included in this chapter, followed by the development of a predictive model of lung mechanics to be used throughout this thesis. In addition, the clinical data used for model analysis is outlined. The overall aim is to present a succinct summary of model methodology and clinical data cohorts underpinning the rest of this thesis

3.2 Current retrospective model-based methods

Two main groups of retrospective lung models exist (Ben-Tal, 2006):

- **Complex, Finite Element Analysis (FEA) models.** The complexity of FEA models allows lung and disease mechanics to be better understood. In particular, FEA models can provide scientists and clinicians with a much more thorough idea of the localised effects of clinical factors, such as patient positioning (Burrowes & Tawhai, 2006), along with expected disease progression and pulmonary effects (Eom, Xu, De, & Shi, 2010; Werner, Ehrhardt, Schmidt, & Handels, 2009). However, for very large scale models, non-identifiability or non-observability can become a serious limitation requiring new identification and statistical approaches or additional data (Chase et al., 2018; Docherty et al., 2011). In many cases, these models are too complex to identify from the clinical data typically available, and are thus

not feasible for clinical use.

- **Variants on simpler, lumped-parameter models.** Lumped parameter models generally define elastic-resistive respiratory behaviours and have a much lower physiological resolution and complexity than FEA models (Ben-Tal, 2006; Major et al., 2018). Alveoli and airways are often initially modelled as a balloon at the end of a pipe or similar (Bates, 2009). The simplicity of these models means they are readily accessible for use in a clinical context. More specifically, they are mathematically identifiable (Docherty et al., 2011; Ljung, 1999; Schranz et al., 2012) from available pressure and flow data at the bedside. However, their simplicity generally means some dynamics are not captured. In particular, a key improvement to be made in lumped-parameter models would be more detailed parameterisation to enable disease evolution to be better understood via better insight into changing lung mechanics.

3.2.1 Finite Element Analysis Models

A range of more complex finite element models seeking to accurately describe the true physiological behaviour of the lungs have been developed (Burrowes, Clark, & Tawhai, 2011; Burrowes & Tawhai, 2006; Crampin et al., 2004; Ma & Bates, 2010; Polak & Lutchen, 2003; Swan et al., 2012; Tawhai & Bates, 2011; Tawhai & Burrowes, 2003, 2008; Tawhai, Hoffman, & Lin, 2009; Tawhai, Pullan, & Hunter, 2000; Tgavalekos, Venegas, Suki, & Lutchen, 2003). These models typically use detailed scale-models of the pulmonary system produced using anatomical information from computed tomography (CT) or other imaging (Tawhai & Burrowes, 2003). Segmented lung data is fitted to a high order mesh, providing a very detailed anatomical model for simulating respiratory mechanics (Tawhai & Bates, 2011). As these models typically have a very high computational cost and require individual CT scans for optimum accuracy, they are often not feasible for use in a clinical setting. They can also include a range of multi-scale models for various lung functions that contribute to gas exchange (Burrowes et al., 2011, 2013;

Burrowes, Swan, Warren, & Tawhai, 2008; Tawhai & Bates, 2011; Tawhai & Burrowes, 2008), and provide valuable information about changes in perfusion and ventilation throughout the lungs (Swan et al., 2012). They can also be used to indicate the extent and progression of disease (Tgavalekos et al., 2005), but not in a personalised manner as they are not identifiable with available data.

There is thus scope for their clinical use in better understanding perfusion and disease state in general, and over time for some patients. Equally, emerging simplified approximations using Bond Graph methods offers the potential to significantly increase computational speed (Safaei, Blanco, Müller, Hellevik, & Hunter, 2018). Combined with enough data or imaging, they provide a link to bring greater detail to simpler elastic-resistive models.

3.2.2 Elastic-Resistive Models

Single Compartment Model

The simplest model of the lung is an elastic balloon at the end of a pipe. The balloon represents the distensible tissues, while the airways are modelled by the pipe (Bates, 2009). From this concept, a single compartment mathematical model is generated. Many variants on this basic model have been established (Ben-Tal, 2006).

A single compartment model was pioneered in 1953, for patients capable of spontaneous breathing (Mead & Whittenberger, 1953). This form of model describes the respiratory system as containing an elastic compliant section representing the lung, along with a resistive component representing the airways (Bates, 2009; Chelucci et al., 1991; van Drunen et al., 2014). This simple model is disproportionally effective for basic analyses. However, as it assumes pressure increases linearly with volume increase, it neglects non-linear flow and other specific dynamics (Bates, 2009; Chiew et al., 2011; Lucangelo et al., 2007).

This model includes the pressure difference *($R\dot{V}(t)$)* in the lungs, and the elastic pressure *($EV(t)$)* in the lungs. Assuming linear flow, it is defined (Bates, 2009):

$$P(t) = EV(t) + R\dot{V}(t) + PEEP \tag{3.1}$$

Where P is the inspiratory pressure delivered to the lungs (cmH_2O), $PEEP$ is the ventilator positive end-expiratory pressure (PEEP) setting (cmH_2O), t is time (s), $V(t)$ is the applied volume (L), $\dot{V}$(t) is the time-dependent flow (L/s), E is the elastance (cmH_2O/L) and R is the resistance (cmH_2O/L*s) (van Drunen et al., 2014).

The low number of parameters in this model means it is easily identifiable using clinically available data, and is computationally inexpensive in its basic form (Chiew, 2013; Chiew et al., 2011). Thus, it can be widely applied in clinical settings with given typical clinical data. It has thus been significantly extended.

SLICE method

The SLICE method was developed by Guttmann et al. in 1995 (Guttmann et al., 1995). Lung mechanics are often non-linear and volume dependent. These issues present a challenge when attempting to fit clinically relevant linear models to data. As a linear piecewise approximation of lung mechanics, the SLICE method splits the tidal volume into a set of 'slices' with a single resistance and single compliance value per volume 'slice'. Combining the resistance and compliance across the delivered volume 'slices' gives quasi-dynamic compliance and resistance values (Guttmann et al., 1995; Zhao, Guttmann, & Möller, 2011, 2012). To further linearise the behaviour, the Rohrer equation (Rohrer, 1925) is used to calculate the tracheal pressure (Guttmann et al., 1995), as opposed to the airway pressure. Equation 3.1 is thus adapted to become:

$$P_{aw,slice}(t) = \frac{V_{slice}(t)}{C_k} + \dot{V}_{slice}(t) x R_k + P_k \tag{3.2}$$

where $P_{aw,slice}$, $\dot{V}_{slice}$, and V_{slice} are the pressure, volume and airway flow for a single slice, respectively (Guttmann et al., 1995). P_k represents the pressure offset for each slice. C_k and R_k are the identified compliance (L/(cmH_2O)) and resistance ((cmH_2O)*s/L*s) for each slice (Zhao et al., 2011).

An adaptive slice model was developed to automate selection of the slice sizes based on the results confidence interval, thereby reducing error while maximising computational efficiency (Zhao et al., 2011). The linearisation of lung mechanics in the SLICE model, along with the additional accuracy in the adaptive form means it remains clinically identifiable, while still providing as many trustworthy estimates of elastance and resistance as possible (Zhao et al., 2011). However, it requires tracheal pressure measurement, which is much more invasive and much less common than ventilator recorded airway pressure.

Time-Varying Elastance Model

Lung elastance is dependent on recruitment, which is a time-varying phenomena (Ma & Bates, 2010; Massa, Allen, & Bates, 2008). Therefore, a method to assess changes in this property throughout the progression of a disease is essential to guide therapy (Chiew et al., 2011; van Drunen et al., 2014). Dynamic lung elastance (E_{drs}) is time-varying elastance changing over a breath (Chiew et al., 2011). It is typically fit over inspiration using the single compartment model in Eq. 1.

Having E_{drs} and a breath-constant lung resistance (R_{rs}) fit to every breath allows the model to be used to optimise PEEP settings (Chiew, Pretty, Shaw, et al., 2015; van Drunen et al., 2014). It can also indicate the occurrence of over-distension or recruitment within the breath (van Drunen et al., 2014).

The time-varying model is defined:

$$P(t) = E_{drs}V(t) + R\dot{V}(t) + PEEP \tag{3.3}$$

where E_{drs} is an overall respiratory system elastance (cmH_2O/L) comprising chest wall elastance, treated as a constant, and lung elastance (assumed to change throughout inspiration (van Drunen et al., 2014)). Resistance is assumed to be a constant over a breath in this model.

Identifying time-varying elastance over a breath also enables detection and monitoring of the incidence and magnitude of asynchronies (Chiew et al., 2018; Kannangara et al., 2016). Asynchrony interrupts MV care and worsens outcomes, as it reflects poor interaction between the patient and ventilator (Chiew et al., 2018; Kannangara et al., 2016). Hence, the model of Equation 3.3 can also be used to address and monitor this clinically important outcome, as well.

Spontaneous Breathing Model

Spontaneously breathing patients apply their own inspiratory efforts on top of a ventilator supported breathing cycle (Langdon, Docherty, Chiew, Damanhuri, & Chase, 2015). A time-varying elastance model was developed to describe the mechanics of spontaneously breathing patients on partial assist mechanical ventilation (Chiew, Pretty, Shaw, et al., 2015). This model utilises a negative time-varying elastance component to describe patient-specific breathing efforts. The overall model is based on the single compartment model of Equation 3.1 and the time-varying model of Equation 3.3, but an adjusted E_{drs} value captures the additional patient effort on top of the ventilator support. The components of this adjusted E_{drs} value are defined:

$$Edrs = E_{chest} + E_{demand}(t) + E_{lung}(t) \tag{3.4}$$

where E_{drs} is the overall time-varying respiratory system elastance (cmH_2O/L), E_{chest} is the constant elastic properties of the chest wall, $E_{lung}(t)$ is a time-varying measure of the elastic properties of the lung, or the collection of alveoli, and $E_{demand}(t)$ is the patient-specific inspiratory demand, which varies from breath-to-breath (Chiew, Pretty, Shaw,

et al., 2015).

Given a value for E_{chest}, the net balance of $E_{demand}(t)$ and $E_{lung}(t)$ can be identified. It may be a positive or negative value as that patient may provide either inspiratory or expiratory pressure. Negative elastance thus accounts and allows for patient breathing efforts separate to the support provided by the ventilator.

The ability of this model to accurately capture mechanics of spontaneously breathing patients without invasive measures extends the clinical ability of minimal models to enable titrating care for all ventilated patients (Chiew, Pretty, Shaw, et al., 2015). Negative elastance and area above this curve allows estimation of breathing effort by the patient. Finally, it lets the same model be used for sedated and spontaneous breathing MV modes, enabling continuity in model-based MV care approach.

Other Elastic-Resistive Models

A range of other elastic-resistive models have been developed (Ben-Tal, 2006). These models include those of Massa et al. (Massa et al., 2008) and Ma et al. (Ma & Bates, 2010), which were used to define the processes of recruitment and derecruitment. Both of these models attempt to capture the specific, time-dependent processes carried out in an airway branch before extending this local model to estimate global lung behaviour based on expected distributions (Massa et al., 2008). It assumes each branch has a critical opening and closing pressure, along with corresponding time constants (Ma & Bates, 2010).

Abboud et al. (Abboud, Barnea, Guber, Narkiss, & Bruderman, 1995) developed a model to capture the lung's flow-volume curve throughout forced expiration. This model was used to more thoroughly investigate the differences in lung stiffness between different lung diseases. Finally, in 2007, Lucangelo et al. adapted Equation 3.1 to capture dysfunctional patient-ventilator interactions such as asynchronies, air-leaks or sudden changes in patient condition (Lucangelo et al., 2007).

3.2.3 Modelling Summary

A range of models have been developed to define lung mechanics. Finite element models are too complex for bedside use in model-predictive and potentially automated care. Simple, mathematically identifiable models have demonstrated the ability to capture clinically relevant dynamics and lung mechanics. However, improvements in the field require the ability to predict the effect of changes in therapy on individual patients and cohorts as a whole, prior to making the change, which has not yet been demonstrated.

3.3 Forward prediction of future lung behaviour

While many pulmonary models have been developed to the point where they can accurately describe elastance and suggest a suitable PEEP level, it is a reactive, retrospective process. For more effective and patient specific treatment, models need to be able to extrapolate from past or current data to predict how the lung will respond to MV setting changes (Langdon, Docherty, Chiew, & Chase, 2016). This predictive capability is demonstrated in glycaemic care (Chase et al., 2011, 2010; J. L. Dickson et al., 2018; Evans et al., 2011; Langdon, Docherty, Mansell, & Chase, 2018; Stewart et al., 2016; Uyttendaele et al., 2018) and is essential in MV care for defining when and how to alter ventilator settings for optimised patient outcomes.

3.3.1 Stochastic Models

Stochastic models use distribution information about a population to predict future behaviour in an individual patient. Stochastic models have been used for predictive models of insulin sensitivity and virtual patient development to ensure safety in semi-automated glycaemic control (Chase et al., 2016, 2018, 2008, 2010; J. L. Dickson et al., 2018; Fisk et al., 2012; Le Compte et al., 2010; Lin et al., 2007). Specifically, these models have been instrumental in the STAR glycaemic control protocol (J. L. N. Dickson, Lynn, Shaw, & Geoffrey Chase, 2019; Evans et al., 2011; Fisk et al., 2012; Le Compte et al., 2012;

Stewart et al., 2016), using information from large amounts of clinical data to inform clinical decisions about future changes in insulin uptake to avoid hyperglycaemic and hypoglycaemic episodes.

However, stochastic modelling may be limited in its application for lung mechanics. Insulin sensitivity is modelled as a one-dimensional problem, either increasing or decreasing over time. More recent work has extended this variable in a model-based glycaemic control scenario to a two-dimensional variable that takes into consideration rate of change by including rate of change (Uyttendaele et al., 2018). However, for lung mechanics models, this variability is spread over a more variable and high, breath-to-breath time resolution.

Notably, the single compartment model of pulmonary mechanics $P = EV + RQ + PEEP$ in Equation 3.1 already has two dimensions. However, once identified this model lacks predictive capability if ventilator settings, such as PEEP, change. To allow for changes in elastance and resistance or ventilator settings over time to be taken into account, the model needs to be of a higher dimension.

3.3.2 NARX Models

Work has been done to predict lung mechanics at a high PEEP using information provided at a lower PEEP (Langdon, Docherty, Chiew, & Chase, 2016; Langdon, Docherty, Chiew, Moeller, & Chase, 2015). A non-linear autoregressive (NARX) resistance and basis function elastance model was developed from a viscoelastic form of the single compartment model (Langdon, Docherty, Chiew, & Chase, 2016; Langdon, Docherty, Chiew, Moeller, & Chase, 2015). Basis functions were developed from overlapping B-spline functions of different orders (Langdon, Docherty, Chiew, & Chase, 2016; Langdon, Docherty, Chiew, Damanhuri, & Chase, 2015; Langdon, Docherty, Chiew, Möller, & Chase, 2016). This model successfully predicts lung behaviour at high PEEP levels using information provided at a lower PEEP setting/value. However, the basis function terms used

cannot be explicitly linked to lung mechanics. This issue reduces the clinical utility of this particular model to be used in a virtual patient, as well as its diagnostic relevance.

3.3.3 Summary

Each of these models is able to provide useful information about current lung response to ventilation and uses clinically-available information. However, each of the models lack the key combination of predictive capabilities and clinical identifiability to be used in determining lung mechanics during future changes in ventilation. In particular, none of these models has been used to forward predict pressure or flow outcome given different mechanical ventilation modes or settings. This work attempts to develop a simple model capturing underlying lung mechanics to be used to predict pressure outcomes given different PEEP and flow conditions.

CHAPTER 4

Clinical Data

4.1 Clinical Data Cohorts

Pressure and flow data from N=21 invasively ventilated patients diagnosed with acute respiratory distress syndrome (ARDS) from ICUs in Germany (N=17) and New Zealand (N=4) (Davidson et al., 2014; Stahl et al., 2006) will be analysed throughout the rest of this thesis. The four patients from New Zealand were part of the CURE pilot trial conducted at Christchurch Hospital Intensive Care Unit (ICU) in August 2016. Pressure-flow data for this cohort was sampled at 50 Hz (Szlavecz et al., 2014). The German data spans eight ICUs, and was collected from September 2000 until February 2002 as part of the McREM trial (Stahl et al., 2006). It was sampled at 125 Hz. All patients were fully sedated and received invasive volume-controlled ventilation via an Endotracheal Tube (ETT).

4.2 CURE Data

This study used pressure-flow data from four mechanically ventilated patients that were treated as part of the CURE pilot trial (ANZTR Number: ACTRN12613001006730) (Szlavecz et al., 2014). The CURE pilot trial was a randomised control trial where the in-

tervention arm received repeated RMs. All patients were intubated and fully sedated, receiving volume controlled MV. Those with APACHE III diagnostic codes associated with prior pulmonary disease admission (asthma, COPD), or neurological, spinal injury, or head trauma, were excluded from the pilot trial.

All patients were fully sedated with muscle relaxants, which is common to prevent spontaneous breathing during RMs. Inclusion criteria for the trial require a PaO_2/FiO_2 ratio (PaO_2/FiO_2 ratio) $<$300 mmHg, classifying the patient as having ARDS according to the Berlin definition (The ARDS Definition Task Force, 2012). Pressure, flow, and time data were extracted at 50Hz from a Puritan Bennett 840 ventilator (Covidien, Boulder, CO, USA). Patient demographic and clinical data is shown in Table 4.1. More information about the CURE trial can be found in (Chiew, Pretty, Shaw, et al., 2015; Davidson et al., 2014; Szlavecz et al., 2014). Only the four patients from the intervention arm of the CURE pilot trial underwent major RMs, per protocol (Szlavecz et al., 2014), and are thus the only data available from this ten patient pilot study for this development and validation study. Each of these patients had mild (200 – 300 mmHg) or moderate (100—200 mmHg) ARDS.

Table 4.1: Patient demographic information.

Patient Number	Sex	Age (years)	LoMV	# RMs	Clinical Diagnostic	P/F Ratio
1	M	33	23 days	2	Peritonitis	177
2	M	77	24 days	2	Legionella pneumonia	209
3	M	61	23 days	2	Staphylococcus Aureus pneumonia	109
4	F	73	2 days	2	Streptococcus pneumonia	155

Each RM comprised two staircase increases and decreases in PEEP. The first was performed to recruit lung volume, and the second to assess lung mechanics at different PEEP levels once recruitment was achieved (Chiew, Pretty, Shaw, et al., 2015; Davidson

et al., 2014). As lung mechanics change throughout an RM, each data set was split into four sections: two upwards and two downwards staircase sections, as shown in Figure 4.1a. PEEP levels containing less than six usable breaths (40% of CURE PEEP levels, 33% of McREM PEEP levels) were excluded to reduce the impact of outliers; this issue occurs when the ventilator does not achieve exactly the stated PEEP in some breaths. The average length of PEEP levels studied in this research was (median [IQR]) 10 [7 – 12] breaths.

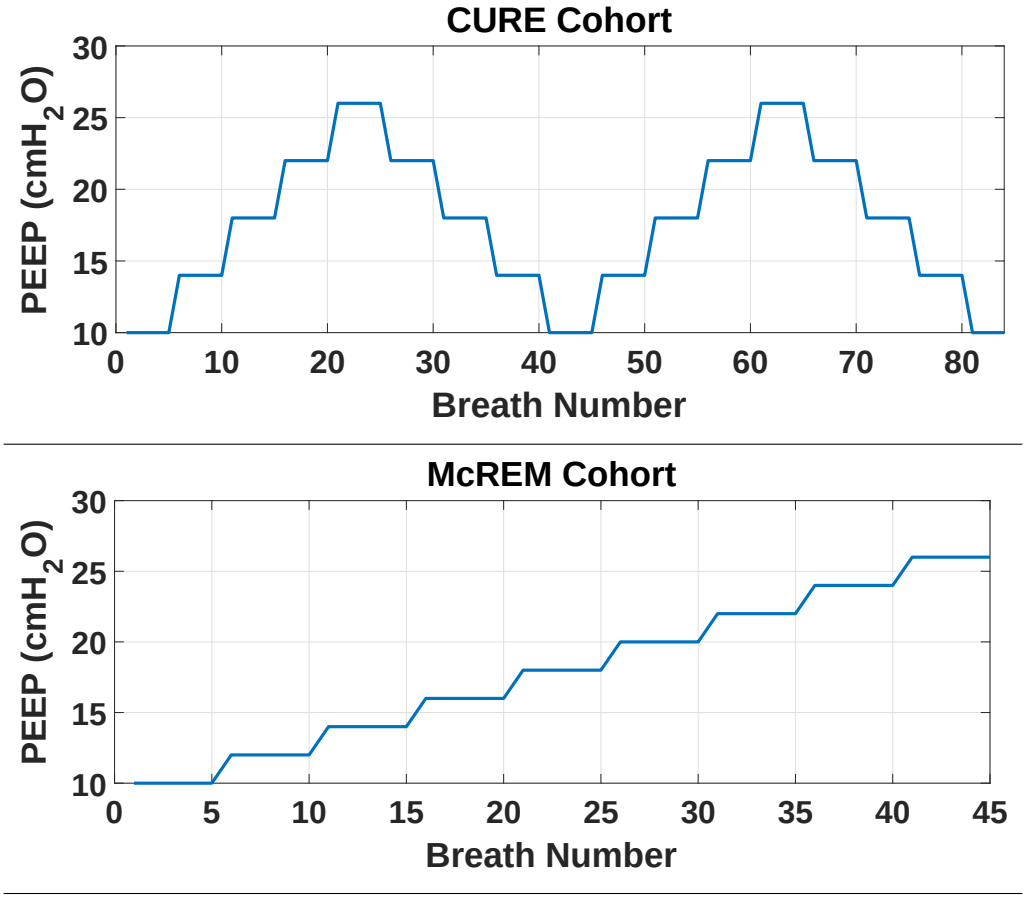

Figure 4.1: Example of RMs used in CURE and McREM trials. The number of breaths spent at each PEEP level are not representative of those found in the data. A more detailed depiction of the breakdown of RM arms for the CURE data can be seen in Chapter 8, Figure 8.1.

4.3 McREM Data

The McREM trial examined whether or not lung mechanical observations differed between measurements taken under static conditions and those taken dynamically. The study had ethics approval under the local ethics committee of each of the eight German ICUs participating in the trial (Stahl et al., 2006). All patients were ventilated with a Draeger Evita 4 (Draeger Medical, Lübeck, Germany) ventilator. Exclusion criteria included patients with obstructive lung disease, presence of a bronchopleural fistula or known air leakage, haemodynamic instability, or being considered ready to wean off ventilation by the attending physician. The maximum PaO_2/FiO_2 ratio was 298 mmHg (PF $<$300 mmHg), which matches the inclusion criteria for the CURE pilot trial. The tidal volume was targeted at 8 ± 2 mL/kg initial body weight. Before the measurements, respiratory rate was adjusted to keep the $PaCO_2$ at around 55 mmHg. Inspiratory time and flow rate were set to obtain an end-inspiratory hold of 0.2 secs. (Stahl et al., 2006) During the protocol, ventilator settings remained unchanged. Patient demographics are shown in Table 4.2.

Each patient underwent a staircase recruitment manoeuvre where PEEP was increased in steps of 2 cmH_2O up to 13 times from ZEEP or to a limit of 26 cmH_2O, as shown in Figure 4.1b. Each PEEP step was maintained for 10 breaths (Stahl et al., 2006). Figure 4.1b shows a typical RM carried out in this study. The McREM study included 28 patients, of which only 17 received RMs that could be used in this study. These latter patients were used in this analysis.

Table 4.2: Patient Demographics for McREM trial

Patient #	Sex	Age	LoMV (Days)	Clinical Diagnostic	P/F Ratio
1	M	37	10	Pneumonia	163
2	M	39	2	Traumatic aortic dissection, lung contusion	170
3	F	50	8	Pancreatitis, pneumonia	202
4	F	49	3	Pneumonia	289
5	M	34	10	Traumatic open brain injury	192
6	M	67	4	Post-resuscitation	234
7	M	39	10	Perf. sigma, peritonitis	188
8	M	42	9	Pneumonia, pancreatitis	235
9	M	51	5	Traumatic brain injury, pneumonia	230
10	M	77	6	Pneumonia	225
11	M	74	10	Subarachnoid and subdural haemorrhage	298
12	M	41	16	Peritonitis	178
13	M	62	2	Subarachnoid haemorrhage	288
14	M	39	7	Traumatic brain injury, pneumonia	143
15	M	74	9	S/P coronary artery, bypass grafting, pneumonia	271
16	M	59	19	ARDS	75
17	M	45	8	Blunt abdominal trauma, pneumonia	173

4.3.1 End-Inspiratory Pause

The McREM trial also administered a 0.2 second long end-inspiratory pause during ventilation for the majority of the patients. End-inspiratory pauses are a held pressure lower than peak pressure after PIP is reached and before expiration begins, as indicated in Figure 4.2 for Patient 8 in the McREM cohort (Stahl et al., 2006). End-inspiratory pauses are used to improve patient ventilation by reducing hypercapnia through reduction of both dead space and $PaCO_2$ levels (Aguirre-Bermeo et al., 2016; Åström et al., 2008; Devaquet et al., 2008).

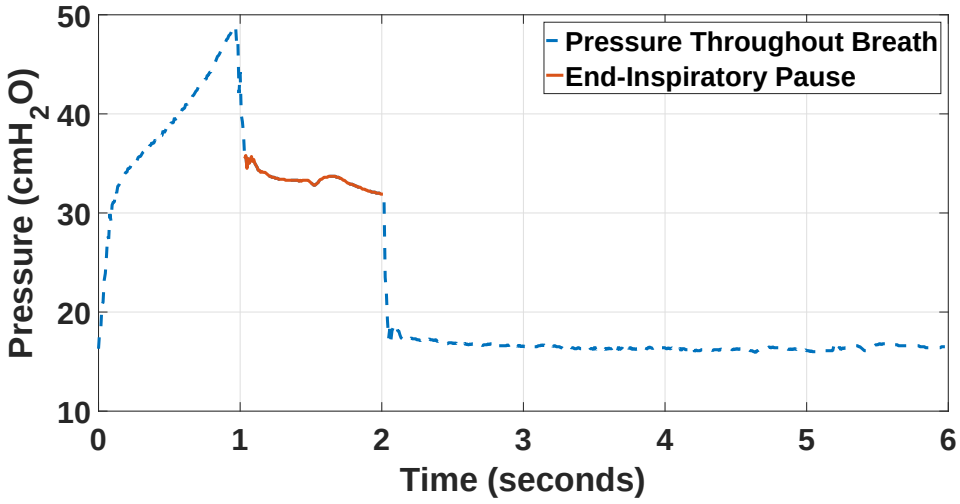

Figure 4.2: Typical end-inspiratory pause for the McREM cohort, shown for Patient 8.

4.4 Data Consolidation

In both cohorts, every breath at each PEEP level was used to create an 'average' breath that was used to fit the model parameters. This was determined using the median values for each parameter at every time-step. This breath was then used for prediction and compared to the average breath at the higher PEEP level. PEEP was taken as the minimum pressure value in a breath, it was rounded to the nearest whole number.

4.5 Summary

In this chapter, the clinical data from the CURE and McREM trial cohorts that will be used throughout the thesis is presented. Additionally, an explanation of the structure of the RMs that are used in each cohort is included.

CHAPTER 5

Development of a Predictive Pulmonary Mechanics Model

5.1 Introduction

In this chapter a predictive pulmonary elastance model is developed to predict the impact of PEEP changes on lung mechanics throughout a staircase recruitment manoeuvre (RM). This model uses physiologically relevant 'basis function' models for elastance and resistance changes over positive end-expiratory pressure (PEEP) steps along with an estimation of the additional lung volume gained (additional lung volume (V_{frc})) to predict peak inspiratory pressure (PIP) over PEEP steps in RMs (Morton, Dickson, Chase, Docherty, Desaive, et al., 2018; Morton, Dickson, Chase, Docherty, Howe, et al., 2018a, 2018b; Morton, Dickson, Docherty, Shaw, & Chase, 2017; Morton, Docherty, Dickson, & Chase, 2018; Morton et al., 2019; Morton, Knopp, et al., 2018). The ability to predict lung response prior to changing ventilator settings would allow clinicians to better assess the trade-off between risk (high pressures and PIP) and reward (alveolar recruitment (increased V_{frc}) and improved gas exchange).

5.2 Modelling Methodology

5.2.1 Model Development

The single compartment model of lung elastance and pressure shown in Equation 3.1 was used as a starting point for model development (Bates, 2009; Chelucci et al., 1991; van Drunen et al., 2014). Pulmonary elastance is defined as a function of both volume and pressure, in two separate basis functions, shown in Figure 5.1. This split allows more specific physiological behaviours of the lungs to be captured, compared with the single, lumped parameter model values in Equation 3.1. The elastance (*E*, cmH2O/L) is defined:

$$E(P(t), V(t)) = E_{rec} + E_{dist} = E_1\Phi_1(V(t)) + E_2\Phi_2(P(t)) \tag{5.1}$$

where *P(t)* is the pressure delivered by the ventilator and *V(t)* is the tidal volume delivered. Φ_1 (*V(t)*) and Φ_2 (*P(t)*) are dimensionless recruitment and distension basis functions, respectively, and E_1 and E_2 are constant coefficients with units (cmH_2O/L).

The recruitment elastance, captures the decreasing rate of recruitment of alveoli with an increase in volume delivered. It is piecewise parabolic with respect to tidal volume above end-expiratory volume at the current PEEP and is defined as zero when $V > V_m$ (Morton et al., 2019). V_m is set to 1L here as this value represents a sensible upper limit on gained recruited volume at the PEEP changes studied, based on clinical observation. Equally, this parameter cannot be easily or uniquely identified for each individual patient or breath, its value is set constant (Docherty et al., 2011). This recruitment basis function is defined:

$$E_{rec} = E_1\Phi_1(V(t)) = \begin{cases} E_1(V - V_m)^2 & if V \leq V_m \\ 0 & if V > V_m \end{cases} \tag{5.2}$$

The distension function (Morton, Dickson, Chase, Docherty, Desaive, et al., 2018; Morton

et al., 2019) captures the increasing elastance with pressure due to distension effects. It is modelled as a linear function, where the value of 60 is the maximum Mechanical Ventilation (MV) pressure considered. This is well above peak limits that are observed or considered safe (Brower et al., 2004). It is defined:

$$E_{dist} = E_2\Phi_2 = E_2\frac{P(t)}{60} \tag{5.3}$$

Airway resistance is a function of flow, and is defined using the Rohrer equation for flow resistance (Flevari et al., 2011; Rohrer, 1925). These terms capture linear and non-linear components of flow resistance, and R_1 and R_2 are constants to be identified. This equation is also similar to those used to model endotracheal tube resistance (Flevari et al., 2011; Jarreau et al., 1999), which is a major form of resistance encountered in MV. Resistance was defined per the structure of the Rohrer equation for flow resistance (Flevari et al., 2011; Rohrer, 1925):

$$R = R_1\Theta_1 + R_2\Theta_2 \tag{5.4}$$

where

$$\Theta_1 = 1 \tag{5.5}$$

$$\Theta_2 = |\dot{V}(t)| \tag{5.6}$$

Combining both the elastance and resistance basis functions into the model of Equation 3.1 yields:

$$P(t) = \left(\underbrace{E_1(V - V_m)^2}_{\text{Recruitment Elastance}} + \underbrace{E_2\frac{P(t)}{60}}_{\text{Distension Elastance}} \right) V(t) + \left(\underbrace{R_1 + R_2\dot{V}(t)}_{\text{Rohrer Resistance}} \right) \dot{V}(t) + PEEP \tag{5.7}$$

where E_1, E_2, R_1, and R_2 are to be identified and the other variables are known.

The general elastance and resistance basis function shapes used in the model are shown

in Figure 5.1 and Table 5.1, and are defined over the pressure range 0-60 cmH_2O and volume range 0-1 L for the elastance basis functions, and a flow range -2 to 2 L/s for the resistance basis functions. These ranges more than cover typical mechanical ventilation ranges. Note that as pressure rises with volume during inspiration, the two elastance basis functions of Equations 5.3 and 5.2 create an overall parabolic shape in combination. This overall shape cannot be directly plotted in sum together as they are functions of pressure and volume, respectively, whose relationship differ for each patient and with MV settings.

Pneumonia-affected lungs often display very heterogeneous localised lung mechanics, with optimal PEEP potentially occurring over a large range (Lorx et al., 2010). Furthermore, airflow resistance in patients presenting with pneumonia-induced ARDS often shows wide variation, making achieving optimal ventilation challenging (Lorx et al., 2010; Wright & Bernard, 1989). The model was developed to account for heterogeneity in lung disease. In particular, where lung stiffness in certain lobes reduces the ability of the lung to be recruited, the model captures this loss of recruitment as increased overall elastance (stiffness), and a decreased ability to gain V_{frc}.

Table 5.1: List of basis function shapes. These basis function shapes are also presented in Figure 5.1.

Relevance	**Title**	**Coefficient**	**A Function of**	**Chosen Shape**
Elastance (Recruitment)	E_{rec}	Φ_1	Volume	Parabolic decay
Elastance (Distension)	E_{dist}	Φ_2	Pressure	Linearly increasing slope
Resistance 1	R_1	θ_1	Constant	Constant value
Resistance 2	R_2	θ_2	Flow	The absolute value of ventilator flow throughout the breath

Basis Function for Elastance (Recruitment)

$$\Phi_1 = (V - V_m)^2$$

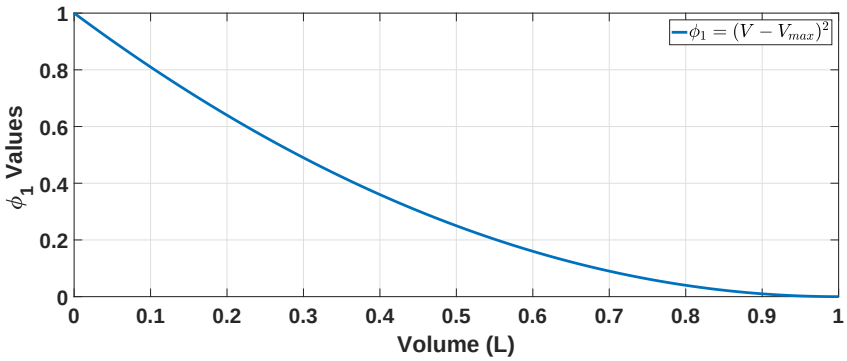

Basis Function for Elastance (Distension)

$$\Phi_2 = \frac{P(t)}{60}$$

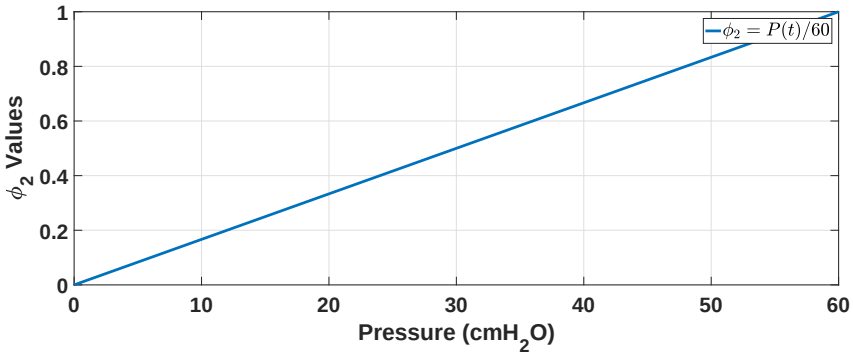

Basis Functions for Resistance

$$\theta_1 = 1,$$
$$\theta_2 = |\dot{V}(t)|$$

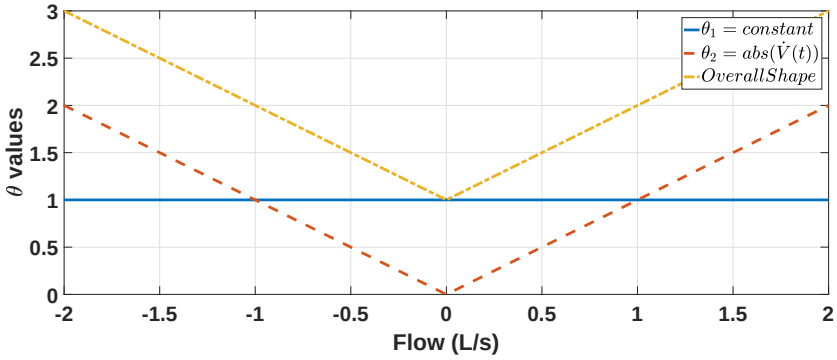

Figure 5.1: Depiction of basis functions for elastance and resistance. The shapes above assume coefficient values of 1. All basis functions are dimensionless.

5.2.2 Model Identification

An identified model can be subsequently used to predict patient-specific outcomes for different settings or pressure and volume, as the basis functions are identified over an entire reasonable range of these variables. The median breaths for each PEEP level (defined in Section 4.4) were used for model identification. Data from the entire breath, including expiration, was used to identify model parameters to identify E_1, E_2, R_1, and R_2 using Equation 5.1. While these points are often discarded in parameter identification, the first data points of each breath were used to capture the viscoelastic behaviour present in this section of ventilation.

Parameter fitting was done independently for every PEEP level in a patient data set. Once a PEEP level was fit, forward prediction to other PEEP levels was achieved using the parameters from the current PEEP level only. Model parameters, E_1, E_2, R_1, and R_2 were identified for the median breath across a PEEP level using MATLABs (The Mathworks, 2017) linear least squares *lsqnonneg* function to constrain all parameters to physiologically possible positive values in MATLAB and clinical data in a problem defined:

$$\begin{bmatrix} min(0, V(t_i) - V_m)^2 \odot V(t_i) & V(t_i) \odot \frac{P(t_i)}{60} & \dot{V}(t_i) & |\dot{V}(t_i)|\dot{V}(t_i) \\ \vdots & \vdots & \vdots & \vdots \end{bmatrix} \begin{bmatrix} E_1 \\ E_2 \\ R_1 \\ R_2 \end{bmatrix} = \begin{bmatrix} P(t_i) - PEEP \\ \vdots \end{bmatrix} \tag{5.8}$$

where $\odot$ indicates pointwise multiplication.

5.2.3 Model Prediction

The solution for an identified model is generated using volume controlled MV and thus specified *V(t)* and $\dot{V}(t)$ are used to simulate *P(t)*. Fit error describes the difference between clinical and simulated data at the same PEEP, and prediction error describes the

difference between clinical and simulated pressure at a higher PEEP. Forward simulation using *V(t)* and $\dot{V}(t)$ inputs at different PEEP levels, which are specified and known ahead of time in volume controlled MV, can be computed to assess prediction and utility.

Prediction was carried out for PEEP increases in each upwards RM arm (shown in Figure 4.1a). There was a focus on prediction on increasing PEEP as an increase in pressure and volume pose a greater immediate risk to patient safety. PIP and gained recruitment volume V_{frc} can be used to reflect the relative gains and risks of mechanical ventilation, for the purposes of avoiding barotrauma and volutrauma. Prediction across PEEP levels also requires calculation of the change in V_{frc} or the volume recruited by a PEEP step change relative to the current PEEP (Lambermont et al., 2008; van Drunen, Chase, et al., 2013). It is assumed that the change in V_{frc} is positive or zero when PEEP is increased, and negative or zero when PEEP is decreased.

Forward simulation of *P(t)* using *V(t)* and $\dot{V}(t)$ given by the volume controlled ventilation mode at different PEEP levels as inputs can be used to assess prediction, and thus the potential clinical utility of the model and overall approach. The change in V_{frc} across a particular PEEP step (n to n+1) is assessed iteratively using:

$$V_{frc}^{n} = \frac{PEEP_{n+1} - PEEP_{n}}{E_1(V_frc - V_m)^2 + \dfrac{E_2 PEEP_{n+1}}{60}} \tag{5.9}$$

The minimum value for $V - V_m$ was set to zero through use of the *min* function in MATLAB.

Incorporating V_{frc}^{n} from Equation 5.9 yields a model to predict *P(t)* using Equation 5.7 and the known volume controlled flow inputs at a new PEEP level ($PEEP_{n+1}$), where the resulting formula is defined:

$$P(t) = \left(\underbrace{E_1((V + V_{frc}) - V_m)^2}_{\text{Recruitment Elastance}} + \underbrace{E_2 \frac{P(t)}{60}}_{\text{Distension Elastance}} \right) V(t) + \left(\underbrace{R_1 + R_2 \dot{V}(t)}_{\text{Rohrer Resistance}} \right) \dot{V}(t) + PEEP \tag{5.10}$$

5.2.4 Model Validation

The same error metrics are used to describe the identified model fit to data (fit error), and the accuracy of the identified model prediction for a higher PEEP level (prediction error). Root Mean Square (RMS) indicates the average sum-squared error residuals throughout the breath. To ensure this value is normalised across all PEEP levels and between data sets with different numbers of data points per breaths, the percentage RMS error is also calculated.

PIP is a key clinical indicator of the risk of ventilator-induced lung injury (VILI) due to barotrauma in volume controlled ventilation (Dreyfuss & Saumon, 1992; Gammon, Shin, & Buchalter, 1992). To assess the clinical relevance and safety of the model, both the error in PIP and its percentage error are calculated for identified model fit and prediction. Finally, predictions are made for 1 – 8 PEEP steps forward for all PEEP levels where there was data. To assess the accuracy of the model across the entire PEEP range, model fit and prediction error are compared across the entire range and for different prediction step sizes. Unless, otherwise stated, PIP (cmH_2O) error is in it's original, signed form, while PIP (%) error is taken as an absolute error.

5.2.5 Summary

This chapter presents a predictive model and parameter identification framework that will be used in subsequent chapters.

CHAPTER 6

Impact of Recruitment Function Shape on Prediction

6.1 Introduction

Prior work suggested the rate of recruitment follows an exponential decay with increasing pressure(Albert et al., 2009; Bates & Irvin, 2002; Crotti et al., 2001; Graham et al., 2005; Harris, Hess, & Venegas, 2000; Massa et al., 2008; Medoff et al., 2000; Mutch et al., 2000; Owens, Hess, Malhotra, Venegas, & Harris, 2008; Ranieri et al., 1991; Sundaresan et al., 2009; Venegas, Harris, & Simon, 1998; Williamson et al., 2011). This decrease in elastance due to recruitment could be mathematically described with different basis functions yielding similar overall shapes. In this chapter, an exponential basis function is compared to a parabolic basis function from Chapter 5, where it is hypothesised the latter will improve identifiability while not sacrificing accuracy. This chapter also serves as model validation for the parabolic model from Chapter 5.

6.2 Methods

A single compartment model is used in conjunction with basis function shapes for elastance and resistance, as presented in Section 5.2.1. This study examines the impact of the difference in recruitment elastance basis function shape (Φ_1) on model identification and PIP prediction. While both the parabolic and exponential models broadly describe elastance as decreasing to a minimum of zero, there are differences in the shape and rate of that decrease, as shown in Figure 6.1 where the exponential of Equation 6.2 has a much steeper initial drop from its maximum value. This comparison can indicate which definition is better across all the data in this study, noting an exponential shape has been very commonly used in previous studies (Crotti et al., 2001; Medoff et al., 2000; Mutch, 2005; Sundaresan et al., 2009; Venegas et al., 1998), and parabolic functions have not been used previously. The overall results should thus provide significant new insight into lung mechanics.

6.3 Model Definition

The definition and identification of the parabolic recruitment function model is outlined in Chapter 5.2, where the parabolic basis function is defined in, Equation 5.2 ($\Phi_1 = E_1(V - V_m)^2$).

In the exponential basis function, an exponential decay is used to describe the relationship between the increasing volume and the rate of alveolar recruitment (Morton, Dickson, Chase, Docherty, Desaive, et al., 2018). This function is defined:

$$E_{rec} = E_1\Phi_1(V(t)) = E_1 e^{b(V(t))} \tag{6.1}$$

where b is a constant controlling the rate of recruitment with increased tidal volume delivered, which also makes it useful for assessing different levels of volume deficiency.

The overall single compartment model with exponential recruitment is defined:

$$P(t) = \left(\underbrace{E_1 e^{b(V(t))}}_{\text{Recruitment Elastance}} + \underbrace{E_2 \frac{P(t)}{60}}_{\text{Distension Elastance}} \right) V(t) + \left(\underbrace{R_1 + R_2 \dot{V}(t)}_{\text{Rohrer Resistance}} \right) \dot{V}(t) + PEEP \quad (6.2)$$

The overall single compartment model for the parabolic case is defined in Equation 5.7 and is repeated here:

$$P(t) = \left(\underbrace{E_1 (V - V_m)^2}_{\text{Recruitment Elastance}} + \underbrace{E_2 \frac{P(t)}{60}}_{\text{Distension Elastance}} \right) V(t) + \left(\underbrace{R_1 + R_2 \dot{V}(t)}_{\text{Rohrer Resistance}} \right) \dot{V}(t) + PEEP$$

The differing shapes of the parabolic and exponential recruitment function are shown in Figure 6.1. The models are fit to the CURE and McREM data cohorts described in Section 4.

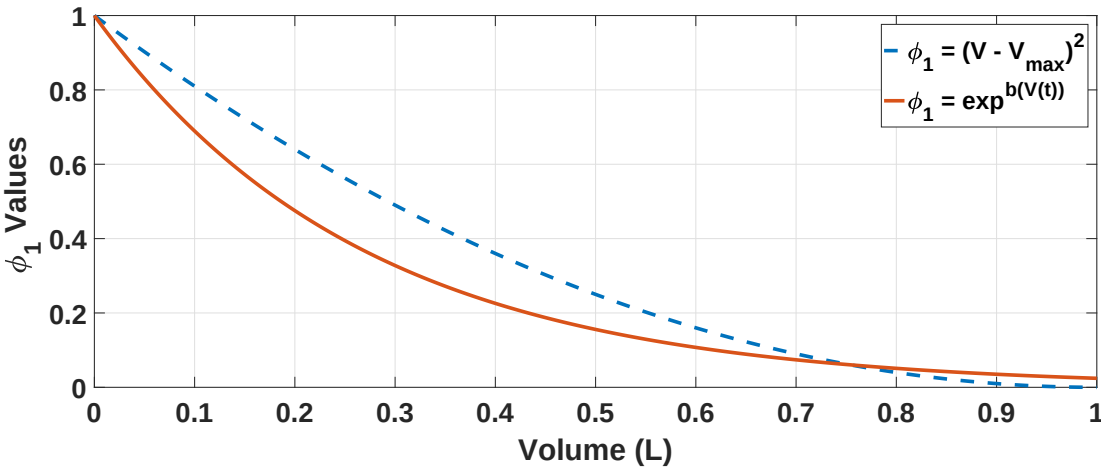

Figure 6.1: Difference in shape between the exponential recruitment function used in Morton, Dickson, Chase, Docherty, Desaive, et al. (2018) and the parabolic function used in Morton et al. (2019). The shapes above assume coefficient values of 1 and an exponential constant, b, of -2.71 for the exponential function.

6.3.1 Exponential Model Identification

Parameters were identified for the entire average breath for both the exponential and parabolic models. Identification methods for the parabolic basis function of Equation 5.2 can be found in Section 5.2.1. In short, a linear least squares method is used to identify $E_1, E_2, R_1 and R_2$, assuming that V_{max} = 1.0. For the exponential model, an iterative linear identification employs three equations defined:

$$\begin{bmatrix} V(t) & V(t) \odot P(t) & \dot{V}(t) & |\dot{V}(t)|\dot{V}(t) \\ \vdots & \vdots & \vdots & \vdots \end{bmatrix} \begin{bmatrix} E_1* \\ E_2 \\ R_1 \\ R_2 \end{bmatrix} = \begin{bmatrix} P(t_i) - PEEP \\ \vdots \end{bmatrix} \tag{6.3}$$

$$\begin{bmatrix} 1 & -V(t) \\ \vdots & \vdots \end{bmatrix} \begin{bmatrix} \ln(E_1) \\ b \end{bmatrix} = \begin{bmatrix} \ln\left(P(t) - PEEP - E_2\frac{P(t)}{60}(V(t) - (R_1 + R_2|\dot{V}(t)|\dot{V}(t)\right) \\ \hline V(t) \\ \vdots \end{bmatrix} \tag{6.4}$$

$$\begin{bmatrix} V(t) \odot P(t) & \dot{V}(t) & |\dot{V}(t)|\dot{V}(t) \\ \vdots & \vdots & \vdots \end{bmatrix} \begin{bmatrix} E_2 \\ R_1 \\ R_2 \end{bmatrix} = \begin{bmatrix} P(t_i) - PEEP - E_1 e^{-bV(t)} V(t) \\ \vdots \end{bmatrix} \tag{6.5}$$

where $\odot$ indicates pointwise multiplication, and where E_2, R_1, and R_2 are estimated from Equation 6.3 to provide an initial estimate for later iterations. Equations 6.4 and 6.5 are then iterated to estimate E_1 and b, then E_2, R_1, and R_2, respectively.

6.3.2 Exponential Model Forward Prediction

Forward simulation of *P(t)* using *V(t)* and $\dot{V}(t)$ inputs at different PEEP levels can be used to assess prediction and thus the potential clinical utility of the model and overall approach. Prediction across PEEP levels requires calculation of the additional lung volume (V_{frc}) induced in a PEEP step relative to the current PEEP. It was assumed V_{frc}

changes would be positive when PEEP was increased and negative when PEEP was decreased.

To determine the change in V_{frc} across a particular PEEP step (V^n_{frc}), a quasi-static solution for V_{frc} was iterated until convergence, $\Delta v^n_{frc} < 0.01\%$, defined:

$$V^n_{frc} = \frac{PEEP_{n+1} - PEEP_n}{E_1 e^{-bV^n_{frc}} + \frac{E_2 PEEP_{n+1}}{60}} \tag{6.6}$$

The final prediction model is shown:

$$P(t) = \left(\underbrace{E_1 e^{b(V(t)+V_{frc})}}_{\text{Recruitment Elastance}} + \underbrace{E_2 \frac{P(t)}{60}}_{\text{Distension Elastance}} \right) V(t) + \left(\underbrace{R_1 + R_2 \dot{V}(t)}_{\text{Rohrer Resistance}} \right) \dot{V}(t) + PEEP \tag{6.7}$$

where V_{frc} modifies the recruitment elastance term.

6.4 Results

6.4.1 Model Fit Results

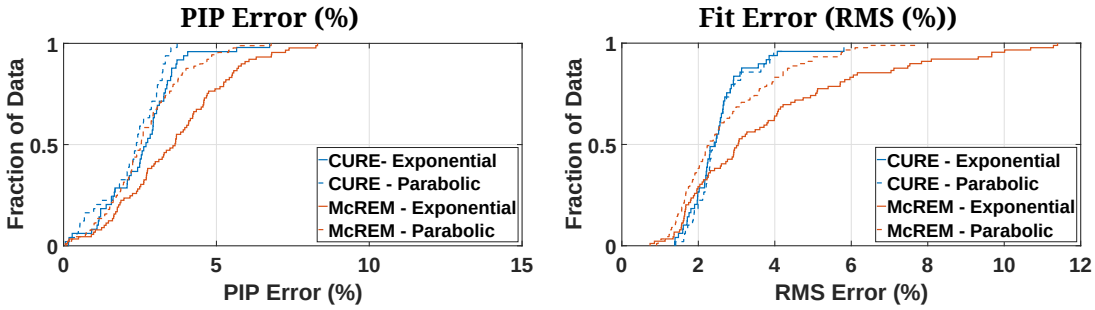

Figure 6.2: CDF comparison of PIP and RMS fitting error results between exponential and parabolic model for elastance as a function of recruitment.

The parabolic and exponential models showed similar accuracy with fitting the data across the CURE cohort. As can be seen in Tables 6.1 and 6.2, both models showed very low fitting error and estimation of the peak inspiratory pressure. More specific comparisons for PIP (%) and RMS (%) error results are shown in the CDFs in Figure 6.2.

The R_2 value was 0 cmH_2O*s/L in most cases as it is constrained from being non-physically

negative. The Rohrer equation's second term using ($|\dot{V}(t)|\dot{V}(t)$) is for high energy flows, where the laminar flows and geometry in mechanical ventilation often do not reach these levels. However, in some cases it is needed for a more accurate fit.

Table 6.1: Summarised model parameters and fitting error (median [IQR]) for the parabolic and exponential model for the CURE cohort.

	Parabolic Model	**Exponential Model**
E_1	5.8 [0.5 - 13.4]	6.7 [0.0 - 14.8]
E_2	55.9 [46.2 - 70.7]	53.9 [46.9 - 74.2]
b	N/A	-5.0 [-7.9 - -2.5]
R_1	6.5 [6.1 - 7.7]	6.4 [6.1 - 7.2]
R_2	0.0 [0.0 - 0.0]	0.0 [0.0 - 0.0]
RMS error (cmH_2O)	1.0 [0.9 - 1.2]	1.1 [1.0 - 1.2]
RMS error (%)	2.4 [2.1 - 2.8]	2.4 [2.0 - 2.8]
PIP error (cmH_2O)	0.8 [0.5 - 1.1]	0.9 [0.6 - 1.2]
PIP error (%)	2.4 [1.6 - 3.0]	2.7 [1.7 - 3.3]

Table 6.2: Summarised model parameters and fitting error (median [IQR]) for the parabolic and exponential model for the McREM cohort.

	Parabolic Model	**Exponential Model**
E_1	14.0 [10.1 - 19.2]	21.7 [14.1 - 27.7]
E_2	47.0 [41.1 - 58.6]	44.0 [32.9 - 61.2]
b	N/A	-3.8 [-5.4 - -0.6]
R_1	8.4 [7.5 - 11.0]	9.0 [7.2 - 12.0]
R_2	0.0 [0.0 - 0.0]	1.4 [0.0 - 3.8]
RMS error (cmH_2O)	0.6 [0.5 - 0.9]	0.9 [0.7 - 1.3]
RMS error (%)	2.3 [1.7 - 3.6]	3.0 [1.9 - 5.1]
PIP error (cmH_2O)	1.0 [0.8 - 1.3]	1.4 [0.9 - 2.0]
PIP error (%)	2.5 [1.7 - 3.4]	3.6 [2.2 - 4.7]

6.4.2 Model Prediction Results

Impact of Recruitment Function Shape

Model predictions for the parabolic model have low RMS and PIP prediction errors across all PEEP changes studied for both cohorts, as shown in Tables 6.3 and 6.4.

Figure 6.3a shows PIP prediction error is lowest across the entire PEEP range studied when the parabolic basis function is used, compared to the exponential model. The difference in error also includes much lower outliers so the 95th percentile errors in Figure 6.3a are 30-40% lower (relative) for both cohorts. Overall, fit and prediction

Table 6.3: Comparison of prediction error (PIP) across the entire clinical recruitment manoeuvre range (14cmH_2O) for the parabolic and exponential model for the CURE and McREM cohorts.

CURE Cohort				
PEEP Change	**PIP Error (cmH_2O)**		**PIP Error (%)**	
	Parabolic Model	**Exponential Model**	**Parabolic Model**	**Exponential Model**
2 cmH_2O	2.8 [2.8 - 3.6]	3.3 [-0.2 - 5.0]	4.1 [2.6 - 5.2]	6.9 [3.4 - 11.2]
4 cmH_2O	1.4 [0.8 - 1.7]	2.9 [1.3 - 3.9]	3.6 [2.7 - 5.0]	7.1 [3.5 - 9.6]
6 cmH_2O	-1.0 [-2.5 - 1.9]	1.7 [-1.4 - 7.2]	4.5 [3.2 - 6.8]	5.3 [3.5 - 14.9]
8 cmH_2O	1.5 [0.3 - 2.6]	4.1 [1.8 - 5.9]	3.6 [1.9 - 6.6]	9.1 [4.5 - 14.2]
10 cmH_2O	-0.6 [-2.2 - 3.7]	4.5 [1.1 - 10.4]	6.3 [4.5 - 8.3]	9.9 [3.1 - 21.3]
12 cmH_2O	2.5 [1.5 - 3.4]	3.4 [-0.1 - 9.2]	7.1 [3.5 - 8.1]	8.3 [1.6 - 20.5]
14 cmH_2O	0.3 [-0.9 - 4.3]	9.6 [2.9 - 13.8]	4.5 [1.0 - 8.8]	19.4 [6.6 - 29.9]
Total	**1.4 [-0.5 - 2.2]**	**3.2 [1.1 - 5.9]**	**4.5 [2.8 - 6.5]**	**8.3 [3.4 - 14.1]**
McREM Cohort				
PEEP Change	**PIP Error (cmH_2O)**		**PIP Error (%)**	
	Parabolic Model	**Exponential Model**	**Parabolic Model**	**Exponential Model**
2 cmH_2O	1.1 [0.3 - 1.4]	3.0 [1.2 - 4.2]	2.7 [1.6 - 3.5]	6.3 [2.9 - 10.8]
4 cmH_2O	1.4 [0.2 - 2.0]	2.7 [0.9 - 4.6]	3.5 [2.0 - 4.4]	6.3 [4.0 - 11.2]
6 cmH_2O	1.7 [-0.1 - 2.4]	2.3 [0.8 - 4.7]	4.3 [3.3 - 5.6]	6.5 [4.0 - 11.2]
8 cmH_2O	2.2 [0.3 - 2.9]	1.6 [-1.0 - 6.3]	5.2 [3.8 - 7.0]	5.5 [3.1 - 13.9]
10 cmH_2O	2.6 [1.4 - 3.6]	0.9 [-2.0 - 4.8]	6.2 [5.0 - 9.1]	4.7 [2.7 - 13.2]
12 cmH_2O	3.4 [2.1 - 5.5]	1.0 [-3.1 - 10.6]	7.2 [5.6 - 11.5]	10.6 [3.4 - 22.0]
14 cmH_2O	6.4 [3.3 - 7.2]	12.8 [4.1 - 14.8]	13.1 [6.7 - 15.1]	26.0 [8.3 - 31.2]
Total	**1.4 [0.3 - 2.2]**	**2.5 [0.9 - 4.6]**	**3.9 [2.4 - 5.3]**	**6.4 [3.5 - 11.5]**

error were low for the parabolic form of the model for all data sets studied.

Prediction error (median [IQR]) for all patients increased as expected with increasing PEEP changes over the range studied (2 cmH_2O - 14 cmH_2O). PIP prediction error was 1.4 [-0.5 - 2.2] cmH_2O (4.5 [2.8 - 6.5]%) for PEEP changes up to 14 cmH_2O using the parabolic model and 3.2 [1.1 - 5.9] cmH_2O and (8.3 [3.4 - 14.1]%) for the exponential model. The prediction error for the parabolic model across the relevant range is likely clinically insignificant, given a 0.5-2 cmH_2O variation in breath to breath PIP.

Examples of specific predictions for the CURE cohort are shown in Figures 6.11 - 6.14 for Patient 1, with predictions starting at 11 cmH_2O, 15 cmH_2O, 23 cmH_2O and 27 cmH_2O, respectively. These figures are shown at the end of the chapter. As can be seen, prediction

Table 6.4: Comparison of prediction fitting error (RMS) across the entire clinical recruitment manoeuvre range (14cmH_2O) for the parabolic and exponential model for the CURE and McREM cohorts.

CURE Cohort				
PEEP Change	**RMS Error (cmH_2O)**		**RMS Error (%)**	
	Parabolic Model	**Exponential Model**	**Parabolic Model**	**Exponential Model**
2 cmH_2O	1.3 [1.0 - 1.4]	2.0 [1.5 - 2.4]	1.3 [-1.0 - 2.2]	4.0 [3.7 - 4.0]
4 cmH_2O	1.1 [1.0 - 1.2]	1.6 [1.5 - 2.1]	2.6 [2.2 - 3.0]	3.4 [2.4 - 4.1]
6 cmH_2O	1.7 [1.4 - 2.0]	2.6 [1.8 - 3.0]	3.6 [3.1 - 4.9]	4.0 [3.3 - 5.2]
8 cmH_2O	1.2 [1.1 - 1.3]	2.0 [1.7 - 2.1]	2.3 [2.1 - 3.2]	4.1 [2.4 - 4.6]
10 cmH_2O	1.8 [1.6 - 2.0]	2.7 [2.3 - 3.9]	3.8 [3.3 - 4.3]	3.7 [3.0 - 6.2]
12 cmH_2O	1.3 [1.3 - 1.6]	2.4 [2.0 - 3.0]	3.2 [2.3 - 3.8]	3.9 [2.2 - 5.6]
14 cmH_2O	1.9 [1.7 - 2.0]	3.2 [2.8 - 5.0]	3.8 [2.6 - 4.0]	5.3 [2.9 - 7.7]
Total	**1.2 [1.1 - 1.6]**	**2.1 [1.6 - 2.6]**	**2.9 [2.3 - 3.6]**	**3.6 [2.8 - 4.8]**
McREM Cohort				
PEEP Change	**RMS Error (cmH_2O)**		**RMS Error (%)**	
	Parabolic Model	**Exponential Model**	**Parabolic Model**	**Exponential Model**
2 cmH_2O	0.7 [0.6 - 1.0]	1.6 [1.1 - 2.2]	2.3 [1.7 - 3.6]	4.1 [2.6 - 6.8]
4 cmH_2O	0.8 [0.6 - 1.0]	1.9 [1.4 - 2.4]	2.3 [1.8 - 3.2]	4.2 [3.2 - 6.3]
6 cmH_2O	0.9 [0.7 - 1.1]	2.0 [1.6 - 2.7]	2.5 [1.9 - 2.9]	4.3 [3.4 - 6.0]
8 cmH_2O	1.1 [0.9 - 1.4]	2.1 [1.7 - 3.0]	2.8 [2.1 - 3.3]	4.4 [3.3 - 7.4]
10 cmH_2O	1.3 [1.0 - 1.9]	2.5 [1.4 - 3.1]	3.8 [2.4 - 4.0]	4.6 [3.1 - 6.3]
12 cmH_2O	1.6 [1.2 - 2.3]	2.9 [1.7 - 3.4]	3.8 [3.2 - 5.1]	5.2 [3.8 - 5.7]
14 cmH_2O	2.9 [1.6 - 2.9]	4.4 [1.9 - 4.7]	6.3 [4.1 - 6.6]	7.2 [3.8 - 7.6]
Total	**0.9 [0.6 - 1.1]**	**2.0 [1.2 - 2.7]**	**2.5 [1.9 - 3.4]**	**4.3 [3.1 - 6.4]**

accuracy increases as the prediction interval decreases. It is expected this trend results from greater certainty in the proportions of recruitment and distension the closer you are to the fitting PEEP.

The McREM cohort showed a similar results trend, as shown in Figures 6.5 - 6.10. These figures are shown at the end of the chapter. The prediction intervals shown range from 2 cmH_2O to 12 cmH_2O. However,intervals of up to 20 cmH_2O were predicted. The McREM data varied from the CURE cohort as each patient received an end-inspiratory pause. As can be seen, the parabolic model was more successful at capturing lung mechanics throughout the end-inspiratory pause. In addition, the exponential model often significantly 'undershot' pressure at the beginning of expiration. However, the parabolic model was more successful at adjusting to the sudden change in lung me-

chanics at this point.

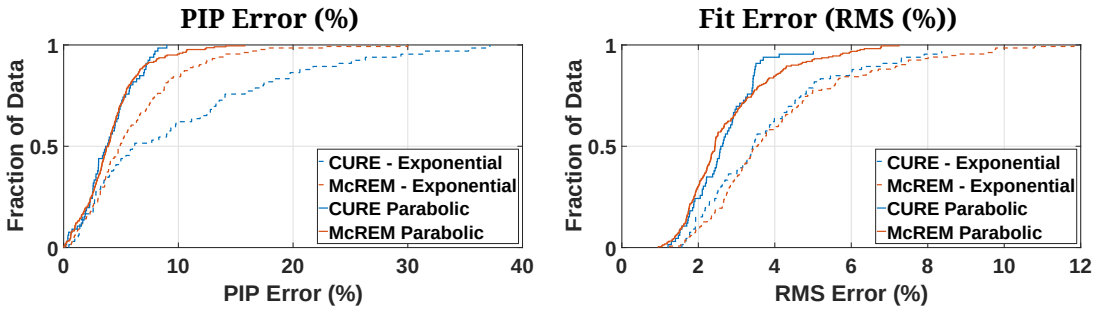

Figure 6.3: CDF comparison of PIP and RMS prediction error results between exponential and parabolic model for elastance as a function of recruitment.

Prediction fit error (RMS) was also lower in the CURE and McREM cohorts, as shown in Figure 6.3b. More specific results can be seen in the boxplots in Figure 6.4, which presents these results by Δ PEEP prediction interval, again showing little sensitivity to this value for the new model. Across each cohort, the parabolic model fit the lung mechanics better throughout the entire breath and more accurately predicted PIP.

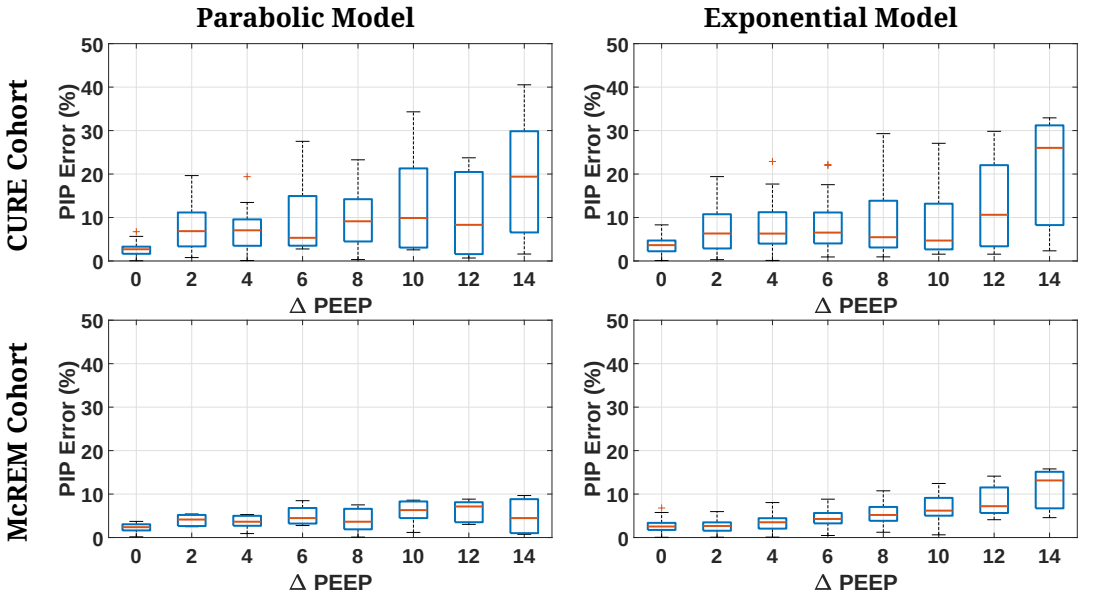

Figure 6.4: Boxplot comparisons of PIP prediction results between exponential and parabolic model for elastance as a function of recruitment. The box plots reflect the CDF in Figure 6.3.

6.5 Discussion

It is always possible that the generic hyperbolic and linear elastance basis functions and/or the Rohrer Equation based resistance basis functions are not the exact or optimal form. Prior work has used exponential recruitment basis functions (Albert et al., 2009; Bates & Irvin, 2002; Crotti et al., 2001; Graham et al., 2005; Harris et al., 2000; Massa et al., 2008; Medoff et al., 2000; Morton, Dickson, Chase, Docherty, Desaive, et al., 2018; Mutch et al., 2000; Owens et al., 2008; Ranieri et al., 1991; Sundaresan et al., 2009; Venegas et al., 1998; Williamson et al., 2011) and other similar shapes may better suit some patients or disease states. However, given the breath to breath variability in typical patients and any noise on the data, differentiating between several similar shaped functions would be difficult. Equally, prior works examining more complex basis functions found no improvement and greater identifiability problems, where identifiability limits the complexity of possible basis function shapes given the limited data (Chase et al., 2018; Docherty et al., 2011).

The higher complexity of the exponential model resulted in tradeoffs between different parameters. However, the simplicity of the parabolic recruitment model enabled clear shapes to be developed. This outcome ensured that the prediction accuracy was consistent, allowing for a higher level of accuracy.

6.6 Summary

In both cohorts studied, the parabolic model both better represented lung mechanics throughout the entire breath and was more accurate at predicting PIP. As was shown in 6.4, significant reductions in prediction error were seen across the entire clinical pressure range when the parabolic model was used as opposed to the exponential. Additionally, as shown in Figures 6.5 - 6.10, the parabolic model was much more effective at capturing lung mechanics throughout an end-inspiratory pause. The parabolic form

of the model shall accordingly be used for the rest of the analyses in this thesis.

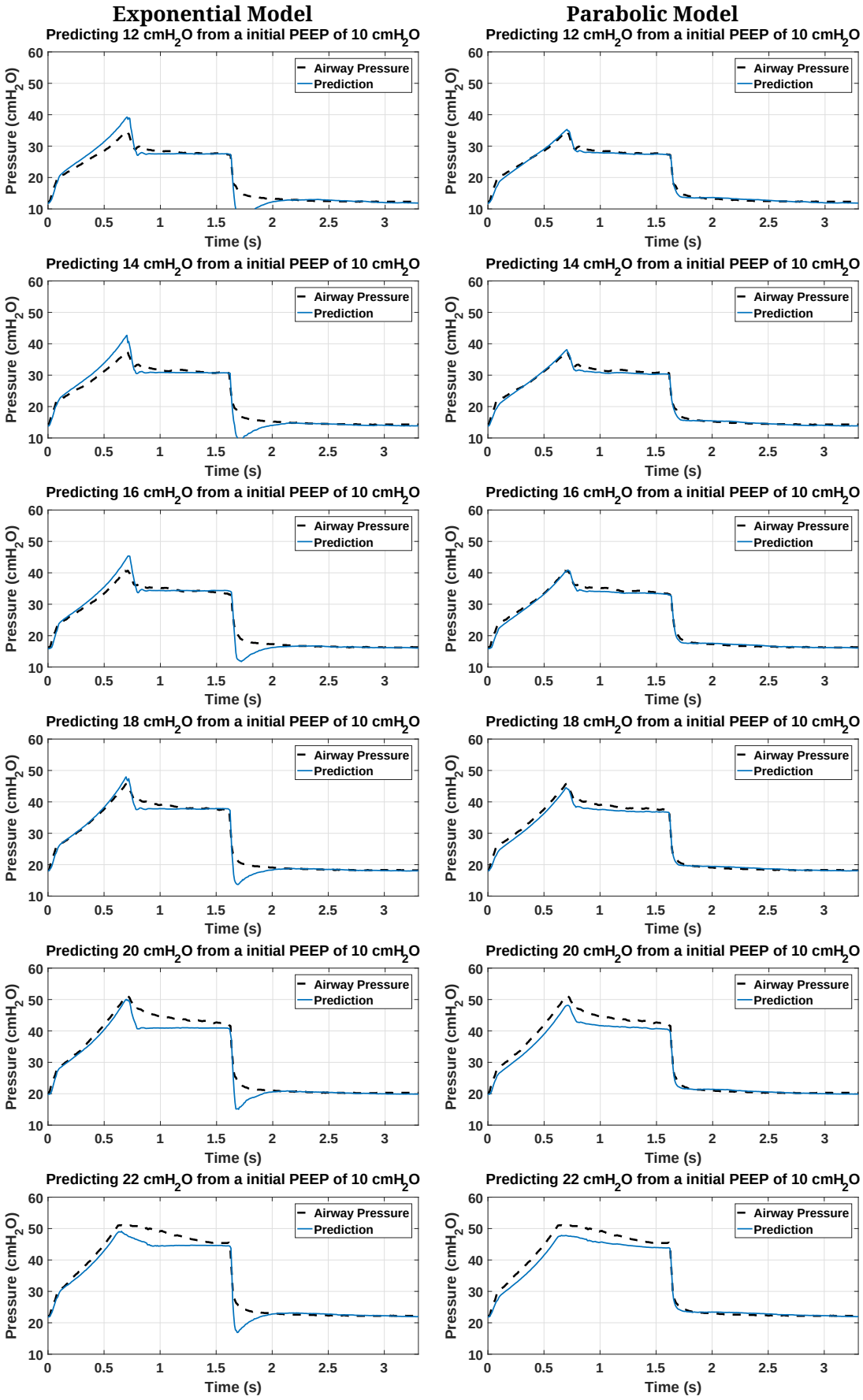

Figure 6.5: Comparison of model prediction results for Patient 5 of the McREM cohort using the exponential and parabolic recruitment functions. Starting at a PEEP of 10 cmH2O, PEEP levels of 12 cmH2O, 14 cmH2O, 16 cmH2O, 18 cmH2O, 20 cmH2O and 22 cmH2O are predicted.

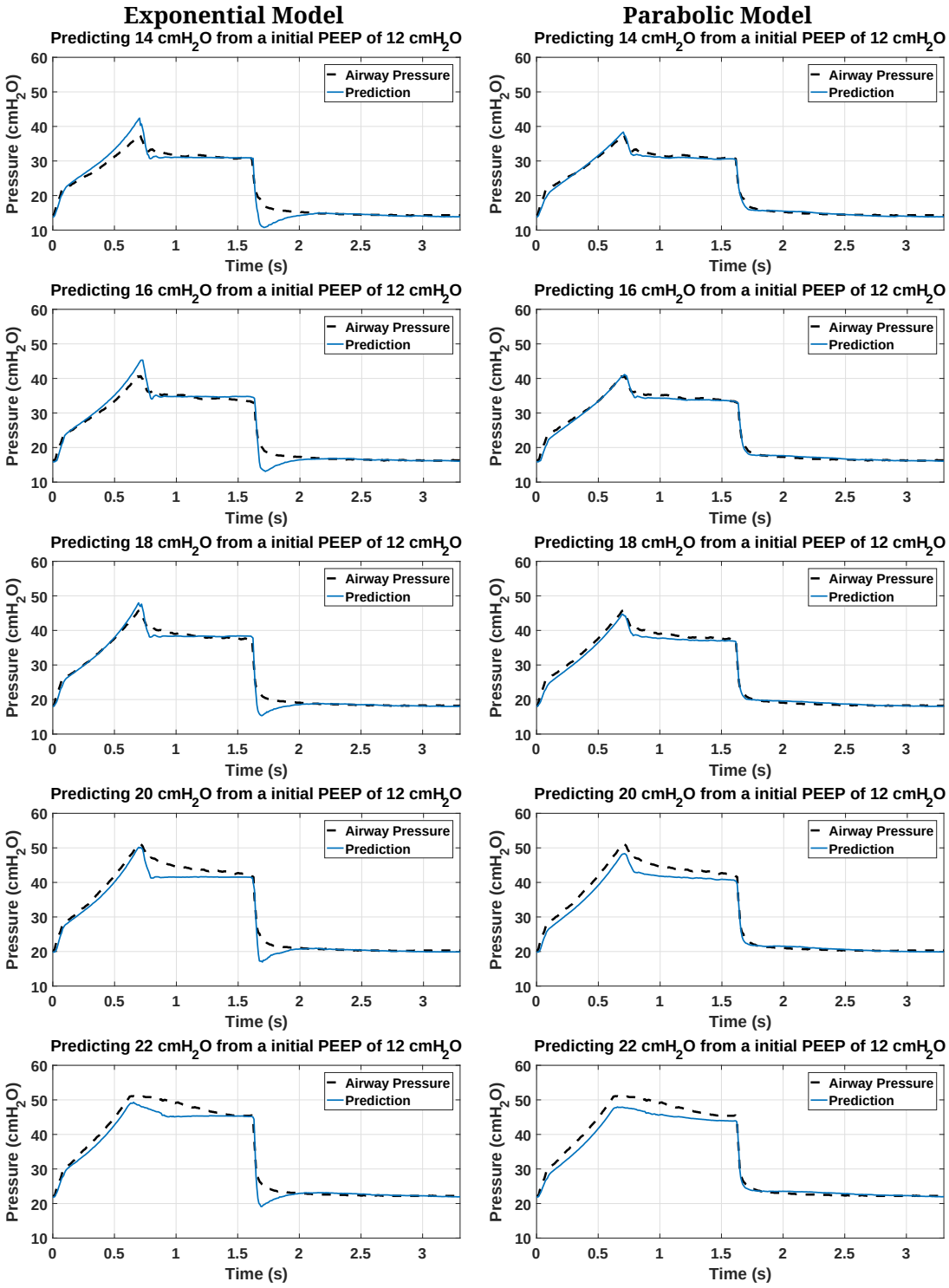

Figure 6.6: Comparison of model prediction results for Patient 5 of the McREM cohort using the exponential and parabolic recruitment functions. Starting at a PEEP of 12 cmH2O, PEEP levels of 14 cmH2O, 16 cmH2O, 18 cmH2O, 20 cmH2O and 22 cmH2O are predicted.

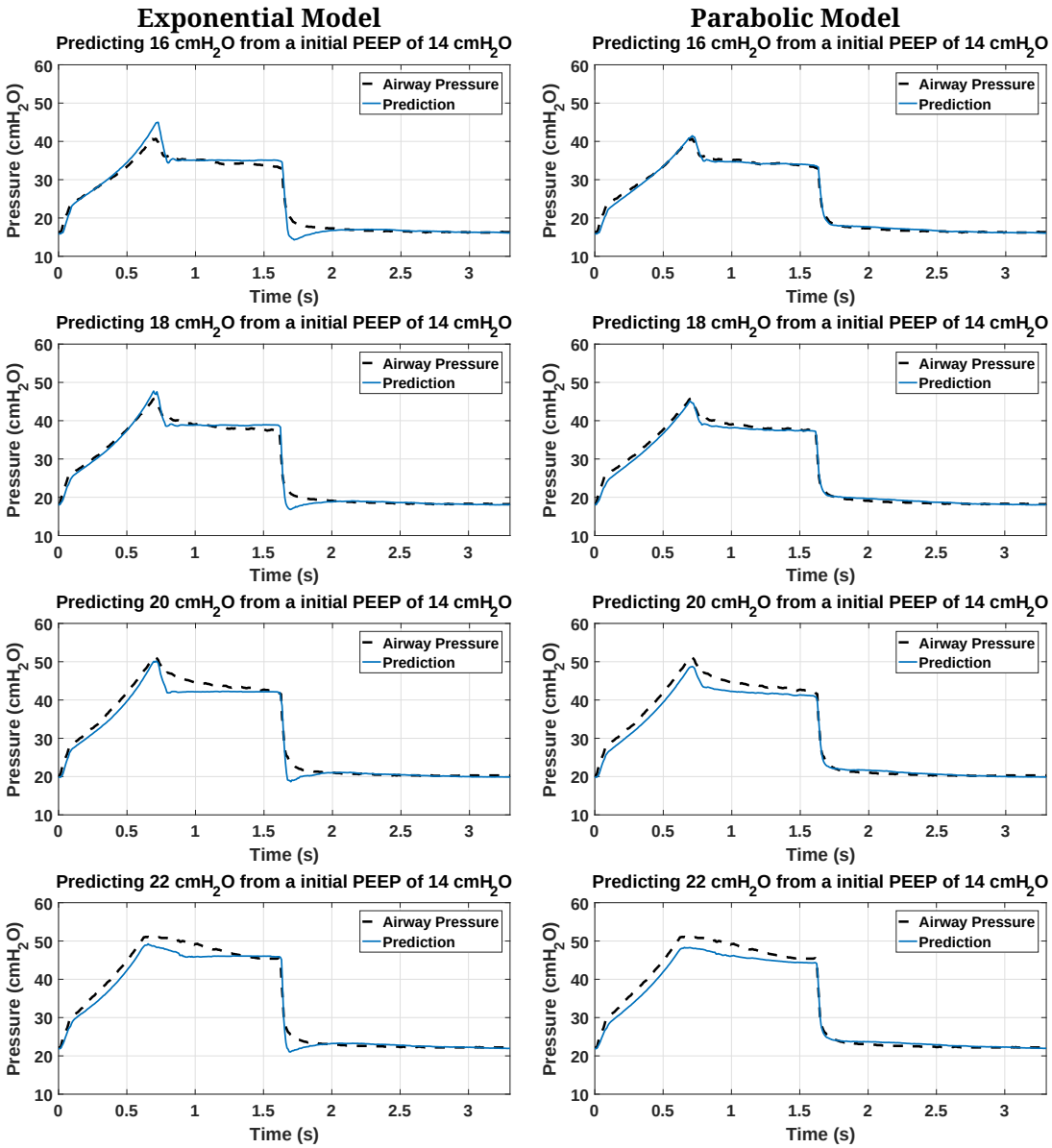

Figure 6.7: Comparison of model prediction results for Patient 5 of the McREM cohort using the exponential and parabolic recruitment functions. Starting at a PEEP of 14 cmH2O, PEEP levels of 16 cmH2O, 18 cmH2O, 20 cmH2O and 22 cmH2O are predicted.

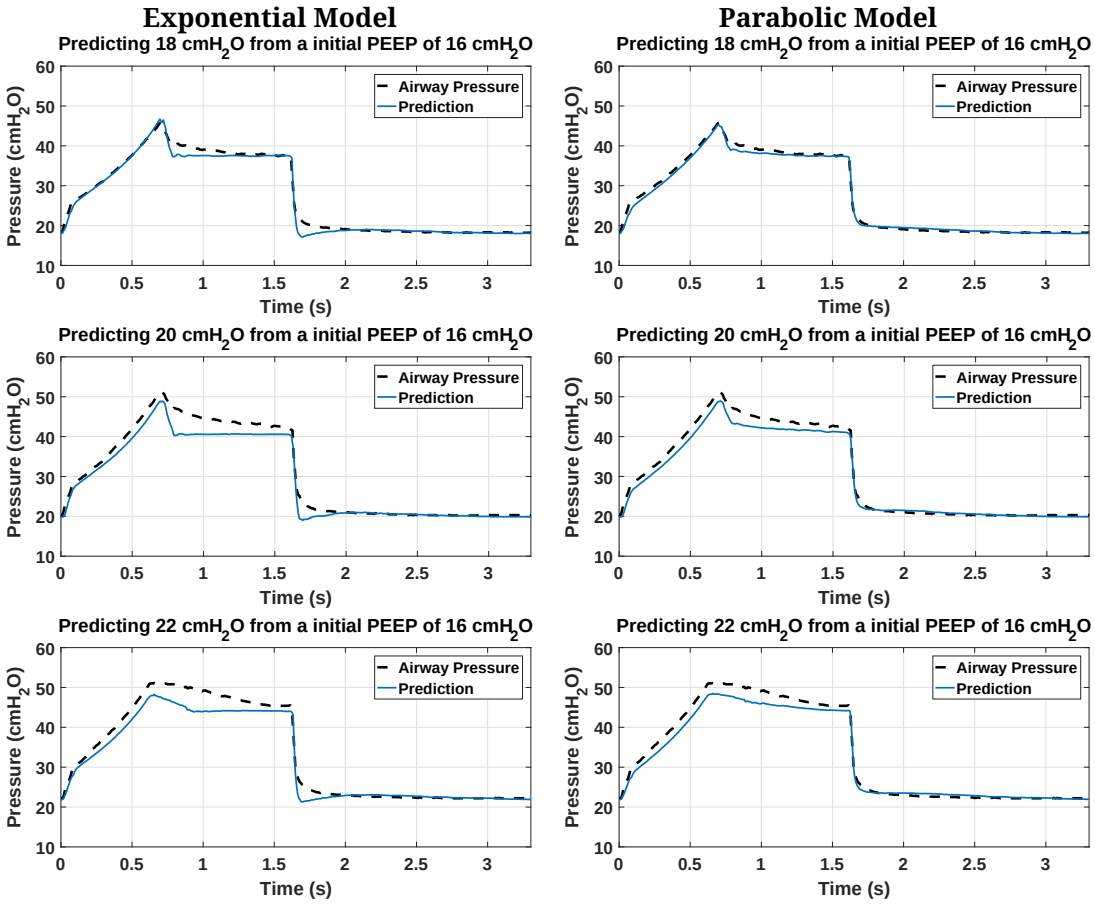

Figure 6.8: Comparison of model prediction results for Patient 5 of the McREM cohort using the exponential and parabolic recruitment functions. Starting at a PEEP of 16 cmH2O, PEEP levels of 18 cmH2O, 20 cmH2O and 22 cmH2O are predicted.

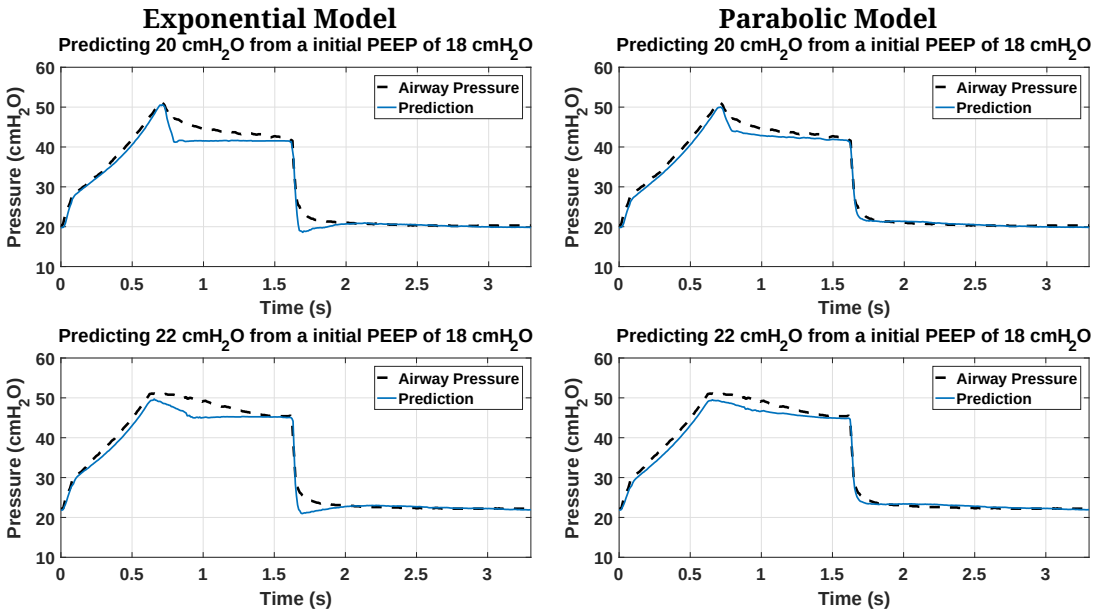

Figure 6.9: Comparison of model prediction results for Patient 5 of the McREM cohort using the exponential and parabolic recruitment functions. Starting at a PEEP of 18 cmH2O, PEEP levels of 20 cmH2O and 22 cmH2O are predicted.

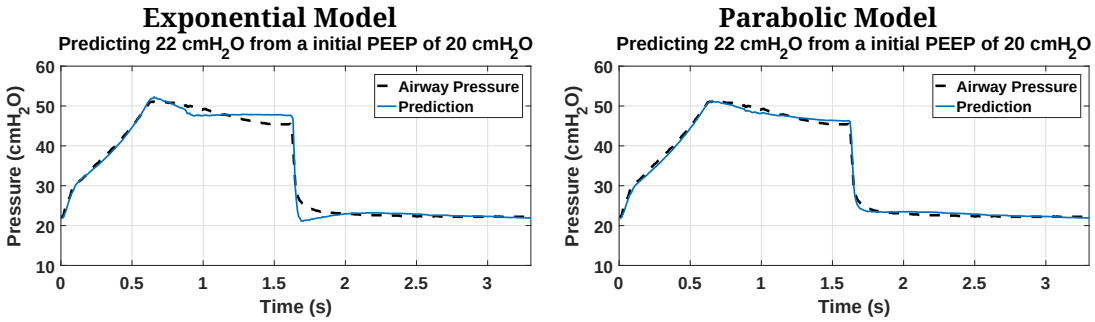

Figure 6.10: Comparison of model prediction results for Patient 5 of the McREM cohort using the exponential and parabolic recruitment functions. Starting at a PEEP of 20 cmH2O, the PEEP level of 22 cmH2O is predicted.

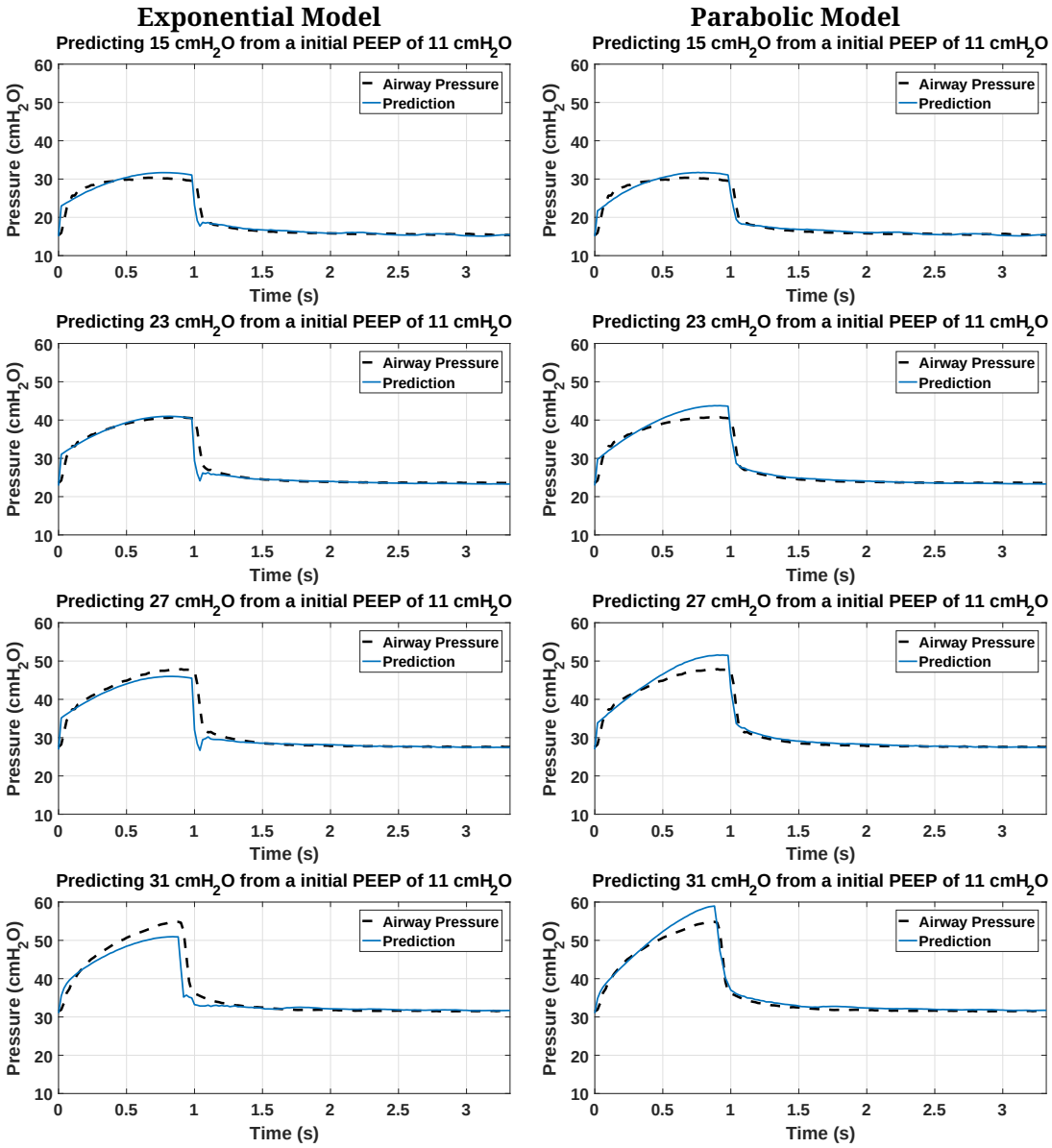

Figure 6.11: Comparison of model prediction results for Patient 1 of the CURE cohort using the exponential and parabolic recruitment functions. Starting at a PEEP of 11 cmH2O, PEEP levels of 15 cmH2O, 23 cmH2O, 27 cmH2O and 31 cmH2O are predicted.

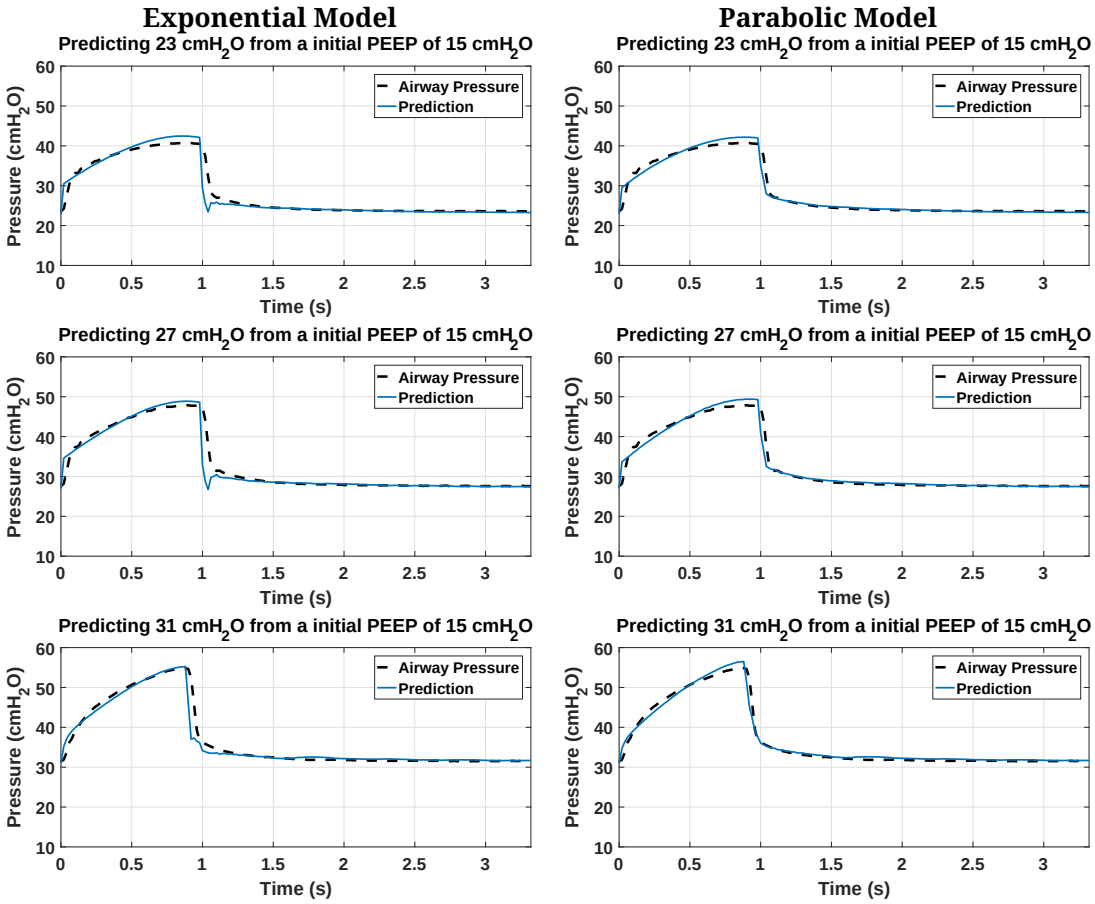

Figure 6.12: Comparison of model prediction results for Patient 1 of the CURE cohort using the exponential and parabolic recruitment functions. Starting at a PEEP of 15 cmH2O, PEEP levels of 23 cmH2O, 27 cmH2O and 31 cmH2O are predicted.

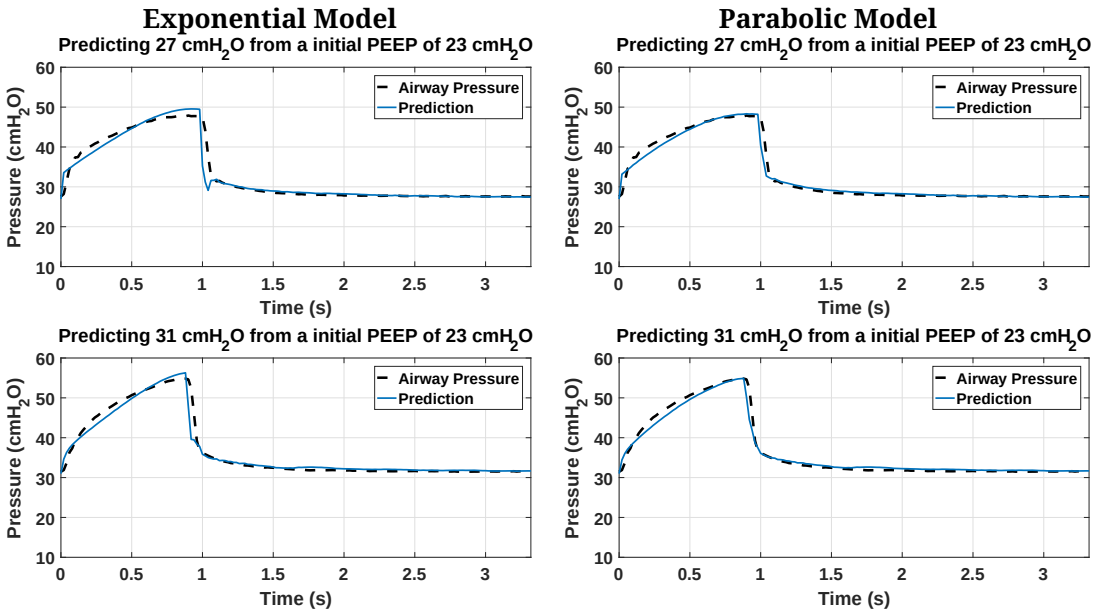

Figure 6.13: Comparison of model prediction results for Patient 1 of the CURE cohort using the exponential and parabolic recruitment functions. Starting at a PEEP of 23 cmH2O, PEEP levels of 27 cmH2O and 31 cmH2O are predicted.

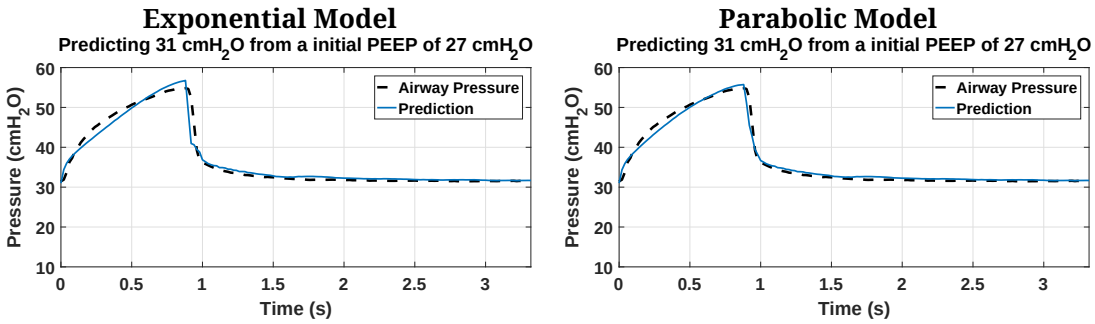

Figure 6.14: Comparison of model prediction results for Patient 1 of the CURE cohort using the exponential and parabolic recruitment functions. Starting at a PEEP of 27 cmH_2O, the PEEP level of 31 cmH_2O is predicted.

CHAPTER 7

Impact of Expiration Data on Prediction

7.1 Introduction

Most pulmonary modelling approaches to optimising mechanical ventilation focuses on the physical changes during inspiration. This focus is due to the increased risk of over-distension and VILI throughout inflation, where expiration is a lessening of these pressures, volumes, and thus risks. However, expiratory lung mechanics differ from those during inspiration (Howe et al., 2018; Möller, Zhao, Stahl, Schumann, & Guttmann, 2008; Schumann et al., 2014; van Drunen, Chiew, et al., 2013). It is believed data from expiration used in concert with that from inspiration could provide useful additional information about patient lung condition to enable more accurate model prediction.

The duration of inspiration and expiration are often unequal in spontaneous breathing, and also in mechanical ventilation to ensure that air has a sufficient time to escape the alveoli. . The inspiration:expiration ratio (I/E ratio) is set to 1:2 in both data cohorts outlined in Sections 4.2 and 4.3 considered in this chapter. The impact of normalising

the expiration data to ensure an equal weighting to inspiration is assessed to find if this modelling and identification method choice improves model fit and prediction.

Work has been done using body plethysmography indicating elastance and airway resistance vary between inspiration and expiration (Möller et al., 2008). Lucangelo et al. suggested using linear least squares fitting to fit a single compartment linear model of Equation 3.1 to inspiration and expiration data independently (Lucangelo et al., 2007). More recent work indicated fitting model parameters to expiration alone could provide erroneous results (Möller et al., 2008), indicating expiration may contain unique mechanics or dynamics not present in inspiration. To investigate this possibility, the model parameters are only identified using inspiration data but are used to predict lung mechanics across the entire breath. This outcome is compared to:

- Fitting the model to inspiration and only predicting inspiration
- Fitting the model to the entire breath and predicting across the entire breath.

These comparisons and analyses allow determination of the presence and impact of any expiration specific mechanics and/or dynamics.

This chapter uses data from the CURE and McREM cohorts to assess the usefulness of expiration data in pulmonary modelling. There is a particular focus on how it impacts the accuracy of elastance prediction throughout recruitment manoeuvres (Morton, Docherty, et al., 2018; Morton et al., 2019).

7.2 Methods

7.2.1 Patient Data

Pressure and flow data from the N=21 invasively ventilated patients diagnosed with acute respiratory distress syndrome (ARDS) from ICUs in Germany (N=17) and New Zealand (N=4) (Davidson et al., 2014; Stahl et al., 2006) outlined in Chapter 4 was analysed.

7.2.2 Impact of Use of Inspiration and Expiration Data on Prediction Accuracy

The model used in this study was the model defined in Section 5.2, specifically Equations 5.7 and 5.10 respectively, as reproduced below.

Overall model for parameter fitting (Equation 5.7):

$$P(t) = \left(\underbrace{E_1(V - V_m)^2}_{\text{Recruitment Elastance}} + \underbrace{E_2 \frac{P(t)}{60}}_{\text{Distension Elastance}} \right) V(t) + \left(\underbrace{R_1 + R_2 \dot{V}(t)}_{\text{Rohrer Resistance}} \right) \dot{V}(t) + PEEP$$

Overall model for prediction (Equation 5.10):

$$P(t) = \left(\underbrace{E_1((V + V_{frc}) - V_m)^2}_{\text{Recruitment Elastance}} + \underbrace{E_2 \frac{P(t)}{60}}_{\text{Distension Elastance}} \right) V(t) + \left(\underbrace{R_1 + R_2 \dot{V}(t)}_{\text{Rohrer Resistance}} \right) \dot{V}(t) + PEEP$$

The model parameters were identified and used for prediction for three cases to test the minimum amount of data required for prediction, and whether the expiratory section of the breath contains different mechanics or dynamics (Möller et al., 2008). Expiration is defined as the point at which ventilator flow first becomes negative after PIP is reached. In the McREM protocol, this point is reached after an end-inspiratory pause, defined in Section 4.3.1. In addition, the first five data points of each breath were excluded, as these points are more reflective of ventilator PEEP adjustment and Monitoring Procedure (PUMP) dynamics than the pressure response of the lung.

The following cases are used for model identification and prediction and compared:

- **Case 1:** The full breath
- **Case 2:** Only the inspiratory section of the breath.
- **Case 3:** Only the inspiratory section for identification, with prediction across the entire breath.

The first two cases both identify the model and predict over the specified portions of the breathing cycle. The last case assesses whether expiration contains unique dynamics, and thus identifies the model over only a portion of the breath, while assessing its

performance across the entire breath.

7.2.3 Necessity of Normalising Expiration Data to the the Length of Inspiration

The I/E ratio in mechanical ventilation often requires a longer expiration time to ensure air is not trapped in the alveoli. This analysis assesses whether or not expiration data should be normalised to the length of inspiration to optimise model accuracy. Both the McREM and CURE cohorts use an I/E ratio of 1:2. To normalise this data, all input measurements (flow and pressure) during expiration were halved prior to model identification and prediction. This data reduction was then compared to the model fit and prediction of Case 1 (fitting and predicting across the entire breath) to assess whether or not normalisation is required.

7.3 Results

7.3.1 General Results

Table 7.1: Impact of the inclusion of expiratory data in prediction accuracy for PEEP increases of up to 16 cmH_2O, indicated by PIP % error (median [IQR]) in the CURE and McREM cohorts. Case 1, Case 2 and Case 3 studied.

CURE Cohort		
	RMS Error (cmH_2O)	**PIP Error (%)**
Case 1: entire breath	1.2 [1.0 - 1.5]	3.8 [2.5 - 5.4]
Case 2: fitted to inspiration	2.2 [1.3 - 3.5]	5.5 [3.8 - 8.7]
Case 3: fitted to inspiration with RMS assessed across entire breath	2.6 [2.0 - 3.0]	5.5 [3.8 - 8.7]
McREM Cohort		
	RMS Error (cmH_2O)	**PIP Error (%)**
Case 1: entire breath	0.9 [0.6 - 1.1]	3.9 [2.4 - 5.3]
Case 2: fitted to inspiration	1.0 [0.7 - 1.5]	1.5 [0.5 - 3.6]
Case 3: fitted to inspiration with RMS assessed across entire breath	1.0 [0.8 - 1.4]	1.5 [0.5 - 3.6]

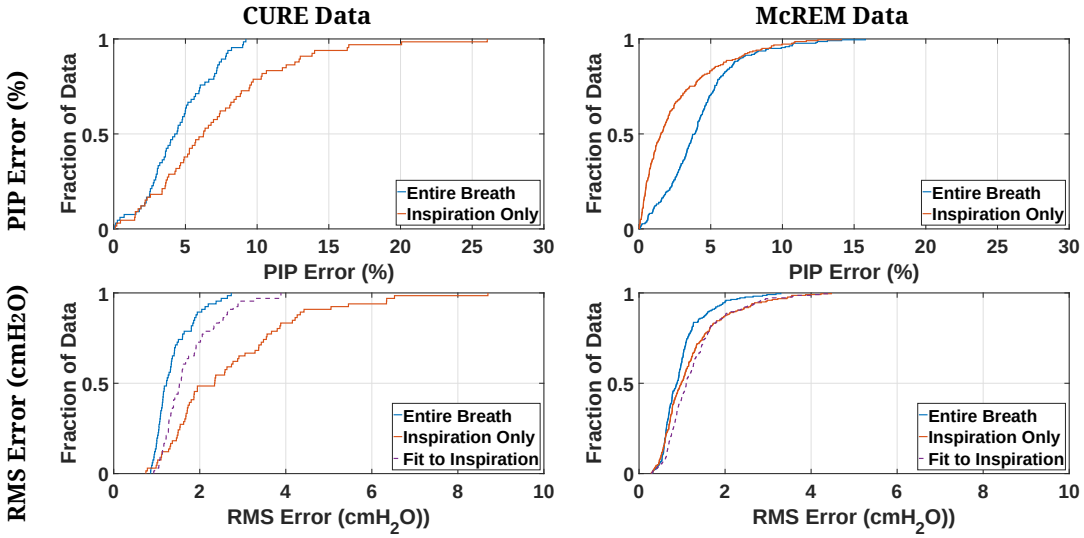

Figure 7.1: Impact of the inclusion of expiration data on prediction of PIP and prediction fit error (RMS) for the CURE and McREM cohorts.

The impact of using different sections of the breath data to fit elastance and resistance was explored for the model outlined in Chapter 5. Results for both cohorts are shown in Table 7.1 and cover Cases 1, 2 and 3, as defined in Section 7.2.2. These results are split into each of the two cohorts, as the end-inspiratory pause used in the McREM clinical trial has an impact on the ability of the model to predict lung mechanics using only

inspiration data to identify the model.

Fitting the data to the entire breath (Case 1) showed a significant improvement to the prediction accuracy in the CURE cohort. In contrast, the inclusion of expiratory data (Case 1) in the model identification did not improve PIP prediction for the McREM data. However, as the PIP (%) IQR error was still relatively low (3.9 [2.4 - 5.3]), it is recommended to continue to use the entire breath for prediction so as to avoid potential parameter tradeoff (Docherty et al., 2011).

Case 3 was included to assess whether or not the expiratory section of the breath included different enough mechanics to warrant a separate fit to inspiration. In the CURE cohort data, there was a significant reduction model prediction accuracy for this case. This result indicates that expiration data may possess significantly different features to inspiration. However, the larger McREM cohort did not show much difference between Case 3 and either Case 1 or 2. Overall, using all available data improved the prediction fit error in both cohorts, as seen in Figures 7.1c and 7.1d and is the best option for improved fitting of lung mechanics.

7.3.2 Specific Cohort Results

CURE Cohort

Figure 7.2 shows the difference in prediction across PEEP levels for Case 1 and Case 2 for a typical patient of the CURE cohort. Case 1 shows a much higher level of accuracy in model fit across inspiration and in prediction of PIP. This difference is particularly pronounced as the prediction interval increases to 8 cmH_2O, where PIP is significantly underestimated. As under-prediction of PIP could lead to less conservative and higher risk treatment decisions, use of the entire breath to fit model parameters is strongly recommended for this clinical cohort.

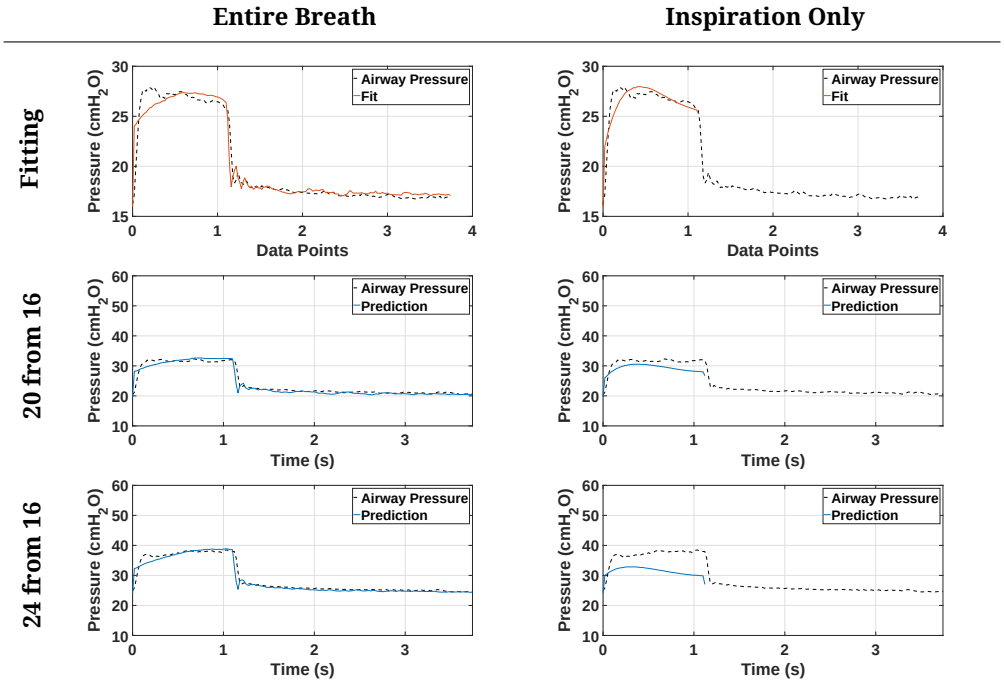

Figure 7.2: Typical effect of the inclusion of expiratory data on prediction across PEEP steps. Patient 2, CURE cohort. Fit of a PEEP of 16 cmH_2O, prediction of a PEEP level of 20 cmH_2O from a PEEP of 16 cmH_2O, and prediction of a PEEP level of 24 cmH_2O from a PEEP level of 16 cmH_2O are shown.

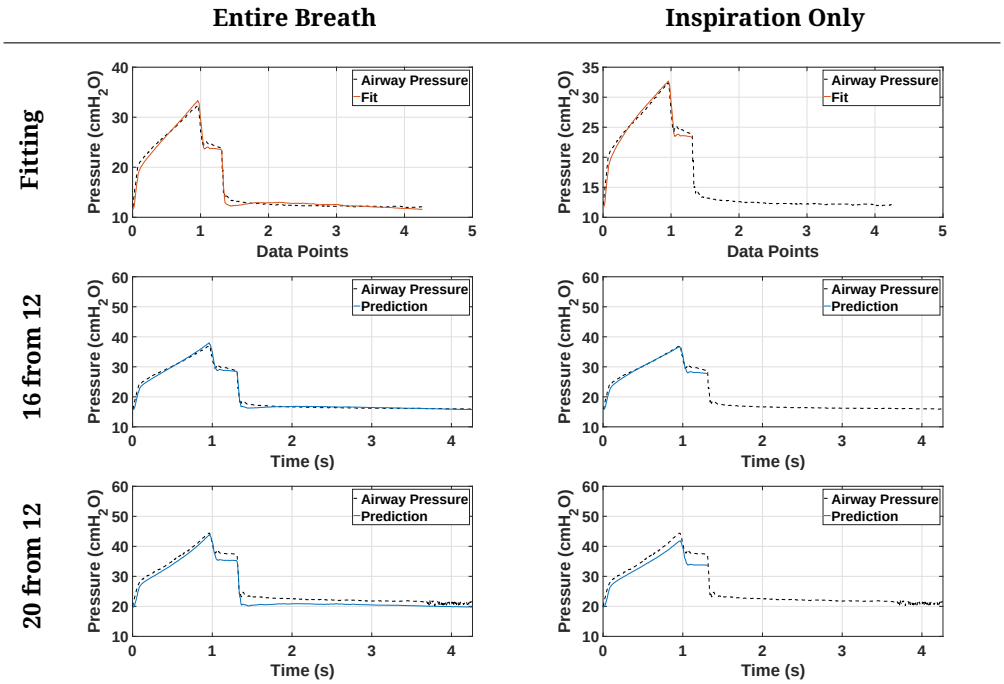

Figure 7.3: Typical effect of the inclusion of expiratory data on prediction. Patient 11, McREM cohort. Fit of a PEEP of 12 cmH_2O, prediction of a PEEP level of 16 cmH_2O from a PEEP of 12 cmH_2O, and prediction of a PEEP level of 20 cmH_2O from a PEEP level of 12 cmH_2O are shown.

McREM Cohort

Both Case 1 and Case 2 provided similar prediction accuracy throughout inspiration up until PIP was achieved, as shown in Figure 7.3. However, in this particular case, the end-inspiratory pause was more accurately predicted when data from the entire breath was used.

7.3.3 Effect of Normalisation on Results

Normalising the expiration data to ensure an equal weighting fit to inspiration data did not improve prediction in the two cohorts studied as shown in Figure 7.4. While overall PIP (%) error stayed fairly constant when normalisation was carried out across both cohorts (from 4.5 [2.8 - 6.5]% to 4.0 [1.6 - 5.6]% for the CURE cohort and from 3.9 [2.4 - 5.3]% to 4.5 [2.5 - 7.0]% for the McREM cohort), the fit error showed a significant increase. While the un-normalised CURE fit had an RMS error of 1.2 [1.1 - 1.6] cmH_2O, when normalised this error increased to 9.2 [8.2 - 10.6] cmH_2O. Similar results were seen for the McREM cohort, with an increase from 0.9 [0.6 - 1.1] cmH_2O to 5.7 [4.5 - 6.7] cmH_2O . More specifically, there was an increase in median RMS percentage error from 2.9% to 60% for the CURE cohort, and 2.5 to 44.9% for the McREM cohort.

7.4 Discussion

Incorporating expiration into model identification had a positive effect on prediction error across both cohorts. Including expiration data improved the prediction RMS error from (median [IQR]) 2.2 [1.3 - 3.5] cmH_2O for only using inspiration data to 1.1 [1.0 - 1.5] cmH_2O in the CURE cohort. Likewise, including expiratory data also improved the McREM prediction fit from 1.0 [0.7 - 1.5] cmH_2O to 0.9 [0.6 - 1.1] cmH_2O. It is expected this improvement occurs because there is a lower chance of parameter trade-off between elastance and resistance. Having each of these parameters explicitly defined enables the model to better capture the mechanical behaviour of the lungs throughout

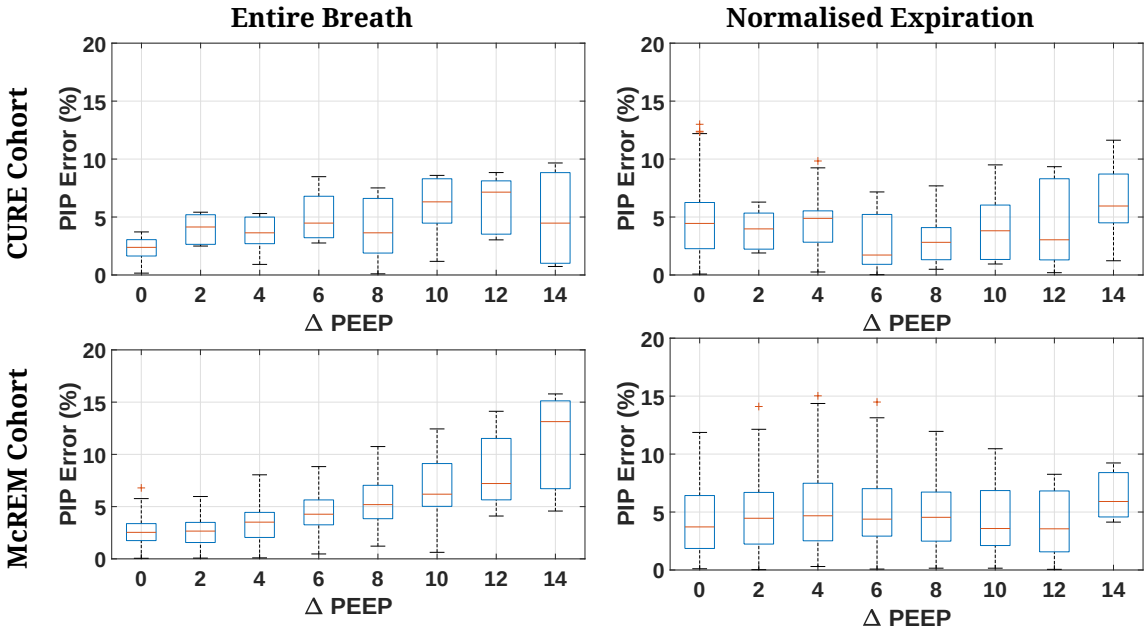

Figure 7.4: Boxplots of prediction error across PEEP steps for the CURE and McREM cohorts.

the entire breathing cycle.

Fitting the parameters to inspiration, before using them to predict across the entire breath, increased RMS error for the CURE cohort (up to 2.6 [2.0 - 3.0] cmH_2O) compared to both Case 1 and Case 2. While Case 2 and Case 3 both use inspiratory data to identify parameters, the larger amount of data RMS is calculated across in Case 3 is expected to increase error. Results stayed relatively constant for the McREM cohort (1.0 [0.8 - 1.4] cmH_2O). This finding could suggest expiration does contain unique dynamics. Alternatively, this finding could also be caused by a higher RMS value due to the model needing to accurately predict a higher number of data point. However, the small change in values in the results indicates these findings may be inconclusive and require further study.

Including expiration data improved PIP prediction for the CURE cohort (PIP error decrease from 5.5 [3.8 - 8.7]% to 3.8 [2.5 - 5.4]%). However, it did not improve for the McREM cohort (PIP error increase from 1.5 [0.5 - 5.6]% to 3.9 [2.4 - 5.3]% . The utilisation of an end-inspiratory pause in the McREM cohort may have had an effect on

the ability of the model to simultaneously fit and predict across both inspiration and expiration. The model was designed to deal with simple, more linear mechanics, and this portion of the breath contains much more non-linear behaviour. Accounting for this drop and hold in pressure immediately after PIP was reached may cause the model to overcompensate by fitting to the smoother transition from the pause into expiration instead of fitting to PIP. It is recommended to continue to incorporate expiratory data into the model identification to reduce the chance of parameter trade-off in the model, which may cause unforeseen issues with prediction in a clinical setting.

Normalising expiration data to achieve an equal I/E ratio neither improved PIP prediction nor prediction fit across PEEP levels in either cohort. Prediction fit, in particular, showed a significant decrease in accuracy with an increase in RMS (%) error from 2.9 to 60% for the CURE cohort, and 2.5 to 44.9% for the McREM cohort. While these findings may not hold true for other I/E ratios, in this case, normalising the data is not recommended.

Both cohorts studied in this chapter were from trials excluding patients with obstructive pulmonary diseases. Obstructive diseases result in reduced gas exchange in the lungs, preventing carbon dioxide from escaping the lungs (Hogg et al., 2004) while also slowing the rate of oxygen reaching the alveoli. As the model has not yet been tested on these patients, it is possible it cannot accurately model expiratory mechanics in these cases. Therefore, future work will need to reinvestigate the utility of this model for these patients.

7.5 Summary

In this chapter, the effect of the inclusion of expiration on the model developed in Chapter 5 was assessed, and found to improve prediction errors due to an anticipated reduction in parameter tradeoff. In addition, normalising the length of expiration to inspiration in this data was found to be unnecessary. In future chapters, data from the entire breath will be used for parameter identification and prediction across PEEP levels.

CHAPTER 8

Overall Model Results

8.1 Introduction

This chapter assesses the utility of the model developed over Chapters 5 - 7 as a whole. It provides extended results and discussion not previously presented. These results represent a definite, more complete outcome from the model developed over Chapters 5 to 7, and explore wider considerations than previously presented.

Fitting and prediction results are provided for both the CURE and McREM cohorts outlined in Chapter 4. In addition, the use of the model to predict both increases and decreases in PEEP level throughout 'mini' recruitment manoeuvres is assessed. Clinically, once a preferred PEEP level is determined, it is rarely significantly altered throughout ventilation. Mini RMs can occasionally be used to make small changes to PEEP and maintain optimal alveolar recruitment and gas exchange (Stahl et al., 2006). However, as patient and lung condition evolves, the optimal PEEP may change. Respiratory models generated from data available at the bedside could be used to predict behaviour at higher or lower PEEP levels without the need for mini RMs, potentially reducing clinician attendance, cost of care and improving patient care and outcomes.

Conditions possibly affecting model efficacy are also considered. First, the impact of the initial PEEP level on model predictions at higher PEEP levels is assessed. The goal of this is to determine whether the model has equivalent relevance and accuracy regardless of what PEEP level at it is implemented in a recruitment manoeuvre (RM). Importantly, this analysis provides better understanding of the relevance and limitations of the model and prediction in a clinical context, particularly at higher PEEP levels where the potential risk of injury with PEEP changes is greater.

8.2 Methods and Analyses

8.2.1 Final Model

The model used was developed in Chapter 5 and optimised in Chapters 6 (use of parabolic recruitment function) and 7 (use of the entire breath to fit and predict). The model forms for fitting and predication are described by Equation 5.7 and Equation 5.10, respectively, and are reproduced in their final forms here for clarity.

Overall model for parameter fitting (Equation 5.7):

$$P(t) = \left(\underbrace{E_1(V - V_m)^2}_{\text{Recruitment Elastance}} + \underbrace{E_2 \frac{P(t)}{60}}_{\text{Distension Elastance}} \right) V(t) + \left(\underbrace{R_1 + R_2 \dot{V}(t)}_{\text{Rohrer Resistance}} \right) \dot{V}(t) + PEEP$$

Overall model for prediction (Equation 5.10):

$$P(t) = \left(\underbrace{E_1((V + V_{frc}) - V_m)^2}_{\text{Recruitment Elastance}} + \underbrace{E_2 \frac{P(t)}{60}}_{\text{Distension Elastance}} \right) V(t) + \left(\underbrace{R_1 + R_2 \dot{V}(t)}_{\text{Rohrer Resistance}} \right) \dot{V}(t) + PEEP$$

8.2.2 Clinical Data Cohorts

CURE and McREM Cohorts

The model was tested on the full RMs carried out in the CURE and McREM cohorts outlined in Chapter 4. Both PIP prediction accuracy and fitting error (RMS) were assessed and compared for each cohort of patient data. A breakdown of how many predictions

were studied at each PEEP interval size are shown in Table 8.1. The variation in the number of breaths at each PEEP level between each cohort is due to the McREM cohort using PEEP interval sizes of 2 cmH_2O, whereas the CURE trial used PEEP steps of 4 cmH_2O. Sometimes the set PEEP increase was not met by the ventilator and in these cases 2, 6, 10, and 14 cmH_2O prediction intervals occurred and were studied.

Table 8.1: **Full CURE and McREM RMs:** Number of predictions studied for each PEEP interval size. This includes both upwards and downwards arms of the CURE RMs.

△ PEEP	CURE Cohort	McREM Cohort
0 cmH_2O	91	89
2 cmH_2O	9	71
4 cmH_2O	45	54
6 cmH_2O	9	40
8 cmH_2O	30	28
10 cmH_2O	9	17
12 cmH_2O	17	8
14 cmH_2O	7	3
Total	**217**	**310**

Mini Recruitment Manoeuvres

To assess whether the model is effective in cases where minimal changes in distension and recruitment are expected, the model was tested on mini recruitment manoeuvre data. In the case of mini RMs, the smaller nature of overall changes in PEEP may affect recruitment dynamics. Thus, results may differ from those found by examining 1-2 larger PEEP changes in a full RM.

As mini recruitment manoeuvres were not used in the McREM trial, only data from the CURE pilot trial defined in Section 4.2 was used in this analysis. As Patient 4 of the CURE cohort did not receive any mini RMs, only the first three patients were studied. Patient 1 received 14 RMs, whereas Patients 2 and 3 each received 2. Of these, 7 of Patient 1's mini RMs and one each of Patient 2 and 3's had enough breaths to enable model analysis. Hence, a total of 172 predictions (Arm 1: 55, Arm 2: 52, Arm 3: 30, Arm 4: 35) were studied across the 4 patients in the CURE trial.

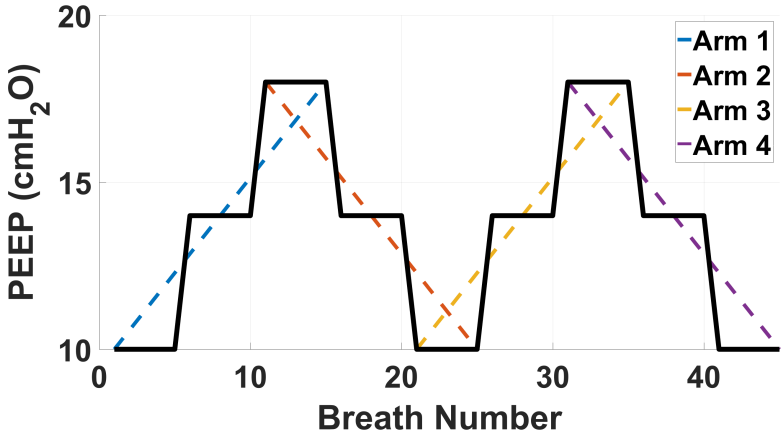

Figure 8.1: Demarcation of data sets across an example mini RM where two staircase manoeuvres are performed. Step size and duration are not necessarily representative of those used in the data.

Mini RMs were comprised of two staircase increases and decreases in PEEP as part of typical MV treatment (Chiew, Pretty, Shaw, et al., 2015; Szlavecz et al., 2014). To capture changes in lung mechanics, each data set was split into four sections, two increasing PEEP and one or two decreasing PEEP sections, shown in Figure 8.1. In a typical mini RM this procedures comprises one or two 4 cmH_2O PEEP increases followed by one or two 4 cmH_2O PEEP decreases. This analysis primarily studies mini RMs, as opposed to full RMs, which can involve many more PEEP increases. The purpose of this analysis is to ensure that the model remains accurate in cases where there are limited changes in either recruitment or distension throughout the entirety of an RM. The efficacy of the model to both fit and predict across mini RMs is assessed.

8.2.3 Conditions of Model Accuracy

To anticipate potential usage limitations of the model, it was tested to see whether or not there were conditions required for accurate prediction. This analysis was carried out using both full and mini RM data as needed, specific data cohorts are outlined below. While not an exhaustive list, the conditions tested in this chapter include:

1. **The impact of initial PEEP level.** To ensure the model performs well regard-

less of what PEEP level during an RM it is used, the impact of initial PEEP level on prediction analysis is considered. This attempts to assess if there is a difference between results from different initial PEEP levels with identical prediction interval sizes of 2 or 6 cmH_2O. Data from both the McREM and CURE trial cohorts defined in Chapter 4 was used in this analysis. As outlined in Chapter 5, the model parameters were identified and used to predict across the RM range.

2. **Accuracy of predicting lung mechanics through a decrease in PEEP level compared with an increase.** Previous chapters examined prediction over the upwards arm of an RM only. While lower risk, downward prediction of pressure outcomes for decreasing PEEP is also of interest. The CURE pilot trial mini RM data outlined in Chapter 4 and Section 8.2.2 along with the full RMs from this trial were used in this analysis. To enable comparison between each set of data, the PEEP changes were not split into specific PEEP changes. Instead, they were delineated as one-step (change of 2-6 cmH_2O), two step (change of 6-11 cmH_2O) and three-step (change of 12-16 cmH_2O).
3. **Accuracy of prediction betwen the first half of an RM (Arm 1 and Arm 2) and the second (Arm 3 and Arm 4).** The CURE pilot trial mini RM data outlined in Chapter 4 and Section 8.2.2 along with the full RMs from this trial were used in this analysis. To enable comparison between each set of data, the PEEP changes were not split into specific PEEP changes. Instead, they were delineated as one-step (change of 2-6 cmH_2O), two step (change of 6-11 cmH_2O) and three-step (change of 12-16 cmH_2O).
4. **Error increase in prediction as PEEP interval increases.** The aim of this analysis is to quantify any potential loss in prediction as the prediction interval increases. Outcomes could enable more confident and robust utilisation of prediction methods clinically. Data from the full RMs carried out in the CURE and McREM trials outlined in Chapter 4 was used in this analysis.

8.3 Results

8.3.1 Overall CURE and McREM Results

Full Recruitment Manoeuvre

Table 8.2: **Full CURE and McREM RMs:** Summarised model parameters and fitting error (median [IQR]) for the CURE and McREM cohort.

	CURE Cohort	McREM Cohort
***E1* (recruitment)**	5.8 [0.5 - 13.4]	14.0 [10.1 - 19.2]
***E2* (distension)**	55.9 [46.2 - 70.7]	47.0 [41.1 - 58.6]
R1	6.5 [6.1 - 7.7]	8.4 [7.5 - 11.0]
R2	0.0 [0.0 - 0.0]	0.0 [0.0 - 0.0]
RMS error (cmH_2O)	1.0 [0.9 - 1.2]	0.6 [0.5 - 0.9]
RMS error (%)	2.4 [2.1 - 2.8]	2.3 [1.7 - 3.6]
PIP error (cmH_2O)	0.8 [0.5 - 1.1]	1.0 [0.8 - 1.3]
PIP error (%)	2.4 [1.6 - 3.0]	2.5 [1.7 - 3.4]

Fitting Results: The model showed a high level of accuracy for capturing and fitting lung mechanics. As can be seen in Table 8.2, the model showed very low fitting error (RMS (%) error of 2.4 [2.1 - 2.8]% for the CURE cohort and 2.3 [1.7 - 3.6]% for the McREM cohort) and estimation of the peak inspiratory pressure (PIP (%) error of 2.4 [1.6 - 3.0]% for the CURE cohort and 2.5 [1.7 - 3.4]% for the McREM cohort) across each of the two cohorts. In addition, as also shown in Table 8.2, both cohorts had similar fitted parameter values.

In particular, the CURE cohort showed slightly higher values for E_2, possibly caused by the CURE trial including PEEP values up to 30 cmH_2O. Thus, distension would have been more greatly represented in the CURE data and identified E_2 values. In contrast, the higher E_1 values for the McREM cohort were potentially caused by this trial including data from a PEEP of 10 cmH_2O up to 24 cmH_2O, which in many patients is within the zone (5 - 25 cmH_2O) where the majority of alveolar recruitment occurs (Borges et al., 2006). As the majority of the CURE data began at a PEEP of 12 cmH_2O, some recruitment may have already occurred prior to the staircase RM commencing, resulting in higher median E_1. The ability of the model to accurately fit the data across both of these

cohorts with similar parameter values for clinically similar patients indicates that the basis functions were well selected.

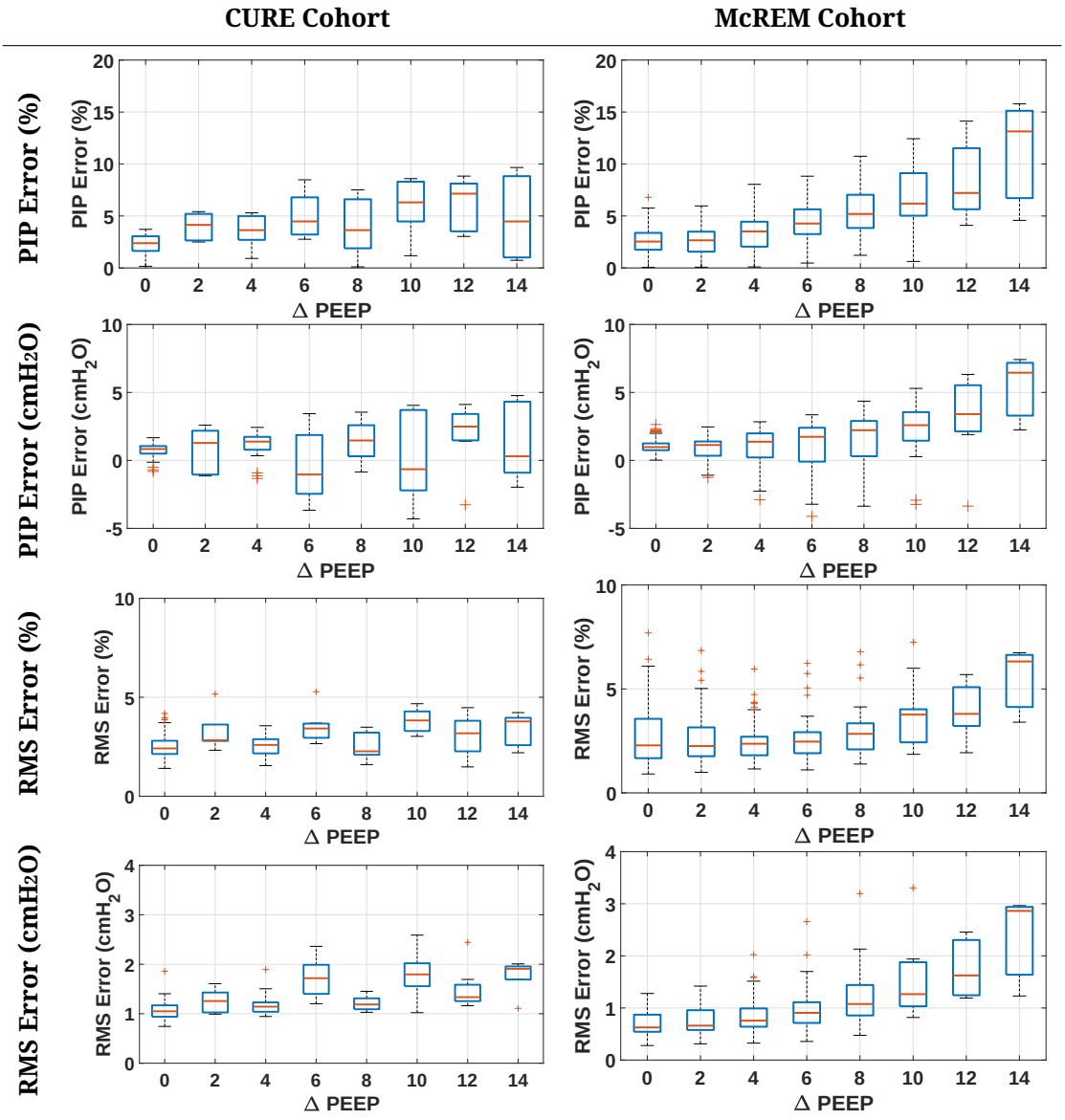

Figure 8.2: **Full CURE and McREM RMs:**Model prediction error results for the final model for the CURE and McREM cohorts for increases of up to 14 cmH2O.

Prediction Results: Cohort results for PIP prediction and fitting error are shown in Figure 8.2. The prediction error was larger for most of the McREM cohort clinical range. It is expected that this greater error is due to the presence of the end inspiratory pause, which is likely non-linear and not well captured by the simple dynamics model used here. However, with the exception of this portion of the breath, the model accurately

predicted airway pressure with less than 10% of fitting error in PEEP increases of up to 14 cmH_2O.

Table 8.3: Compiled model prediction results for CURE and McREM cohorts. PIP error (%) is an absolute value, while PIP error (cmH_2O) is signed.

CURE Cohort				
PEEP Change	**PIP Error (cmH_2O)**	**PIP Error (%)**	**RMS Error (cmH_2O)**	**RMS Error (%)**
2 cmH_2O	2.8 [2.8 - 3.6]	4.1 [2.6 - 5.2]	1.3 [1.0 - 1.4]	1.3 [-1.0 - 2.2]
4 cmH_2O	1.4 [0.8 - 1.7]	3.6 [2.7 - 5.0]	1.1 [1.0 - 1.2]	2.6 [2.2 - 3.0]
6 cmH_2O	-1.0 [-2.5 - 1.9]	4.5 [3.2 - 6.8]	1.7 [1.4 - 2.0]	3.6 [3.1 - 4.9]
8 cmH_2O	1.5 [0.3 - 2.6]	3.6 [1.9 - 6.6]	1.2 [1.1 - 1.3]	2.3 [2.1 - 3.2]
10 cmH_2O	-0.6 [-2.2 - 3.7]	6.3 [4.5 - 8.3]	1.8 [1.6 - 2.0]	3.8 [3.3 - 4.3]
12 cmH_2O	2.5 [1.5 - 3.4]	7.1 [3.5 - 8.1]	1.3 [1.3 - 1.6]	3.2 [2.3 - 3.8]
14 cmH_2O	0.3 [-0.9 - 4.3]	4.5 [1.0 - 8.8]	1.9 [1.7 - 2.0]	3.8 [2.6 - 4.0]
Total	**1.4 [-0.5 - 2.2]**	**4.5 [2.8 - 6.5]**	**1.2 [1.1 - 1.6]**	**2.9 [2.3 - 3.6]**
McREM Cohort				
PEEP Change	**PIP Error (cmH_2O)**	**PIP Error (%)**	**RMS Error (cmH_2O)**	**RMS Error (%)**
2 cmH_2O	1.1 [0.3 - 1.4]	2.7 [1.6 - 3.5]	0.7 [0.6 - 1.0]	2.3 [1.7 - 3.6]
4 cmH_2O	1.4 [0.2 - 2.0]	3.5 [2.0 - 4.4]	0.8 [0.6 - 1.0]	2.3 [1.8 - 3.2]
6 cmH_2O	1.7 [-0.1 - 2.4]	4.3 [3.3 - 5.6]	0.9 [0.7 - 1.1]	2.5 [1.9 - 2.9]
8 cmH_2O	2.2 [0.3 - 2.9]	5.2 [3.8 - 7.0]	1.1 [0.9 - 1.4]	2.8 [2.1 - 3.3]
10 cmH_2O	2.6 [1.4 - 3.6]	6.2 [5.0 - 9.1]	1.3 [1.0 - 1.9]	3.8 [2.4 - 4.0]
12 cmH_2O	3.4 [2.1 - 5.5]	7.2 [5.6 - 11.5]	1.6 [1.2 - 2.3]	3.8 [3.2 - 5.1]
14 cmH_2O	6.4 [3.3 - 7.2]	13.1 [6.7 - 15.1]	2.9 [1.6 - 2.9]	6.3 [4.1 - 6.6]
Total	**1.4 [0.3 - 2.2]**	**3.9 [2.4 - 5.3]**	**0.9 [0.6 - 1.1]**	**2.5 [1.9 - 3.4]**

Tabularised prediction results across the entire clinical RM range are presented in Table 8.3. Prediction results are similar in both cohorts, with 4.5 [2.8 - 6.5]% (1.4 [-0.5 - 2.2] cmH_2O) PIP error for the CURE cohort and 3.9 [2.4 - 5.3]% (1.4 [0.3 - 2.2] cmH_2O) for the McREM cohort for PEEP changes of up to 14 cmH_2O. RMS error was 2.9 [2.3 - 3.6]% (1.2 [1.1 - 1.6] cmH_2O) for the CURE cohort and 2.5 [1.9 - 3.4]% (0.9 [0.6 - 1.1] cmH_2O) for the McREM cohort.

As shown in Figure 8.2 and in Table 8.3, both PIP prediction error and fitting error increased with the size of prediction interval. While each cohort had similar error for smaller interval predictions ($<$6 cmH_2O), the McREM cohort, but displayed higher error for larger predictions for both PIP prediction and fitting accuracy. PIP prediction error showed a steady increase for the McREM cohort however stayed reasonably constant for the CURE trial data.

Table 8.4: **Full CURE RMs:** Model prediction error (median [IQR]) results for one-step, two-step and three-step predictions. Upwards and downwards predictions are compared. PIP error (%) is an absolute value, while PIP error (cmH_2O) is signed.

One-Step Prediction (2 - 6 cmH_2O)		
Error Metric	**Upwards Prediction**	**Downwards Prediction**
PIP Error (cmH_2O)	0.8 [-0.3 - 1.6]	0.9 [-0.1 - 1.4]
PIP Error (%)	0.0 [0.0 - 0.0]	0.0 [0.0 - 0.0]
RMS Error (cmH_2O)	1.1 [1.0 - 1.3]	1.1 [1.0 - 1.3]
RMS Error (%)	3.1 [2.4 - 3.6]	3.0 [2.3 - 3.5]
Two-Step Prediction (7 - 11 cmH_2O)		
Error Metric	**Upwards Prediction**	**Downwards Prediction**
PIP Error (cmH_2O)	1.0 [-0.5 - 1.9]	0.5 [-0.7 - 1.7]
PIP Error (%)	0.0 [0.0 - 0.1]	0.0 [0.0 - 0.1]
RMS Error (cmH_2O)	1.3 [1.1 - 1.6]	1.3 [1.1 - 1.5]
RMS Error (%)	4.0 [2.7 - 5.1]	3.6 [3.0 - 4.6]
Three-Step Prediction (12 - 16 cmH_2O)		
Error Metric	**Upwards Prediction**	**Downwards Prediction**
PIP Error (cmH_2O)	-0.0 [-1.7 - 1.8]	0.3 [-1.5 - 2.4]
PIP Error (%)	0.1 [0.0 - 0.1]	0.0 [0.0 - 0.1]
RMS Error (cmH_2O)	1.6 [1.3 - 2.1]	1.4 [1.3 - 1.8]
RMS Error (%)	4.1 [3.3 - 7.1]	4.1 [3.3 - 5.5]

Table 8.4 shows the variation in prediction across PEEP changes between upwards arms (1 and 3) and downwards arms (2 and 4), as defined in Figure 8.1. Table 8.5 splits this information into individual arms. Upwards and downwards predictions show similar accuracy for both PIP prediction and RMS error across the entirety of the prediction range. PIP (%) error for downwards predictions was 0.0 [0.0 - 0.0]%, 0.0 [0.0 - 0.1]% and 0.1 [0.0 - 0.1]% for one, two and three-step predictions, respectively. In comparison, for the downwards predictions, the PIP (%) errors were 0.0 [0.0 - 0.0]%, [0.0 - 0.1]% and 0.0 [0.0 - 0.1]% for the same step sizes. However, as can be seen in the signed PIP (cmH_2O) errors in Table 8.4, PIP was more frequently over-predicted in upwards arms. This result is clinically useful as an over-prediction of PIP could lead to more conservative treatment. Whereas, the slight tendency of the model to under-predict PIP in downwards arms would not have much of an effect on clinical value, as there is less patient risk when pressure is decreasing. There was very little difference between these results and those of individual arms, suggesting in full RMs, there is little difference in model prediction accuracy between the first and second half of a staircase RM.

Table 8.5: **Full CURE RMs:** Model prediction error (median [IQR]) results comparing each arm of an full RM for one-step and two-step prediction. PIP error (%) is an absolute value, while PIP error (cmH_2O) is signed.

One-Step Prediction (2 - 6 cmH_2O)				
Error Metric	**Arm 1**	**Arm 2**	**Arm 3**	**Arm 4**
PIP Error (cmH_2O)	1.2 [0.1 - 2.1]	0.4 [-0.3 - 1.5]	1.3 [0.3 - 1.7]	0.5 [-0.1 - 1.3]
PIP Error (%)	0.0 [0.0 - 0.1]	0.0 [0.0 - 0.0]	0.0 [0.0 - 0.0]	0.0 [0.0 - 0.0]
RMS Error (cmH_2O)	1.2 [1.0 - 1.3]	1.1 [0.9 - 1.3]	1.2 [1.0 - 1.3]	1.1 [0.9 - 1.3]
RMS Error (%)	2.7 [2.3 - 3.5]	3.1 [2.5 - 3.8]	3.0 [2.6 - 3.3]	2.7 [1.9 - 3.6]
Two-Step Prediction (7 - 11 cmH_2O)				
Error Metric	**Arm 1**	**Arm 2**	**Arm 3**	**Arm 4**
PIP Error (cmH_2O)	0.9 [-0.0 - 2.2]	1.2 [-0.5 - 1.8]	1.5 [-0.2 - 3.1]	-0.0 [-1.1 - 1.4]
PIP Error (%)	0.0 [0.0 - 0.1]	0.1 [0.0 - 0.1]	0.0 [0.0 - 0.1]	0.0 [0.0 - 0.1]
RMS Error (cmH_2O)	1.2 [1.1 - 1.4]	1.3 [1.1 - 1.6]	1.3 [1.1 - 1.4]	1.3 [1.1 - 1.6]
RMS Error (%)	2.6 [2.2 - 4.1]	4.3 [3.4 - 7.0]	3.3 [2.6 - 3.6]	4.1 [3.2 - 5.2]
Three-Step Prediction (12 - 16 cmH_2O)				
Error Metric	**Arm 1**	**Arm 2**	**Arm 3**	**Arm 4**
PIP Error (cmH_2O)	1.8 [-0.5 - 3.0]	Not	2.4 [1.0 - 4.2]	-0.4 [-1.7 - 0.5]
PIP Error (%)	0.0 [0.0 - 0.1]	Enough	0.1 [0.0 - 0.1]	0.0 [0.0 - 0.1]
RMS Error (cmH_2O)	1.4 [1.3 - 1.7]	Data for	1.5 [1.3 - 1.8]	1.4 [1.3 - 1.8]
RMS Error (%)	2.9 [2.6 - 3.6]	IQR	3.3 [2.5 - 3.9]	5.2 [3.9 - 5.9]

Mini Recruitment Manoeuvre

Fitting Results: Elastance and resistance functions were fit across 3 patients, over 1056 breaths. PIP fitting error was 0.4 [0.3 - 0.5] cmH_2O (0.0 [0.0 - 0.0] %) and RMS error was 0.9 [0.7 - 1.2] cmH_2O (2.5 [1.6 - 3.3] %). Both error metrics (PIP error and RMS error) have very low values, indicating the model fits the lung behaviour well in all arms of the mini RMs studied.

Prediction Results: The model showed high accuracy in predicting upwards throughout mini RMs, as shown in Table 8.6. PIP (%) error was 0.0 [0.0 - 0.0]% for a one-step prediction and 0.0 [0.0 - 0.1]% for two-steps. As shown by the signed PIP (cmH_2O) errors of 0.5 [-0.1 - 0.9] (one step) and 0.4 [-0.3 - 1.2] (two steps), the model showed a tendency to over-estimate pressure when predicting upwards arms. Greater prediction accuracy was seen in the upwards arms of the recruitment manoeuvre than the downwards, however this difference was minimal. Fitting error was also low for both upwards and downwards predictions. The high accuracy of the model to fit lung mechanics (RMS er-

Table 8.6: **Mini CURE RMs:** Model prediction error (median [IQR]) results for one-step and two-step prediction. Upwards and downwards predictions are compared. PIP error (%) is an absolute value, while PIP error (cmH_2O) is signed.

One-Step Prediction (2 - 6 cmH_2O)		
Error Metric	**Upwards Prediction**	**Downwards Prediction**
PIP Error (cmH_2O)	0.5 [-0.1 - 0.9]	0.4 [-0.2 - 1.0]
PIP Error (%)	0.0 [0.0 - 0.0]	0.0 [0.0 - 0.0]
RMS Error (cmH_2O)	1.0 [0.9 - 1.2]	0.9 [0.8 - 1.3]
RMS Error (%)	2.8 [2.1 - 3.6]	2.9 [1.9 - 3.8]
Two-Step Prediction (7 - 11 cmH_2O)		
Error Metric	**Upwards Prediction**	**Downwards Prediction**
PIP Error (cmH_2O)	0.4 [-0.3 - 1.2]	0.2 [-0.7 - 1.0]
PIP Error (%)	0.0 [0.0 - 0.1]	0.0 [0.0 - 0.0]
RMS Error (cmH_2O)	1.2 [1.0 - 1.4]	1.2 [1.0 - 1.4]
RMS Error (%)	3.8 [2.6 - 4.7]	3.2 [2.5 - 4.6]

ror) and fit PIP (PIP error) when predicting both upwards and downwards indicates the capability of the model to be able to re-assess the best PEEP level for a patients condition throughout ventilation.

Table 8.7: **Mini CURE RMs:** Model prediction error (median [IQR]) results comparing each arm of an mini RM for one-step and two-step prediction. PIP error (%) is an absolute value, while PIP error (cmH_2O) is signed.

One-Step Prediction (2 - 6 cmH_2O)				
Error Metric	**Arm 1**	**Arm 2**	**Arm 3**	**Arm 4**
PIP Error (cmH_2O)	-0.1 [-0.3 - 0.2]	0.8 [0.5 - 1.2]	0.1 [-0.4 - 0.4]	0.7 [0.4 - 1.0]
PIP Error (%)	0.0 [0.0 - 0.0]	0.0 [0.0 - 0.0]	0.0 [0.0 - 0.0]	0.0 [0.0 - 0.0]
RMS Error (cmH_2O)	1.0 [0.9 - 1.2]	1.0 [0.8 - 1.2]	0.9 [0.7 - 1.2]	1.1 [0.8 - 1.3]
RMS Error (%)	2.3 [1.7 - 2.5]	3.6 [3.0 - 4.1]	2.0 [1.6 - 3.0]	3.8 [3.1 - 4.7]
Two-Step Prediction (7 - 11 cmH_2O)				
Error Metric	**Arm 1**	**Arm 2**	**Arm 3**	**Arm 4**
PIP Error (cmH_2O)	-1.0 [-1.3 - -0.0]	1.2 [0.5 - 1.7]	-0.5 [-0.8 - 0.7]	0.6 [0.2 - 1.3]
PIP Error (%)	0.0 [0.0 - 0.0]	0.0 [0.0 - 0.1]	0.0 [0.0 - 0.0]	0.0 [0.0 - 0.1]
RMS Error (cmH_2O)	1.2 [1.0 - 1.4]	1.2 [0.9 - 1.4]	1.0 [0.8 - 1.3]	1.2 [1.1 - 1.4]
RMS Error (%)	2.2 [1.8 - 2.6]	4.5 [3.9 - 4.9]	2.5 [2.0 - 2.9]	4.6 [4.1 - 5.3]

As can be seen in Table 8.7, there was very little difference in prediction error between Arms 1 and 2, and Arms 3 and 4 of the mini RMs. As mini RMs are often used to maintain oxygenation and reduce the impacts of time-dependent de-recruitment, this may vary from the results from a full RM. As described in Section 4.2, the purpose of the first half of the RM is to recruit alveoli while the second is to assess lung mechanics. Prediction

results for Patients 1-3 are shown in Table 8.6 with (median [IQR]) PIP error of 0.5 [-0.1 - 0.9] cmH2O for a one-step increase in PEEP level and 0.4 [-0.3 - 1.2] cmH2O for a two-step increase. The specific prediction results for Patient 1, RM 3 are shown in Figure 8.3. Prediction results for other mini RMs are provided in Appendix A (Chapter 12).

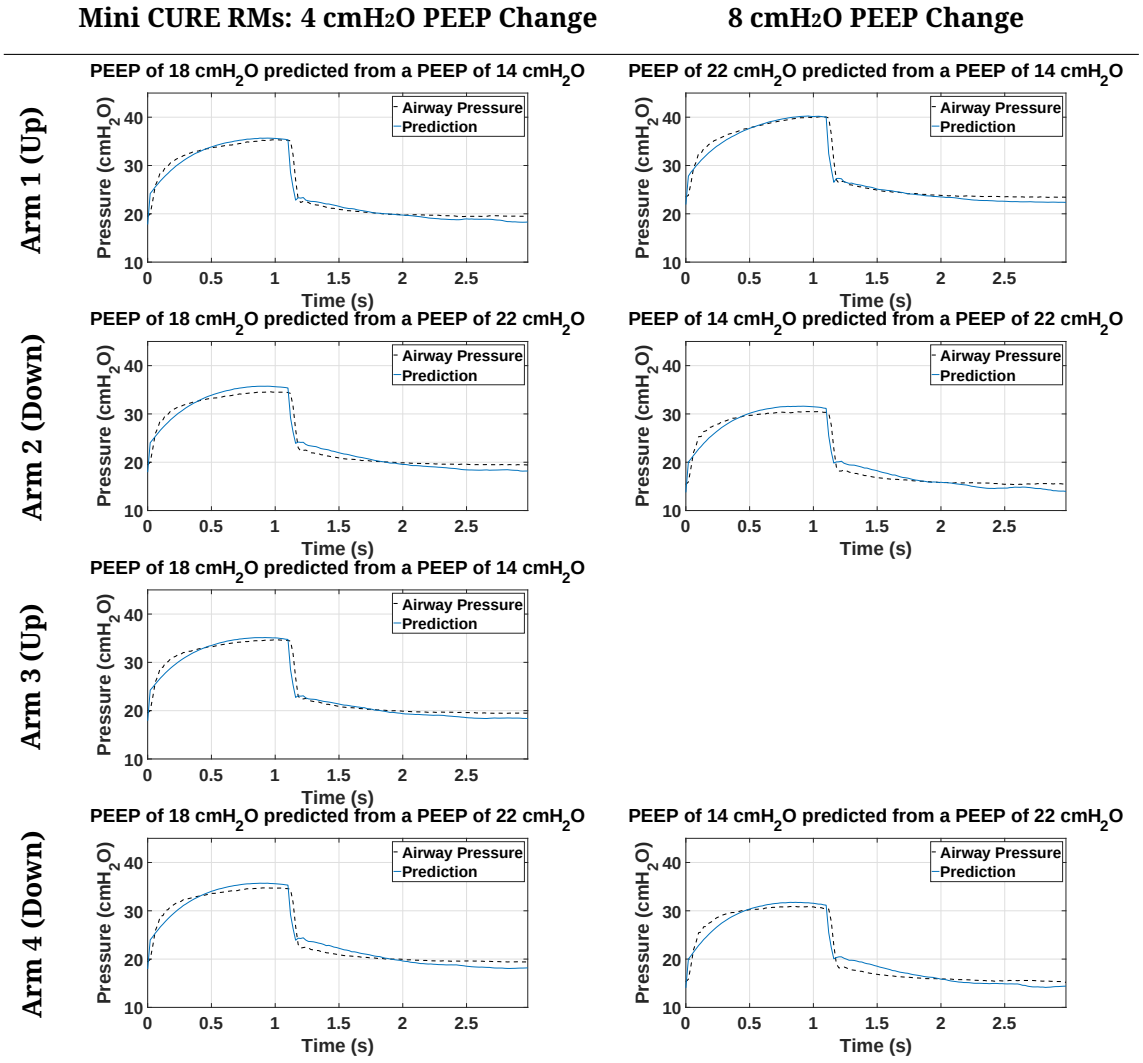

Figure 8.3: **Mini CURE RMs:** Prediction results for Patient 1, RM 3 across all arms. The blue, solid line shows the model prediction and the dashed black line indicates the median airway pressure at that PEEP level.

8.3.2 Impact of Initial PEEP Level

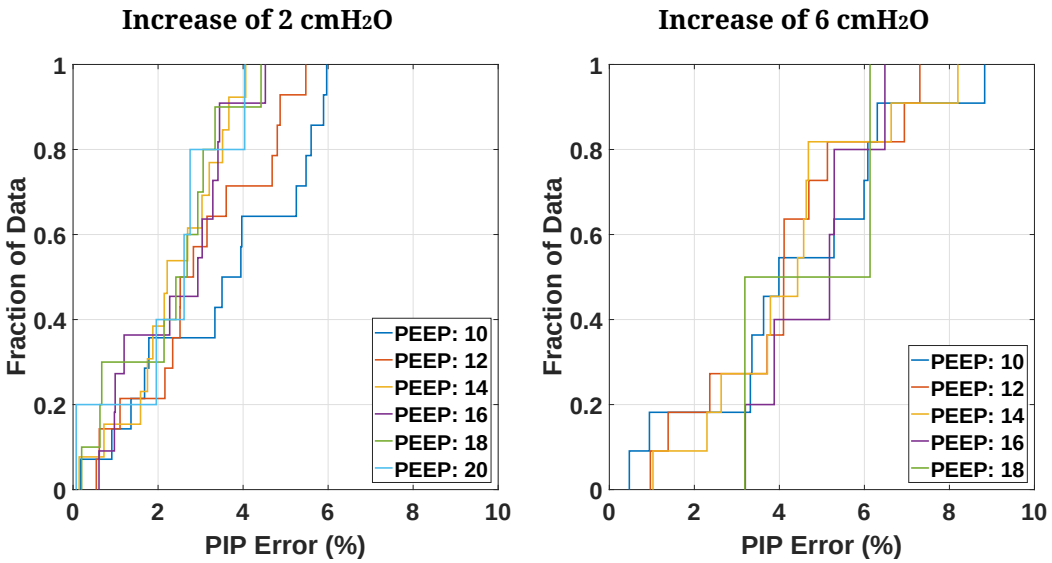

Figure 8.4: **McREM RMs:** Cumulative distribution functions (CDFs) showing consistent prediction errors across all PEEP levels for step increases of 2 and 6 cmH_2O using the parabolic basis function model. The PEEP shown in the legend is the initial PEEP level from which a prediction is made.

To ensure higher levels of clinical relevance for the model, the impact of the initial PEEP level was assessed. This study helps to ensure that the model has clinical benefit and can be used at any point of a RM. The cumulative distribution function (CDFs) in Figure 8.4 show that prediction errors are similar for all initial PEEP levels, irrespective of whether the PEEP step increase magnitude is 2 cmH_2O or 6 cmH_2O. There is thus no noticeable sensitivity to PEEP level or PEEP interval in prediction error. Figure 8.4 shows prediction error is reasonably consistent across variable PEEP levels used to generate prediction and consistent prediction ranges. The errors are still clinically acceptable and relatively small compared to inter- and intra- patient variability, but do grow as the model is "stretched" to predict over larger intervals. For comparison, the median [IQR] variation in PIP across each PEEP level was 1.2 [0.8 - 1.9] cmH_2O, with 95% of the data up 4.3 cmH_2O for the McREM cohort. The CURE cohort had (median [IQR]) variation of 1.3 [0.9 - 2.4] cmH_2O with a 95% value of 11.2 cmH_2O. The success at prediction in the results thus validates the choice of basis function shapes, as well as their potential

to accurately capture mechanics outside the range of breath data used to identify their parameters.

8.4 Discussion

8.4.1 General Model Efficacy and Clinical Implications

As shown in Table 8.3, the model predicts lung mechanics with very high accuracy over the entire expected MV pressure range (14 cmH_2O) with (median [IQR]) PIP Error of 1.4 [-0.5 - 2.2] cmH_2O (CURE cohort) and 1.4 [0.3 - 2.2] cmH_2O (McREM cohort). In addition, as also shown in Table 8.3, a total prediction RMS error of 1.2 [1.1 - 1.6] (CURE) and 0.9 [0.6-1.1] (McREM) cmH_2O was achieved. These preliminary results show the model is capable of predicting respiratory responses of critically ill patients during RMs using data from a baseline PEEP level. The ability of the model to predict across such a large PEEP change interval suggests the basis functions chosen for distension and recruitment provide an accurate depiction of the pulmonary processes occurring throughout a RM.

Prediction of potential respiratory mechanics at different MV settings may allow more informed decisions around ventilation practice to be made. In addition, these sorts of predictions could be used to test potential treatment strategies *in silico*, rather than direct testing in patient cohorts, thus increasing safety. One potential application is the estimation of PEEP for minimum elastance (M. Amato et al., 1998; Chiew, Pretty, Docherty, et al., 2015) without the need to perform RM steps at much higher pressures, reducing risk and personalising care. In addition, the model would also offer clinicians an idea of the risk of over-distension resulting from excessive airway pressure and volume at any PEEP.

The model was tested on median breaths at each PEEP level. However, due to intra-patient variability there was variation in what the PIP of each breath at a PEEP level

was. The median [IQR] variation in PIP across each PEEP level was 1.2 [0.8 - 1.9] cmH_2O, with 95% of the data up 4.3 cmH_2O for the McREM cohort. The CURE cohort had (median [IQR]) variation of 1.3 [0.9 - 2.4] cmH_2O with a 95% value of 11.2 cmH_2O. As shown in Table 8.3, the model was within this variation for predictions up to 8 cmH_2O ahead for the CURE cohort and 4 cmH_2O for the McREM cohort, which is two PEEP steps ahead for each protocol. This suggests that these low errors are clinically insignificant in these cases.

The overall capability of this model should make the process of PEEP titration to find minimum elastance and the implementation of RMs much safer and more efficient. However, there was some variation in over- and under- prediction of PIP (cmH_2O), as shown in Table 8.3, caused by the variance in whether the effects of either recruitment or distension were having a more significant effect on lung mechanics at that pressure. Estimating at exactly what point this change in mechanics occurs is difficult to achieve for an individual patient due to high levels of variability.

Due to this variation, it is not clinically advisable to base PEEP settings on a sole prediction of lung mechanics at a PEEP level 14 cmH_2O higher than the current one. Smaller predictions of a single step would be more commonly used to ensure patient safety. Equally, the method could be extended to include data from more than the current PEEP step to further reduce errors (Langdon, Docherty, Chiew, & Chase, 2016; Langdon, Docherty, Chiew, Möller, & Chase, 2016).

The analysis carried out in Chapters 5 - 7 and in this chapter focussed on volume controlled ventilation data, where pressure is the uncontrolled factor. While these experiments use volume controlled ventilation, the field is increasingly changing towards pressure controlled ventilation. However, the methods presented are readily generalisable to the choice of controlled variables (volume or pressure) and fitted model outputs (pressure or volume). Future work will utilise pressure control data to forward predict volume outcomes across a recruitment manoeuvre, where peak tidal volume could be a

clinically interesting risk metric. The ultimate goal of MV is to maximise recruitment of alveoli and thus gas exchange, while minimising incidences of VILI (Bates & Irvin, 2002; Lambermont et al., 2008; Mercat et al., 2008; Rocco et al., 2010; Valentini et al., 2014), which is supported by the model prediction results presented here.

Model Prediction across Mini RMs

To assess whether the model is effective in cases where minimal changes in distension and recruitment are expected, the model was tested on mini recruitment data. The results presented in Tables 8.6 and 8.7 suggest the model captures lung dynamics across a nearer, more local pressure range very well with PIP (%) error of 0.0 [0.0 -0.1]% in increases of PEEP up to 11 cmH_2O. This low level of error indicates the model would be clinically useful for making small changes to PEEP levels throughout treatment as patient condition evolves.

Fitting results were accurate across all PEEP levels and arms in each mini RM studied, with a median PIP % error less than 10% and a median RMS (%) error less than 7% in all cases. The model showed good accuracy in predicting noth upwards and downwards across entire mini RMs. Fitting error across one PEEP level was similar in both upwards and downwards arms with (median [IQR]) RMS error of 1.2 [1.0 - 1.4] cmH_2O for two-step prediction. The model was more accurate at predicting PIP when predicting upwards both one and two steps, in the majority of cases over-predicting peak pressure. This over-prediction is clinically important as it is presenting the conservative case, reducing the change of over-distension and VILI.

Predicting downwards often results in an under-prediction of PIP. However, as pressure is decreasing between the steps this error is much less likely to result in VILI. This difference is likely due to the variation in mechanics between recruitment and derecruitment resulting in the recruitment basis function holding less relevance for the downwards arms in the mini RMs. The ability of the model to predict lung mechanic

changes with such high accuracy in mini RMs is a strong indication that it maintains efficacy even when there are small changes in distension and recruitment.

8.4.2 Conditions of Model Accuracy

Four model conditions were tested in this chapter to assess their impact on model accuracy.

1. **The impact of initial PEEP level.** This was found to not have an impact on prediction accuracy in the cohorts studied. This means that the model has the versatility to be used in a variety of contexts. It could be used to predict across an entire RM to work out approximate point (starting point of 10 cmH_2O) or minimum elastance, or partway through the process (18 cmH_2O (when additional information about patient condition is available)) to ensure that the initial prediction was accurate prior to further increasing pressure. In addition, it could be used to make small alterations to PEEP level in mini RMs.
2. **Accuracy of predicting lung mechanics through a decrease in PEEP level compared with an increase.** While the absolute (%) error of PIP estimation was not changed by the direction of prediction, predicting across a decrease in PEEP often resulted in an under-prediction for both the full and mini RMs. Predicting an increase in PEEP level tended slightly towards over-predicting PIP however showed reasonably similar amounts of over- and under-predictions
3. **Accuracy of prediction betwen the first half of an RM (Arm 1 and Arm 2) and the second (Arm 3 and Arm 4).** There was not a difference in model accuracy between the first and second half of RMs for both the mini and full RMs.
4. **Error increase in prediction as PEEP interval increases.** Error tended to increase as PEEP prediction interval increased in all cohorts and RM types studied. While both PIP prediction and fitting error (RMS) error levels stayed reasonably constant in increases of up to 6 cmH_2O, steady increases occurred past this point.

8.5 Summary

This chapter has provided a general overview of model development and efficacy. In addition, the potential utility of this ability in mini RMs has been investigated. Analysis carried out in this chapter has also suggested that there is little change in model efficacy if any of the studied model conditions were changed. The high level of accuracy and robustness of this model indicates that it could hold clinical relevance.

CHAPTER 9

Estimation of Additional Lung Volume Gained through PEEP Increases

9.1 Introduction

Functional Residual Capacity (FRC) represents recruited lung volume at zero end-expiratory pressure (ZEEP), or at atmospheric pressure after normal expiration (Bates, 2009; Major et al., 2018; van Drunen, Chase, et al., 2013). A less studied impact of increasing PEEP is the added pressure results in an increased end-expiratory (recruited) lung volume, or dynamic function residual capacity. It is essentially the residual additional lung volume additional lung volume (V_{frc}), due to alveolar recruitment at this higher pressure (Dellamonica et al., 2011; van Drunen, Chase, et al., 2013; Wallet et al., 2013).

Determining V_{frc} is often invasive, or requires imaging that either cannot be carried out at the bedside or is not available in every care unit. Estimating changes in V_{frc} across each RM step could aid PEEP optimisation by enabling clinicians to better manage risk

vs reward, and minimise the risk of lung damage. Potentially, PEEP could be titrated based on V_{frc} as this volume is the direct goal of applying PEEP.

This chapter assesses the accuracy of a model-based method of V_{frc} estimation against raw volume data, and investigates how much this accuracy affects the predictive abilities of the model developed in Chapter 5.

9.2 Methods

9.2.1 Patient Data

Pressure and flow data from the N=21 invasively ventilated patients diagnosed with acute respiratory distress syndrome (ARDS) from ICUs in Germany (N=17) and New Zealand (N=4) (Davidson et al., 2014; Stahl et al., 2006) outlined in Chapter 4 was analysed.

9.2.2 Models Used in Analysis

The model used in this study was the model defined in Section 5.2. Specifically, Equations 5.7 and 5.10, respectively as reproduced below.

Overall model for parameter fitting (Equation 5.7):

$$P(t) = \left(\underbrace{E_1(V - V_m)^2}_{\text{Recruitment Elastance}} + \underbrace{E_2 \frac{P(t)}{60}}_{\text{Distension Elastance}} \right) V(t) + \left(\underbrace{R_1 + R_2 \dot{V}(t)}_{\text{Rohrer Resistance}} \right) \dot{V}(t) + PEEP$$

Overall model for prediction (Equation 5.10):

$$P(t) = \left(\underbrace{E_1((V + V_{frc}) - V_m)^2}_{\text{Recruitment Elastance}} + \underbrace{E_2 \frac{P(t)}{60}}_{\text{Distension Elastance}} \right) V(t) + \left(\underbrace{R_1 + R_2 \dot{V}(t)}_{\text{Rohrer Resistance}} \right) \dot{V}(t) + PEEP$$

Calculation of V_{frc}

The change in volume due to an increase in PEEP (V_{frc}) was calculated using a steady state assumption applied to the elastance component of the overarching model equa-

tion of Equation 5.7. It is defined in Equation 5.9 and reproduced below for clarity:

$$V_{frc}^{n} = \frac{PEEP_{n+1} - PEEP_{n})}{E_1(V_frc - V_m)^2 + \frac{E_2 PEEP_{n+1}}{60}}$$

Where V_{frc} across a particular PEEP step from n to n+1 is denoted V_{frc}^{n}. This equation (Equation 5.9) was iterated until convergence ($\triangle V_{frc}^{n}$ <0.01%). The minimum value for $V - V_m$ was set to zero through use of the *min* function in MATLAB. V_{frc} was calculated in this manner across all PEEP steps in all RMs.

Calculating V_{frc} from Clinical Data

Volume was calculated across the final breath at $PEEP_n$ and the first breath at $PEEP_{n+1}$ by integrating clinical flow data with respect to time. V_{frc} was determined to be the difference in end expiratory volume across this PEEP change thus matching the definition as volume retained by increased PEEP. For 2 steps up in PEEP, V_{frc} across this larger PEEP change was calculated as the sum of the two V_{frc} calculations for each single step up in PEEP. This calculation was used to avoid flow sensor noise causing drift effects confounding volume estimation. The same additive process was also used for step increases of 3 PEEP levels and higher.

9.2.3 Validation of Results

The error between the modelled V_{frc} estimate and the calculated clinical V_{frc} value was determined for each PEEP step. The percentage error was also calculated. However, absolute percent error was used.PEEP steps of less than 2 cmH_2O were not included in the analysis as these were often due to a change in PEEP level not being achieved.

Forward simulation of Equation 5.10 using previously identified parameters and with a V_{frc} shift in the volumetric recruitment elastance function (V(t) $\rightarrow$ V(t) + V_{frc}) was used to compare model fit of this forward prediction a forward-prediction of the model to that using the calculated clinical V_{frc} value. Model fit was assessed via the difference between model and clinical peak inspiratory pressure, a clinical outcome as it is an

indicator of the risk of ventilator-induced lung injury (VILI).

9.3 Results

9.3.1 Accuracy of V_{frc} Estimation

Table 9.1 shows V_{frc} estimate errors tend to increase with increasing PEEP interval size. However, many of the larger errors were under-estimations of V_{frc}. This under-estimation is clinically preferable to over-estimation as it would encourage more conservative treatment plans due to reduced predicted response to a PEEP change with less risk of patient harm.

Table 9.1: V_{frc} error (L) (median [IQR]) for each PEEP interval size for the CURE and McREM cohorts.

$\triangle$ PEEP	CURE Cohort V_{frc} Error (L)	McREM Cohort V_{frc} Error (L)
2 cmH_2O	0.03 [-0.03 - 0.07]	0.00 [-0.04 - 0.02]
4 cmH_2O	-0.03 [-0.09 - 0.00]	-0.00 [-0.07 - 0.03]
6 cmH_2O	0.12 [-0.11 - 0.14]	-0.03 [-0.07 - 0.01]
8 cmH_2O	-0.11 [-0.14 - -0.04]	-0.04 [-0.16 - -0.02]
10 cmH_2O	-0.12 [-0.17 - 0.05]	-0.13 [-0.24 - -0.03]
12 cmH_2O	-0.11 [-0.22 - -0.07]	-0.13 [-0.32 - -0.02]
14 cmH_2O	-0.08 [-0.13 - -0.04]	-0.29 [-0.33 - -0.09]

The boxplots in Figure 9.1 suggest the V_{frc} estimate was more accurate in the CURE cohort than in the McREM cohort with median absolute errors of around 15% for changes in PEEP level up to 14 cmH_2O. In addition, the McREM cohort also demonstrated more cases of under-estimation of V_{frc}.

The outliers shown in the boxplots are defined as cases where the data point is more than 1.5 times the IQR away from the box. While these values are high percentage errors, this magnitude of error is due to the small volume increases being estimated making these errors seem larger than they are clinically. For example, the largest clinical V_{frc} value for the CURE cohort was 0.68 L whereas in the McREM cohort this was 0.76 L. In comparison to these values, the average lung capacity of an adult is around 6 L.

9.3.2 Validation of V_{frc} Estimation

The fitted elastance curves for each PEEP level are shown for two cases in Figure 9.2. When curve was offset with the estimated V_{frc} change from the starting PEEP level, they overlapped into a parabolic shape in most cases studied. As expected, the recruitment elastance was often steeper earlier in the recruitment manoeuvre than at higher PEEP levels such as 20 or 22 cmH_2O where distension is expected to be the primary dynamic.

9.3.3 Effect of V_{frc} Estimation Accuracy on Model Prediction

Figure 9.3 shows there is very little improvement in PIP prediction when the model V_{frc} estimate is replaced with the exact, calculated clinical V_{frc} value. Tables 9.2 - 9.21 presented at the end of the chapter show detailed V_{frc} estimation and prediction results for the 21 patients studied. PIP prediction was less accurate in the McREM cohort than in the CURE cohort when the clinical V_{frc} was used, mimicking the results from Chapters 6 - 8. This result and the small difference in error between the prediction when using the modelled V_{frc} value and the clinical V_{frc} indicates the larger errors in this cohort are caused more by the elastance and resistance basis functions not completely capturing the non-linear behaviour, than by Equation 5.9 not capturing the true value of V_{frc}.

9.4 Discussion

The model provided good estimation of V_{frc} across a range of patients and PEEP levels with a median [IQR] error of 0.03[-0.09 - 0.00]L (CURE cohort) and -0.00 [-0.07 - 0.03]L (McREM cohort) for PEEP increases of up to 4 cmH_2O. For an increase of up to 8 cmH_2O, the model estimated V_{frc} with error of -0.11 [-0.14 - -0.04]L for the CURE cohort and -0.04 [-0.16 - -0.02]L for the McREM cohort. This high accuracy in a non-invasive V_{frc} estimation which can be carried out using information readily available at the bedside and without any added workload will aid in clinical decision making.

In particular, precise V_{frc} knowledge could aid the management of the trade-off between added recruited volume and increasing the airway pressure applied to the lung. For example, Patient 4, Arm 3 (Table 9.21 shows significant saturation of V_{frc} gains to low values at higher PEEP, indicating very little recruited volume is gained for an increase in risk of VILI. This method thus offers a non-invasive means to titrate pressures based on recruited volume instead of, or in addition to, elastance or pressure.

As demonstrated in Figure 9.3, using the clinical V_{frc} value showed limited improvements to model prediction of PIP over using the modelled V_{frc} estimate. In PEEP increases of 4 cmH_2O PIP (%) error, the modelled V_{frc} estimate was 4.0 [2.9 - 5.0]% whereas when this value was replaced with the calculated clinical V_{frc} value it only decreased to 3.6 [1.9 - 4.5]% for the CURE cohort. For the McREM cohort, substituting the modelled V_{frc} estimate (PIP (%) error of 3.5 [2.0 - 4.4]%) with the clinical value (PIP (%) error of 3.6 [1.9 - 4.5]%) had no effect on the prediction accuracy across a 4 cmH_2O PEEP increase. This lack of change indicates better V_{frc} estimation can provide no further information with the current model and basis function.

In addition to the high accuracy of results, the estimated values of V_{frc} showed expected physical behaviour. In particular, increasing positive end-expiratory pressure (PEEP) has falling V_{frc}, as expected with diminishing available volume at higher PEEP. While there were a few outlier values of V_{frc} error, generally results were internally consistent within patients and reflected clinically and physiologically expected trends. Future work could look at reducing these outliers by identifying models over several PEEP steps, by aggregating average breaths across a PEEP level, or by statistical analysis of trends in larger data sets.

The initial analysis carried out in this study used data from a limited number of patients. In addition, 3 of the 4 patients in the CURE cohort presented with forms of bacterial pneumonia, which may lead to reduced pulmonary recruitability along with limiting patient disease type (Lorx et al., 2010). However, all patients studied across both

cohorts had PF $<$300 mmHg, meeting ARDS guideline definitions for impaired function (Brower et al., 2000). To mitigate the impact of this sample size, a large number of breaths and RM steps were studied from each patient to ensure a diverse range of lung mechanics was assessed.

Pneumonia-affected lungs often display heterogeneous behaviour across different pulmonary regions, with optimal PEEP potentially occurring over a large range (Lorx et al., 2010). Furthermore, airflow resistance in patients presenting with pneumonia-induced ARDS often shows wide variation, making achieving optimal ventilation challenging (Lorx et al., 2010). Therefore, the ability of this model to accurately estimate V_{frc} across a range of PEEP changes is promising for clinical use.

The model used to determine a value of V_{frc} assumed a steady state system, and showed very good accuracy at estimating the measured change in volume. There was a strong correlation between low error in V_{frc} and good accuracy in prediction results. Thus, future work into developing a more accurate estimation of the volume gained throughout a RM would further aid clinician ability to set the optimal PEEP levels. The results also offer a clinical opportunity to titrate PEEP based on the estimated lung volume recruited, a direct indication of the success of an RM. This combined with prediction of the point of minimum elastance would allow clinicians to manage the trade-off between the risk of VILI and lung recruitment.

9.5 Summary

In this study a model-based method to predict additional recruited lung volume (V_{frc}) gained throughout a recruitment manoeuvre was developed and validated against clinical data. Initial results were promising with high accuracy shown in both approximating V_{frc} and using this information to predict lung behaviour at higher PEEP levels. The results offer a clinical opportunity to titrate PEEP based on the estimated lung volume recruited. Combined with prediction of the point of minimum elastance this would al-

low clinicians to manage the trade-off between the risk of VILI and lung recruitment, improving patient outcomes.

Table 9.2: Prediction results for Patient 1 of the McREM cohort.

$PEEP_n$ **(cmH2O)**	$PEEP_{n+1}$ **(cmH2O)**	**PEEP Change (cmH2O)**	**RMS Error (cmH2O)**	**RMS Error (%)**	**PIP Error (cmH2O)**	**PIP Error (%)**	**Clinical *Vfrc* (L)**	**Model *Vfrc* Estimate (L)**	***Vfrc* Error (L)**
10	**12**	2	1.1	5.0	2.0	5.5	0.09	0.08	0.01
	14	4	1.0	4.0	2.6	6.5	0.17	0.17	0.00
	16	6	1.0	3.7	2.6	6.0	0.29	0.27	0.01
	18	8	1.1	3.2	3.2	7.0	0.39	0.38	0.00
12	**14**	2	0.9	3.9	2.2	5.5	0.08	0.08	0.00
	16	4	0.9	3.6	1.9	4.4	0.20	0.17	0.02
	18	6	0.9	3.0	2.4	5.1	0.30	0.27	0.03
14	**16**	2	0.9	3.6	1.0	2.2	0.12	0.09	0.03
	18	4	1.0	3.1	1.2	2.6	0.22	0.18	0.03
16	**18**	2	0.9	3.1	1.4	2.9	0.10	0.09	0.02

Table 9.3: Prediction results for Patient 2 of the McREM cohort.

$PEEP_n$ **(cmH2O)**	$PEEP_{n+1}$ **(cmH2O)**	**PEEP Change (cmH2O)**	**RMS Error (cmH2O)**	**RMS Error (%)**	**PIP Error (cmH2O)**	**PIP Error (%)**	**Clinical *Vfrc* (L)**	**Model *Vfrc* Estimate (L)**	***Vfrc* Error (L)**
10	**12**	2	0.5	2.4	1.4	3.9	0.08	0.07	0.01
	14	4	0.7	2.4	2.0	5.5	0.16	0.15	0.01
	16	6	0.9	2.3	2.5	6.3	0.17	0.24	0.07
	18	8	1.0	2.4	2.9	6.7	0.17	0.33	0.16
	20	10	1.1	2.5	2.9	6.2	0.18	0.43	0.25
12	**14**	2	0.5	2.0	1.3	3.6	0.08	0.08	0.01
	16	4	0.6	1.8	1.6	4.1	0.09	0.16	0.07
	18	6	0.6	1.7	1.8	4.1	0.09	0.25	0.15
	20	8	0.7	1.8	1.7	3.6	0.10	0.34	0.24
14	**16**	2	0.4	1.5	0.9	2.1	0.01	0.08	0.07
	18	4	0.5	1.5	0.8	1.8	0.01	0.17	0.16
	20	6	0.5	1.5	0.5	1.0	0.02	0.26	0.24
16	**18**	2	0.4	1.4	0.5	1.2	0.00	0.08	0.08
	20	4	0.5	1.5	0.1	0.1	0.01	0.17	0.16

Table 9.4: Prediction results for Patient 3 of the McREM cohort.

$PEEP_n$ (cmH2O)	$PEEP_{n+1}$ (cmH2O)	PEEP Change (cmH2O)	RMS Error (cmH2O)	RMS Error (%)	PIP Error (cmH2O)	PIP Error (%)	Clinical *Vfrc* (L)	Model *Vfrc* Estimate (L)	*Vfrc* Error (L)
10	**12**	2	1.1	4.7	2.3	6.0	0.00	0.08	0.08
	14	4	1.0	4.7	2.2	5.3	0.02	0.18	0.15
	16	6	0.9	2.1	1.5	3.4	0.13	0.28	0.15
	18	8	0.7	1.5	2.3	4.8	0.24	0.39	0.15
	20	10	0.8	1.9	2.6	5.3	0.37	0.50	0.13
	22	12	1.2	1.9	3.2	6.5	0.38	0.60	0.23
12	**14**	2	1.0	4.2	2.1	4.9	0.02	0.10	0.08
	16	4	0.9	2.0	1.3	2.9	0.13	0.20	0.07
	18	6	0.7	1.4	2.0	4.1	0.24	0.31	0.06
	20	8	0.8	1.8	2.3	4.6	0.37	0.41	0.04
	22	10	1.2	1.9	2.9	5.9	0.38	0.50	0.13
14	**16**	2	1.0	1.9	1.4	3.0	0.11	0.11	0.00
	18	4	0.7	1.3	2.0	4.2	0.22	0.22	0.00
	20	6	0.8	1.7	2.3	4.6	0.35	0.32	0.03
	22	8	1.2	2.0	2.9	5.9	0.35	0.41	0.05
16	**18**	2	0.7	1.7	2.2	4.5	0.11	0.09	0.02
	20	4	0.7	1.6	2.2	4.5	0.24	0.18	0.06
	22	6	1.0	1.8	2.6	5.2	0.24	0.27	0.03
18	**20**	2	0.7	1.6	1.6	3.3	0.13	0.10	0.03
	22	4	1.0	1.7	2.0	4.1	0.13	0.19	0.06
20	**22**	2	0.9	1.8	2.0	4.0	0.01	0.09	0.08

Table 9.5: Prediction results for Patient 5 of the McREM cohort.

$PEEP_n$ (cmH2O)	$PEEP_{n+1}$ (cmH2O)	PEEP Change (cmH2O)	RMS Error (cmH2O)	RMS Error (%)	PIP Error (cmH2O)	PIP Error (%)	Clinical *Vfrc* (L)	Model *Vfrc* Estimate (L)	*Vfrc* Error (L)
10	**12**	2	0.6	2.4	0.6	1.8	0.09	0.07	0.02
	14	4	0.6	2.3	0.6	1.7	0.19	0.15	0.04
	16	6	0.7	1.9	0.2	0.5	0.28	0.23	0.05
	18	8	1.0	2.6	-1.3	2.8	0.36	0.31	0.05
	20	10	1.9	3.8	-2.9	5.7	0.47	0.39	0.08
	22	12	2.0	3.8	-3.4	6.6	0.54	0.47	0.07
12	**14**	2	0.6	2.1	0.9	2.3	0.10	0.07	0.03
	16	4	0.6	1.7	0.4	1.1	0.19	0.15	0.04
	18	6	0.9	2.5	-1.1	2.4	0.27	0.23	0.04
	20	8	1.8	3.7	-2.8	5.4	0.38	0.31	0.07
	22	10	1.9	3.8	-3.2	6.3	0.45	0.38	0.07
14	**16**	2	0.5	1.6	0.8	1.9	0.09	0.08	0.01
	18	4	0.8	2.2	-0.7	1.5	0.17	0.16	0.02
	20	6	1.6	3.4	-2.4	4.6	0.28	0.23	0.05
	22	8	1.7	3.5	-2.9	5.6	0.35	0.30	0.04
16	**18**	2	0.7	1.9	-0.5	1.0	0.09	0.08	0.01
	20	4	1.5	3.2	-2.2	4.3	0.19	0.15	0.04
	22	6	1.7	3.4	-2.7	5.3	0.26	0.23	0.03
18	**20**	2	1.1	2.4	-1.1	2.1	0.10	0.08	0.03
	22	4	1.2	2.6	-1.7	3.3	0.17	0.15	0.03
20	**22**	2	0.6	1.6	0.0	0.1	0.07	0.07	0.00

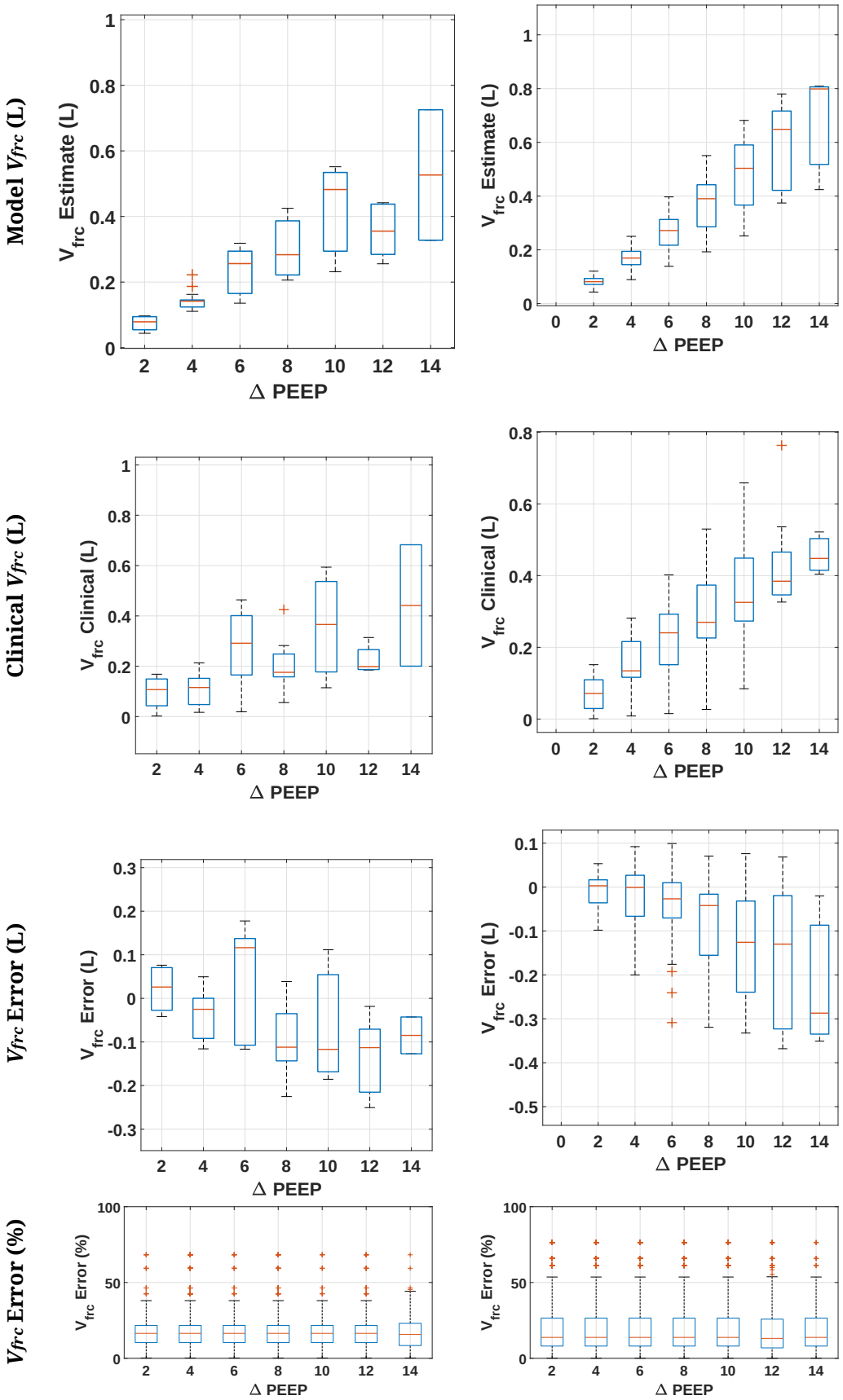

Figure 9.1: Boxplot of V_{frc} results separated by PEEP interval size for the CURE and McREM cohorts.

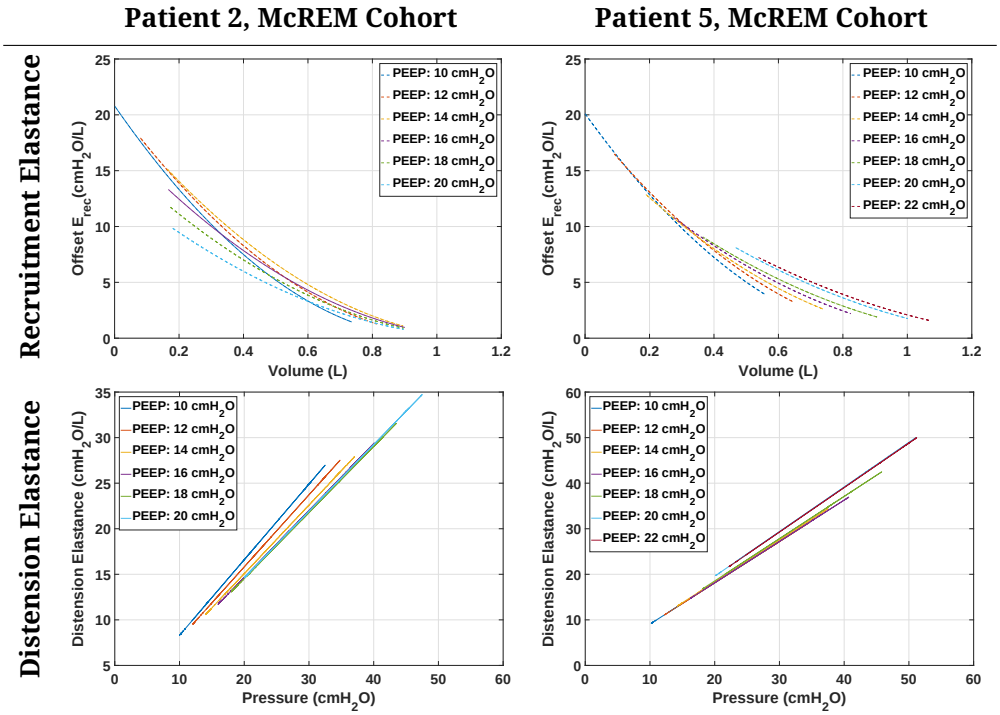

Figure 9.2: Recruitment and distension elastance curves across PEEP steps, including the associated volume gain offsets relative to the lowest PEEP data.

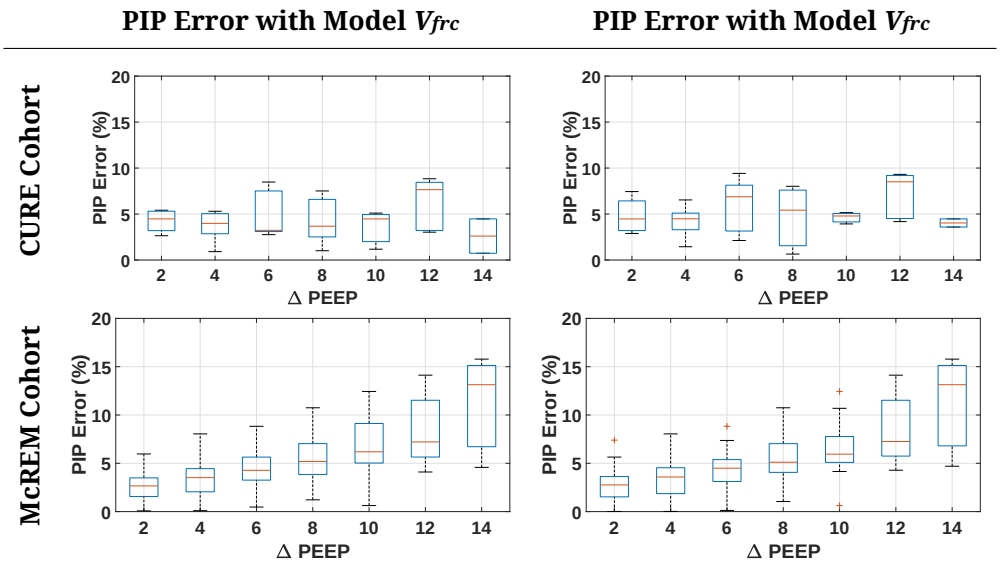

Figure 9.3: Boxplot of $Vfrc$ results separated by PEEP interval size for the CURE and McREM cohorts.

Table 9.6: Prediction results for Patient 6 of the McREM cohort.

$PEEP_n$ (cmH2O)	$PEEP_{n+1}$ (cmH2O)	PEEP Change (cmH2O)	RMS Error (cmH2O)	RMS Error (%)	PIP Error (cmH2O)	PIP Error (%)	Clinical *Vfrc* (L)	Model *Vfrc* Estimate (L)	*Vfrc* Error (L)
10	**12**	2	0.6	3.1	1.4	3.5	0.08	0.08	0.00
	14	4	0.6	2.5	1.6	3.7	0.17	0.17	0.00
12	**14**	2	0.6	2.5	1.1	2.5	0.09	0.08	0.01

Table 9.7: Prediction results for Patient 7 of the McREM cohort.

$PEEP_n$ (cmH2O)	$PEEP_{n+1}$ (cmH2O)	PEEP Change (cmH2O)	RMS Error (cmH2O)	RMS Error (%)	PIP Error (cmH2O)	PIP Error (%)	Clinical *Vfrc* (L)	Model *Vfrc* Estimate (L)	*Vfrc* Error (L)
10	**12**	2	0.5	2.1	0.6	1.7	0.08	0.07	0.01
	14	4	0.7	2.4	0.0	0.1	0.16	0.15	0.01
	16	6	0.9	2.6	-0.4	0.9	0.21	0.23	0.01
12	**14**	2	0.6	2.2	0.2	0.5	0.08	0.07	0.00
	16	4	0.8	2.4	-0.3	0.6	0.13	0.15	0.01
14	**16**	2	0.6	1.8	0.3	0.7	0.06	0.07	0.02

Table 9.8: Prediction results for Patient 8 of the McREM cohort.

$PEEP_n$ (cmH2O)	$PEEP_{n+1}$ (cmH2O)	PEEP Change (cmH2O)	RMS Error (cmH2O)	RMS Error (%)	PIP Error (cmH2O)	PIP Error (%)	Clinical *Vfrc* (L)	Model *Vfrc* Estimate (L)	*Vfrc* Error (L)
10	**12**	2	1.2	4.5	2.5	5.9	0.13	0.08	0.05
	14	4	1.1	3.3	2.4	5.4	0.26	0.17	0.09
	16	6	1.1	2.7	2.5	5.3	0.38	0.28	0.10
	18	8	1.2	2.8	2.5	5.1	0.38	0.41	0.03
	20	10	1.3	2.6	3.3	6.6	0.40	0.58	0.18
12	**14**	2	1.1	3.3	2.1	4.7	0.13	0.08	0.04
	16	4	1.1	2.6	2.0	4.2	0.24	0.18	0.06
	18	6	1.1	2.5	1.8	3.7	0.25	0.29	0.04
	20	8	1.2	2.3	2.6	5.2	0.27	0.42	0.15
14	**16**	2	1.0	2.7	1.9	4.1	0.12	0.09	0.03
	18	4	1.1	2.3	1.6	3.3	0.12	0.18	0.06
	20	6	1.1	2.1	2.2	4.4	0.14	0.29	0.15
16	**18**	2	1.0	2.3	1.7	3.4	0.01	0.08	0.08
	20	4	1.0	2.2	2.0	4.1	0.02	0.18	0.15

Table 9.9: Prediction results for Patient 9 of the McREM cohort.

$PEEP_n$ (cmH2O)	$PEEP_{n+1}$ (cmH2O)	PEEP Change (cmH2O)	RMS Error (cmH2O)	RMS Error (%)	PIP Error (cmH2O)	PIP Error (%)	Clinical *Vfrc* (L)	Model *Vfrc* Estimate (L)	*Vfrc* Error (L)
10	**12**	2	0.8	3.5	1.7	5.3	0.15	0.11	0.04
	14	4	0.8	3.1	1.7	4.8	0.28	0.25	0.03
	16	6	0.9	2.4	2.3	6.1	0.40	0.40	0.01
	18	8	1.0	2.5	2.9	7.1	0.53	0.55	0.02
	20	10	1.0	2.3	3.2	7.4	0.66	0.68	0.02
	22	12	1.3	3.0	3.6	7.9	0.76	0.78	0.02
12	**14**	2	0.7	3.2	1.0	2.8	0.13	0.12	0.01
	16	4	0.8	2.4	1.4	3.7	0.25	0.25	0.00
	18	6	0.8	2.5	1.9	4.7	0.38	0.39	0.01
	20	8	0.8	1.9	2.2	5.0	0.51	0.53	0.03
	22	10	0.9	2.3	2.5	5.5	0.61	0.65	0.04
14	**16**	2	0.7	2.5	1.4	3.7	0.12	0.12	0.00
	18	4	0.8	2.4	1.8	4.4	0.25	0.25	0.00
	20	6	0.7	1.9	2.0	4.7	0.38	0.38	0.00
	22	8	0.8	2.2	2.4	5.2	0.48	0.50	0.02
16	**18**	2	0.7	2.5	1.4	3.4	0.13	0.11	0.01
	20	4	0.6	2.0	1.5	3.4	0.26	0.24	0.02
	22	6	0.6	1.8	1.8	3.9	0.36	0.36	0.00
18	**20**	2	0.6	2.0	1.2	2.7	0.13	0.12	0.01
	22	4	0.6	1.7	1.3	2.9	0.23	0.23	0.00
20	**22**	2	0.6	1.8	1.2	2.6	0.10	0.12	0.01

Table 9.10: Prediction results for Patient 10 of the McREM cohort.

$PEEP_n$ (cmH2O)	$PEEP_{n+1}$ (cmH2O)	PEEP Change (cmH2O)	RMS Error (cmH2O)	RMS Error (%)	PIP Error (cmH2O)	PIP Error (%)	Clinical *Vfrc* (L)	Model *Vfrc* Estimate (L)	*Vfrc* Error (L)
10	**11**	13	2	0.9	4.3	1.2	2.5	0.01	0.05

Table 9.11: Prediction results for Patient 11 of the McREM cohort.

$PEEP_n$ (cmH2O)	$PEEP_{n+1}$ (cmH2O)	PEEP Change (cmH2O)	RMS Error (cmH2O)	RMS Error (%)	PIP Error (cmH2O)	PIP Error (%)	Clinical *Vfrc* (L)	Model *Vfrc* Estimate (L)	*Vfrc* Error (L)
10	**12**	2	0.7	3.0	1.3	4.0	0.11	0.08	0.03
	14	4	0.6	2.4	1.5	4.3	0.22	0.17	0.05
	16	6	0.6	1.9	1.3	3.6	0.33	0.27	0.06
	18	8	0.6	1.7	1.2	2.9	0.44	0.39	0.05
	20	10	1.6	6.0	0.3	0.6	0.45	0.52	0.06
12	**14**	2	0.6	2.3	1.1	3.2	0.11	0.09	0.02
	16	4	0.6	1.9	0.9	2.4	0.22	0.18	0.03
	18	6	0.6	1.8	0.6	1.4	0.32	0.29	0.04
	20	8	1.6	6.2	-0.5	1.2	0.34	0.40	0.06
14	**16**	2	0.6	1.9	0.6	1.8	0.11	0.09	0.02
	18	4	0.7	1.8	0.2	0.6	0.22	0.19	0.03
	20	6	1.7	6.2	-1.0	2.3	0.24	0.30	0.06
16	**18**	2	0.6	1.7	0.4	1.0	0.11	0.10	0.01
	20	4	1.6	6.0	-0.9	2.0	0.13	0.19	0.07
18	**20**	2	1.4	5.4	-0.3	0.6	0.02	0.10	0.08

Table 9.12: Prediction results for Patient 12 of the McREM cohort.

$PEEP_n$ **(cmH2O)**	$PEEP_{n+1}$ **(cmH2O)**	**PEEP Change (cmH2O)**	**RMS Error (cmH2O)**	**RMS Error (%)**	**PIP Error (cmH2O)**	**PIP Error (%)**	**Clinical *Vfrc* (L)**	**Model *Vfrc* Estimate (L)**	***Vfrc* Error (L)**
12	**14**	2	0.4	1.7	0.2	0.6	0.05	0.06	0.00
	16	4	0.3	1.2	0.2	0.6	0.12	0.12	0.00
	18	6	0.4	1.1	-0.4	1.0	0.19	0.18	0.00
	20	8	0.5	1.4	-0.8	1.8	0.25	0.25	0.00
14	**16**	2	0.3	1.2	0.1	0.1	0.07	0.06	0.01
	18	4	0.4	1.2	-0.6	1.6	0.13	0.12	0.01
	20	6	0.6	1.5	-1.1	2.6	0.19	0.18	0.01
16	**18**	2	0.3	1.0	-0.2	0.6	0.07	0.06	0.00
	20	4	0.4	1.2	-0.6	1.5	0.13	0.13	0.00
18	**20**	2	0.3	1.1	-0.3	0.7	0.06	0.06	0.00

Table 9.13: Prediction results for Patient 13 of the McREM cohort.

$PEEP_n$ **(cmH2O)**	$PEEP_{n+1}$ **(cmH2O)**	**PEEP Change (cmH2O)**	**RMS Error (cmH2O)**	**RMS Error (%)**	**PIP Error (cmH2O)**	**PIP Error (%)**	**Clinical *Vfrc* (L)**	**Model *Vfrc* Estimate (L)**	***Vfrc* Error (L)**
10	**12**	2	1.3	6.8	-0.4	0.9	0.07	0.04	0.02

Table 9.14: Prediction results for Patient 14 of the McREM cohort.

$PEEP_n$ **(cmH2O)**	$PEEP_{n+1}$ **(cmH2O)**	**PEEP Change (cmH2O)**	**RMS Error (cmH2O)**	**RMS Error (%)**	**PIP Error (cmH2O)**	**PIP Error (%)**	**Clinical *Vfrc* (L)**	**Model *Vfrc* Estimate (L)**	***Vfrc* Error (L)**
10	**12**	2	0.6	2.9	1.1	3.3	0.06	0.06	0.00
	14	4	0.6	2.5	1.0	2.8	0.12	0.13	0.01
	16	6	0.7	2.9	1.3	3.3	0.18	0.19	0.01
	18	8	0.9	3.1	1.7	4.0	0.24	0.26	0.01
	20	10	0.9	3.0	1.8	4.3	0.30	0.32	0.02
	22	12	1.2	3.8	1.9	4.1	0.35	0.37	0.02
	24	14	1.2	3.4	2.2	4.6	0.40	0.42	0.02
12	**14**	2	0.6	2.1	0.9	2.5	0.06	0.07	0.01
	16	4	0.6	2.5	1.3	3.3	0.12	0.14	0.02
	18	6	0.8	2.8	1.7	4.1	0.18	0.21	0.03
	20	8	0.9	2.9	1.9	4.4	0.24	0.27	0.03
	22	10	1.2	3.8	2.0	4.3	0.29	0.32	0.04
	24	12	1.3	3.4	2.4	4.8	0.34	0.37	0.03
14	**16**	2	0.6	2.3	1.0	2.7	0.06	0.07	0.01
	18	4	0.7	2.5	1.4	3.5	0.12	0.14	0.02
	20	6	0.8	2.4	1.6	3.7	0.18	0.20	0.03
	22	8	1.0	3.3	1.6	3.5	0.23	0.26	0.03
	24	10	1.0	2.9	1.9	3.9	0.28	0.32	0.03
16	**18**	2	0.6	2.1	1.2	3.0	0.06	0.08	0.01
	20	4	0.7	2.0	1.5	3.4	0.12	0.14	0.03
	22	6	0.9	2.7	1.5	3.2	0.17	0.21	0.04
	24	8	0.9	2.5	1.8	3.6	0.22	0.27	0.04
18	**20**	2	0.6	1.8	1.3	2.9	0.05	0.08	0.02
	22	4	0.8	2.3	1.3	2.8	0.11	0.14	0.04
	24	6	0.8	2.1	1.6	3.2	0.16	0.21	0.05
20	**22**	2	0.7	2.0	0.9	2.0	0.05	0.07	0.02
	24	4	0.6	1.8	1.1	2.3	0.11	0.14	0.03
22	**24**	2	0.6	1.6	1.1	2.3	0.05	0.08	0.03

Table 9.15: Prediction results for Patient 15 of the McREM cohort.

$PEEP_n$ (cmH2O)	$PEEP_{n+1}$ (cmH2O)	PEEP Change (cmH2O)	RMS Error (cmH2O)	RMS Error (%)	PIP Error (cmH2O)	PIP Error (%)	Clinical *Vfrc* (L)	Model *Vfrc* Estimate (L)	*Vfrc* Error (L)
10	**12**	2	0.7	3.2	1.9	5.6	0.13	0.09	0.04
	14	4	0.9	2.7	2.8	8.0	0.25	0.19	0.06
	16	6	1.1	3.0	3.4	8.8	0.25	0.31	0.06
	18	8	1.5	3.4	4.4	10.7	0.26	0.45	0.19
	20	10	1.9	4.0	5.3	12.4	0.27	0.60	0.33
	22	12	2.5	5.2	6.3	14.1	0.39	0.72	0.33
	24	14	3.0	6.3	7.4	15.8	0.52	0.81	0.29
	26	16	3.6	8.2	8.1	16.6	0.57	0.87	0.30
12	**14**	2	0.6	2.3	1.7	4.8	0.12	0.09	0.03
	16	4	0.8	2.4	2.1	5.4	0.12	0.20	0.08
	18	6	1.0	2.5	3.0	7.3	0.13	0.32	0.19
	20	8	1.4	2.9	3.8	9.0	0.15	0.46	0.32
	22	10	1.8	4.0	4.8	10.7	0.27	0.60	0.33
	24	12	2.3	5.0	5.8	12.3	0.40	0.71	0.32
	26	14	2.9	6.7	6.4	13.1	0.45	0.80	0.35
14	**16**	2	0.6	2.2	1.2	3.2	0.00	0.10	0.10
	18	4	0.7	1.9	2.0	4.9	0.01	0.21	0.20
	20	6	1.0	2.2	2.8	6.6	0.02	0.33	0.31
	22	8	1.4	3.1	3.7	8.3	0.14	0.46	0.32
	24	10	1.8	4.0	4.7	9.9	0.27	0.59	0.31
	26	12	2.3	5.7	5.3	10.7	0.33	0.69	0.37
16	**18**	2	0.5	1.7	1.3	3.3	0.01	0.10	0.09
	20	4	0.7	1.6	2.1	4.9	0.02	0.20	0.18
	22	6	1.0	2.5	2.9	6.5	0.14	0.32	0.18
	24	8	1.4	3.3	3.8	8.1	0.27	0.44	0.17
	26	10	1.9	4.8	4.3	8.9	0.33	0.56	0.24
18	**20**	2	0.5	1.4	1.3	3.1	0.01	0.10	0.09
	22	4	0.8	2.0	2.0	4.5	0.13	0.21	0.07
	24	6	1.0	2.7	2.9	6.1	0.26	0.32	0.06
	26	8	1.5	4.1	3.4	6.9	0.32	0.44	0.13
20	**22**	2	0.6	1.7	1.2	2.8	0.12	0.10	0.02
	24	4	0.7	2.1	2.0	4.2	0.25	0.21	0.04
	26	6	1.2	3.5	2.4	5.0	0.30	0.33	0.03
22	**24**	2	0.5	1.5	1.4	3.1	0.13	0.11	0.02
	26	4	0.9	2.7	1.8	3.7	0.18	0.23	0.05
24	**26**	2	0.8	2.2	1.3	2.7	0.05	0.12	0.07

Table 9.16: Prediction results for Patient 17 of the McREM cohort.

$PEEP_n$ **(cmH2O)**	$PEEP_{n+1}$ **(cmH2O)**	**PEEP Change (cmH2O)**	**RMS Error (cmH2O)**	**RMS Error (%)**	**PIP Error (cmH2O)**	**PIP Error (%)**	**Clinical *Vfrc* (L)**	**Model *Vfrc* Estimate (L)**	***Vfrc* Error (L)**
10	**12**	2	1.0	4.4	0.1	0.3	0.00	0.04	0.04
	14	4	1.0	3.7	-0.5	1.4	0.02	0.09	0.07
	16	6	1.5	4.7	-1.7	3.9	0.02	0.14	0.12
	18	8	2.1	5.5	-3.4	7.1	0.03	0.19	0.17
	20	10	3.3	7.2	-5.3	10.4	0.08	0.25	0.17
12	**14**	2	1.0	3.6	-0.4	1.0	0.01	0.04	0.03
	16	4	1.4	4.4	-1.5	3.5	0.02	0.09	0.08
	18	6	2.0	5.0	-3.2	6.8	0.02	0.14	0.12
	20	8	3.2	6.8	-5.1	10.1	0.08	0.20	0.11
14	**16**	2	1.1	3.6	-0.6	1.5	0.00	0.05	0.04
	18	4	1.6	4.1	-2.3	4.8	0.01	0.09	0.08
	20	6	2.7	5.7	-4.1	8.1	0.07	0.14	0.07
16	**18**	2	1.1	3.0	-1.1	2.3	0.01	0.05	0.04
	20	4	2.0	4.3	-2.9	5.7	0.07	0.09	0.03
18	**20**	2	1.3	3.0	-1.3	2.5	0.06	0.05	0.01

Table 9.17: Prediction results for Patient 18 of the McREM cohort.

$PEEP_n$ **(cmH2O)**	$PEEP_{n+1}$ **(cmH2O)**	**PEEP Change (cmH2O)**	**RMS Error (cmH2O)**	**RMS Error (%)**	**PIP Error (cmH2O)**	**PIP Error (%)**	**Clinical *Vfrc* (L)**	**Model *Vfrc* Estimate (L)**	***Vfrc* Error (L)**
10	**12**	2	1.2	5.8	0.7	1.4	0.06	0.05	0.01
	14	4	1.1	4.3	0.6	1.1	0.13	0.10	0.03
12	**14**	2	1.0	4.4	1.2	2.2	0.07	0.05	0.02

Table 9.18: Prediction results for Patient 1 (Arms 1 and 3) of the CURE cohort.

$PEEP_n$ **(cmH2O)**	$PEEP_{n+1}$ **(cmH2O)**	**PEEP Change (cmH2O)**	**RMS Error (cmH2O)**	**RMS Error (%)**	**PIP Error (cmH2O)**	**PIP Error (%)**	**Clinical *Vfrc* (L)**	**Model *Vfrc* Estimate (L)**	***Vfrc* Error (L)**
Arm 1									
11	**15**	4	1.0	2.9	1.4	4.6	0.16	0.15	0.01
	20	9	1.3	3.6	2.8	7.7	0.17	0.34	0.16
	23	12	1.3	2.2	3.1	7.5	0.31	0.44	0.13
	27	16	1.5	2.2	3.7	7.7	0.34	0.56	0.21
15	**20**	5	1.1	3.1	1.6	4.6	0.02	0.19	0.17
	23	8	1.0	1.7	1.5	3.6	0.16	0.30	0.14
	27	12	1.2	1.5	1.5	3.2	0.19	0.44	0.25
20	**23**	3	1.0	1.6	0.9	2.2	0.14	0.13	0.01
	27	7	1.2	1.3	0.9	1.8	0.17	0.28	0.12
23	**27**	4	1.1	1.5	0.4	0.9	0.03	0.14	0.12
Arm 3									
10	**11**	1	1.2	6.4	1.2	4.5	0.00	0.03	0.02
10	**15**	5	1.1	3.9	1.5	4.6	0.14	0.14	0.01
10	**19**	9	1.0	2.8	1.6	4.4	0.17	0.27	0.09
10	**23**	13	1.1	2.5	2.0	4.6	0.20	0.41	0.21
11	**15**	4	0.9	2.5	1.6	5.1	0.14	0.14	0.00
11	**19**	8	1.1	2.5	2.4	6.5	0.17	0.29	0.12
11	**23**	12	1.4	2.8	3.4	7.8	0.20	0.41	0.22
15	**19**	4	0.9	2.0	1.1	3.1	0.03	0.14	0.12
15	**23**	8	1.1	2.1	1.4	3.3	0.06	0.28	0.23
19	**23**	4	1.1	2.0	0.9	2.1	0.03	0.14	0.11

Table 9.19: Prediction results for Patient 2 (Arms 1 and 3) of the CURE cohort.

$PEEP_n$ (cmH2O)	$PEEP_{n+1}$ (cmH2O)	PEEP Change (cmH2O)	RMS Error (cmH2O)	RMS Error (%)	PIP Error (cmH2O)	PIP Error (%)	Clinical *Vfrc* (L)	Model *Vfrc* Estimate (L)	*Vfrc* Error (L)
Arm 1									
13	**14**	1	0.8	2.5	0.1	0.3	0.00	0.04	0.04
13	**16**	3	1.0	2.8	-0.8	3.0	0.09	0.14	0.06
13	**20**	7	1.2	3.2	-0.8	2.4	0.22	0.37	0.15
13	**21**	8	1.1	2.3	-0.8	2.5	0.22	0.42	0.21
13	**24**	11	1.6	3.6	-1.3	3.3	0.37	0.59	0.23
13	**27**	14	1.9	4.2	-2.0	4.5	0.68	0.73	0.04
14	**16**	2	1.0	2.9	-1.0	3.7	0.08	0.10	0.01
14	**20**	6	1.3	3.4	-1.0	3.2	0.21	0.32	0.10
14	**21**	7	1.2	2.4	-1.2	3.5	0.22	0.38	0.16
14	**24**	10	1.7	4.0	-1.7	4.5	0.37	0.55	0.19
14	**27**	13	2.1	4.6	-2.5	5.7	0.68	0.69	0.01
16	**20**	4	1.1	2.6	0.3	1.1	0.13	0.22	0.09
16	**21**	5	1.1	2.7	0.4	1.3	0.13	0.27	0.14
16	**24**	8	1.2	2.1	0.4	1.0	0.28	0.40	0.11
16	**27**	11	1.5	2.6	0.0	0.0	0.60	0.50	0.10
20	**21**	1	1.2	3.5	-0.1	0.3	0.00	0.04	0.04
20	**24**	4	1.4	2.5	-1.3	3.4	0.15	0.16	0.01
20	**27**	7	2.0	4.1	-3.0	6.7	0.47	0.30	0.17
21	**24**	3	1.3	2.9	-0.5	1.3	0.15	0.15	0.00
21	**27**	6	1.7	3.7	-1.4	3.2	0.46	0.29	0.18
24	**27**	3	1.4	2.4	-1.4	3.1	0.31	0.10	0.21
Arm 3									
16	**17**	1	1.0	2.5	0.3	1.0	0.19	0.04	0.15
16	**20**	4	1.2	2.2	-0.9	2.8	0.21	0.19	0.03
16	**24**	8	1.2	2.1	-0.5	1.4	0.43	0.39	0.04
16	**26**	10	2.0	4.7	-2.2	5.1	0.59	0.48	0.11
17	**20**	3	1.2	2.0	-1.3	3.8	0.02	0.13	0.11
17	**24**	7	1.3	2.3	-1.0	2.8	0.23	0.33	0.10
17	**26**	9	2.1	4.9	-2.9	6.6	0.40	0.43	0.03
20	**24**	4	1.4	2.6	-1.1	3.0	0.21	0.16	0.05
20	**26**	6	2.4	5.3	-3.7	8.5	0.38	0.26	0.12
24	**26**	2	1.6	3.6	-1.1	2.6	0.17	0.09	0.08

Table 9.20: Prediction results for Patient 3 (Arms 1 and 3) of the CURE cohort.

$PEEP_n$ (cmH2O)	$PEEP_{n+1}$ (cmH2O)	PEEP Change (cmH2O)	RMS Error (cmH2O)	RMS Error (%)	PIP Error (cmH2O)	PIP Error (%)	Clinical *Vfrc* (L)	Model *Vfrc* Estimate (L)	*Vfrc* Error (L)
Arm 1									
13	**17**	4	1.1	3.2	1.5	4.6	0.13	0.14	0.01
	21	8	1.3	3.0	1.5	3.7	0.25	0.26	0.01
	24	11	1.5	2.3	1.5	3.3	0.40	0.33	0.06
17	**21**	4	1.3	2.9	1.1	2.9	0.12	0.14	0.02
	24	7	1.4	2.3	1.2	2.6	0.27	0.23	0.04
21	**24**	3	1.4	2.5	1.6	3.4	0.15	0.11	0.04
Arm 3									
13	**17**	4	1.2	3.4	1.5	4.3	0.11	0.14	0.02
	20	7	1.3	2.9	1.7	4.2	0.27	0.22	0.05
	24	11	1.6	3.5	2.7	5.9	0.43	0.32	0.11
	26	13	1.8	3.7	3.7	7.7	0.56	0.36	0.21
17	**20**	3	1.3	2.9	1.4	3.6	0.16	0.11	0.05
	24	7	1.5	3.4	2.5	5.5	0.32	0.22	0.10
	26	9	1.7	3.5	3.6	7.4	0.45	0.26	0.19
20	**24**	4	1.5	3.6	2.4	5.3	0.16	0.12	0.04
	26	6	1.7	3.6	3.4	7.2	0.29	0.18	0.12
24	**26**	2	1.4	2.8	2.6	5.4	0.13	0.07	0.07

Table 9.21: Prediction results for Patient 4 (Arms 1 and 3) of the CURE cohort.

$PEEP_n$ (cmH2O)	$PEEP_{n+1}$ (cmH2O)	PEEP Change (cmH2O)	RMS Error (cmH2O)	RMS Error (%)	PIP Error (cmH2O)	PIP Error (%)	Clinical *Vfrc* (L)	Model *Vfrc* Estimate (L)	*Vfrc* Error (L)
Arm 1									
11	**13**	2	1.0	5.2	1.3	5.2	0.00	0.04	0.04
	21	10	1.0	3.0	0.4	1.2	0.11	0.23	0.12
	25	14	1.1	2.7	0.3	0.7	0.20	0.33	0.13
	29	18	1.2	2.4	0.2	0.4	0.28	0.42	0.13
13	**21**	8	1.1	3.2	2.4	6.6	0.11	0.22	0.11
	25	12	1.5	3.8	3.5	8.5	0.20	0.30	0.10
	29	16	1.9	4.1	4.4	9.5	0.28	0.35	0.07
17	**21**	4	1.0	2.8	1.9	5.2	0.10	0.13	0.03
	25	8	1.3	3.4	3.1	7.5	0.18	0.22	0.04
	29	12	1.7	3.8	4.1	8.8	0.27	0.28	0.02
21	**25**	4	1.0	2.8	2.1	5.1	0.09	0.12	0.03
	29	8	1.4	3.2	3.1	6.6	0.17	0.21	0.04
25	**29**	4	1.1	2.6	1.7	3.6	0.08	0.11	0.03
Arm 3									
16	**21**	5	1.1	4.0	1.0	2.7	0.02	0.11	0.09
	25	9	1.2	3.5	1.0	2.4	0.07	0.20	0.12
	28	12	1.3	3.5	1.4	3.0	0.19	0.26	0.07
21	**25**	4	1.1	2.9	2.1	5.0	0.05	0.11	0.07
	28	7	1.3	3.3	3.3	7.0	0.16	0.18	0.02
25	**28**	3	1.1	2.7	1.9	4.1	0.11	0.08	0.03

CHAPTER 10

Conclusions

Mechanical ventilation MV is a core life-support therapy for patients suffering from respiratory failure or acute respiratory distress syndrome (ARDS). Respiratory failure is a secondary outcome of a range of injuries and diseases, and results in almost half of all Intensive Care Unit (ICU) patients receiving some form of MV. Funding the increasing demand for ICU is a major economic and social issue and MV, in particular, can double the cost per day due to significant patient variability, over-sedation, and the large amount of clinician time required for patient management.

Reducing cost and increasing productivity in this area requires both a decrease in the average duration of MV by improving care, and a reduction in clinical workload. Both could be achieved by safely automating all or part of MV care via model-based dynamic systems modelling. The development of the first virtual patients, extends these models in this research to include lung mechanics prediction, providing clinicians with information about how a patient will respond to a change in treatment prior to making that change, improving patient treatment while reducing clinical workload. Virtual patients leads directly to the creation of virtual cohorts, extending impact by enabling *in-silico* design and testing of clinical protocols, speeding up the development of new treatment

plans.

All major changes in clinical ICU care are based on major clinical trial results, which are often poorly designed or powered. The high level of patient variability and the non-normal distribution of the key clinical outcome, length of mechanical ventilation, means many MV RCTs struggle to achieve statistical significance. As a result of this, RCTs often require a very large sample size to achieve statistical power to prevent inconclusive findings that cannot be extrapolated to other care units. This thesis first presents a non-parametric method to estimate required sample sizes for MV trials to achieve statistical power. A Monte-Carlo simulation method was developed and used to investigate several outcome metrics of ventilation treatment. As these metrics have highly skewed distributions, it also included the impact of imposing clinically relevant exclusion criteria on study power to enable better design for significance. Overall, a Monte-Carlo simulation approach using local cohort data combined with objective patient selection criteria can yield better design of ventilation studies to desired power and significance, with fewer patients per arm than traditional trial design methods, which in turn reduces patient burden and risk. In addition, composite outcome metrics, such as VFD, should be used when a difference in mortality is also expected between the two cohorts. The non-parametric approach developed is readily generalisable to a range of trial types where outcome data is similarly skewed.

This thesis next developed a virtual patient model for use in staircase recruitment manoeuvres. The virtual patient model was designed to provide accurate predictions about how a patient's lungs will respond to increases in positive end-expiratory pressure (PEEP), while only using measurements that are easily accessible at the patient bedside. Lung mechanics were captured using a well-validated single compartment model adapted to include basis functions for elastance and resistance. Elastance was defined using separate basis functions for the effects of alveolar recruitment and distension on elastance. Resistance basis functions were developed with respect to flow

and followed the form of the Rohrer equation (Rohrer, 1925). The ability of these virtual patients to accurately identify, fit, and predict patient-specific mechanics across the wide range of presenting conditions studied suggests these basis functions accurately capture the lung dynamics that occur in a RM. As titrating PEEP to minimum elastance has been suggested to improve patient outcomes, providing this accurate information to clinicians about patient-specific lung mechanics could enable them to better optimise ventilation.

The virtual patient model was validated against pressure-flow data from 21 patients to assess how accurately it could predict peak inspiratory pressure (PIP) at a higher PEEP level. As PIP is a key indicator of the risk of over-distension, it provides valuable information to the clinician about at which PEEP level the RM should either stop, or much smaller incremental changes should be made. Achieving prediction across PEEP levels was done by adding a novel, model estimated value for additional lung volume (V_{frc}), the volume gained or lost from a change in PEEP. This value provides clinicians with additional information about whether it is beneficial to increase PEEP levels as additional recruited volume is the main goal of RMs. The ability to estimate PIP and the V_{frc} gain (or saturation of this gain) would allow clinicians to decide if increases in PIP are likely to achieve the desired recruitment, and as they are numeric values enables automation and optimisation if defined.

The incorporation of virtual patient methods into mechanical ventilation will aid the healthcare sector in meeting increasing demand in intensive care units. In particular, a change from more generic protocols to the use of predictive, patient-specific models will improve individual patient outcomes while also reducing clinical workload. The efficacy of the physiologically relevant model in determining lung behaviour throughout an entire RM in ventilation indicates it could be used as a diagnostic clinical tool. The future use of virtual patients and cohorts will also allow new treatments and therapies to be safely and more efficiently tested, allowing for faster advancements in the field.

CHAPTER 11

Future Work

Further development of this research could focus on a range of different areas. Much of this would require additional information about the lungs which cannot be solely provided by information about mechanics.

Extension to Pressure Controlled Ventilation

At this stage, the model is only capable of working with volume controlled ventilation to reduce the risk of barotrauma. However, volutrauma is an equivalent risk for pressure controlled ventilation. The model could be extended to use information about pressure inputs to predict tidal volume across positive end-expiratory pressure (PEEP) increases.

Virtual Cohorts

The first of these developments would focus on virtual cohorts. While a virtual patient model is used to personalise and optimise care for an individual patient by predicting response to a change in treatment prior to implementing the change, virtual cohorts offer a method of safely and efficiently validating the effect that testing new treatments can have on a population of patients (Chase et al., 2016). A validated in-silico virtual trial platform could reduce the number of Phase II and III human trials (Chase et al.,

2018). It would thus be a substantial development in mechanical ventilation, as two of the main metrics for judging an improvement in treatment across a cohort (length of mechanical ventilation and ventilator-free days (Schoenfeld & Bernard, 2002)) are both highly skewed (Morton, Chiew, et al., 2017). This skew requires a large number of patients in a given clinical trial to reach statistical power (Morton, Chiew, et al., 2017). Capitalising on the recent FDA change to recognising virtual trials (Smalley, 2018) as a method of testing medical treatments, having virtual cohorts to test new mechanical ventilation protocols would allow the field to move forward much faster.

More Investigation into V_{frc}

While this thesis has developed an accurate method for estimating the additional lung volume gained from a RM, more research needs to be conducted into how much additional lung volume (V_{frc}) is required for a RM to be considered useful. While population statistics can provide general information about lung capacity in healthy individuals, the variation in patients suffering from respiratory failure means this information needs to be personalised to ensure that long-term damage is not caused to the lungs. The emergence of bedside accessible, non-invasive imaging techniques such as EIT will also be increasingly essential for this application and to further improve care.

Determination of Optimal PEEP

A further question may ask how optimal PEEP can be defined for patients and how best to continually assess and alter this value. While research has indicated titration of PEEP to minimum elastance results in good patient outcomes (Carvalho et al., 2007; Chiew, Pretty, Shaw, et al., 2015; Lambermont et al., 2008; Pintado et al., 2013), this approach may not hold true for all cohorts of patients. Potentially, V_{frc} should also be considered in setting PEEP and other MV settings. In addition, lung mechanics often change as lung condition evolves and previously opened alveoli collapse, necessitating another RM or change in MV settings. Assuming perfect prediction of lung response throughout

these RMs, their optimal frequency needs to be considered – whether additional gains in oxygenation are worth potential lung injury from changes in pressure. All of these methods will require the models and methods first, before their clinical investigation.

Combination with Gas Exchange Models

Ultimately MV is about maintaining blood oxygenation. Mechanical models can also be combined with gas exchange models and bedside oxygenation data to allow the effect that RMs have on oxygenation, specifically the existence of pulmonary shunt, to be better understood. Elastance and resistance values calculated from pressure and flow data offer information about the mechanical health of the lungs and subsequent alveolar recruitment. However, the success of oxygen and carbon dioxide diffusion from the alveoli to the bloodstream cannot be determined from mechanical information alone. Combining mechanical and gas exchange models would provide clinicians with more data to be able to better optimise care.

CHAPTER 12

Appendix A

This appendix presents additional mini RM (Morton, Dickson, Chase, Docherty, Howe, et al., 2018b) results from Chapter 8 .

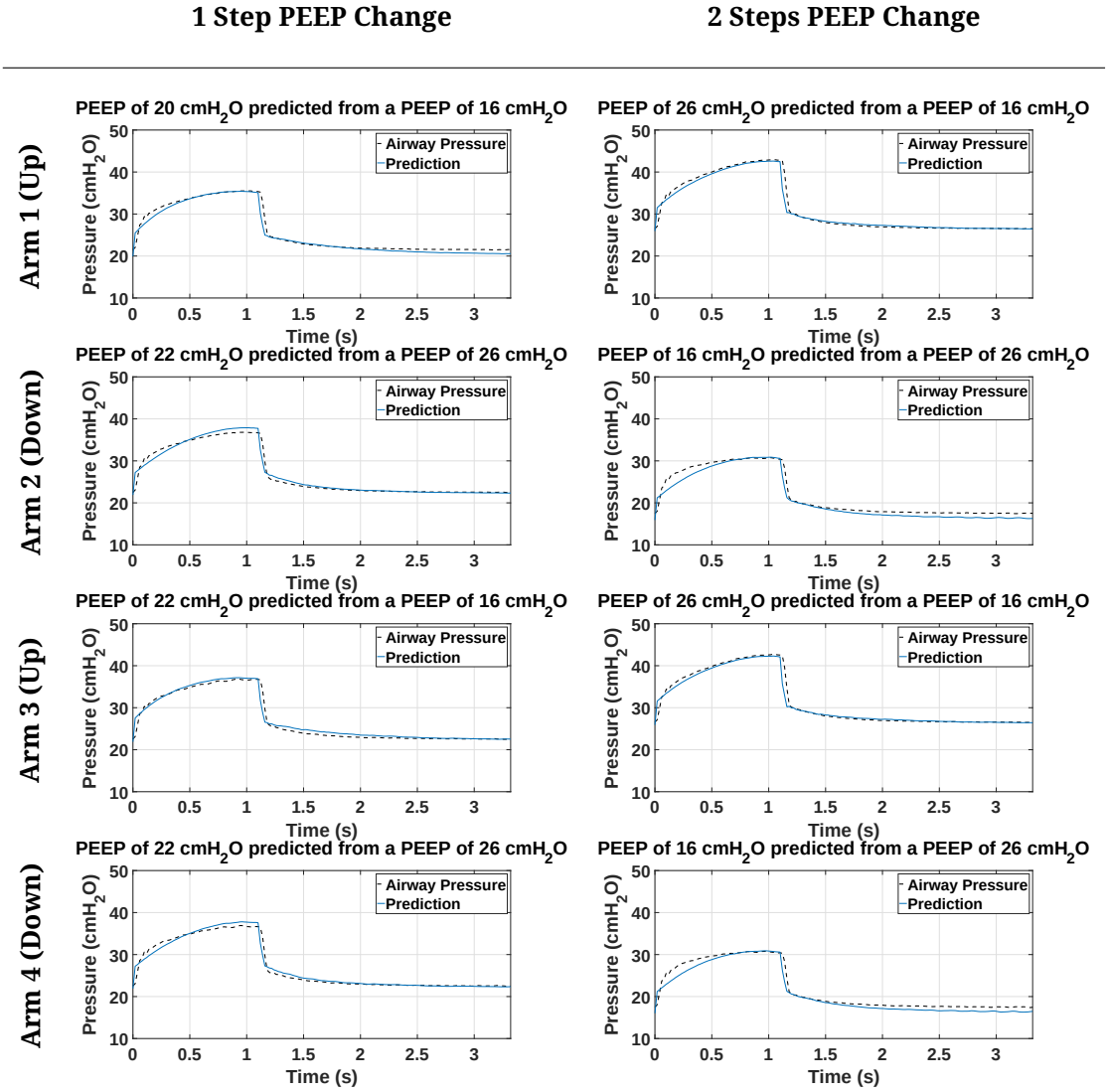

Figure 12.1: Prediction results for Patient 1, RM 1 across all arms. The blue, solid line shows the model prediction and the dashed black line indicates the median airway pressure at that PEEP level.

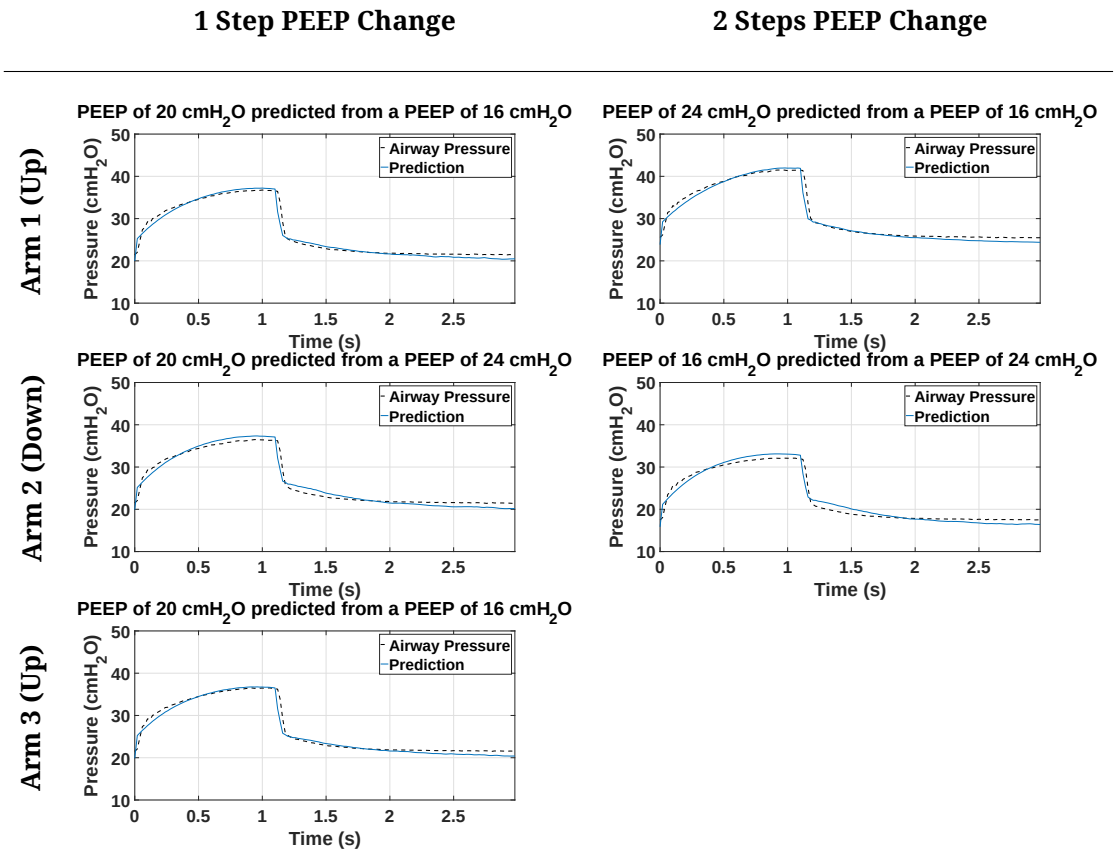

Figure 12.2: Prediction results for Patient 1, RM 2 across all arms. The blue, solid line shows the model prediction and the dashed black line indicates the median airway pressure at that PEEP level.

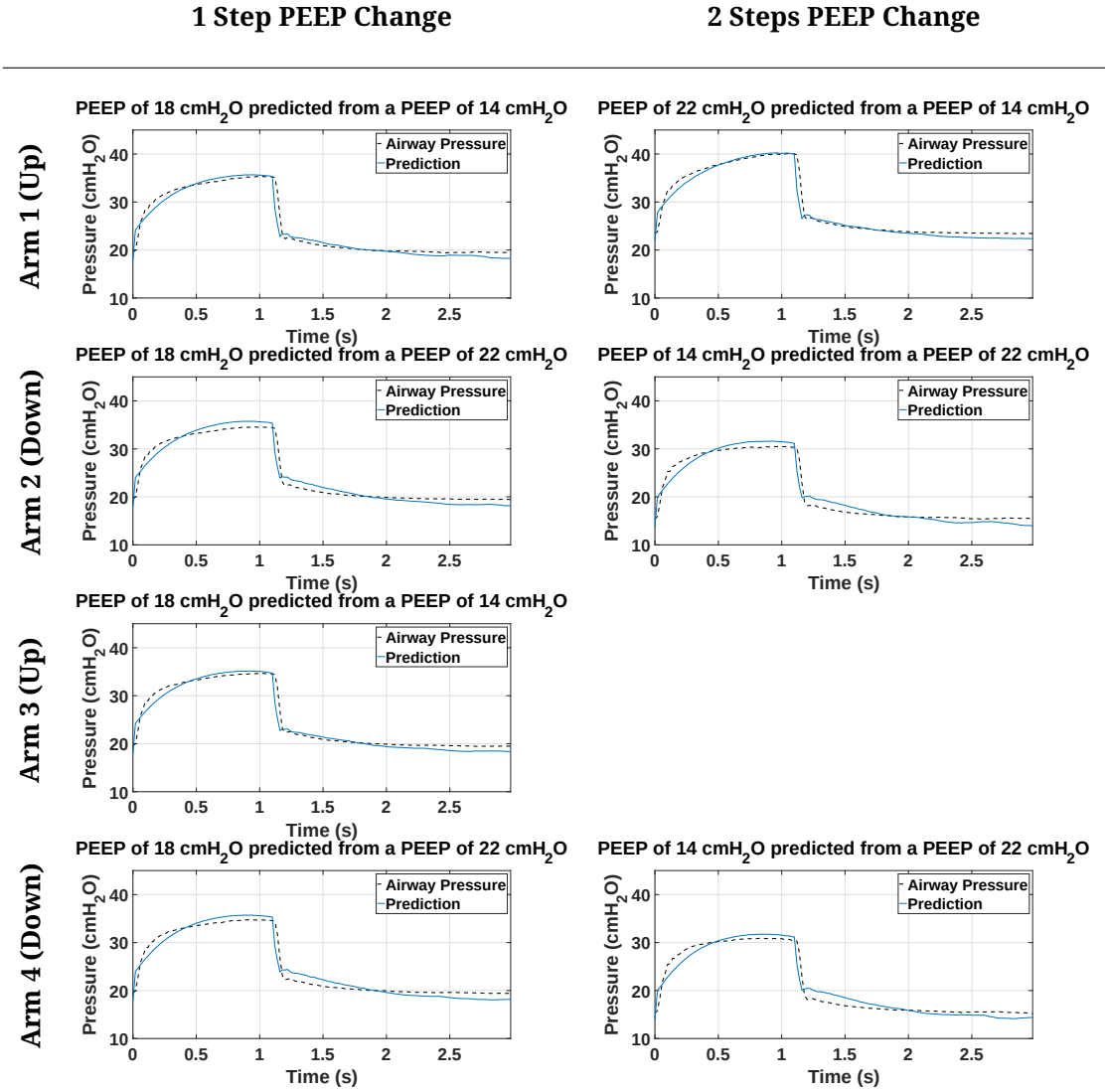

Figure 12.3: Prediction results for Patient 1, RM 3 across all arms. The blue, solid line shows the model prediction and the dashed black line indicates the median airway pressure at that PEEP level.

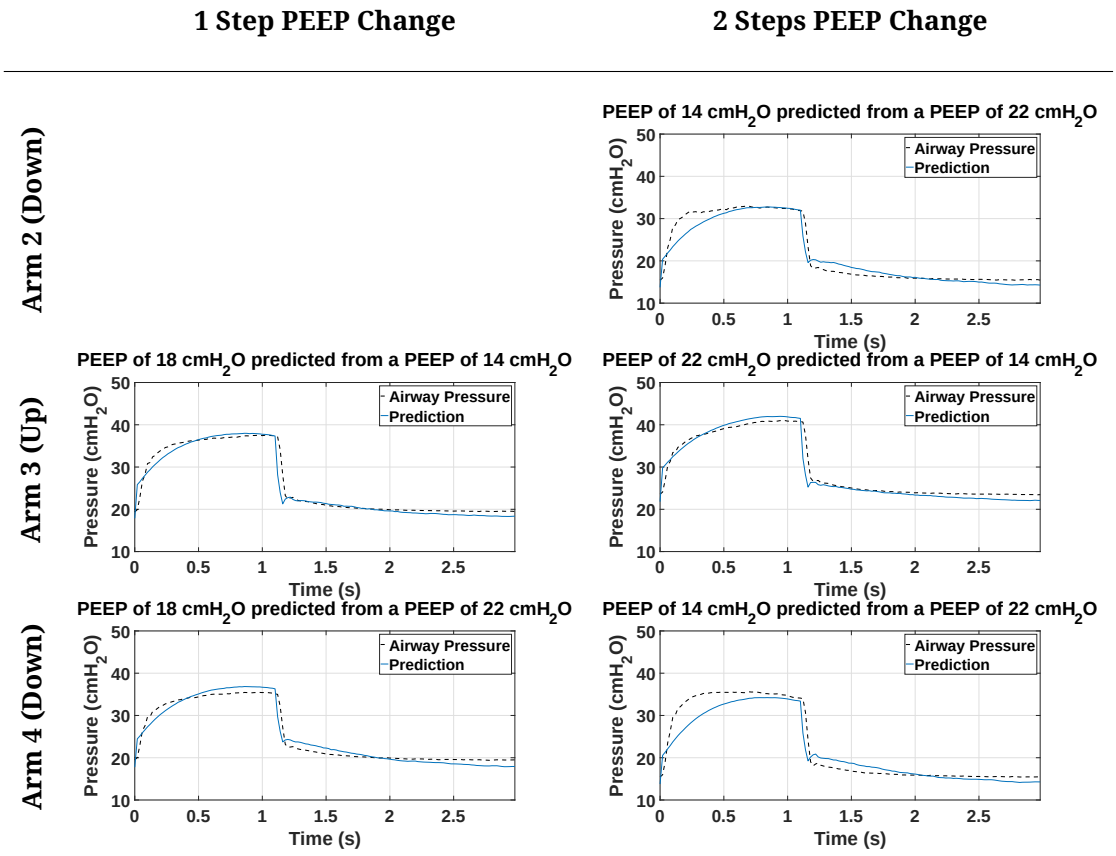

Figure 12.4: Prediction results for Patient 1, RM 5 across all arms. The blue, solid line shows the model prediction and the dashed black line indicates the median airway pressure at that PEEP level.

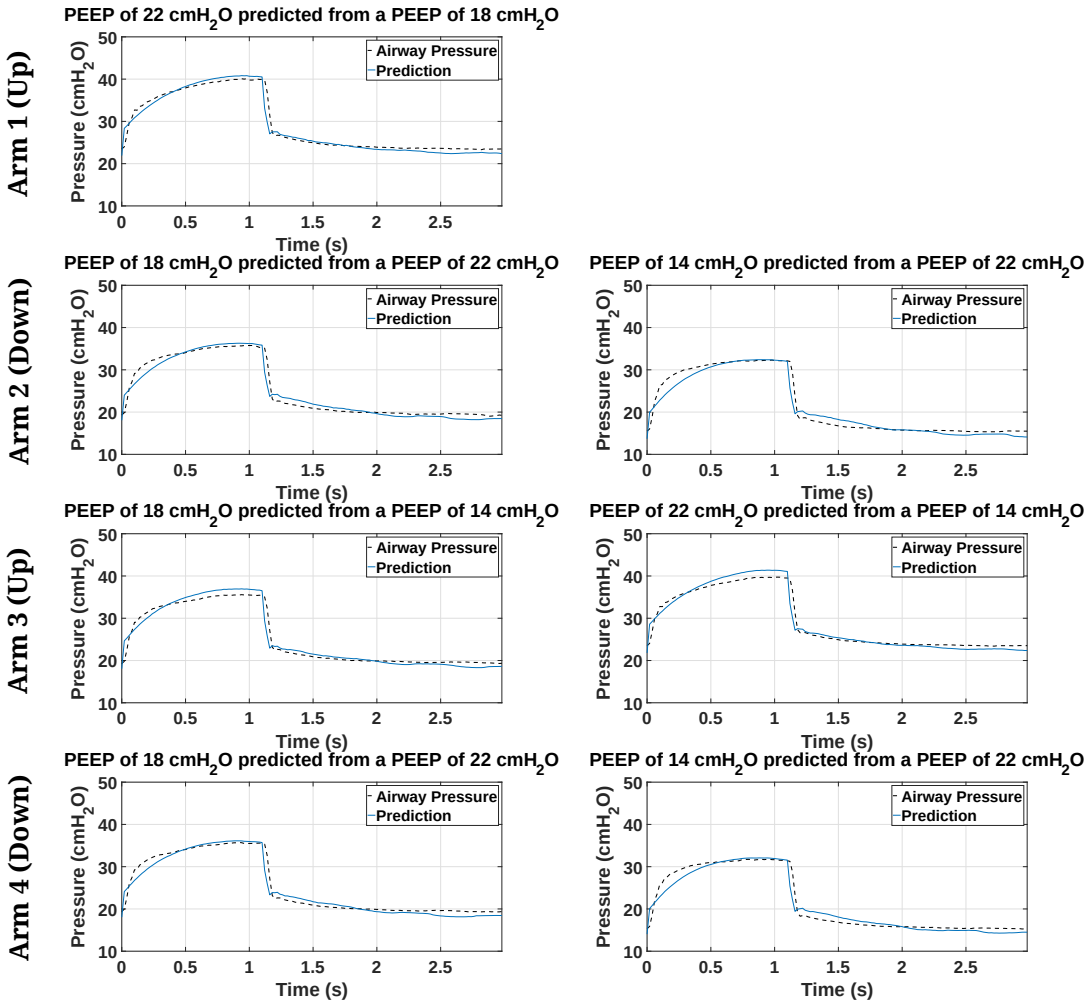

Figure 12.5: Prediction results for Patient 1, RM 6 across all arms. The blue, solid line shows the model prediction and the dashed black line indicates the median airway pressure at that PEEP level.

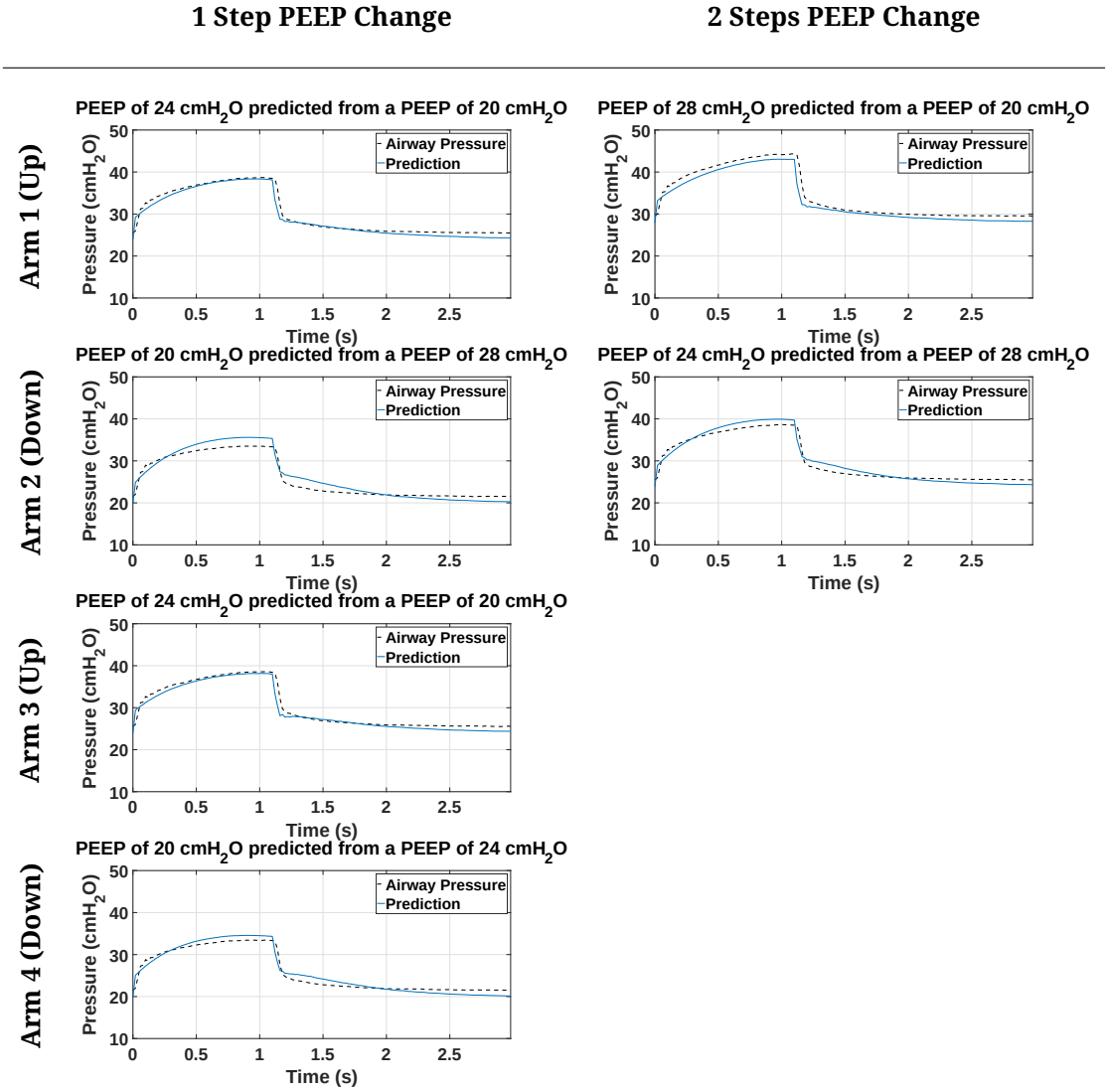

Figure 12.6: Prediction results for Patient 1, RM 7 across all arms. The blue, solid line shows the model prediction and the dashed black line indicates the median airway pressure at that PEEP level.

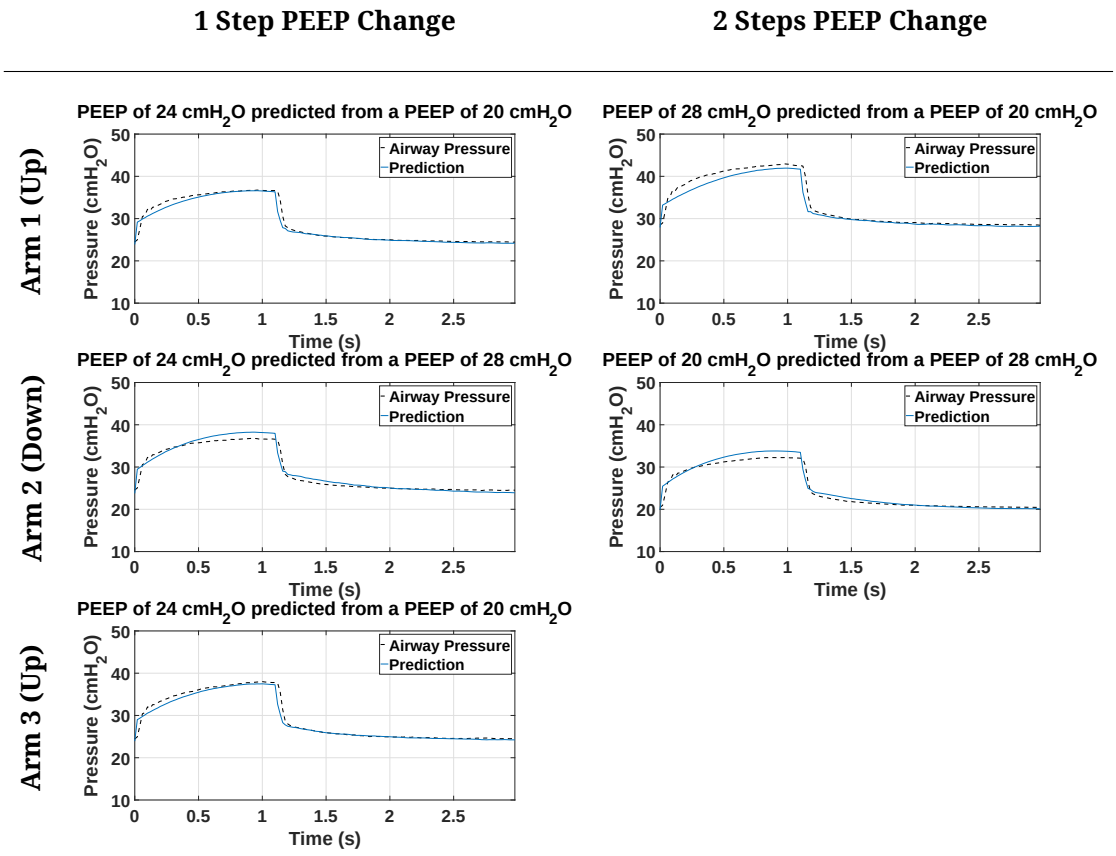

Figure 12.7: Prediction results for Patient 1, RM 9 across all arms. The blue, solid line shows the model prediction and the dashed black line indicates the median airway pressure at that PEEP level.

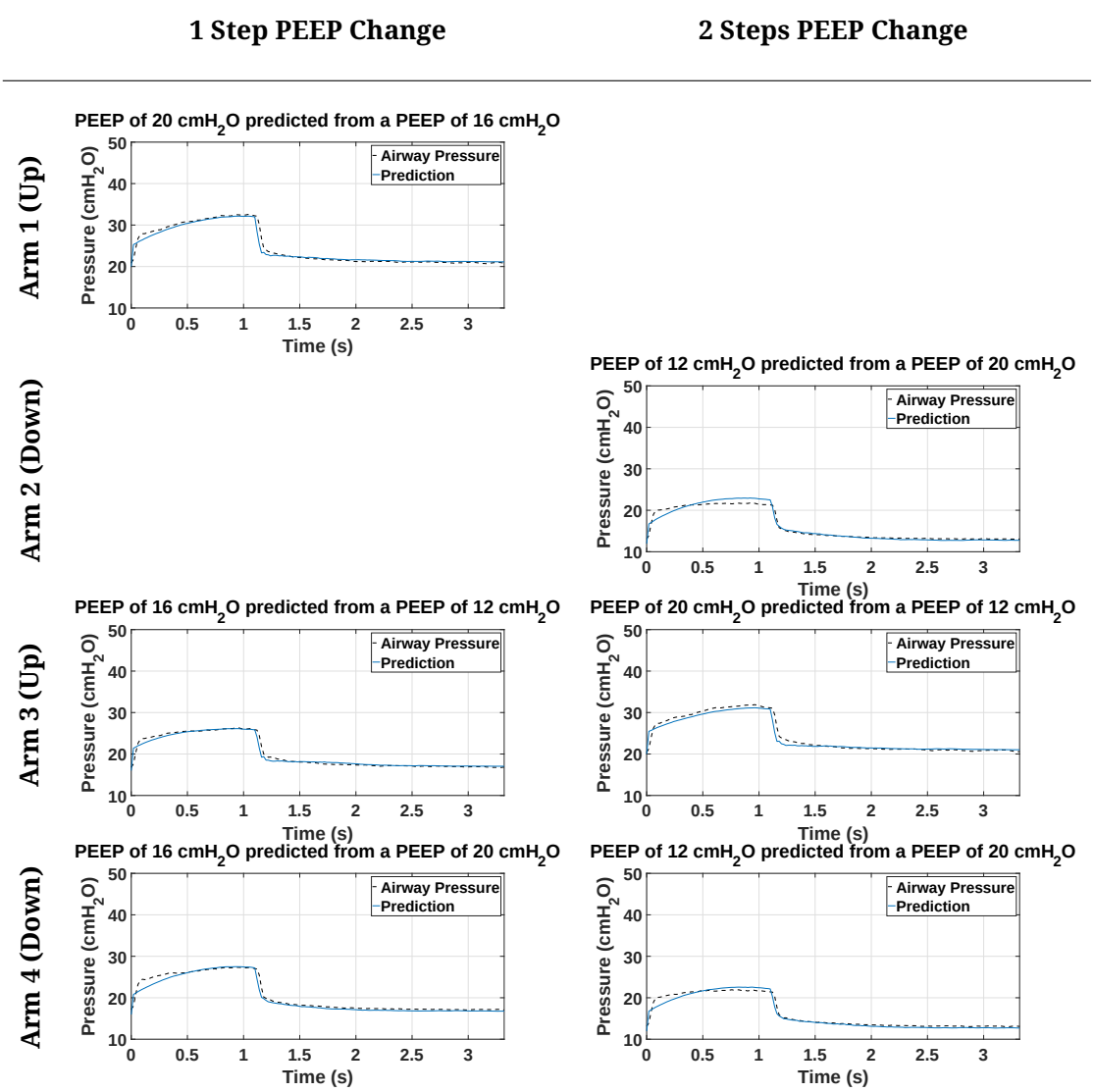

Figure 12.8: Prediction results for Patient 2, RM 1 across all arms. The blue, solid line shows the model prediction and the dashed black line indicates the median airway pressure at that PEEP level.

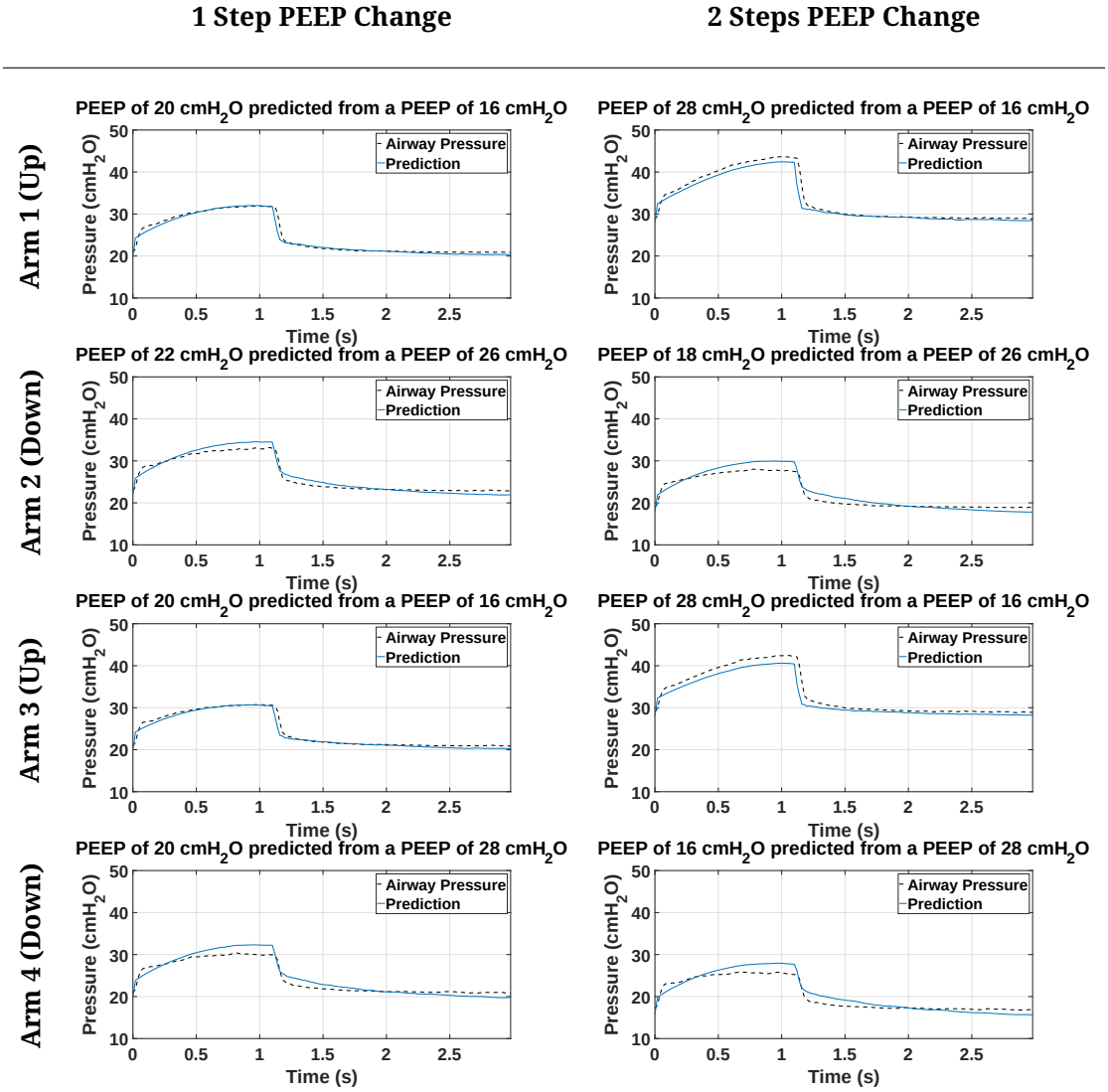

Figure 12.9: Prediction results for Patient 3, RM 1 across all arms. The blue, solid line shows the model prediction and the dashed black line indicates the median airway pressure at that PEEP level.

References

Abboud, S., Barnea, O., Guber, A., Narkiss, N., & Bruderman, I. (1995). Maximum expiratory flow-volume curve: Mathematical model and experimental results. *Medical Engineering and Physics*, *17*(5), 332–336. doi: 10.1016/1350-4533(95)97312-D

Aboab, J., Louis, B., Jonson, B., & Brochard, L. (2006). Relation between PaO2/FIO2 ratio and FIO2 - A mathematical description. *Applied Physiology in Intensive Care Medicine (Second Edition)*, 57–60. doi: 10.1007/978-3-642-01769-8_14

Aguirre-Bermeo, H., Morán, I., Bottiroli, M., Italiano, S., Parrilla, F. J., Plazolles, E., … Mancebo, J. (2016). End-inspiratory pause prolongation in acute respiratory distress syndrome patients: effects on gas exchange and mechanics. *Annals of Intensive Care*, *6*(1). doi: 10.1186/s13613-016-0183-z

Ahrens, T. (2004). *Monitoring carbon dioxide in critical care: The newest vital sign?* (Vol. 16) (No. 3 SPEC. ISS.). doi: 10.1016/j.ccell.2004.05.002

Albaiceta, G. M., & Blanch, L. (2011). Beyond volutrauma in ARDS - the critical role of lung tissue deformation. *Critical Care*, *15*(2), 304. Retrieved from http://ccforum.biomedcentral.com/articles/10.1186/cc10052 doi: 10.1186/cc10052

Albert, S. P., Dirocco, J. D., Allen, G. B., Bates, J. H., Lafollette, R., Kubiak, B. D., … Nieman, G. F. (2009). The role of time and pressure on alveolar recruitment. *Journal of Applied Physiology*, *106*(3), 757–765. doi: 10.1152/japplphysiol.90735.2008

Altman, D. G., & Bland, J. M. (1995). *Absence of evidence is not evidence of absence.*

(Vol. 311) (No. 7003). doi: 10.1136/bmj.311.7003.485

Alviar, C. L., Miller, P. E., McAreavey, D., Katz, J. N., Lee, B., Moriyama, B., ... Morrow, D. A. (2018). Positive Pressure Ventilation in the Cardiac Intensive Care Unit. *Journal of the American College of Cardiology*, *72*(13), 1532–1553. doi: 10.1016/j.jacc.2018.06.074

Amato, M., Barbas, C., Medeiros, D., Magaldi, R., & Schettino, G. (1998). Effect of a protective-ventilation strategy on mortality in the acute respiratory distress syndrome. *The New England Journal of Medicine*, *338*(6), 347–354. doi: 10.1056/NEJM199802053380602

Amato, M. B., Meade, M. O., Slutsky, A. S., Brochard, L., Costa, E. L. V., Schoenfeld, D. a., ... Brower, R. G. (2015). Driving Pressure and Survival in the Acute Respiratory Distress Syndrome. *The New England Journal of Medicine*, *372*(8), 747–755. Retrieved from http://www.nejm.org/doi/abs/10.1056/NEJMsa1410639 doi: 10.1056/NEJMsa1410639

Ashbaugh, D. G., Bigelow, D. B., Petty, T. L., & Levine, B. E. (1967). Acute respiratory distress in adults. *The Lancet*, *7*(1), 60–61. doi: 10.1016/S0140-6736(67)90168-7

Åström, E., Uttman, L., Niklason, L., Aboab, J., Brochard, L., & Jonson, B. (2008). Pattern of inspiratory gas delivery affects CO2 elimination in health and after acute lung injury. *Intensive Care Medicine*, *34*(2), 377–384. doi: 10.1007/s00134-007-0840-7

Bastarache, J. A., & Blackwell, T. S. (2009). Development of animal models for the acute respiratory distress syndrome. *Disease Models & Mechanisms*, *2*(5-6), 218–223. Retrieved from http://dmm.biologists.org/cgi/doi/10.1242/dmm.001677 doi: 10.1242/dmm.001677

Bates, J. H. (2009). *Lung Mechanics: An Inverse Modeling Approach*. Cambridge University Press.

Bates, J. H., & Irvin, C. G. (2002). Time dependence of recruitment and derecruitment in the lung - a theoretical model. *Journal of Applied Physiology*, *93*(2), 705–713. Retrieved from http://jap.physiology.org/lookup/doi/10.1152/

japplphysiol.01274.2001 doi: 10.1152/japplphysiol.01274.2001

Ben-Tal, A. (2006). Simplified models for gas exchange in the human lungs. *Journal of Theoretical Biology*, *238*(2), 474–495. doi: 10.1016/j.jtbi.2005.06.005

Bhardwaj, S. S., Camacho, F., Derrow, A., Fleischer, A. B., & Feldman, S. R. (2004). Statistical Significance and Clinical Relevance. *Archives of Dermatology*, *140*(12), 1520–1523. Retrieved from http://archderm.jamanetwork.com/article.aspx?doi=10.1001/archderm.140.12.1520 doi: 10.1001/archderm.140.12.1520

Blanch, L., & Villagrá, A. (2004). Recruitment maneuvers might not always be appropriate in ARDS. *Critical Care Medicine*, *32*(12), 2540–2541. doi: 10.1097/01.CCM.0000148083.82109.CB

Bland, J. M., & Altman, D. G. (1986). Statistical methods for assessing agreement between two methods of clinical measurement. *The Lancet*, *327*(8476), 307–310.

Blum, C. A., Nigro, N., Briel, M., Schuetz, P., Ullmer, E., Suter-Widmer, I., ... Christ-Crain, M. (2015). Adjunct prednisone therapy for patients with community-acquired pneumonia: a multicentre, double-blind, randomised, placebo-controlled trial. *The Lancet*, 1511–1518. Retrieved from http://www.ncbi.nlm.nih.gov/pubmed/25608756 doi: 10.1016/S0140-6736(14)62447-8

Borges, B., Okamoto, V. N., Matos, G. F. J., Caramez, M. P. R., Arantes, P. R., Barros, F., ... Amato, M. B. (2006). Reversibility of lung collapse and hypoxemia in early acute respiratory distress syndrome. *American Journal of Respiratory and Critical Care Medicine*, *174*(3), 268–278. doi: 10.1164/rccm.200506-976OC

Breen, D., Churches, T., Hawker, F., & Torzillo, P. J. (2002). Acute respiratory failure secondary to chronic obstructive pulmonary disease treated in the intensive care unit - a long term follow up study. *Thorax*, *57*(1), 29–33. Retrieved from http://www.pubmedcentral.nih.gov/articlerender.fcgi?artid=1746171{&}tool=pmcentrez{&}rendertype=abstract doi: 10.1136/thorax.57.1.29

Briel, M., Meade, M. O., Mercat, A., Brower, R. G., Talmor, D., Walter, S. D., ... Guyatt,

G. H. (2010). Higher vs Lower Positive End-Expiratory Pressure in Patients With Acute Lung Injury. *JAMA: The Journal of the American Medical Association*, *303*(9), 865–873. Retrieved from http://jama.jamanetwork.com/article.aspx?doi=10.1001/jama.2010.218 doi: 10.1001/jama.2010.218

Brochard, L., Rauss, A., Benito, S., Conti, G., Mancebo, J., Rekik, N., ... Lemaire, F. (1994). Comparison of three methods of gradual withdrawal from ventilatory support during weaning from mechanical ventilation. *American Journal of Respiratory and Critical Care Medicine*, *150*(4), 896–903. doi: 10.1164/ajrccm.150.4.7921460

Brower, R. G., Lanken, P. N., Macintyre, N., Matthay, M. A., Morris, A., Ancukiewicz, M., ... The National Heart Lung and Blood Institute ARDS Clinical Trials (2004). Higher versus Lower Positive End-Expiratory Pressures in Patients with the Acute Respiratory Distress Syndrome. *The New England Journal of Medicine*, *351*(4), 113–116. doi: 10.1056/NEJMp1415160

Brower, R. G., Matthay, M. A., Morris, A., Schoenfeld, D. A., Thompson, B. T., Wheeler, A., & The Acute Respiratory Distress Syndrome Network. (2000). Ventilation With Lower Tidal Volumes As Compared With Traditional Tidal Volumes for Acute Lung Injury and the Acute Respiratory Distress Syndrome. *The New England Journal of Medicine*, *342*(18), 1301–1308. doi: 10.1056/NEJM200005043421801

Burrowes, K. S., Clark, A. R., & Tawhai, M. H. (2011). Blood flow redistribution and ventilation-perfusion mismatch during embolic pulmonary arterial occlusion. *Pulmonary Circulation*, *1*(3), 365–76. Retrieved from http://www.ncbi.nlm.nih.gov/pubmed/22140626{%}5Cnhttp://www.pubmedcentral.nih.gov/articlerender.fcgi?artid=PMC3224428 doi: 10.4103/2045-8932.87302

Burrowes, K. S., De Backer, J., Smallwood, R., Sterk, P. J., Gut, I., Wirix-Speetjens, R., ... Brightling, C. (2013). Multi-scale computational models of the airways to unravel the pathophysiological mechanisms in asthma and chronic obstructive pulmonary disease (AirPROM). *Interface Focus*, *3*(2). doi: 10.1098/rsfs.2012.0057

Burrowes, K. S., Swan, A. J., Warren, N. J., & Tawhai, M. H. (2008). Towards a virtual lung: Multi-scale, multi-physics modelling of the pulmonary system. *Philosophical Transactions of the Royal Society A: Mathematical, Physical and Engineering Sciences*, *366*(1879), 3247–3263. doi: 10.1098/rsta.2008.0073

Burrowes, K. S., & Tawhai, M. H. (2006). Computational predictions of pulmonary blood flow gradients: Gravity versus structure. *Respiratory Physiology and Neurobiology*, *154*(3), 515–523. doi: 10.1016/j.resp.2005.11.007

Carvalho, A. R. S., Jandre, F. C., Pino, A. V., Bozza, F. a., Salluh, J., Rodrigues, R., ... Giannella-Neto, A. (2007). Positive end-expiratory pressure at minimal respiratory elastance represents the best compromise between mechanical stress and lung aeration in oleic acid induced lung injury. *Critical Care*, *11*(4), R86. doi: 10.1186/cc6093

Cavalcanti, A. B., Suzumura, É. A., Laranjeira, L. N., Paisani, D. d. M., Damiani, L. P., Guimarães, H. P., ... Ribeiro de Carvalho, C. R. (2017). Effect of Lung Recruitment and Titrated Positive End-Expiratory Pressure (PEEP) vs Low PEEP on Mortality in Patients With Acute Respiratory Distress Syndrome. *JAMA: The Journal of the American Medical Association*, *318*(14), 1335. Retrieved from http://jama.jamanetwork.com/article.aspx?doi=10.1001/jama.2017.14171 doi: 10.1001/jama.2017.14171

Chase, J. G., Desaive, T., & Preiser, J.-C. (2016). Virtual patients and virtual cohorts - a new way to think about the design and implementation of personalised ICU treatments. In J.-L. Vincent (Ed.), *Annual update in intensive care and emergency medicine 2016* (Vol. 2, pp. 435–448). Springer.

Chase, J. G., Le Compte, A. J., Preiser, J.-C., Shaw, G. M., Penning, S., & Desaive, T. (2011). Physiological modeling, tight glycemic control, and the ICU clinician: what are models and how can they affect practice? *Annals of Intensive Care*, *1*(11). Retrieved from http://annalsofintensivecare.springeropen.com/articles/10.1186/2110-5820-1-11 doi: 10.1186/2110-5820-1-11

Chase, J. G., Moeller, K., Shaw, G. M., Schranz, C., Chiew, Y.-S., & Desaive, T. (2014). When the value of gold is zero. *BMC Research Notes*, *7*(1), 5–7. doi: 10.1186/1756-0500-7-404

Chase, J. G., Preiser, J.-C., Dickson, J. L., Pironet, A., Chiew, Y.-S., Pretty, C. G., ... Desaive, T. (2018). Next-generation, personalised, model-based critical care medicine: a state-of-the art review of in silico virtual patient models, methods, and cohorts, and how to validation them. *BioMedical Engineering OnLine*, *17*(1), 24.

Chase, J. G., Shaw, G. M., Le Compte, A., Lonergan, T., Willacy, M., Wong, X. W., ... Hann, C. (2008). Implementation and evaluation of the SPRINT protocol for tight glycaemic control in critically ill patients: A clinical practice change. *Critical Care*, *12*(2), 1–15. doi: 10.1186/cc6868

Chase, J. G., Suhaimi, F., Penning, S., Preiser, J.-C., Le Compte, A. J., Lin, J., ... Desaive, T. (2010). Validation of a model-based virtual trials method for tight glycemic control in intensive care. *BioMedical Engineering OnLine*, *9*(1), 84. Retrieved from http://www.biomedical-engineering-online.com/content/9/1/84http://www.pubmedcentral.nih.gov/articlerender.fcgi?artid=3224899{&}tool=pmcentrez{&}rendertype=abstract doi: 10.1186/1475-925X-9-84

Chelucci, G. L., Brunett, F., Ava-santuccit, J. D., Dhainautt, J. F., Paccalyt, D., Armaganidis, A., & Lockhartt, A. (1991). A single-compartment model cannot describe passive expiration in intubated, paralysed humans. *European Respiratory Journal*, *4*, 458–464.

Chiew, Y.-S. (2013). *Model-Based Mechanical Ventilation for the Critically Ill* (Unpublished doctoral dissertation).

Chiew, Y.-S., Chase, J. G., Shaw, G. M., Sundaresan, A., & Desaive, T. (2011). Model-based PEEP Optimisation in Mechanical Ventilation. *BioMedical Engineering OnLine*, *10*(1), 111. Retrieved from http://www.biomedical-engineering-online.com/content/10/1/111 doi: 10.1186/1475-925X-10-111

Chiew, Y.-S., Pretty, C. G., Docherty, P. D., Lambermont, B., Shaw, G. M., Desaive, T., & Chase, J. G. (2015). Time-Varying Respiratory System Elastance: A Physiological Model for Patients Who Are Spontaneously Breathing. *PLoS ONE*, *10*(1), e0114847. Retrieved from http://dx.plos.org/10.1371/journal.pone.0114847 doi: 10.1371/journal.pone.0114847

Chiew, Y.-S., Pretty, C. G., Moltchanova, E., Scarrott, C., Redmond, D., Shaw, G. M., & Chase, J. G. (2015). Reducing the Length of Mechanical Ventilation with Significance - A Case Study of Sample Size Estimation Trial Design Using Monte-Carlo Simulation. In *9th ifac symposium on biological and medical systems, 31 aug-2 sep 2015*. Berlin.

Chiew, Y.-S., Pretty, C. G., Shaw, G. M., Chiew, Y. W., Lambermont, B., Desaive, T., & Chase, J. G. (2015). Feasibility of titrating PEEP to minimum elastance for mechanically ventilated patients. *Pilot and Feasibility Studies*, *1*(1), 1–10. doi: 10.1186/s40814-015-0006-2

Chiew, Y.-S., Tan, C. P., Chase, J. G., Chiew, Y. W., Desaive, T., Ralib, A. M., & Mat Nor, M. B. (2018). Assessing mechanical ventilation asynchrony through iterative airway pressure reconstruction. *Computer Methods and Programs in Biomedicine*, *157*, 217–224. Retrieved from https://doi.org/10.1016/j.cmpb.2018.02.007 doi: 10.1016/j.cmpb.2018.02.007

Chiumello, D., Carlesso, E., Cadringher, P., Caironi, P., Valenza, F., Polli, F., ... Gattinoni, L. (2008). Lung stress and strain during mechanical ventilation for acute respiratory distress syndrome. *American Journal of Respiratory and Critical Care Medicine*, *178*(4), 346–355. doi: 10.1164/rccm.200710-1589OC

Cobelli, C., & DiStefano, J. J. (1980). Parameter and structural identifiability concepts and ambiguities: a critical review and analysis. *American Journal of Physiology-Regulatory, Integrative and Comparative Physiology*, *239*(1), R7–R24. Retrieved from http://www.physiology.org/doi/10.1152/ajpregu.1980.239.1.R7 doi: 10.1152/ajpregu.1980.239.1.R7

Cohen, I. L., & Booth, F. V. (1994, aug). Cost containment and mechanical ventilation in the United States. *New horizons (Baltimore, Md.)*, *2*(3), 283–90. Retrieved from http://www.ncbi.nlm.nih.gov/pubmed/8087585

Corrado, A., & Gorini, M. (2002). Negative-pressure ventilation - Is there still a role? *European Respiratory Journal*, *20*(1), 187–197. doi: 10.1183/09031936.02.00302602

Crampin, E. J., Halstead, M., Hunter, P., Nielsen, P., Noble, D., Smith, N., & Tawhai, M. H. (2004). Computational physiology and the physiome project. *Experimental Physiology*, *89*(1), 1–26. doi: 10.1113/expphysiol.2003.026740

Crotti, S., Mascheroni, D., Caironi, P., Pelosi, P., Ronzoni, G., Mondino, M., ... Gattinoni, L. (2001). Recruitment and derecruitment during acute respiratory failure: a clinical study. *American Journal of Respiratory and Critical Care Medicine*, *164*(1), 131–40. Retrieved from http://www.ncbi.nlm.nih.gov/pubmed/11435251 doi: 10.1164/ajrccm.164.1.2007010

Das, A., Cole, O., Chikhani, M., Wang, W., Ali, T., Haque, M., ... Hardman, J. G. (2015). Evaluation of lung recruitment maneuvers in acute respiratory distress syndrome using computer simulation. *Critical Care*, *19*(1). doi: 10.1186/s13054-014-0723-6

Dasta, J. F., McLaughlin, T. P., Mody, S. H., & Piech, C. T. (2005). Daily cost of an intensive care unit day - The contribution of mechanical ventilation. *Critical Care Medicine*, *33*(6), 1266–1271. Retrieved from http://content.wkhealth.com/linkback/openurl?sid=WKPTLP:landingpage{&}an=00003246-200506000-00013 doi: 10.1097/01.CCM.0000164543.14619.00

Davidson, S. M., Redmond, D. P., Laing, H., White, R., Radzi, F., Chiew, Y.-S., ... Chase, J. G. (2014). Clinical Utilisation of Respiratory Elastance (CURE): Pilot trials for the optimisation of mechanical ventilation settings for the critically Ill. *IFAC Proceedings Volumes (IFAC-PapersOnline)*, *19*(October), 8403–8408. doi: 10.13140/2.1.1772.2882

Deans, K. J., Minneci, P. C., Cui, X., Banks, S. M., Natanson, C., & Eichacker, P. Q. (2005). *Mechanical ventilation in ARDS: One size does not fit all.* (Vol. 33) (No. 5). doi: 10

.1097/01.CCM.0000162384.71993.A3

Dellamonica, J., Lerolle, N., Sargentini, C., Beduneau, G., Di Marco, F., Mercat, A., ... Brochard, L. (2011). PEEP-induced changes in lung volume in acute respiratory distress syndrome. Two methods to estimate alveolar recruitment. *Intensive Care Medicine*, *37*(10), 1595–1604. doi: 10.1007/s00134-011-2333-y

de Matos, G. F., Stanzani, F., Passos, R. H., Fontana, M. F., Albaladejo, R., Caserta, R. E., ... Barbas, C. S. (2012). How large is the lung recruitability in early acute respiratory distress syndrome: A prospective case series of patients monitored by computed tomography. *Critical Care*, *16*(1), R4. Retrieved from `http://ccforum.com/content/16/1/R4` doi: 10.1186/cc10602

Devaquet, J., Jonson, B., Niklason, L., Si Larbi, A.-G., Uttman, L., Aboab, J., & Brochard, L. (2008). Effects of inspiratory pause on CO2 elimination and arterial PCO2 in acute lung injury. *Journal of Applied Physiology*, *105*(6), 1944–1949. doi: 10.1152/japplphysiol.90682.2008

Dickson, J. L., Gunn, C. A., & Chase, J. G. (2014). Humans are Horribly Variable. *International Journal of Clinical and Medical Imaging*, *1*(2), 1000142.

Dickson, J. L., Stewart, K. W., Pretty, C. G., Flechet, M., Desaive, T., Penning, S., ... Chase, J. G. (2018). Generalisability of a Virtual Trials Method for Glycaemic Control in Intensive Care. *IEEE Transactions on Biomedical Engineering*, *65*(7), 1543–1553. doi: 10.1109/TBME.2017.2686432

Dickson, J. L. N., Lynn, A. M., Shaw, G. M., & Geoffrey Chase, J. (2019). Safe and effective glycaemic control in premature infants: Observational clinical results from the computerised STAR-GRYPHON protocol. *Archives of Disease in Childhood: Fetal and Neonatal Edition*, *104*(2), F205–F211. doi: 10.1136/archdischild-2017-314072

DiRocco, J. D., Carney, D. E., & Nieman, G. F. (2007). Correlation between alveolar recruitment/derecruitment and inflection points on the pressure-volume curve. *Intensive Care Medicine*, *33*(7), 1204–1211. doi: 10.1007/s00134-007-0629-8

Docherty, P. D., Chase, J. G., Lotz, T. F., & Desaive, T. (2011). A graphical method

for practical and informative identifiability analyses of physiological models - a case study of insulin kinetics and sensitivity. *BioMedical Engineering OnLine*, *10*(1), 39. Retrieved from http://www.biomedical-engineering-online.com/content/10/1/39 doi: 10.1186/1475-925X-10-39

Donahoe, M. (2011). Acute respiratory distress syndrome: A clinical review. *Pulmonary Circulation*, *1*(2), 192–211. Retrieved from http://www.pubmedcentral.nih.gov/articlerender.fcgi?artid=3198645{&}tool=pmcentrez{&}rendertype=abstract doi: 10.4103/2045-8932.83454

Dreyfuss, D., & Saumon, G. (1992). Barotrauma is volutrauma, but which volume is the one responsible? *Intensive Care Medicine*, *18*, 139–141.

Dreyfuss, D., & Saumon, G. (1998). Ventilator-induced lung injury - Lessons from experimental studies. *American Journal of Respiratory and Critical Care Medicine*, *157*(1), 294–323. doi: 10.1164/ajrccm.157.1.9604014

Dyhr, T., Laursen, N., & Larsson, A. (2002). Effects of lung recruitment maneuver and positive end-expiratory pressure on lung volume, respiratory mechanics and alveolar gas mixing in patients ventilated after cardiac surgery. *Acta Anaesthesiologica Scandinavica*, *46*(6), 717–25. doi: importanceofPEEPafterwards

Eom, J., Xu, X. G., De, S., & Shi, C. (2010). Predictive modeling of lung motion over the entire respiratory cycle using measured pressure-volume data, 4DCT images, and finite-element analysis. *Medical Physics*, *37*(8), 4389–4400. doi: 10.1118/1.3455276

Evans, A., Shaw, G. M., Le Compte, A., Tan, C.-S., Ward, L., Steel, J., ... Chase, J. G. (2011). Pilot proof of concept clinical trials of Stochastic Targeted (STAR) glycemic control. *Annals of Intensive Care*, *1*(1), 38. doi: 10.1186/2110-5820-1-38

Fisk, L. M., Le Compte, A. J., Shaw, G. M., Penning, S., Desaive, T., & Chase, J. G. (2012). STAR development and protocol comparison. *IEEE Transactions on Biomedical Engineering*, *59*(12), 3357–3364. doi: 10.1109/TBME.2012.2214384

Fletcher, G., & Barber, J. L. (1966). *Lung mechanics and physiologic shunt during spontaneous breathing in normal subjects.* (Vol. 27) (No. 5). doi: 10.1097/00000542

-196609000-00015

Flevari, A. G., Maniatis, N., Kremiotis, T., Siempos, I., Betrosian, A. P., Roussos, C., ... Armaganidis, A. (2011). Rohrer's constant, K2, as a factor of determining inspiratory resistance of common adult endotracheal tubes. *Anaesthesia & Intensive Care*, *39*(3), 410–417.

Futier, E., Constantin, J.-M., Paugam-Burtz, C., Pascal, J., Eurin, M., Neuschwander, A., ... Jaber, S. (2013). A Trial of Intraoperative Low-Tidal-Volume Ventilation in Abdominal Surgery. *New England Journal of Medicine*, *369*(5), 428–437. Retrieved from http://www.nejm.org/doi/10.1056/NEJMoa1301082 doi: 10.1056/NEJMoa1301082

Gammon, R. B., Shin, M. S., & Buchalter, S. E. (1992). Pulmonary Barotrauma in Mechanical Ventilation: Patterns and Risk Factors. *Chest*, *102*(2), 568–572.

Garcia, C. S. N. B., Prota, L. F. M., Morales, M. M., Romero, P. V., Zin, W. a., & Rocco, P. R. M. (2006). Understanding the mechanisms of lung mechanical stress. *Brazilian Journal of Medical and Biological Research*, *39*(6), 697–706. doi: 10.1590/S0100-879X2006000600001

Gastañaga, V. M., McLaren, C. E., & Delfino, R. J. (2006). Power calculations for generalized linear models in observational longitudinal studies: A simulation approach in SAS. *Computer Methods and Programs in Biomedicine*, *84*(1), 27–33. doi: 10.1016/j.cmpb.2006.07.011

Gattinoni, L., Carlesso, E., Brazzi, L., & Caironi, P. (2010). Positive end-expiratory pressure. *Current Opinion in Critical Care*, *16*(1), 39–44. doi: 10.1097/MCC.0b013e3283354723

Gattinoni, L., & Pesenti, A. (2005). The concept of "baby lung". *Intensive Care Medicine*, *31*(6), 776–784. Retrieved from http://link.springer.com/10.1007/s00134-005-2627-z doi: 10.1007/s00134-005-2627-z

Girard, T. D., & Bernard, G. R. (2007). Mechanical ventilation in ARDS: A state-of-the-art review. *Chest*, *131*(3), 921–929. doi: 10.1378/chest.06-1515

Gong, B., Krueger-Ziolek, S., Moeller, K., Schullcke, B., & Zhao, Z. (2015). Electrical impedance tomography: Functional lung imaging on its way to clinical practice? *Expert Review of Respiratory Medicine*, *9*(6), 721–737. Retrieved from http://dx.doi.org/10.1586/17476348.2015.1103650 doi: 10.1586/17476348.2015.1103650

Graham, M. R., Haberman, C. J., Brewster, J. F., Girling, L. G., McManus, B. M., & Mutch, W. A. C. (2005). Mathematical modelling to centre low tidal volumes following acute lung injury: A study with biologically variable ventilation. *Respiratory Research*, *6*, 1–11. doi: 10.1186/1465-9921-6-64

Grasso, F., Engelberts, D., Helm, E., Frndova, H., Jarvis, S., Talakoub, O., ... Kavanagh, B. P. (2008). Negative-pressure ventilation - Better oxygenation and less lung injury. *American Journal of Respiratory and Critical Care Medicine*, *177*(4), 412–418. doi: 10.1164/rccm.200707-1004OC

Grasso, S., Stripoli, T., Sacchi, M., Trerotoli, P., Staffieri, F., Franchini, D., ... Fiore, T. (2009). Inhomogeneity of lung parenchyma during the open lung strategy - A computed tomography scan study. *American Journal of Respiratory and Critical Care Medicine*, *180*(5), 415–423. doi: 10.1164/rccm.200901-0156OC

Guttmann, J., Eberhard, L., Fabry, B., Bertschmann, W., Zeravik, J., Adolph, M., ... Wolff, G. (1995). Time constant/volume relationship of passive expiration in mechanically ventilated ARDS patients. *European Respiratory Journal*, *8*(1), 114–120. doi: 10.1183/09031936.95.08010114

Hager, D. N., Krishnan, J. a., Hayden, D. L., & Brower, R. G. (2005). Tidal volume reduction in patients with acute lung injury when plateau pressures are not high. *American Journal of Respiratory and Critical Care Medicine*, *172*(10), 1241–1245. doi: 10.1164/rccm.200501-048CP

Halter, J. M., Steinberg, J. M., Schiller, H. J., Dasilva, M., Gatto, L. A., Landas, S., & Nieman, G. F. (2003). Positive end-expiratory pressure after a recruitment maneuver prevents both alveolar collapse and recruitment{/}derecruitment. *Amer-*

ican Journal of Respiratory and Critical Care Medicine, *167*(12), 1620–1626. doi: 10.1164/rccm.200205-435OC

Harris, R. S., Hess, D. R., & Venegas, J. G. (2000). An Objective Analysis of the Pressure-Volume Curve in the Acute Respiratory Distress Syndrome. *American Journal of Respiratory & Critical Care Medicine*, *161*, 432–439.

Herridge, M., Cheung, A., Tansey, C., Matte-Martyn, A., Diaz-Granados, N., Al-Saidi, F., ... Slutsky, A. S. (2003). One-Year Outcomes in Survivors of the Acute Respiratory Distress Syndrome. *The New England Journal of Medicine*, *348*(8), 683–693. doi: 10.1136/jech.2009.090662

Herridge, M., Tansey, C., Matte, A., Tomlinson, G., Diaz-Granados, N., Cooper, A., ... Cheung, A. (2011). Functional Disability 5 Years after Acute Respiratory Distress Syndrome. *The New England Journal of Medicine*, *364*(14), 1315–1323. doi: 10.1056/NEJMoa1706198

Hess, D. R. (2015). Recruitment Maneuvers and PEEP Titration. *Respiratory Care*, *60*(11), 1688–1704.

Hickling, K. G. (1998). The Pressure–Volume Curve Is Greatly Modified by Recruitment A Mathematical Model of ARDS Lungs. *American Journal of Respiratory & Critical Care Medicine*, *158*(1), 194–202. doi: 10.1164/ajrccm.158.1.9708049

Hodgson, C. L., Tuxen, D. V., Davies, A. R., Bailey, M. J., Higgins, A. M., Holland, A. E., ... Nichol, A. D. (2011). A randomised controlled trial of an open lung strategy with staircase recruitment, titrated PEEP and targeted low airway pressures in patients with acute respiratory distress syndrome. *Critical Care*, *15*(3), R133. doi: 10.1186/cc10249

Hogg, J. C., Chu, F., Utokaparch, S., Woods, R., Elliott, M., Buzatu, L., ... Paré, P. D. (2004). The Nature of Small-Airway Obstruction in Chronic Obstructive Pulmonary Disease. *The New England Journal of Medicine*, *350*(26), 2645–2654.

Howe, S. L., Chase, J. G., Redmond, D. P., Morton, S. E., Kim, K. T., Pretty, C. G., ... Desaive, T. (2018). Estimation of Inspiratory Respiratory Elastance Using Expiratory

Data. *IFAC-PapersOnLine*, *51*(27), 204–208. Retrieved from https://doi.org/10.1016/j.ifacol.2018.11.642 doi: 10.1016/j.ifacol.2018.11.642

Iglesias, M., Martinez, E., Badia, J. R., Macchiarini, P., Iglesias, M., Martinez, E., & Badia, J. R. (2008). Severe Acute Respiratory Distress Syndrome. In *Advances in extracorporeal perfusion therapies* (pp. 237–244). doi: 10.1016/j.athoracsur.2007.06.004

Jandre, F. C., Modesto, F. C., Carvalho, A. R. S., & Giannella-Neto, A. (2008). The endotracheal tube biases the estimates of pulmonary recruitment and overdistension. *Medical and Biological Engineering and Computing*, *46*(1), 69–73. doi: 10.1007/s11517-007-0227-5

Jarreau, P. H., Louis, B., Dassieu, G., Desfrere, L., Blanchard, P. W., Moriette, G., ... Harf, A. (1999). Estimation of inspiratory pressure drop in neonatal and pediatric endotracheal tubes. *Journal of Applied Physiology*, *87*(1), 36–46.

Jobe, A. H. (2009). Lung Recruitment for Ventilation: Does It Work, and is It Safe? *Journal of Pediatrics*, *154*(5), 635–636. Retrieved from http://dx.doi.org/10.1016/j.jpeds.2009.01.059 doi: 10.1016/j.jpeds.2009.01.059

Jubran, A. (2015). Pulse oximetry. *Critical Care*, *75*(889), 703. Retrieved from http://dx.doi.org/10.1186/s13054-015-0984-8 doi: 10.1016/S0953-7112(05)80086-9

Kacmarek, R. M., Villar, J., Sulemanji, D., Montiel, R., Ferrando, C., Blanco, J., ... Suarez-Sipmann, F. (2016). Open lung approach for the acute respiratory distress syndrome - A pilot, randomized controlled trial. *Critical Care Medicine*, *44*(1), 32–42. doi: 10.1097/CCM.0000000000001383

Kannangara, D. O., Newberry, F., Howe, S., Major, V., Redmond, D., Szlavecs, A., ... Chase, J. G. (2016). Estimating the true respiratory mechanics during asynchronous pressure controlled ventilation. *Biomedical Signal Processing and Control*, *30*, 70–78. Retrieved from http://dx.doi.org/10.1016/j.bspc.2016.06.014 doi: 10.1016/j.bspc.2016.06.014

Kárason, S., Antonsen, K., & Aneman, A. (2002). Ventilator treatment in the Nordic countries. A multicenter survey. *Acta Anaesthesiologica Scandinavica*, *46*(9), 1053–

61. Retrieved from http://www.ncbi.nlm.nih.gov/pubmed/12366498 doi: 10.1034/j.1399-6576.2002.460901.x

Kheir, J. N., Walsh, B. K., Smallwood, C. D., Rettig, J. S., Thompson, J. E., Gomez-Laberge, C., ... Arnold, J. H. (2013). Comparison of 2 lung recruitment strategies in children with acute lung injury. *Respiratory Care*, *58*(8), 1280–1290. doi: http://dx.doi.org/10.4187/respcare.01808

Kim, E.-k., Miller, I. A. N., Landree, L. E., Borisy-rudin, F. F., Brown, P., Tihan, T., ... Ronnett, G. V. (2002). Topographical distribution of pulmonary perfusion and ventilation, assessed by PET in supine and prone humans GUIDO. *Translational Physiology*, 867–879.

Lambermont, B., Ghuysen, A., Janssen, N., Morimont, P., Hartstein, G., Gerard, P., & D'Orio, V. (2008). Comparison of functional residual capacity and static compliance of the respiratory system during a positive end-expiratory pressure (PEEP) ramp procedure in an experimental model of acute respiratory distress syndrome. *Critical Care*, *12*(4), R91. Retrieved from http://www.pubmedcentral.nih.gov/articlerender.fcgi?artid=2575573{&}tool=pmcentrez{&}rendertype=abstract doi: 10.1186/cc6961

Langdon, R., Docherty, P. D., Chiew, Y.-S., & Chase, J. G. (2016). Extrapolation of a non-linear autoregressive model of pulmonary mechanics. *Mathematical Biosciences*, *284*, 32–39. doi: 10.1016/j.mbs.2016.08.001

Langdon, R., Docherty, P. D., Chiew, Y.-S., Damanhuri, N. S., & Chase, J. G. (2015). Implementation of a non-linear autoregressive model with modified Gauss-Newton parameter identification to determine pulmonary mechanics of respiratory patients that are intermittently resisting ventilator flow patterns. *IFAC-PapersOnLine*, *28*(20), 354–359. doi: 10.1016/j.ifacol.2015.10.165

Langdon, R., Docherty, P. D., Chiew, Y.-S., Moeller, K., & Chase, J. G. (2015). Interpolation within a recruitment manoeuvre using a non-linear autoregressive model

of pulmonary mechanics. *IFAC-PapersOnLine*, *28*(20), 297–302. doi: 10.1016/j.ifacol.2015.10.155

Langdon, R., Docherty, P. D., Chiew, Y.-S., Möller, K., & Chase, J. G. (2016). Use of basis functions within a non-linear autoregressive model of pulmonary mechanics. *Biomedical Signal Processing and Control*, *27*, 44–50. doi: 10.1016/j.bspc.2016.01.010

Langdon, R., Docherty, P. D., Mansell, E. J., & Chase, J. G. (2018). Accurate and precise prediction of insulin sensitivity variance in critically ill patients. *Biomedical Signal Processing and Control*, *39*, 327–335. Retrieved from http://dx.doi.org/10.1016/j.bspc.2017.08.010 doi: 10.1016/j.bspc.2017.08.010

Laufer, B., Docherty, P. D., Knörzer, A., Chiew, Y.-S., Langdon, R., Möller, K., & Chase, J. G. (2017). Performance of variations of the dynamic elastance model in lung mechanics. *Control Engineering Practice*, *58*, 262–267. Retrieved from http://dx.doi.org/10.1016/j.conengprac.2016.03.004 doi: 10.1016/j.conengprac.2016.03.004

Le Compte, A. J., Lee, D. S., Chase, J. G., Lin, J., Lynn, A., & Shaw, G. M. (2010). Blood glucose prediction using stochastic modeling in neonatal intensive care. *IEEE Transactions on Biomedical Engineering*, *57*(3), 509–518. doi: 10.1109/TBME.2009.2035517

Le Compte, A. J., Pretty, C. G., Chase, J. G., Lynn, A. M., Lin, J., & Shaw, G. M. (2012). Pilot study of a model-based approach to blood glucose control in very-low-birthweight neonates. *BMC Pediatrics*, *12*. doi: 10.1186/1471-2431-12-117

Lin, J., Lee, D., Chase, J. G., Shaw, G. M., Compte, A. L., Lotz, T., ... Hann, C. E. (2007). Stochastic Modelling of Insulin Sensitivity and Adaptive Glycemic Control for Critical Care. *Computer Methods and Programs in Biomedicine*, *89*(2), 141–152.

Lipes, J., Bojmehrani, A., & Lellouche, F. (2012). Low tidal volume ventilation in patients without acute respiratory distress syndrome - A paradigm shift in mechanical ventilation. *Critical Care Research and Practice*, *2012*. doi: 10.1155/2012/416862

Ljung, L. (1999). *System identification : theory for the user* (2nd Editio ed.). Upper Saddle River, NJ: Prentice Hall.

Lorx, A., Suki, B., Hercsuth, M., Szabó, B., Pénzes, I., Boda, K., & Hantos, Z. (2010). Airway and tissue mechanics in ventilated patients with pneumonia. *Respiratory Physiology and Neurobiology*, *171*(2), 101–109. doi: 10.1016/j.resp.2010.03.004

Lucangelo, U., Bernabè, F., & Blanch, L. (2007). Lung mechanics at the bedside - make it simple. *Current Opinion in Critical Care*, *13*(1), 64–72. doi: 10.1097/MCC.0b013e32801162df

Luecke, T., & Pelosi, P. (2005). Clinical review: Positive end-expiratory pressure and cardiac output. *Critical Care*, *9*(6), 607–21. Retrieved from http://www.pubmedcentral.nih.gov/articlerender.fcgi?artid=1414045{&}tool=pmcentrez{&}rendertype=abstract doi: 10.1186/cc3877

Ma, B., & Bates, J. H. (2010). Modeling the complex dynamics of derecruitment in the lung. *Annals of Biomedical Engineering*, *38*(11), 3466–3477. doi: 10.1007/s10439-010-0095-2

Maca, J., Jor, O., Holub, M., Sklienka, P., Bur a, F., Burda, M., . . . Ev ik, P. (2017). Past and Present ARDS Mortality Rates: A Systematic Review. *Respiratory Care*, *62*(1), 113–122. Retrieved from http://rc.rcjournal.com/cgi/doi/10.4187/respcare.04716 doi: 10.4187/respcare.04716

Major, V., Shaw, G. M., & Chase, J. G. (2018). Biomedical Engineer's Guide to the Clinical Aspects of Intensive Care Mechanical Ventilation. *BioMedical Engineering OnLine*. Retrieved from https://doi.org/10.1186/s12938-018-0599-9 doi: 10.1186/s12938-018-0599-9

Malhotra, A. (2008). Low-Tidal-Volume Ventilation in the Acute Respiratory Distress Syndrome. *New England Journal of Medicine*, *357*(11), 1113–1120. Retrieved from http://www.ncbi.nlm.nih.gov/pubmed/17855672{%}5Cnhttp://www.pubmedcentral.nih.gov/articlerender.fcgi?artid=PMC2287190{%}5Cnhttp://www.nejm.org/doi/abs/10.1056/

NEJMct074213 doi: 10.1097/SA.0b013e31817c3742

Marini, J. J. (1994). Ventilation of the acute respiratory distress syndrome - looking for Mr. Goodmode. *Anesthesiology*, *80*(5), 972–975.

Massa, C. B., Allen, G. B., & Bates, J. H. (2008). Modeling the dynamics of recruitment and derecruitment in mice with acute lung injury. *Journal of Applied Physiology*, *105*(6), 1813–1821. Retrieved from http://jap.physiology.org/cgi/doi/10.1152/japplphysiol.90806.2008 doi: 10.1152/japplphysiol.90806.2008

Maxwell, J. H. (1986). The Iron Lung - Halfway Technology or Necessary Step? *The Milbank Quarterly*, *64*(1), 3. doi: 10.2307/3350003

Mead, J., & Whittenberger, J. L. (1953). Physical Properties of Human Lungs Measured During Spontaneous Respiration. *Journal of Applied Physiology*, *5*(12), 779–796. Retrieved from http://jap.physiology.org/content/5/12/779.short

Meade, M. O., Cook, D. J., Arabi, Y. M., Cooper, D. J., Davies, A. R., Hand, L. E., ... Stewart, T. E. (2008). Ventilation Strategy Using Low Tidal Volumes, Recruitment Maneuvers, and High Positive End-Expiratory Pressure for Acute Lung Injury and Acute Respiratory Distress Syndrome. *JAMA: The Journal of the American Medical Association*, *299*(6), 637–645. Retrieved from http://archderm.jamanetwork.com/article.aspx?articleid=181425http://jama.jamanetwork.com/article.aspx?doi=10.1001/jama.299.6.637 doi: 10.1001/jama.299.6.637

Meade, M. O., Cook, D. J., Griffith, L. E., Rrt, L. E. H., Lapinsky, S. E., Stewart, T. E., ... Guyatt, G. H. (2008). A Study of the Physiologic Responses to a Lung Recruitment Maneuver in Acute Lung Injury and Acute Respiratory Distress Syndrome. *Respiratory Care*, *53*(11), 1441–1449.

Medoff, B. D., Harris, R. S., Kesselman, H., Venegas, J. G., Amato, M. B., & Hess, D. (2000). Use of recruitment maneuvers and high-positive end-expiratory pressure in a patient with acute respiratory distress syndrome. *Critical Care Medicine*, *28*(4), 1210–6. Retrieved from http://www.ncbi.nlm.nih.gov/pubmed/10809308

Mercat, A., Richard, J.-C. M., Vielle, B., Jaber, S., Osman, D., Diehl, J.-L., ... for the Expiratory Pressure (Express) Study Group (2008). Positive End-Expiratory Pressure Setting in Adults With Acute Lung Injury and Acute Respiratory Distress Syndrome. *JAMA: The Journal of the American Medical Association*, *299*(6), 646. Retrieved from http://jama.jamanetwork.com/article.aspx?doi=10.1001/jama.299.6.646 doi: 10.1001/jama.299.6.646

Metnitz, P. G., Metnitz, B., Moreno, R. P., Bauer, P., Sorbo, L. D., Hoermann, C., ... Ranieri, V. M. (2009). Epidemiology of Mechanical Ventilation: Analysis of the SAPS 3 Database. *Intensive Care Medicine*, *35*(5), 816–824. doi: 10.1007/s00134-009-1449-9

Moher, D., Dulberg, C., & Wells, G. (1994). Statistical Power, Sample Size, and Their Reporting in Randomized Controlled Trials. *Journal of American Medical Association*, *272*(2), 122–124. doi: doi:10.1001/jama.1994.03520020048013

Möller, K., Zhao, Z., Stahl, C., Schumann, S., & Guttmann, J. (2008). On the separate determination of lung mechanics in in- and expiration. *IFMBE Proceedings*, *22*, 2049–2052. doi: 10.1007/978-3-540-89208-3_488

Mols, G., Priebe, H. J., & Guttmann, J. (2006). Alveolar recruitment in acute lung injury. *British Journal of Anaesthesia*, *96*(2), 156–166. doi: 10.1093/bja/aei299

Morton, S. E., Chiew, Y.-S., Pretty, C. G., Moltchanova, E., Scarrott, C., Redmond, D. P., ... Chase, J. G. (2017). Effective sample size estimation for a mechanical ventilation trial through Monte-Carlo simulation - Length of mechanical ventilation and Ventilator Free Days. *Mathematical Biosciences*, *284*, 21–31. Retrieved from http://dx.doi.org/10.1016/j.mbs.2016.06.001 doi: 10.1016/j.mbs.2016.06.001

Morton, S. E., Dickson, J. L., Chase, J. G., Docherty, P. D., Desaive, T., Howe, S. L., ... Tawhai, M. H. (2018). A virtual patient model for mechanical ventilation. *Computer Methods and Programs in Biomedicine*, *165*, 77–87. Retrieved from https://doi.org/10.1016/j.cmpb.2018.08.004 doi: https://doi.org/10.1016/j.cmpb.2018.08.004

Morton, S. E., Dickson, J. L., Chase, J. G., Docherty, P. D., Howe, S. L., Shaw, G. M., & Tawhai, M. H. (2018a). Basis function identification of lung mechanics in mechanical ventilation for predicting outcomes of therapy changes : A first virtual patient. *IFAC-PapersOnLine*, *51*(15), 299–304. Retrieved from https://doi.org/10.1016/j.ifacol.2018.09.151 doi: 10.1016/j.ifacol.2018.09.151

Morton, S. E., Dickson, J. L., Chase, J. G., Docherty, P. D., Howe, S. L., Shaw, G. M., & Tawhai, M. H. (2018b). Development of a Predictive Pulmonary Elastance Model to Describe Lung Mechanics throughout Recruitment Manoeuvres. *IFAC-PapersOnLine*, *51*(27), 215–220. Retrieved from https://doi.org/10.1016/j.ifacol.2018.11.640 doi: 10.1016/j.ifacol.2018.11.640

Morton, S. E., Dickson, J. L., Docherty, P. D., Shaw, G. M., & Chase, J. G. (2017). Development of a predictive model for pulmonary elastance. *New Zealand Medical Journal*, *130*(1459), 79–82.

Morton, S. E., Docherty, P. D., Dickson, J. L., & Chase, J. G. (2018). An analysis of the impact of the inclusion of expiration data on the fitting of a predictive pulmonary elastance model. *Current Directions in Biomedical Engineering*, *4*(1), 255–258.

Morton, S. E., Knopp, J. L., Chase, J. G., Möller, K., Docherty, P., Shaw, G. M., & Tawhai, M. (2019). Predictive Virtual Patient Modelling of Mechanical Ventilation: Impact of Recruitment Function. *Annals of Biomedical Engineering*, *47*(7), 1626–1641. Retrieved from http://link.springer.com/10.1007/s10439-019-02253-w doi: 10.1007/s10439-019-02253-w

Morton, S. E., Knopp, J. L., Docherty, P. D., Shaw, G. M., & Chase, J. G. (2018). Validation of a Model-based Method for Estimating Functional Volume Gains during Recruitment Manoeuvres in Mechanical Ventilation. *IFAC-PapersOnLine*, *51*(27), 231–236. Retrieved from https://doi.org/10.1016/j.ifacol.2018.11.637 doi: 10.1016/j.ifacol.2018.11.637

Motulsky, H. (1995). *Intuitive Biostatistics* (Vol. 17). Retrieved from http://www.bio.ri.ccf.org/ASA{_}TSHS/pdf/TSHSnews10fall.pdf doi: 10.1002/(SICI)1097

-0258(19981215)17:23⟨2804::AID-SIM964⟩3.0.CO;2-A

Mutch, W. A. C. (2005). Convexity, Jensen's inequality, and benefits of noisy or biologically variable life support. *Proceedings of SPIE*, *5841*, 1–8. Retrieved from http://link.aip.org/link/?PSI/5841/1/1{&}Agg=doi doi: 10.1117/12.612588

Mutch, W. A. C., Harms, S., Graham, M. R., Kowalski, S. E., Girling, L. G., & Lefevre, G. R. (2000). Biologically variable or naturally noisy mechanical ventilation recruits atelectatic lung. *American Journal of Respiratory and Critical Care Medicine*, *162*(1), 319–323. doi: 10.1164/ajrccm.162.1.9903120

Nieman, G. F., Satalin, J., Andrews, P., Wilcox, K., Aiash, H., Baker, S., ... Habashi, N. M. (2018, dec). Preemptive mechanical ventilation based on dynamic physiology in the alveolar microenvironment. *Journal of Trauma and Acute Care Surgery*, *85*(6), 1081–1091. Retrieved from http://insights.ovid.com/crossref?an=01586154-201812000-00008 doi: 10.1097/TA.0000000000002050

Nieman, G. F., Satalin, J., Kollisch-Singule, M., Andrews, P., Aiash, H., Habashi, N. M., & Gatto, L. A. (2017). Physiology in Medicine: Understanding dynamic alveolar physiology to minimize ventilator-induced lung injury. *Journal of Applied Physiology*, *122*(6), 1516–1522. Retrieved from http://jap.physiology.org/lookup/doi/10.1152/japplphysiol.00123.2017 doi: 10.1152/japplphysiol.00123.2017

Ochs, M., Nyengaard, J. R., Jung, A., Knudsen, L., Voigt, M., Wahlers, T., ... Gundersen, H. J. G. (2004). The Number of Alveoli in the Human Lung. *American Journal of Respiratory and Critical Care Medicine*, *169*(1), 120–124. Retrieved from http://www.atsjournals.org/doi/full/10.1164/rccm.200308-1107OC{#}.VhZZOnVStBc{%}5Cnhttp://www.atsjournals.org/doi/abs/10.1164/rccm.200308-1107OC doi: 10.1164/rccm.200308-1107OC

Owens, R. L., Hess, D. R., Malhotra, A., Venegas, J. G., & Harris, R. S. (2008). Effect of the chest wall on pressure-volume curve analysis of acute respiratory distress syndrome lungs. *Critical Care Medicine*, *36*(11), 2980–2985. doi: 10.1097/CCM.0b013e318186afcb

Pelosi, P., Goldner, M., Mckibben, A., Adams, A. B., Eccher, G., Caironi, P., ... Marini, J. J. (2001). Recruitment and Derecruitment During Acute Respiratory Failure. *American Journal of Respiratory and Critical Care Medicine*, *164*, 122–130.

Petrie, A., Bulman, J. S., & Osborn, J. F. (2002). Further statistics in dentistry. Part 4: Clinical trials 2. *British Dental Journal*, *193*(10), 557–561. doi: 10.1038/sj.bdj.4801627

Petrucci, N., & De Feo, C. (2013). Lung protective ventilation strategy for the acute respiratory distress syndrome. *Cochrane database of systematic reviews*, *2*(4), CD003844. doi: 10.1002/14651858.CD003844.pub4

Petty, T. L., & Ashbaugh, D. G. (1971). The Adult Respiratory Distress Syndrome: Clinical Features , Factors Influencing Prognosis and Principles of Management The Adult Respiratory Distress Syndrome *. *Chest*.

Pinhu, L., Whitehead, T., Evans, T. W., & Griffiths, M. (2003). Ventilator-associated lung injury. *The Lancet*, *6736*(January 2014). doi: 10.1016/S0140-6736(03)12329-X

Pintado, M.-C., de Pablo, R., Trascasa, M., Milicua, J.-M., Rogero, S., Daguerre, M., ... Sánchez-García, M. (2013). Individualized PEEP setting in subjects with ARDS: a randomized controlled pilot study. *Respiratory Care*, *58*(9), 1416–23. Retrieved from http://www.ncbi.nlm.nih.gov/pubmed/23362167 doi: 10.4187/respcare.02068

Polak, A. G., & Lutchen, K. R. (2003). Computational model for forced expiration from asymmetric normal lungs. *Annals of Biomedical Engineering*, *31*(8), 891–907. doi: 10.1114/1.1588651

Ranieri, V. M., Eissa, N. T., Corbeil, C., Chassé, M., Braidy, J., Matar, N., & Milic-Emili, J. (1991, sep). Effects of Positive End-expiratory Pressure on Alveolar Recruitment and Gas Exchange in Patients with the Adult Respiratory Distress Syndrome. *American Review of Respiratory Disease*, *144*(3_pt_1), 544–551. Retrieved from http://www.atsjournals.org/doi/abs/10.1164/ajrccm/144.3{_}Pt{_}1.544 doi: 10.1164/ajrccm/144.3_Pt_1.544

Ranieri, V. M., Suter, P. M., Tullio, R. D., Dayer, J. M., Brienza, A., Bruno, F., & Slutsky, A. S. (2011). Effect of Mechanical Ventilation on Inflammatory Mediators in Patients with Acute Respiratory Distress Syndrome. *Journal of the American Medical Association*, *281*(1), 54–61.

Richardson, D. B. (2003). Power Calculations for Survival Analyses Via Monte Carlo Estimation. *American Journal of Industrial Medicine*, *44*(5), 532–539. doi: 10.1002/ajim.10310

Riedlinger, A., Kretschmer, J., & Möller, K. (2015). On the practical identifiability of a two - parameter model of pulmonary gas exchange. *BioMedical Engineering OnLine*, 1–15. doi: 10.1186/s12938-015-0077-6

Rocco, P. R. M., Pelosi, P., & de Abreu, M. G. (2010). Pros and cons of recruitment maneuvers in acute lung injury and acute respiratory distress syndrome. *Expert Review of Respiratory Medicine*, *4*(4), 479–489. doi: 10.1586/ers.10.43

Rohrer, F. (1925). Physiologie der Atembewegung. In *Handbuch der normalen und pathologischen physiologie: Vol 2* (pp. 70–127). Berlin: Springer-Verlag.

Safaei, S., Blanco, P. J., Müller, L. O., Hellevik, L. R., & Hunter, P. J. (2018). Bond graph model of cerebral circulation: Toward clinically feasible systemic blood flow simulations. *Frontiers in Physiology*, *9*(MAR), 1–15. doi: 10.3389/fphys.2018.00148

Schoenfeld, D. A., & Bernard, G. R. (2002). Statistical evaluation of ventilator-free days as an efficacy measure in clinical trials of treatments for acute respiratory distress syndrome. , *30*(8).

Schranz, C., Docherty, P. D., Chiew, Y.-S., Chase, J. G., & Möller, K. (2012). Structural identifiability and practical applicability of an alveolar recruitment model for ARDS patients. *IEEE Transactions on Biomedical Engineering*, *59*(12), 3396–3404. doi: 10.1109/TBME.2012.2216526

Schumann, S., Goebel, U., Haberstroh, J., Vimlati, L., Schneider, M., Lichtwarck-Aschoff, M., & Guttm. (2014). Determination of respiratory system mechanics during inspiration and expiration by FLow-controlled Expiration (FLEX): A pilot study in

anesthetized pigs. *Minerva Anestesiologica*, *80*(1), 19–28.

Simonis, F. D., Binnekade, J. M., Braber, A., Gelissen, H. P., Heidt, J., Horn, J., ... Schultz, M. J. (2015). PReVENT: protective ventilation in patients without ARDS at start of ventilation- study protocol for a randomized controlled trial. *Trials*, *16*(1), 226. Retrieved from ???http://www.pubmedcentral.nih.gov/articlerender.fcgi?artid=4453265{&}tool=pmcentrez{&}rendertype=abstract doi: 10.1186/s13063-015-0759-1

Slutsky, A. S. (1993). ACCP Consensus Conference - Mechanical Ventilation. *Chest*, *104*(6), 1833–1859. doi: 10.1378/chest.110.3.866-a

Slutsky, A. S. (1999). Lung injury caused by mechanical ventilation. *Chest*, *116*(1 Suppl), 9S–15S. Retrieved from http://www.ncbi.nlm.nih.gov/pubmed/24667617 doi: 10.1378/chest.116.suppl

Slutsky, A. S., & Ranieri, V. M. (2000). Mechanical ventilation: lessons from the ARDSNet trial. *Respiratory Research*, *1*(2), 73–77. doi: 10.1186/rr15

Slutsky, A. S., & Ranieri, V. M. (2014). Ventilator-Induced Lung Injury. *The New England Journal of Medicine*, *370*, 980. doi: http://dx.doi.org/10.1108/17506200710779521

Slutsky, A. S., & Tremblay, L. N. (1998). Multiple System Organ Failure - Is Mechanical Ventilation a Contributing Factor? *American Journal of Physiology*, *157*(16), 1721–1725.

Smalley, E. (2018). Clinical trials go virtual, big pharma dives in. *Nature Biotechnology*, *36*(7), 561–562. Retrieved from http://www.nature.com/doifinder/10.1038/nbt0718-561 doi: 10.1038/nbt0718-561

Spieth, P. M., & Gama de Abreu, M. (2012). Lung recruitment in ARDS - We are still confused, but on a higher PEEP level. *Critical Care*, *16*(1), 9–10. doi: 10.1186/cc11177

Stahl, C. A., Moeller, K., Schumann, S., Kuhlen, R., Sydow, M., Putensen, C., & Guttmann, J. (2006). Dynamic versus static respiratory mechanics in acute lung injury and acute respiratory distress syndrome. *Critical Care Medicine*, *34*(8), 2090–2098. doi:

10.1097/01.CCM.0000227220.67613.0D

Stenqvist, O. (2003). Practical assessment of respiratory mechanics. *British Journal of Anaesthesia*, *91*(1), 92–105. doi: 10.1093/bja/aeg141

Stewart, K. W., Pretty, C. G., Tomlinson, H., Thomas, F. L., Homlok, J., Noémi, S. N., ... Chase, J. G. (2016). Safety, efficacy and clinical generalization of the STAR protocol: a retrospective analysis. *Annals of Intensive Care*, *6*(1). doi: 10.1186/s13613-016-0125-9

Strøm, T., Martinussen, T., & Toft, P. (2010). A protocol of no sedation for critically ill patients receiving mechanical ventilation - a randomised trial. *The Lancet*, *375*(9713), 475–480. Retrieved from http://linkinghub.elsevier.com/retrieve/pii/S0140673609620729 doi: 10.1016/S0140-6736(09)62072-9

Suarez-Sipmann, F. (2014). New modes of assisted mechanical ventilation. *Medicina Intensiva (English Edition)*, *38*(4), 249–260. Retrieved from http://linkinghub.elsevier.com/retrieve/pii/S2173572714000216 doi: 10.1016/j.medine.2014.04.001

Suarez-Sipmann, F., Böhm, S. H., Tusman, G., Pesch, T., Thamm, O., Reissmann, H., ... Hedenstierna, G. (2007). Use of dynamic compliance for open lung positive end-expiratory pressure titration in an experimental study. *Critical Care Medicine*, *35*(1), 214–221. doi: 10.1097/01.CCM.0000251131.40301.E2

Sundaresan, A., & Chase, J. G. (2012). Positive end expiratory pressure in patients with acute respiratory distress syndrome - The past, present and future. *Biomedical Signal Processing and Control*, *7*(2), 93–103. doi: 10.1016/j.bspc.2011.03.001

Sundaresan, A., Yuta, T., Hann, C. E., Chase, J. G., Shaw, G. M., & Geoffrey Chase, J. (2009). A minimal model of lung mechanics and model-based markers for optimizing ventilator treatment in ARDS patients. *Computer Methods and Programs in Biomedicine*, *95*(2), 166–180. doi: 10.1016/j.cmpb.2009.02.008

Surrowes, K. S. (2005). *An anatomically-based mathematical model of the human pulmonary circulation* (Unpublished doctoral dissertation).

Swan, A. J., Clark, A. R., & Tawhai, M. H. (2012). A computational model of the topographic distribution of ventilation in healthy human lungs. *Journal of Theoretical Biology*, *300*, 222–231. Retrieved from http://dx.doi.org/10.1016/j.jtbi.2012.01.042 doi: 10.1016/j.jtbi.2012.01.042

Szlavecz, A., Chiew, Y.-S., Redmond, D. P., Beatson, A., Glassenbury, D., Corbett, S., ... Chase, J. G. (2014). The Clinical Utilisation of Respiratory Elastance Software (CURE Soft): a bedside software for real-time respiratory mechanics monitoring and mechanical ventilation management. *BioMedical Engineering OnLine*, *13*(1), 140. doi: 10.1186/1475-925X-13-140

Tawhai, M. H., & Bates, J. H. (2011). Multi-scale lung modeling. *Journal of Applied Physiology*, *110*(5), 1466–1472. Retrieved from http://jap.physiology.org/cgi/doi/10.1152/japplphysiol.01289.2010 doi: 10.1152/japplphysiol.01289.2010

Tawhai, M. H., & Burrowes, K. S. (2003). Developing integrative computational models of pulmonary structure. *Anatomical record. Part B, New anatomist*, *275*(1), 207–218. doi: 10.1002/ar.b.10034

Tawhai, M. H., & Burrowes, K. S. (2008). Multi-scale Models of the Lung Airways and Vascular System. *Integration in Respiratory Control*, *605*(5), 190–194.

Tawhai, M. H., Hoffman, E., & Lin, C.-L. (2009). The lung physiome: merging imaging-based measures with predictive computational models. *Wiley Interdisciplinary Reviews: Systems Biology and Medicine 2009*, *1*(1), 61–62.

Tawhai, M. H., Pullan, A. J., & Hunter, P. J. (2000). Generation of an Anatomically Based Three-Dimensional Model of the Conducting Airways. *Annals of Biomedical Engineering*, *28*(7), 793–802. Retrieved from http://link.springer.com/10.1114/1.1289457 doi: 10.1114/1.1289457

Tehrani, F. T. (2012). A closed-loop system for control of the fraction of inspired oxygen and the positive end-expiratory pressure in mechanical ventilation. *Computers in Biology and Medicine*, *42*(11), 1150–1156. Retrieved from http://dx.doi.org/

10.1016/j.compbiomed.2012.09.007 doi: 10.1016/j.compbiomed.2012.09.007

Terragni, P., Rosboch, G., Tealdi, A., Corno, E., Menaldo, E., Davini, O., ... Ranieri, V. M. (2007). Tidal hyperinflation during low tidal volume ventilation in acute respiratory distress syndrome. *American Journal of Respiratory & Critical Care Medicine*, *175*(2), 160–166. Retrieved from http://search.ebscohost.com/login.aspx?direct=true{&}db=c8h{&}AN=2009503529{&}site=ehost-live doi: 10.1164/rccm.200607-915OC

Terragni, P., Rosboch, G. L., Lisi, A., Viale, A. G., & Ranieri, V. M. (2003). How respiratory system mechanics may help in minimising ventilator-induced lung injury in ARDS patients. *European Respiratory Journal*, *22*(Suppl. 42), 15–21. doi: 10.1183/09031936.03.00420303

Tgavalekos, N. T., Tawhai, M. H., Harris, R. S., Mush, G., Vidal-Melo, M., Venegas, J. G., & Lutchen, K. R. (2005). Identifying airways responsible for heterogeneous ventilation and mechanical dysfunction in asthma: an image functional modeling approach. *Journal of Applied Physiology*, *99*(6), 2388–2397. Retrieved from http://jap.physiology.org/cgi/doi/10.1152/japplphysiol.00391.2005 doi: 10.1152/japplphysiol.00391.2005

Tgavalekos, N. T., Venegas, J. G., Suki, B., & Lutchen, K. R. (2003). Relation Between Structure, Function, and Imaging in a Three-Dimensional Model of the Lung. *Annals of Biomedical Engineering*, *31*(4), 363–373. doi: 10.1114/1.1557972

The ARDS Definition Task Force. (2012). Acute Respiratory Distress Syndrome : The Berlin Definition. *JAMA: The Journal of the American Medical Association*, *307*(23), 2526–2533. doi: 10.1001/jama.2012.5669

The Mathworks. (2017). *MATLAB R2017a.* Natick, Massachusetts: The Mathworks.

Thomson, A. (1997). The role of negative pressure ventilation. *Archives of Disease in Childhood*, *77*, 454–458. doi: 10.1136/adc.79.1.94b

Trundle, S., & Rawat, S. (2011). Measurement of pH, SpO2, and end tidal CO2. *Anaesthesia & Intensive Care Medicine*, *12*(12), 565–567. doi: 10.1016/j.mpaic.2011.09.011

Tusman, G., Groisman, I., Fiolo, F. E., Scandurra, A., Arca, J. M., Krumrick, G., ... Sipmann, F. S. (2014). Noninvasive monitoring of lung recruitment maneuvers in morbidly obese patients: The role of pulse oximetry and volumetric capnography. *Anesthesia and Analgesia*, *118*(1), 137–144. doi: 10.1213/01.ane.0000438350.29240.08

Uyttendaele, V., Dickson, J. L., Morton, S. E., Shaw, G. M., Desaive, T., & Chase, J. G. (2018). Changes in Identified, Model-based Insulin Sensitivity can be used to Improve Risk and Variability Forecasting in Glycaemic Control. *IFAC-PapersOnLine*, *51*(15), 311–316.

Valentini, R., Aquino-Esperanza, J., Bonelli, I., & Maskin, P. (2014). Gas exchange and lung mechanics in patients with acute respiratory distress syndrome: comparison of three different strategies of positive end expiratory pressure. *Journal of Critical Care*, *30*(2), 334–340. Retrieved from http://www.sciencedirect.com/science/article/pii/S0883944114004857 doi: 10.1016/j.jcrc.2014.11.019.

Van Der Lee, J. H., Tanck, M. W., Wesseling, J., & Offringa, M. (2009). Pitfalls in the design and analysis of paediatric clinical trials: A case of a 'failed' multi-centre study, and potential solutions. *Acta Paediatrica, International Journal of Paediatrics*, *98*(2), 385–391. doi: 10.1111/j.1651-2227.2008.01048.x

van Drunen, E. J., Chase, J. G., Chiew, Y.-S., Shaw, G. M., & Desaive, T. (2013). Analysis of different model-based approaches for estimating dFRC for real-time application. *BioMedical Engineering OnLine*, *12*(1), 9. doi: 10.1186/1475-925X-12-9

van Drunen, E. J., Chiew, Y.-S., Chase, J. G., Shaw, G. M., Lambermont, B., Janssen, N., ... Desaive, T. (2013). Expiratory model-based method to monitor ARDS disease state. *BioMedical Engineering OnLine*, *12*(1), 1. Retrieved from BioMedicalEngineeringOnLine doi: 10.1186/1475-925X-12-57

van Drunen, E. J., Chiew, Y.-S., Pretty, C. G., Shaw, G. M., Lambermont, B., Janssen, N., ... Desaive, T. (2014). Visualisation of time-varying respiratory system elastance in experimental ARDS animal models. *BMC Pulmonary Medicine*, *14*(1), 1–9. Re-

trieved from BMCPulmonaryMedicine doi: 10.1186/1471-2466-14-33

Venegas, J. G., Harris, R. S., & Simon, B. A. (1998). A comprehensive equation for the pulmonary pressure-volume curve. *Journal of Applied Physiology*, *84*(1), 389–395.

Villar, J., Kacmarek, R. M., Perez-Mendez, L., & Aguirre-Jaime, A. (2006). A high positive end-expiratory pressure, low tidal volume ventilatory strategy improves outcome in persistent acute respiratory distress syndrome - A randomized controlled trial. *Critical Care Medicine*, *34*(5), 1311–1318. doi: 10.1097/01.CCM.0000215598.84885.01

Villar, J., & Slutsky, A. S. (1996). PEEP or no PEEP: That is not the question. *Respiratory Care*, *3*(6), 361–368.

Wallet, F., Delannoy, B., Haquin, A., Debord, S., Leray, V., Bourdin, G., ... Guerin, C. (2013). Evaluation of Recruited Lung Volume at Inspiratory Plateau Pressure With PEEP Using Bedside Digital Chest X-ray in Patients With Acute Lung Injury{/}ARDS. *Respiratory Care*, *58*(3), 416–423. Retrieved from http://rc.rcjournal.com/cgi/doi/10.4187/respcare.01893 doi: 10.4187/respcare.01893

Webb, P. (2016). Rarotonga. In S. Levine (Ed.), *Pacific ways: Government and politics in the pacific islands* (2nd ed.). Wellington: Victoria University Press.

Werner, R., Ehrhardt, J., Schmidt, R., & Handels, H. (2009). Patient-specific finite element modeling of respiratory lung motion using 4D CT image data. *Medical Physics*, *36*(5), 1500–1511. doi: 10.1118/1.3101820

West, J. B. (2012). *Respiratory Physiology: The Essentials* (9th ed.). Baltimore: Lippincott Williams & Wilkins.

Wheatley, C. M., Dickinson, J. L., Mackey, D. a., Craig, J. E., & Sale, M. M. (2002). Retinopathy of prematurity: recent advances in our understanding. *Archives of Disease in Childhood. Fetal and neonatal edition*, *87*(2), F78–82. Retrieved from http://www.pubmedcentral.nih.gov/articlerender.fcgi?artid=1721447{&}tool=pmcentrez{&}rendertype=abstract doi: 10.1136/bjo.86.6.696

Whitley, E., & Ball, J. (2002). Statistics review 4: sample size calculations. *Critical Care*, *6*(4), 335–41. Retrieved from http://www.ncbi.nlm.nih.gov/pubmed/12225610 doi: 10.1186/cc1521

Williamson, J. P., McLaughlin, R. A., Noffsinger, W. J., James, A. L., Baker, V. A., Curatolo, A., ... Eastwood, P. R. (2011). Elastic properties of the central airways in obstructive lung diseases measured using anatomical optical coherence tomography. *American Journal of Respiratory and Critical Care Medicine*, *183*(5), 612–619. doi: 10.1164/rccm.201002-0178OC

Wright, P., & Bernard, G. R. (1989). The role of airflow resistance in patients with the adult respiratory distress syndrome. *American Review of Respiratory Disease*, *139*(5), 1169–1174. doi: 10.1164/ajrccm/139.5.1169

Wunsch, H., Linde-zwirble, W. T., Angus, D. C., Hartman, M. E., Milbrandt, E. B., & Kahn, J. M. (2010). The epidemiology of mechanical ventilation use in the United States. *Critical Care Medicine*, *38*(10), 1947–1953. doi: 10.1097/CCM.0b013e3181ef4460

Yuta, T. (2007). Minimal model of lung mechanics for optimising ventilator therapy in critical care. (July). Retrieved from http://ir.canterbury.ac.nz/handle/10092/1608

Zhao, Z., Guttmann, J., & Möller, K. (2011). Adaptive SLICE method: an enhanced method to determine nonlinear dynamic respiratory system mechanics. *Physiological Measurement*, *33*(1), 51–64. doi: 10.1088/0967-3334/33/1/51

Zhao, Z., Guttmann, J., & Möller, K. (2012). Assessment of a volume-dependent dynamic respiratory system compliance in ALI/ARDS by pooling breathing cycles. *Physiological Measurement*, *33*(8), N61–N67. doi: 10.1088/0967-3334/33/8/N61

Zick, G., Elke, G., Becher, T., Schädler, D., Pulletz, S., Freitag-Wolf, S., ... Frerichs, I. (2013). Effect of PEEP and Tidal Volume on Ventilation Distribution and End-Expiratory Lung Volume: A Prospective Experimental Animal and Pilot Clinical Study. *PLoS ONE*, *8*(8). doi: 10.1371/journal.pone.0072675